





28577256



This is to certify that the

dissertation entitled

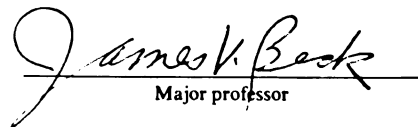
ESTIMATION OF THE THERMAL AND KINETIC PROPERTIES
ASSOCIATED WITH CARBON/EPOXY COMPOSITE MATERIALS
DURING AND AFTER CURING

presented by

Elaine Patricia Scott

has been accepted towards fulfillment
of the requirements for

Ph. D. degree in Mechanical Engineering


Major professor

Date December 8, 1989

**PLACE IN RETURN BOX to remove this checkout from your record.
TO AVOID FINES return on or before date due.**

DATE DUE DATE DUE DATE DUE		
<u>DAN 10 1996</u>	_____	_____
_____	_____	_____
_____	_____	_____
_____	_____	_____
_____	_____	_____
_____	_____	_____
_____	_____	_____

ESTIMATE

ASSOCIATE

**ESTIMATION OF THE THERMAL AND KINETIC PROPERTIES
ASSOCIATED WITH CARBON/EPOXY COMPOSITE MATERIALS
DURING AND AFTER CURING**

By

Elaine Patricia Scott

A DISSERTATION

Submitted to
Michigan State University
in partial fulfillment of the requirements
for the degree of

DOCTOR OF PHILOSOPHY

Department of Mechanical Engineering

1989

6054936

ABSTRACT

ESTIMATION OF THE THERMAL AND KINETIC PROPERTIES ASSOCIATED WITH CARBON/EPOXY COMPOSITE MATERIALS DURING AND AFTER CURING

By

Elaine Patricia Scott

The use of high performance composite materials in a variety of applications has grown rapidly in recent years. A thorough understanding of these materials with regards to thermal characteristics properties is essential in developing new processing methods and product applications. The focus of this research is on the estimation of the thermal properties (specifically thermal conductivity and the product of density and specific heat) of cured carbon fiber/amine-epoxy matrix composites, and on the estimation of both thermal and kinetic properties of these materials during curing. The kinetic properties include the activation energy constants.

The thermal properties of the cured composites were first estimated using an estimation procedure based on the minimization of a least squares function which incorporates both calculated and measured temperatures. Differential scanning calorimetry (DSC) was used in the next phase of this study for the estimation of the kinetic parameters associated with the curing of an EPON 828 amine-epoxy system, using several different kinetic models.

The final phase of this study related to the estimation of thermal properties during the curing process. The simultaneous estimation of thermal conductivity and the product of density and specific heat during the curing process has not previously been attempted. A least squares function incorporating both calculated and measured

temperatures was
tions during curing
analysis. This proc
an experiment wa
during the curing p

The thermal c
heat were determin
temperature for two
EPON 828 epoxy w
similar epoxy system
model was presented
for the estimation of
perature data, and
used in obtaining exp

temperatures was again used, and the heat generation resulting from the kinetic reactions during curing was accounted for in the analysis, using the results of the DSC analysis. This procedure was evaluated using simulated temperature data. In addition, an experiment was designed and evaluated for use in obtaining temperature data during the curing process with this estimation scheme.

The thermal conductivity perpendicular to the fiber axis and the density-specific heat were determined for the cured AS4-EPON 828 composite materials as functions of temperature for two different fiber orientations. The kinetic parameters obtained for EPON 828 epoxy were in good agreement with previously published kinetic data for similar epoxy systems during the first half of the curing cycle, and a new reaction rate model was presented for the second half of the curing process. Finally, the procedure for the estimation of thermal properties during curing was verified using simulated temperature data, and improvements were proposed for the techniques and equipment used in obtaining experimental temperatures.

LIST OF TABLES .

LIST OF FIGURES

LIST OF SYMBOLS

CHAPTER 1. Intro

CHAPTER 2. Lite

2.1 Estimation

Composi

2.1.1 E

C

2.1.2 E

F

2.2 Estimation

2.2.1 K

2.2.2 D

2.2.3 C

2.2.4 C

E

2.3 Estimation

Systems

2.3.1 M

Carbon/

2.3.2 E

di

TABLE OF CONTENTS

	PAGE
LIST OF TABLES	xi
LIST OF FIGURES	xvii
LIST OF SYMBOLS	xxii
 CHAPTER 1. Introduction	 1
CHAPTER 2. Literature Review	6
2.1 Estimation of Thermal Properties of	
Composite Materials	6
2.1.1 Estimation of Thermal Properties of Composite and	
Other Anisotropic Materials	7
2.1.2 Estimation of Thermal Properties of Cured Carbon	
Fiber-Reinforced Composites	9
2.2 Estimation of Kinetic Parameters in Epoxy-Based Systems	10
2.2.1 Kinetics of Amine-Epoxy Systems	11
2.2.2 Differential Scanning Calorimetry (DSC)	12
2.2.3 Cure Kinetics using DSC	13
2.2.4 Cure Kinetics of Neat vs. Carbon Fiber Reinforced	
Epoxy Systems	15
2.3 Estimation of Thermal Properties in Carbon/Epoxy Composite	
Systems during Curing	16
2.3.1 Mathematical Models to Simulate Heat Transfer in	
Carbon/Epoxy Composite Materials during Curing	16
2.3.2 Estimation of Thermal Properties of Composites	
during Curing	17

2.4 Minimization

Properties

2.4.1 T

2.4.2 T

2.4.3 T

2.4.4 M

De

CHAPTER 3. Theor

3.1 Estimation

Composite

3.1.1 He

Con

3.1.2 Est

3.2 Estimation

3.2.1 Re

Cu

3.2.2 Re

Cu

3.2.3 Sel

The

3.3 Estimation

Curing . .

3.3.1 He

du

3.3.2 Pa

3.4 Optimal E

Thermal P

3.4.1 Ob

Op

3.4.2 Op

2.4 Minimization Methods used for the Estimation of Thermal	
Properties	17
2.4.1 The Gauss Method	18
2.4.2 The Steepest Descent Method	19
2.4.3 The Conjugate Gradient Method	20
2.4.4 Methods of Determining the Matrix	
Derivatives	20
CHAPTER 3. Theoretical Considerations	22
3.1 Estimation of Thermal Properties in Cured	
Composite Materials	23
3.1.1 Heat Conduction in Cured Carbon-Fiber Reinforced	
Composites	23
3.1.2 Estimation of Thermal Properties	24
3.2 Estimation of Kinetic Parameters	25
3.2.1 Reaction Kinetics for Degree of	
Cure < 50%	26
3.2.2 Reaction Models for Degree of	
Cure > 50%	30
3.2.3 Selection of Kinetic Models for the Determination of	
Thermal Properties	31
3.3 Estimation of Thermal Properties during	
Curing	31
3.3.1 Heat Conduction in Carbon Fiber Reinforced Composites	
during Curing	32
3.3.2 Parameter Estimation Method	33
3.4 Optimal Experimental Design Criterion for the Estimation of	
Thermal Properties	34
3.4.1 Objectives for the Experimental Design	
Optimization	34
3.4.2 Optimal Experimental Design Criterion	35

CHAPTER 4. Exp

4.1 Experime:

Composi

4.1.1 P

S

4

4.

4.

4.

4.1.2 Exp

4.1

4.1

4.1.3 Data

Hea

4.1

4.1

4.1

4.1

4.1.4 Tran

4.1.5 Expe

4.1.6 Fibe

4.2 Differential

4.2.1 Sam

4.2.2 Diffe

4.2

4.2

4.2

4.2.3 Expe

CHAPTER 4. Experimental Procedures	41
4.1 Experiments for the Estimation of Thermal Properties in Cured	
Composite	41
4.1.1 Preparation of the Composite	
Samples	42
4.1.1.1 Epoxy Preparation	42
4.1.1.2 Prepreg Preparation	44
4.1.1.3 Stacking Procedure	52
4.1.1.4 Consolidation	55
4.1.2 Experimental Set-up	57
4.1.2.1 Thermocouple Fabrication	59
4.1.2.2 Experimental Set-up Assembly	61
4.1.3 Data Acquisition System and Controlled	
Heat Flux	64
4.1.3.1 Data Acquisition Hardware	64
4.1.3.2 Signal Conditioning	64
4.1.3.3 Data Acquisition Programs	66
4.1.3.4 Controlled Heat Flux	66
4.1.4 Transient Temperature Experiments	66
4.1.5 Experimental Parameters	67
4.1.6 Fiber Volume Fraction	68
4.2 Differential Scanning Calorimetry Experiments	70
4.2.1 Sample Preparation for DSC Experiments	70
4.2.2 Differential Scanning Calorimeter Operation	72
4.2.2.1 Differential Scanning	
Calorimeter Set Up Procedure	72
4.2.2.2 Initialization Procedure for	
the DuPont 910 Calorimeter	74
4.2.2.3 Post-Processing Procedure	75
4.2.3 Experimental Parameters	78

4.3 Transient

4.3.1 Sa

4

4

4.3.2 Ex

4.3.3 Da

4

4.3

4.3

4.3

4.3.4 Exp

Me

4.3.5 Exp

CHAPTER 5. Results

5.1 Estimation

Composite

5.1.1 An

5.1

5.1

5.1

5.1

5.1.2 Est

He

5.1

5.1

4.3 Transient Temperature Measurements during Curing	80
4.3.1 Sample Preparation	82
4.3.1.1 Heater Preparation	82
4.3.1.2 Stacking Procedure	82
4.3.2 Experimental Set-up	84
4.3.3 Data Acquisition and Controlled Heat Flux	86
4.3.3.1 The VAXlab Data Acquisition Hardware	88
4.3.3.2 Signal Amplification	91
4.3.3.3 Controlled Heat Flux	92
4.3.3.4 Data Acquisition Program	93
4.3.4 Experimental Procedure for Transient Temperature Measurements during Curing	96
4.3.5 Experimental Parameters	98
CHAPTER 5. Results and Discussion	102
5.1 Estimation of Thermal Properties of Cured AS4/EPON 828-mPDA Composite Materials	104
5.1.1 Analysis of the Estimation Procedure	105
5.1.1.1 The Residuals	105
5.1.1.2 The Sensitivity Coefficients of the Estimated Parameters	108
5.1.1.3 The Sequential Estimates of the Estimated Parameters	110
5.1.1.4 Insights into the Experimental Design	110
5.1.2 Estimation of Thermal Conductivity and Density-Specific Heat of Cured AS4/EPON 828 Composite Materials	112
5.1.2.1 Experiments using $[0^\circ]_{24}$ Samples	112
5.1.2.2 Experiments using $[0^\circ, \pm 30^\circ, \pm 60^\circ, 90^\circ]_{2(\text{sym})}$ Samples	119

5

5

5.2 Estimation

EPON 82

5.2.1 De

of

5.2.2 Pa

(no

5.2

5.2

5.2.3 DL

5.2.4 Sel

tion

5.3 Estimation

Curing . .

5.3.1 Ana

Da

5.3

5.3

5.3.2 Ana

Exp

5.3

5.3

5.3

5.1.2.3	Comparison of Results from $[0^\circ]_{24}$ and $[0^\circ, \pm 30^\circ, \pm 60^\circ, 90^\circ]_{2(\text{sym})}$ Samples	122
5.1.2.4	Comparison with Previously Published Results	125
5.2	Estimation of Kinetic Parameters Associated with the Curing of EPON 828/mPDA Epoxy	125
5.2.1	Determination of the Total Heat of Reaction and Degree of Cure	127
5.2.2	Parameter Estimation for Autocatalyzed Cure Kinetics (no diffusion)	127
5.2.2.1	Estimation of Rate constants and Exponents	129
5.2.2.2	Estimation of the Activation Energy Constants and the Pre-Exponential Factors	133
5.2.3	Diffusion Controlled Reactions and Parameter Estimation..	137
5.2.4	Selection of Kinetic Parameters for Use in the Estimation of Thermal Properties during Curing	138
5.3	Estimation of Thermal Properties of Composite Materials during Curing	141
5.3.1	Analysis of the Estimation Procedure using Simulated Data	142
5.3.1.1	Description of Test Cases	142
5.3.1.2	Results from Test Cases	146
5.3.2	Analysis of the Estimation of Thermal Properties from Experimental Data	154
5.3.2.1	Results from Experimental Data	156
5.3.2.2	Investigation of Possible Errors in the Estimation of Thermal Properties during Curing	170
5.3.2.3	Improvements in the Experimental Design for the Estimation of Thermal Properties in Composite	

Materials during Curing	176
CHAPTER 6. Summary and Conclusions	179
APPENDIX A. One Dimensional Curing Program, CURE1D	183
A.1 Summary of Program	183
A.2 Program Listing for CURE1D	185
APPENDIX B. Data Aquisition Program, DATA_DA_AD	215
B.1 Summary of Program	215
B.2 Program Listing for DATA_DA_AD	217
APPENDIX C. Parameter Estimation Results from Experimental Repetitions	
using Cured Composite Samples	238
BIBLIOGRAPHY	247

Table 4.1 Fabrication

Transient Experiments

Table 4.2 Experimental

Composite Systems

Table 4.3 Fiber Volume

Numerical Values

Table 4.4 Experimental

Experiments

Table 5.1 Average

Effective Thermal

and Effective

EPON 828-1

Table 5.2 Estimation

Linear Regression

Perpendicular

$\rho_{c,p}$ of Cure

Table 5.3 Average

Effective Thermal

Effective Deformation

AS4/EPON

Table 5.4 Comparison

Perpendicular

LIST OF TABLES

	PAGE
Table 4.1 Fabrication Parameters for Cured Composite Disks used in Transient Experiments	58
Table 4.2 Experimental Parameters for Transient Experiments using Cured Composite Samples	69
Table 4.3 Fiber Volume Fractions using Acid Digestion Analysis and Optical Numerical Volumetric Analysis (ONVfA)	71
Table 4.4 Experimental Parameters for Differential Scanning Calorimetry Experiments	81
Table 5.1 Averaged Estimated Values and 95% Confidence Intervals for Effective Thermal Conductivity, k , Perpendicular to the Fiber Axis and Effective Density-Specific Heat, ρc_p , of Cured $[0^\circ]_{24}$ AS4/ EPON 828-mPDA Composites	113
Table 5.2 Estimated Parameters and 95% Confidence Intervals for the Linear Regression of Both Effective Thermal Conductivity, k , Perpendicular to the Fibers and Effective Density-Specific Heat, ρc_p , of Cured $[0^\circ]_{24}$ AS4/EPON 828-mPDA Composites	120
Table 5.3 Averaged Estimated Values and 95% Confidence Intervals for Effective Thermal Conductivity, k , Perpendicular to the Fiber Axis and Effective Density-Specific Heat, ρc_p , of Cured $[0^\circ, \pm 30^\circ, \pm 60^\circ, 90^\circ]_{2(\text{sym})}$ AS4/EPON 828-mPDA Composites	121
Table 5.4 Comparison of Estimated Effective Thermal Conductivity, k , Perpendicular to the Fiber Axis with Previously Published	

Results

Table 5.5 Total H

Scanning Ca

EPON 828/r

Table 5.6 Rate Co

(3.4) and Deg

Epoxy, using

Table 5.7 Rate Con

95% Confiden

Values, α , Le

Squares Meth

Table 5.8 Rate Con

Intervals, De

Less than 50

(1976) Metho

Table 5.9 Rate Co

dence Interv

α , Less than

Table 5.10 Activa

Factors, A_1

and Estimati

(3.6), for Deg

EPON 828/r

Table 5.11 Rate C

95% Confide

Values, α , G

Table 5.12 Test Ca

Density-Spec

Materials

Results	126
Table 5.5 Total Heat of Reaction Calculated from Dynamic Differential Scanning Calorimetry Experiments (Exp. 2.1) using EPON 828/mPDA Epoxy	128
Table 5.6 Rate Constants, c_1 and c_2, and Exponent, m, Determined from eq. (3.4) and Degree of Cure Values, α, Less than 50% for EPON 828/mPDA Epoxy, using the Ryan and Dutta (1979) Method	130
Table 5.7 Rate Constants, c_1 and c_2, and Exponent, m, and Associated 95% Confidence Intervals, Determined from eq. (3.4) and Degree of Cure Values, α, Less than 50% for EPON 828/mPDA Epoxy, using a Least Squares Method	131
Table 5.8 Rate Constants, c_1 and c_2, and Associated 95% Confidence Intervals, Determined from eq. (3.5) and Degree of Cure Values, α, Less than 50% for EPON 828/mPDA Epoxy, using the Sourour and Kamal (1976) Method	132
Table 5.9 Rate Constant, c_1, and Exponent, n, and Associated 95% Confidence Intervals, Determined from eq. (3.6) and Degree of Cure Values, α, Less than 50% for EPON 828/mPDA Epoxy	134
Table 5.10 Activation Energy Constants, E_1 and E_2, and Pre-Exponential Factors, A_1 and A_2, Determined from the Arrhenius Relationship (eq. 3.7) and Estimated Rate Constants Estimated from eqs. (3.4), (3.5), and (3.6), for Degree of Cure Values, α, Less than 50% for EPON 828/mPDA Epoxy	136
Table 5.11 Rate Constant, c_1, and Diffusion Constant, D, and Associated 95% Confidence Intervals Determined from eq. (3.16) and Degree of Cure Values, α, Greater than 50% for EPON 828/mPDA Epoxy	139
Table 5.12 Test Cases for the Estimation of Thermal Conductivity, k, and Density-Specific Heat, ρc_p, from Simulated Data for Composite Materials	147

Table 5.13 Estim.

the Fibers a

95% Confid.

Temperature

Properties: k

Table 5.14 Estima

the Fibers and

Confidence In

Temperature d

Properties: k =

Table 5.15 Estimate

the Fibers and

95% Confiden

Temperature c

Properties: k (

ρc_p (MJ/m³ °C

Table 5.16 Estim

the Fibers and

95% Confiden

Temperature

Properties: k

ρc_p (MJ/m³ °C

Table 5.17 Compar

and Density-s

eq. (5.6) and

Table 5.18 Estima

k and Effect

mPDA Comp

Only in Exp.

Table 5.13	Estimated Effective Thermal Conductivity, k , Perpendicular to the Fibers and Density-Specific Heat, ρc_p , and the Associated 95% Confidence Intervals for a Simulated Composite with an Initial Temperature of 75°C, an Initial Degree of Cure of 0.40, and Thermal Properties: $k = 0.83 \text{ W/m}^\circ\text{C}$ and $\rho c_p = 1.84 \text{ MJ/m}^3 \text{ }^\circ\text{C}$	149
Table 5.14	Estimated Effective Thermal Conductivity, k , Perpendicular to the Fibers and Density-Specific Heat, ρc_p , and the Associated 95% Confidence Intervals for a Simulated Composite with an Initial Temperature of 125°C, an Initial Degree of Cure of 0.80, and Thermal Properties: $k = 0.83 \text{ W/m}^\circ\text{C}$ and $\rho c_p = 1.84 \text{ MJ/m}^3 \text{ }^\circ\text{C}$	150
Table 5.15	Estimated Effective Thermal Conductivity, k , Perpendicular to the Fibers and Density-Specific Heat, ρc_p , and the Associated 95% Confidence Intervals for a Simulated Composite with an Initial Temperature of 75°C, an Initial Degree of Cure of 0.40, and Thermal Properties: $k \text{ (W/m}^\circ\text{C)} = 0.6678 + 9.03 \times 10^{-4}T + 0.0742\alpha$, and $\rho c_p \text{ (MJ/m}^3 \text{ }^\circ\text{C)} = 1.251 + 0.0045T + 0.139\alpha$	152
Table 5.16	Estimated Effective Thermal Conductivity, k , Perpendicular to the Fibers and Density-Specific Heat, ρc_p , and the Associated 95% Confidence Intervals for a Simulated Composite with an Initial Temperature of 125°C, an Initial Degree of Cure of 0.80, and Thermal Properties: $k \text{ (W/m}^\circ\text{C)} = 0.6678 + 9.03 \times 10^{-4}T + 0.0742\alpha$, and $\rho c_p \text{ (MJ/m}^3 \text{ }^\circ\text{C)} = 1.251 + 0.0045T + 0.139\alpha$	153
Table 5.17	Comparison of Averaged Estimated Thermal Conductivity, \bar{k} , and Density-Specific Heat, $\overline{\rho c_p}$, Values with Values Calculated Using eq. (5.6) and (5.7)	155
Table 5.18	Estimation of Thermal Conductivity Perpendicular to the Fibers, k , and Effective Density-Specific Heat, ρc_p , of Cured AS4/EPON 828-mPDA Composites using Temperature Data from the Top Composite Section Only in Exp. 3.3	161

Table 5.19 Estim

k, and Effect

mPDA Comp

Section Only

Table 5.20 Estima

k, and Effect

Composites d

Section Only

Table 5.21 Estima

k, and Effect

Composites d

Composite S

Table 5.22 Estima

k, and Effect

Composites

Sections in

Table 5.23 Estim

k, and Effect

Composites

Bottom Cor

Table 5.24 Estim

k, and Effect

Composites

Bottom Cor

Table 5.25 Estim

k, and Effect

Composites

Sections in

Measured P

Protection L

Table 5.19 Estimation of Thermal Conductivity Perpendicular to the Fibers, k, and Effective Density-Specific Heat, ρc_p , of Cured AS4/EPON 828- mPDA Composites using Temperature Data from the Bottom Composite Section Only in Exp. 3.3	162
Table 5.20 Estimation of Thermal Conductivity Perpendicular to the Fibers, k, and Effective Density-Specific Heat, ρc_p , of AS4/EPON 828-mPDA Composites during Curing using Temperature Data from the Top Composite Section Only in Exp. 3.2	163
Table 5.21 Estimation of Thermal Conductivity Perpendicular to the Fibers, k, and Effective Density-Specific Heat, ρc_p , of AS4/EPON 828-mPDA Composites during Curing using Temperature Data from the Bottom Composite Section Only in Exp. 3.2	164
Table 5.22 Estimation of Thermal Conductivity Perpendicular to the Fibers, k, and Effective Density-Specific Heat, ρc_p , of Cured AS4/EPON 828-mPDA Composites using Temperature Data from Both Top and Bottom Composite Sections in Exp. 3.3	168
Table 5.23 Estimation of Thermal Conductivity Perpendicular to the Fibers, k, and Effective Density-Specific Heat, ρc_p , of AS4/EPON 828-mPDA Composites during Curing using Temperature Data from Both Top and Bottom Composite Sections in Exp. 3.2	168
Table 5.24 Estimation of Thermal Conductivity Perpendicular to the Fibers, k, and Effective Density-Specific Heat, ρc_p , of AS4/EPON 828-mPDA Composites during Curing using Temperature Data from Both Top and Bottom Composite Sections in Exp. 3.1	169
Table 5.25 Estimation of Thermal Conductivity Perpendicular to the Fibers, k, and Effective Density-Specific Heat, ρc_p , of Cured AS4/EPON 828-mPDA Composites using Temperature Data from Both Top and Bottom Composite Sections in Exp. 3.3, with Applied Heat Flux Calculated From the Measured Power Input and the Surface Area of the Aluminum Foil Protection Layer	177

Table A.1 Descrip

CUREID

Table B.1 Descrip

DATA_DA_A

Table C.1 Estimate

the Fiber Axis

AS4/EPON 82

Temperature c

Table C.2 Estimate

the Fiber Axis

AS4/EPON 82

Temperature c

Table C.3 Estimate

the Fiber Axis

AS4/EPON 82

Temperature c

Table C.4 Estimate

the Fiber Axis

AS4/EPON 82

Temperature c

Table C.5 Estimate

the Fiber Axis

AS4/EPON 82

Temperature c

Table C.6 Estimate

the Fiber Axis

$10^\circ, \pm 30^\circ, \pm 60^\circ$

Experiments

Table A.1 Description of the One Dimensional Curing Program,

<i>CURE1D</i>	184
---------------	-------	-----

Table B.1 Description of the Data Acquisition Program,

<i>DATA_DA_AD</i>	216
-------------------	-------	-----

Table C.1 Estimated Effective Thermal Conductivity, k , Perpendicular tothe Fiber Axis and Density-Specific Heat, ρc_p , of Cured $[0^\circ]_{24}$

AS4/EPON 828-mPDA Composites from Experiments with an Initial

Temperature of Approximately 25°C	239
-----------------------------------	-------	-----

Table C.2 Estimated Effective Thermal Conductivity, k , Perpendicular tothe Fiber Axis and Density-Specific Heat, ρc_p , of Cured $[0^\circ]_{24}$

AS4/EPON 828-mPDA Composites from Experiments with an Initial

Temperature of Approximately 50°C	240
-----------------------------------	-------	-----

Table C.3 Estimated Effective Thermal Conductivity, k , Perpendicular tothe Fiber Axis and Density-Specific Heat, ρc_p , of Cured $[0^\circ]_{24}$

AS4/EPON 828-mPDA Composites from Experiments with an Initial

Temperature of Approximately 75°C	241
-----------------------------------	-------	-----

Table C.4 Estimated Effective Thermal Conductivity, k , Perpendicular tothe Fiber Axis and Density-Specific Heat, ρc_p , of Cured $[0^\circ]_{24}$

AS4/EPON 828-mPDA Composites from Experiments with an Initial

Temperature of Approximately 100°C	242
------------------------------------	-------	-----

Table C.5 Estimated Effective Thermal Conductivity, k , Perpendicular tothe Fiber Axis and Density-Specific Heat, ρc_p , of Cured $[0^\circ]_{24}$

AS4/EPON 828-mPDA Composites from Experiments with an Initial

Temperature of Approximately 125°C	243
------------------------------------	-------	-----

Table C.6 Estimated Effective Thermal Conductivity, k , Perpendicular tothe Fiber Axis and Density-Specific Heat, ρc_p , of Cured $[0^\circ, \pm 30^\circ, \pm 60^\circ, 90^\circ]_{2(\text{sym})}$ AS4/EPON 828-mPDA Composites from

Experiments with an Initial Temperature of Approximately 25°C	244
---	------	-----

Table C.7 Estima

the Fiber Ax

$(0^\circ, \pm 30^\circ, \pm$

Experiments

Table C.8 Estima

the Fiber Ax

$(0^\circ, \pm 30^\circ, \pm 6$

Experiments

Table C.7	Estimated Effective Thermal Conductivity, k , Perpendicular to the Fiber Axis and Density-Specific Heat, ρc_p , of Cured $[0^\circ, \pm 30^\circ, \pm 60^\circ, 90^\circ]_{2(s_{ym})}$ AS4/EPON 828-mPDA Composites from Experiments with an Initial Temperature of Approximately 50°C	245
-----------	--	------	-----

Table C.8	Estimated Effective Thermal Conductivity, k , Perpendicular to the Fiber Axis and Density-Specific Heat, ρc_p , of Cured $[0^\circ, \pm 30^\circ, \pm 60^\circ, 90^\circ]_{2(s_{ym})}$ AS4/EPON 828-mPDA Composites from Experiments with an Initial Temperature of Approximately 75°C	246
-----------	--	------	-----

LIST OF FIGURES

	PAGE
Figure 3.1 Dimensionless Experimental Design Criterion, Δ^+ , for Different Dimensionless Heating Times, t_1^+ , and a Dimension-less Heat Generation Term, g^+ , equal to 0.1	39
Figure 3.2 Dimensionless Experimental Design Criterion, Δ^+ , for Different Dimensionless Heating Times, t_1^+ , and a Dimension-less Heat Generation Term, g^+ , equal to 1.0 (dimensionless)	39
Figure 4.1 Hot Melt Prepregger (Research Tools Corporation)	45
Figure 4.2a Schematic of Single Spool Mount on Hot-Melt Prepregger	46
Figure 4.2b Photograph of Single Spool Mount	46
Figure 4.3a Schematic of Guide Roller, Furnace, and Tension Rollers on Hot-Melt Prepregger	47
Figure 4.3b Photograph of Fibers Through Guide Roller, Furnace, and Tension Rollers	47
Figure 4.4a,b Schematic (left) and Photograph (right) of Resin Pot Assembly on Hot-Melt Prepregger	49
Figure 4.5 Detailed View of Resin Pot, Die (A-A), and Pin Guide (from left to right)	50
Figure 4.6 Hot-Melt Prepregger Control Panel	50
Figure 4.7 Stacking for Orientation for the First Six Parallel and the First Six Quasi-isotropic Laminates for the $[0^\circ]_{24}$ and the $[0^\circ, \pm 30^\circ, \pm 60^\circ, 90^\circ]_{2(\text{sym})}$ Composite Disks	53
Figure 4.8 Cut-Away View of Stacked Prepreg Laminate	56

Figure 4.9 Prepa

Thermoco

Figure 4.10 Therm

Temperatu

Figure 4.11 An Ex

using Cure

Figure 4.12 Schem

Cured Comp

Figure 4.13 DuPon

Figure 4.14a DuPo

Cell (left), SH

Ceramic Lid

Figure 4.14b Close

in Calorimet

Figure 4.15 Heat o

Experiment

Figure 4.16 Determ

from a Dyn

Figure 4.17 Stacke

Heaters. (Ph

Figure 4.18 Stacke

Bag

Figure 4.19 Mecha

Figure 4.20 Schem

during Curi

Figure 4.21 Schem

during Curi

Figure 4.9 Prepared Thermocouple (ANSI Type E) with Close-up View of Thermocouple Junction	60
Figure 4.10 Thermocouple Placements on Composite Disks Used in Transient Temperature Experiments	62
Figure 4.11 An Experimental Set-up for Transient Temperature Measurements using Cured Composite Samples	63
Figure 4.12 Schematic of Data Acquisition for Transient Experiments using Cured Composite Samples	65
Figure 4.13 DuPont Instruments 910 Differential Scanning Calorimeter	73
Figure 4.14a DuPont Instruments 910 Differential Scanning Calorimeter Cell (left), Showing Bell Jar (right), Cell Cover (center), and Ceramic Lid (on cell)	76
Figure 4.14b Close-up View of Samples Pan (right) and Reference Pan (left) in Calorimeter Cell Shown Above	76
Figure 4.15 Heat of Reaction Data from One Repetition of the Dynamic DSC Experiment using DuPont Thermal Analysis Plotting Subroutines	77
Figure 4.16 Determination of Temperatures for Isothermal DSC Experiments from a Dynamic DSC Experiment	79
Figure 4.17 Stacked Composite Prepreg, Instrumented with Thermocouples and Heaters. (Photograph taken after curing.)	85
Figure 4.18 Stacked and Instrumented Composite Prepreg Sealed in a Vacuum Bag	85
Figure 4.19 Mechanical Press with Composite Laminate in Place	87
Figure 4.20 Schematic of Data Acquisition for First Transient Experiment during Curing	89
Figure 4.21 Schematic of Data Acquisition for Second Transient Experiment during Curing	90

Figure 4.22 Sch

Figure 4.23 Ther

First Tran

Bottom to

are Number

Figure 4.24 Therm

Second Tra

Bottom to T

are Number

Boldface typ

Figure 5.1. Residua

Surface (TC

the Heated S

No. 9 (Initial

Figure 5.2. Sensitiv

at the Heate

Repetition o

Figure 5.3. Sequen

Specific Hea

(initial temp

Figure 5.4. Estima

to the Fiber

Composites

Figure 5.5. Estima

Cured [0°]₂

Figure 5.6. Estima

to the Fiber

EPON 828-r

Figure 5.7. Estima

Figure 4.22 Schematic of Data Acquisition Program <i>DATA_DA_AD</i>	94
Figure 4.23 Thermocouple (T.C.) Locations in Prepreg Laminate for the First Transient Experiment during Curing. Plies are Numbered from Bottom to Top, and the Thermocouples used in the Data Acquisition are Numbers 1, 2, 10 and 11 (shown in Boldface type)	100
Figure 4.24 Thermocouple (T.C.) Locations in Prepreg Laminate for the Second Transient Experiment during Curing. Plies are Numbered from Bottom to Top, and the Thermocouples used in the Data Acquisition are Numbers 1, 3, 4, 6, 7, 10, 11, 12, 13, and 14 (shown in Boldface type)	102
Figure 5.1. Residuals ($^{\circ}\text{C}$) for Two Thermocouples Located at the Heated Surface (TC #1 and TC #2) and One Thermocouple Located 3.3 mm from the Heated Surface (TC #5) for the Second Repetition of Experiment No. 9 (initial temperature $\approx 100^{\circ}\text{C}$)	106
Figure 5.2. Sensitivity Coefficients, X_1 ($k\partial T/\partial k$) and X_2 ($\rho c_p \partial T/\partial \rho c_p$), at the Heated Surface and 3.3 mm from the Heated Surface for Second Repetition of Experiment No. 9	109
Figure 5.3. Sequential Estimation of Thermal Conductivity, k , and Density Specific Heat, ρc_p , from the Second Repetition of Experiment No. 9 (initial temperature $\approx 100^{\circ}\text{C}$)	111
Figure 5.4. Estimation of Effective Thermal Conductivity Perpendicular to the Fiber Axis, k , of Cured $[0^{\circ}]_{24}$ AS4/EPON 828-mPDA Composites	117
Figure 5.5. Estimation of Effective Density-Specific Heat, ρc_p , of Cured $[0^{\circ}]_{24}$ AS4/EPON 828-mPDA Composites	116
Figure 5.6. Estimation of Effective Thermal Conductivity Perpendicular to the Fiber Axis, k , of Cured $[0^{\circ}, \pm 30^{\circ}, \pm 60^{\circ}, 90^{\circ}]_{2(s y m)}$ AS4/EPON 828-mPDA Composites	123
Figure 5.7. Estimation of Effective Density-Specific Heat, ρc_p , of Cured	

$[0^\circ, \pm 30^\circ]$

Figure 5.8. Comparison of
Conductivity
and Cured
Composites

Figure 5.9. Comparison of
Density-Specific
 $[0^\circ, \pm 30^\circ, \pm 45^\circ]$

Figure 5.10 Arrhenius
eqs. (3.4), (3.5)
(kJ/mole $^\circ$ K)

Figure 5.11 Arrhenius
eqs. (3.4), (3.5)
(kJ/mole $^\circ$ K)

Figure 5.12 Residual
Errors with
Locations

Figure 5.13 Temperature
Thermocouple
Curing (Ex)

Figure 5.14 Temperature
Thermocouple
Curing (Ex)

Figure 5.15 Temperature
Transient
Cured Composites

Figure 5.16 Residual
TC#1, TC#2

$[0^\circ, \pm 30^\circ, \pm 60^\circ, 90^\circ]_{2(sym)}$ AS4/EPON 828-mPDA Composites	123
Figure 5.8. Comparison of Linear Regression Curves for Effective Thermal Conductivity Perpendicular to the Fiber Axis, k , of Cured $[0^\circ]_{24}$ and Cured $[0^\circ, \pm 30^\circ, \pm 60^\circ, 90^\circ]_{2(sym)}$ AS4/EPON 828-mPDA Composites	124
Figure 5.9. Comparison of Linear Regression Curves for Effective Density-Specific Heat, ρc_p , of Cured $[0^\circ]_{24}$ and Cured $[0^\circ, \pm 30^\circ, \pm 60^\circ, 90^\circ]_{2(sym)}$ AS4/EPON 828-mPDA Composites	124
Figure 5.10 Arrhenius Relationship for the First Rate Constant, c_1 in eqs. (3.4), (3.5), and (3.6): $\ln(c_1)$ versus $1/RT_a$ (R = Gas Const. (kJ/mole $^\circ$ K); T_a = Abs. Temp. ($^\circ$ K))	135
Figure 5.11 Arrhenius Relationship for the Second Rate Constant, c_2 in eqs. (3.4), (3.5), and (3.6): $\ln(c_2)$ versus $1/RT_a$ (R = Gas Const. (kJ/mole $^\circ$ K); T_a = Abs. Temp. ($^\circ$ K))	135
Figure 5.12 Residuals for a Simulated Test Case, using Input Temperature Errors with a Standard Deviation of 0.25°C , at Four Different Locations (total thickness equal to 4.5 mm)	148
Figure 5.13 Temperature Measurements and Applied Heat Flux from Four Thermocouples in the First Transient Temperature Experiment during Curing (Exp. 1)	157
Figure 5.14 Temperature Measurements and Applied Heat Flux from Six Thermocouples in the Second Transient Temperature Experiment during Curing (Exp. 2)	158
Figure 5.15 Temperatures Resulting from the Simulation of the Second Transient Experiment (3.2) using Thermal Properties Estimated from Cured Composite at 100°C	159
Figure 5.16 Residuals Associated with Three of the Five Thermocouples (TC#1, TC#2, and TC#3) Located at the Heated Surface for the Fifth	

Heat Flux

Figure 5.17 Temper

11th, 14th

as Function

Heater

Figure 5.18 Temper

12th, and 1

second expe

Midsection o

Figure 5.19 Temper

11th, and 14

first experim

Midsection o

Heat Flux Pulse in Exp. 3.3	171
Figure 5.17 Temperature Measurements at the End of the 2nd, 5th, 8th, 11th, 14th, and 17th Heat Flux Pulses in Exp. 3.3 (cured composites) as Functions of Thermocouple Location from the Midsection of the Heater	173
Figure 5.18 Temperature Measurements at the End of the 2nd, 4th, 6th, 9th, 12th, and 15th Heat Flux Pulses in Exp. 3.2 (uncured composites; second experiment) as Functions of Thermocouple Location from the Midsection of the Heater	174
Figure 5.19 Temperature Measurements at the End of the 2nd, 4th, 6th, 9th, 11th, and 14th Heat Flux Pulses in Exp. 3.1 (uncured composites; first experiment) as Functions of Thermocouple Location from the Midsection of the Heater	175

ac	Primary
ac_1	Second
ac_2	Tertiary
A, A_1, A_2	Pre-exp
b	Estima
	density
B	Amine
B^{avg}	Averag
C, C_1, C_2	rate co
C, C_1	rate co
C_p	Specif
C	Epoxi
C_1	Initial
C_{1j}	Comp
D	Diffus
D, D_1	Regres
	tempe
e	Epoxi
E, E_1, E_2	Activa
H	Heat c
h	Heat g
h	Heat g
h	Gain f
h	Total h
h	Reside

LIST OF SYMBOLS

ae_1	Primary amine
ae_2	Secondary amine
ae_3	Tertiary amine
A_1, A_2, A_3	Pre-exponential factors used in kinetic models
\mathbf{b}	Estimated parameter vector; contains thermal conductivity (W/m°C) and density-specific heat (J/m ³ °C) values
B	Amine to epoxide equivalency ratio
B^{avg}	Average of binary temperature data
c_1, c_2, c_3	rate constants (s-1) in epoxide reactions
c'_1, c'_2	rate constants (s-1) in resident epoxide reactions
c_p	Specific heat (J/kg°C)
C	Epoxide consumed in kinetic reactions during curing (moles)
C_0	Initial epoxide in kinetic reactions during curing (moles)
C_{ij}	Components of the optimal experimental design criterion
D	Diffusion constant
D_0, D_1	Regression parameters for the diffusion constant, D , as a linear function of temperature
e	Epoxide
E_1, E_2, E_3	Activation Energy Constants (kJ/mole)
H	Heat of reaction (J)
g	Heat generation (constant) (J/m ³)
g_i	Gain for i th thermocouple (°C)
H_t	Total heat of reaction (J)
HX_0	Resident hydroxyl (impurities)

HX_a	Hydr
k	Therm
k_{eff}	Effect
k_f	Therm
k_m	Therm
k, k, k_s	Regres
	peratu
L	Thickn
m	Expone
m, m_1	Regress
	ture
n	Expone
n_t	Numbe
n, n_1	Regress
	ture
P	Marchi
q	Heat flu
R	Gas cor
S	Least s
t	Time (s
t^2	Time at
t_s	Total h
t_a	Time a
	(sec)
T	Temper
T_1	Temper
T_{max}	Maximu
T_d	design
T_i	Initial t
T_c	Calcula

HX_a	Hydroxide group resulting from amine-epoxide addition reaction
k	Thermal conductivity (W/m°C)
k_{eff}	Effective thermal conductivity (W/m°C)
k_f	Thermal conductivity of fibers (W/m°C)
k_m	Thermal conductivity of matrix (W/m°C)
k_1, k_2, k_3	Regression parameters for thermal conductivity as a linear function of temperature and degree of cure
L	Thickness (m)
m	Exponential constants in kinetic models (dimensionless)
m_0, m_1	Regression parameters for the exponent, m , as a linear function of temperature
n	Exponential constants in kinetic models (dimensionless)
n_t	Number of experimental time steps
n_0, n_1	Regression parameters for the exponent, n , as a linear function of temperature
P	Marching direction in steepest descent method
q	Heat flux (W/m ²)
R	Gas constants (mole°K/kJ)
S	Least squares function
t	Time (sec)
t^n	Time at nth time step (sec)
t_0	Total heat of reaction (sec)
t_1	Time at the end of the heat flux in optimal experimental design analysis (sec)
T	Temperature (°C)
T_L	Temperature at boundary where $x = L$ (°C)
T_{max}	Maximum temperature up to time nth time step in optimal experimental design criterion analysis (°C)
T_0	Initial temperature (°C)
T	Calculated temperatures (vector) (°C)

v	Measured
v^a	Adjusted
v_f	Fiber volu
w	Weighting
x	Position of
x	Sensitivity
y	Measured
z	Zero' adj
α	Degree of
α_D	Degree of
α_p	Degree of
β	Weighting
β	Eigenval
λ	Paramete
λ	specific l
λ	Paramet
λ	mal con
ρ	Density
ρ_p	Density
ρ_p, ρ_{p^2}	Regress
ρ_{p^2}	tion of t
λ	Optimal
Γ	Matrix

Superscripts

$+$ dimens

Subscripts

T top

B bottom

V	Measured thermocouple voltage (volts)
V^a	Adjusted thermocouple voltage (volts)
V_f	Fiber volume fraction (dimensionless)
W	Weighting matrix for least squares function
x	Position along the x-axis (m)
X	Sensitivity coefficient matrix
Y	Measured temperatures (vector) (°C)
z	'Zero' adjustment for thermocouples (°C)
α	Degree of cure (dimensionless)
α_D	Degree of cure where diffusion becomes significant
α_p	Degree of cure at maximum degree of cure rate (dimensionless)
α	Weighting factor in steepest descent method
β	Eigenvalues
<u>β</u>	Parameter vector; contains thermal conductivity (W/m°C) and density-specific heat (J/m ³ °C) values
<u>β</u>[^]	Parameter vector from minimization of least squares function; contains thermal conductivity (W/m°C) and density-specific heat (J/m ³ °C) values
ρ	Density (kg/m ³)
ρc_p	Density-specific heat product (J/m ³ °C)
ρc_{p1}, ρc_{p2}, ρc_{p3}	Regression parameters for thermal conductivity as a linear function of temperature and degree of cure
Δ	Optimal experimental design criterion
∇	Matrix derivative operator

Superscripts

+ dimensionless

Subscripts

T top

B bottom

In general, a com-
tain a new material
regards to strength and
vehicle applications. In
boats were fabricated
widespread use of
materials, has only a
materials are common
especially with regard
to their generally low
use of composites with
the strength and dur-

However, the
aero-related industries
suspension components
and rudder designs
submarine designs.
has produced a number
rowing oars, bicycle
could be athlete, the

Chapter 1

Introduction

In general, a composite is simply the combination of two or more materials to obtain a new material with some improved or new characteristics, particularly with regards to strength and weight. The use of composite materials in construction and vehicle applications has been in effect since the early Egyptian days when bricks and boats were fabricated from mud fortified with reeds and chopped straw. However, the widespread use of modern day composites, which utilize new high-performance materials, has only come into being during the last 20 years. These high-performance materials are commonly associated with the aeronautics and aerospace industries, especially with regards to the military, where composites are particularly attractive due to their generally low-weight/high-strength characteristics. One of the most notable use of composites was in the design of the all-composite Voyager aircraft, which proved the strength and durability of the materials in its non-stop flight around the world.

However, the use of high-performance composites is by no means limited to the aero-related industries. The automotive industry has used composites in body and suspension components, and the boating industry has incorporated composites in hull and rudder designs. The U.S. Navy has a particular interest in composites in ship and submarine designs. Another important industry is the sporting goods industry, which has produced a multitude of composite golf clubs, tennis rackets, racket ball rackets, rowing oars, bicycles, skis, and poles for pole vaulting designed to give the athlete, or would be athlete, the extra edge to hit harder, go faster, and jump higher.

Modern day composites are made of a variety of materials. Due to the fact that they are often flaked or filled (Vins), they have a particular interest in enhancing fibers bound in them. The materials include glass, carbon, Kevlar, epoxies, polyimides, polyamides, and carbon fiber-epoxy matrix. They are classified as thermoset materials because they cure and thus bind to the substrate.

It is the application of these materials provided the motivation for the development of applied heat loads and failure. Accurate knowledge of the thermal behavior, very important in the design of the curing process, is essential to the thermal characteristics of the product which is strong and durable. The design of these thermal characteristics which maximizes performance is the key to the success of the product.

The thermal response of the material is a function of the forces which lead to the response. The responses are characterized by the composite material, namely, the addition, during the curing process, of the reactions, in which the material is the focal point of the reaction. The AS4 fibers (Hercules)

Modern day composites are formulated in a variety of ways from many different materials. Due to this variability, they are often classified as fiber, particulate, laminar, flaked or filled (Vinson and Sierakowski, 1987). The fiber-reinforced composites are of particular interest in this study. These composites are typically composed of strength enhancing fibers bound together in a relatively low density matrix material. The fibrous materials include glass, Kevlar, carbon, and boron, and the matrix materials include epoxies, polyimides, phenolics and aluminum. The focus of this study is on continuous carbon fiber-epoxy matrix composites. The epoxies used in these composites are classified as thermoset materials since both heat and pressure are required for the epoxy to cure and thus bind to the fibers.

It is the application of heat on composites both during and after curing that has provided the motivation for this study. The thermal responses of cured composites to applied heat loads induce thermal stresses, which can possibly lead to structural failure. Accurate knowledge of the thermal characteristics of the composites are, therefore, very important with regards any design application in a nonisothermal environment. The thermal response of composites is also pertinent with respect to the design of the curing cycle. In the worst case scenario, a lack of understanding of the thermal characteristics of the composite during curing could lead to an unevenly cured product which is structurally unsafe. In the best of worlds, a thorough understanding of these thermal characteristics would lead to the design of an optimal curing cycle which maximizes product quality and minimizes cost.

The thermal responses of interest in this study are the result of applied heat fluxes which lead to conductive heat transfer within the composite. These thermal responses are characterized by the intrinsic thermal properties of the particular composite material, namely the thermal conductivity and the density-specific heat product. In addition, during curing, the epoxy matrix composites of interest undergo exothermic reactions, in which the rate of heat generation is characterized by the kinetic properties of the composite. It is the determination of these thermal and kinetic properties which is the focal point of this study. The particular composite used in this study consists of AS4 fibers (Hercules Aerospace Corp.) and with an EPON 828 epoxy matrix (Shell

Chemical Comp.).
posite with a high s
only on the determin
both the analytical a
which are not neces
here.

The overall obj
imation of thermal p
during curing; and, t
tion of thermal prop
least squares functio
ments within the co
transient and both
estimated simultane
have typically meas
ments. This approa
Al-Araj, 1974; Coun
icular instance is
property values as f
thermal conductivit
heat product of cur
and fiber orientation.

The second a
This is shown to b
estimation of ther
parameters which
rate constants and
established proced
studies (Sourour a
cycle, the effort of

Chemical Comp.). This is a moderate temperature ($<150^{\circ}\text{C}$) high-performance composite with a high strength versus weight ratio. The emphasis in this study was not only on the determination of specific properties values, but also on the development of both the analytical and experimental procedures for the estimation of these properties, which are not necessarily limited in application to the specific composite investigated here.

The overall objectives of this study can be divided into three major areas: the estimation of thermal properties in cured composites; the estimation of kinetic properties during curing; and, the estimation of thermal properties during curing. In the estimation of thermal properties of cured composites, a minimization procedure involving a least squares function is employed which utilizes experimental temperature measurements within the composite. This approach is unique in that the experiments are transient and both the thermal conductivity and density-specific heat properties are estimated simultaneously. Previous studies (Lee and Taylor, 1975; Ishikawa, 1980) have typically measured these two properties in composites in independent experiments. This approach has been used, however, for homogeneous materials (Beck and Al-Araji, 1974; Courville and Beck, 1988; Farnia, 1976), and the emphasis in this particular instance is on developing an experimental design and on obtaining specific property values as functions of temperature. The specific objectives are to estimate the thermal conductivity perpendicular to the fiber axis direction and the density-specific heat product of cured AS4/EPON 828 composite materials as functions of temperature and fiber orientation.

The second area of interest is the estimation of kinetic properties during curing. This is shown to be fundamentally linked to the third overall objective relating to the estimation of thermal properties during curing. The kinetic properties are those parameters which characterize the chemical reactions during curing, and they include rate constants and activation energy constants. These properties are estimated using established procedures using differential scanning calorimetry (DSC). Unlike previous studies (Sourour and Kamal, 1976) which have only focused on the first half of the cure cycle, the effort of this study was to estimate the kinetic properties which characterize

the exothermic reaction
characterize these reactions
are assumed to follow
this case, efforts were
be used in the estimation
this area were to estimate
epoxy from DSC data
epoxy systems, and the
system.

Previous efforts
the interruption of the
measurement (Mojovic
unique because the p
viscosity and density-spe
process as functions
estimation problem is d

The proposed
study for the estimation
analysis is complicated
This estimation process
necessitated the develop
process. Due to the
aspects, the focus o
direct, rather on obtai
this case are first to
thermal conductivity
the parameter estimat
properties of cured e
epoxy system. The
appropriate experimen

the exothermic reactions throughout the entire cure cycle. The kinetic properties which characterize these reactions typically involve the determination of rate constants which are assumed to follow an Arrhenius relationship (Barton, 1985) with temperature. In this case, efforts were directed towards obtaining specific properties values which could be used in the estimation of thermal properties during curing. The specific objectives in this area were to estimate the kinetic properties associated with the curing of EPON 828 epoxy from DSC data using the various kinetic models found in the literature for similar epoxy systems, and to select the most appropriate model(s) for this particular epoxy system.

Previous efforts for the estimation of thermal properties during curing required the interruption of the curing process and/or separate experiments for each property measurement (Mojović and Mei, 1987). The focus of this investigation is new and unique because the procedures permit the thermal properties, namely thermal conductivity and density-specific heat, to be measured simultaneously throughout the curing process as functions of both temperature and completeness or degree of cure. The estimation problem is difficult in both the analytical and experimental aspects.

The proposed procedure involves the minimization techniques utilized in this study for the estimation of the thermal properties of cured composites; however, this analysis is complicated by the exothermic chemical reactions occurring during curing. This estimation procedure also required transient temperatures measurements, which necessitated the development of new experimental designs applicable during the curing process. Due to the complexity of this problem in both analytical and experimental aspects, the focus of these efforts were on the development of the estimation procedures, rather on obtaining specific property values. Therefore, the specific objectives in this case are first to develop and verify the analytical procedures for the estimation of thermal conductivity and density-specific heat during curing. This would incorporate the parameter estimation techniques utilized in this study for the estimation of thermal properties of cured composites and the results of the kinetic analysis of the EPON 828 epoxy system. The second objective involves the development and testing of an appropriate experimental design for use in recording transient temperature measurements

during curing. The

functions of tempera

during curing. The final objective is to, if possible, measure specific property values as functions of temperature and degree of cure using this experimental design.

A review of the
composite materials
estimation of therm
this area with regard
is devoted to the te
posite systems dur
to estimate rate co
niques which have
are presented in t
methods which
materials. These
with analytical so
thermal conductiv

2.1 Estimation of

The method
materials have in
techniques used
and anisotropic

Chapter 2

Literature Review

A review of the literature for the estimation of thermal and kinetic properties in composite materials is given in this chapter. In the first section, the emphasis is on the estimation of thermal properties in cured composites. There have been many studies in this area with regards to both theoretical and experimental methods. The next section is devoted to the techniques used in estimating kinetic properties of epoxy-based composite systems during curing. These methods utilize differential scanning calorimetry to estimate rate constants which characterize the curing of the composites. The techniques which have been used to estimate thermal properties during the curing process are presented in the third section. This is followed by a final section on minimization methods which have been used to estimate thermal properties in homogeneous materials. These methods provide a means of coupling experimental measurements with analytical solutions, and they allow for the simultaneous determination of both thermal conductivity and the product of density and specific heat.

2.1 Estimation of Thermal Properties of Composite Materials

The methods used for the estimation of thermal properties in cured composite materials have included both experimental and analytical techniques. A synopsis of the techniques used to estimate thermal properties in composite materials and other related anisotropic materials is first presented in Section 2.1.1. This is followed by a

review of previous
fiber-reinforced com

2.1.1 Estimation of

The problem of
anisotropic composi
aspect of importance
least two different ty
thermal properties.

been concentrated in

The first area
properties from a m
timation of thermal
in this area. Most o
ductivities of the in
known, along with
original theories by
such models for th
Hasselman and Jo
diameter and the
matrix. Ziebland (1
conductivity was ca
model for the heat
expressed mathema

$$k_{eff} =$$

where k_{eff} is the eff
nal conductivities

review of previous research devoted to the estimation of thermal properties of carbon fiber-reinforced composites, in particular.

2.1.1 Estimation of Thermal Properties of Composite and Other Anisotropic Materials

The problem of estimating thermal properties, such as thermal conductivity, in anisotropic composites is interesting and challenging in that not only is the directional aspect of importance, but also because composites, by definition, are composed of at least two different types of materials (i.e., the fiber and matrix materials), with differing thermal properties. The existing literature on this subject indicates that research has been concentrated in two different areas for the solution of this problem.

The first area is focused on the determination of the effective or overall thermal properties from a mathematical analysis of the components of the composite. The estimation of thermal conductivity, in particular, has been the main focus of the studies in this area. Most of these methods are based on the assumption that the thermal conductivities of the individual composite elements, namely the matrix and the fiber, are known, along with the void fraction of the fibers. These models are based on the original theories by Maxwell and Rayleigh (Hasselman and Johnson, 1987). Several such models for the effective thermal conductivity of composites were proposed by Hasselman and Johnson (1987). These models also required knowledge of the fiber diameter and the interfacial thermal barrier resistance between the fiber and the matrix. Ziebland (1977) presented a simpler approach in which the effective thermal conductivity was calculated using a unit-cube model with rectangular coordinates. The model for the heat flux perpendicular to the fiber length (fiber and matrix in series) is expressed mathematically as

$$k_{\text{eff}} = \frac{k_m k_f}{V_f k_m + (1 - V_f) k_f}$$

where k_{eff} is the effective thermal conductivity of the composite, k_m and k_f are the thermal conductivities of the matrix and the fiber, respectively, and V_f is the fiber volume

fraction. Ziebland
al. (1987) also used
Combining this app
a generalized expres
directions, given th
fiber axis. Similar
thermal conductivity
one and two-directio
fective thermal cond
element analysis of a
numerical method w
method with the met
posite. In this pro
component system us

The other focus
been on experimental
experimental method
involve one or two th
Ziebland (1977) desc
determined solely fro
where thermal condu
conductivity. Three
apparatus with a hea
cell with heater gua
paratus, which uses
used the later metho
composites as a func
rative apparatus simi
construction. Quasi
crossed by Ziebland f

fraction. Ziebland also included models for cross-ply and fabric laminates. James et al. (1987) also used the unit-cube approach, but with a cylindrical model for the fiber. Combining this approach with a finite difference model for heat flow within composites, a generalized expression was obtained for the effective thermal conductivities in off-axis directions, given the effective thermal conductivity parallel and perpendicular to the fiber axis. Similarly, Mottram and Taylor (1987b) developed expressions for effective thermal conductivity parallel and perpendicular to the fiber axis, which included both one and two-directional composite laminates. Han and Cosner (1981) analyzed the effective thermal conductivity of composites with different void fractions, using a finite element analysis of a unit composite cell, with heat flow perpendicular to the fibers. A numerical method was presented by Dul'nev et al. (1977) which combined Rayleigh's method with the method of grids to estimate the effective thermal conductivity of a composite. In this procedure, each block defined by a grid was analyzed as a two component system using Rayleigh's approach.

The other focus of attention for the determination of the thermal properties has been on experimental methods. In the estimation of thermal conductivity, most of these experimental methods are conducted at steady state conditions. Most of these methods involve one or two thin samples which are placed in between heated or cooled plates. Ziebland (1977) describes these methods as absolute, where thermal conductivity is determined solely from an energy balance of the steady state conditions, or relative, where thermal conductivity is determined by reference to a substance of known thermal conductivity. Three of the absolute methods mentioned by Ziebland are the flat plate apparatus with a heater guard, which uses one flat test specimen, the coaxial cylinder cell with heater guard, which uses a cylindrical test specimen, and a two-plate apparatus, which uses two test specimens and is generally preferred. Harris et al. (1982) used the latter method in estimating the thermal conductivity of Kevlar fiber-reinforced composites as a function of temperature and fiber direction. The relative methods involve apparatus similar to the two-plate apparatus, but they are more complex in their construction. Quasi-steady state experiments, using similar apparatus, were also discussed by Ziebland for materials with low thermal conductivity.

Another technique for determining thermal capacity, and thermal conductivity (1961). In this method a filament which is coated with a material of known thermal capacity response is used. The thermal diffusivity of the material is determined to reach one half of the maximum value from the maximum value determined from the method. This method was used by Beck and Schummel, Jr. et al. to determine the thermal diffusivity of matrix samples as follows:

Other methods for determining thermal properties. Beck and Schummel, Jr. et al. have used a thermal conductivity method of estimation analogous to the procedure where the thermal conductivity is determined by Springer and Tsai. This method is based on the filament and matrix material.

2.1.2 Estimation of Thermal Conductivity

Most of the problems in determining thermal conductivity of materials has been found to be the estimation of the thermal conductivity of the material.

Another technique for the experimental determination of thermal diffusivity, heat capacity, and thermal conductivity is the laser-flash method presented by Parker et al. (1961). In this method, a laser pulse is directed on a sample a few millimeters thick which is coated with carbon to prevent direct transmission of the beam, and the temperature response of the specimen at the rear surface is monitored by optical means. The thermal diffusivity is then determined from the time required for the back surface to reach one half of the maximum temperature rise, and the heat capacity is determined from the maximum temperature rise of the specimen. The thermal conductivity can be determined from the thermal diffusivity, the heat capacity, and the density. This method was used by Brennan et al. (1982) to determine the thermal conductivity and thermal diffusivity of thin amorphous silicon carbide fibers from composite and neat matrix samples as functions of temperature, and by Mottram and Taylor (1987a) to determine the thermal diffusivity of silica-phenolic composites.

Other methods have also been considered in the determination of thermal properties. Beck and Al-Araji (1974) presented a method of estimating thermal conductivity and density-specific heat independently from a single transient experiment. Schimmel, Jr. et al. (1977) presented a solution for the determination of the effective thermal conductivity of a multi-layer laminate based on an analytical solution for a two-layer composite transient system with known thermal properties of the components. A method of estimating thermal conductivity in unidirectional materials which is analogous to the problem of longitudinal shear loading of a unidirectional composite, where the thermal conductivity is analogous to the average shear moduli, was proposed by Springer and Tsai (1967). This method was compared to a thermal model in which the filament and matrix were assumed to be arranged in series.

2.1.2 Estimation of Thermal Properties of Cured Carbon Fiber Composites

Most of the previous research on the estimation of thermal properties, such as thermal conductivity and thermal diffusivity, of carbon fiber-reinforced composite materials has been for cured composites. The methods used in the determination of

these properties included both exper

The laser-flas

along with an abso

thermal diffusivity a

505) and graphite

thermal diffusivities

conductivities estim

igated the effects

orientation, and spec

composites using th

followed by the fiber

behavior of the compo

to determine thermal

posites as a function

(1987b), and the the

in different fiber dir

Ishikawa (198

composite systems

on the solution of t

Springer and Tsai

knowledge of the th

analytical results w

infrared radiation m

2.2 Estimation of

The kinetic P
and activation ene
composite systems

these properties included some of the techniques described in Section 2.1.1., and they included both experimental and analytical aspects.

The laser-flash method (Parker et al. 1961) was used by Lee and Taylor (1975) along with an absolute method, which required cylindrical samples, to determine the thermal diffusivity and the effective thermal conductivity of carbon fiber-reinforced (PX 505) and graphite fiber-reinforced (Morganite II and Thornal 50 S) composites. The thermal diffusivities of the graphite fibers were determined from the effective thermal conductivities estimated using the absolute method. Taylor and Kelsic (1986) investigated the effects of fiber fraction, fiber/matrix thermal conductivity ratio, fiber orientation, and specimen length on thermal diffusivity of unidirectional fiber-reinforced composites using the laser-flash technique. They found that the conductivity ratio, followed by the fiber volume fraction were the major factors affecting the thermal behavior of the composite. Mottram and Taylor (1987a) also used the laser-flash method to determine thermal diffusivity of woven and unwoven carbon fiber-phenolic resin composites as a function of temperature. This work was continued (Mottram and Taylor (1987b), and the thermal conductivity of the carbon-phenolic composite was determined in different fiber directions using the Maxwell-Rayleigh approach.

Ishikawa (1980) analytically determined the thermal conductivity of carbon/epoxy composite systems under steady-state conditions using a Fourier series analysis based on the solution of the longitudinal shear problem. This is the same approach used by Springer and Tsai (1967). This solution was two dimensional, and it required knowledge of the thermal conductivity of the matrix and the fiber volume fraction. The analytical results were compared with experimental results using a technique called the infrared radiation method.

2.2 Estimation of Kinetics Parameters in Epoxy-Based Systems

The kinetic parameters of importance in this section include the rate constants and activation energy constants which characterize the curing of amine-epoxy based composite systems. A discussion of the cure kinetics of amine-epoxy systems is first

presented, followed
vious studies in the
given these studies
calorimetry. Finally,
composite systems

2.2.1 Kinetics of A

The epoxy sys
which the initial re
stages, the reaction
searchers have use
describe the kinetics

Most of the re
based on the mecha
rate determining ste
epoxide and hydroxy
is a two tiered proc
epoxide reactions.
additives), HX_o :

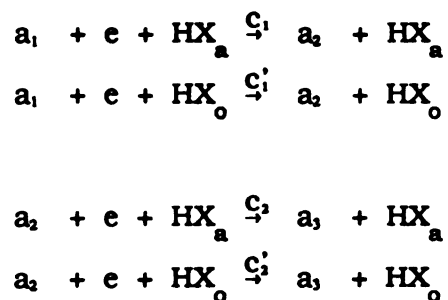
in these reactions.
epoxide, and the C_1
following overall kin

presented, followed by review of differential scanning calorimetry. A summary of previous studies in the estimation of kinetic parameters in amine-epoxy systems is then given; these studies all utilize experimental results obtained using differential scanning calorimetry. Finally, a brief discussion is included on the use of neat vs. reinforced composite systems with regards to the estimation of kinetic parameters.

2.2.1 Kinetics of Amine-Epoxy Systems

The epoxy system of interest in this investigation is an amine-epoxy system in which the initial reaction is accelerated due to autocatalyzation, while in the latter stages, the reaction is diffusion controlled. Due to the complexity of the system, researchers have used relatively simple models over limited ranges of conversion to describe the kinetics of the reactions.

Most of the reaction models for the initial phase of the amine-epoxy cure are based on the mechanisms proposed by Schechter et al. (1956) and Smith (1961). The rate determining step of the reaction scheme is assumed to be the reaction of amine, epoxide and hydroxyl (or other proton-donor species, HX) (Barton, 1985). This scheme is a two tiered process, which involves reactions of the hydroxyls formed in the amine-epoxide reactions, HX_a , and the resident hydroxyls in the system (impurities or additives), HX_o :



In these reactions, a_1 , a_2 , and a_3 are primary, secondary, and tertiary amines, e is the epoxide, and the c_1 and c_1' values ($i = 1, 2$) are the reaction rates. From this scheme, the following overall kinetic equation was derived (Barton, 1985):

$$\frac{dC}{dt} =$$

where C is the epoxy
tions of HX_0 and th
primary and second

2.2.2 Differential Scanning

Differential scanning

Committee of the Inter-

nique in which the

are subjected to a

DSC has proven to

such as those occur

The underlying assu

the reacting substan

dC/dt in eq. 2.1).

There are two

compensation mode wh

heaters and platinum

sample and referen

resistance with ex

Scanning Calorimet

consists of a sample

enclosed platform i

section and the heat

within the sample a

of milligrams) and

sample pan, and th

platform, and the r

$$\frac{dC}{dt} = (c_1 C_0 + c_2 C)(e_0 - C)(a_1 + a_2) \quad (2.1)$$

where C is the epoxide consumed at a given time, t ; C_0 and e_0 are the initial concentrations of HX_0 and the epoxide, respectively; and, a_1 and a_2 are the concentrations of the primary and secondary amines.

2.2.2 Differential Scanning Calorimetry (DSC)

Differential scanning calorimetry (DSC) has been defined by the Nomenclature Committee of the International Confederation for Thermal Analysis (ICTA) as a technique in which the difference in energy inputs into a substance and reference material are subjected to a controlled temperature program (Barton, 1985). The technique of DSC has proven to be a useful method for the investigation of exothermic reactions, such as those occurring during the curing of epoxy resins (Fava, 1968; Rabek, 1980). The underlying assumption in DSC kinetics is that the difference in heat flow between the reacting substance and the reference material is proportional to the reaction rate (dC/dt in eq. 2.1).

There are two types of DSC instruments. The first operates under a power compensation mode which utilizes separate sample and reference holders with individual heaters and platinum thermometers. The second type operates in a heat flux mode; the sample and reference are in separate containers connected by a controlled thermal resistance with external thermocouples. The DuPont Instruments 910 Differential Scanning Calorimeter cell, used in this study, operates in the heat flux mode. This cell consists of a sample chamber in which the empty reference and sample pans rest on an enclosed platform instrumented with thermocouples. In using both the power compensation and the heat flux DSC instruments, it is assumed that the temperature gradients within the sample are very small. This requires the use of small samples (on the order of milligrams) and the assurance of good thermal contact between the sample and the sample pan, and the same degree of thermal contact between the sample pan and the platform, and the reference pan and the platform.

Two experimen-
kinetic modeling o
are conducted at d
By assuming an a
temperature studie
perature can be d
which a sample is h
times referred to as
In this case, both th
proportional to the r
been limited to very
nth order kinetics).

2.2.3 Cure Kinetics

Several resear-
sants of a bisphen
epoxy system, which
ains two rate cons
The first rate const
of the reaction is e
are present, c_1 is
generalized kinetic

$$\frac{d\alpha}{dt} =$$

where, α is the fr
(1979) used this r
con rate data from
 $n = 2$). An Arrhe
perature:

Two experimental methods involving the use of DSC are commonly used in the kinetic modeling of exothermic systems. In the first instance, isothermal experiments are conducted at different temperatures, and the rate of heat flow is recorded with time. By assuming an appropriate kinetic model, rate constants can be determined for each temperature studied, and then the relationship between these rate constants and temperature can be determined. The second method involves dynamic experiments in which a sample is heated at a linear rate throughout the curing process. This is sometimes referred to as the Borchardt and Daniels method (Borchardt and Daniels, 1957). In this case, both the time and temperature dependence of the conversion rate (which is proportional to the reaction rate) may be found simultaneously. Use of this method has been limited to very simple kinetic models in which only one rate constant is found (i.e., nth order kinetics).

2.2.3 Cure Kinetics using DSC

Several researchers have used a generalized form of eq. (2.1) to identify rate constants of a bisphenol-A-diglycidylether (BADGE) and meta-phenylenediamine (mPDA) epoxy system, which is similar to the epoxy investigated here. The kinetic model contains two rate constants, consistent with the mechanisms presented by Barton (1985). The first rate constant, c_1 , represents nth order kinetics, while the autocatalytic nature of the reaction is evident by the second rate constant, c_2 . Therefore, if no impurities are present, c_1 is equal to zero, and the reaction is completely autocatalyzed. The generalized kinetic equation is

$$\frac{d\alpha}{dt} = (c_1 + c_2 \alpha^m)(1 - \alpha)^n \quad (2.2)$$

where, α is the fractional conversion, and m and n are constants. Ryan and Dutta (1979) used this model to determine the rate constants c_1 and c_2 from maximum reaction rate data from isothermal DSC experiments, assuming a second order reaction ($m + n = 2$). An Arrhenius relationship was assumed between the rate constants and temperature:

$$c_1 =$$

This relationship w

diffusion controlled

Equation (2.4)

similar epoxy system

in an tetraglycidyl-

used this model in

in studying curing

(1987) used this m

of $\alpha > 58\%$. Hagn

in glass fiber-BAD

In an earlier

$$\frac{d\alpha}{dt}$$

where B is the an

using isothermal

assuming an Arr

or 50%: at that t

tion for conversio

in studying Herc

for $\alpha > 30\%$.

Prime (19

BADGE/MPDA

DSC experiment

model, and nth o

$$\frac{d\alpha}{dt}$$

$$c_i = A_i \exp(-E_i/RT) \quad i = 1, 2 \quad (2.3)$$

This relationship was shown to follow conversion rates up to 90%, with no evidence of a diffusion controlled reaction.

Equation (2.2) was also used by several researchers to describe curing in other similar epoxy systems. Mijović et al. (1984) used this model to determine rate constants in an tetraglycidyl-4,4'-diminodiphenylmethane epoxy system, and Moroni et al. (1986) used this model in studying BADGE and 1,4 butanedioldiglycidylether resin mixtures. In studying curing kinetics in BADGE/ethylenediamine epoxies, Chern and Poehlein (1987) used this model and found that diffusion controlled the reaction rates for values of $\alpha > 58\%$. Hagnauer et al. (1983) also used this model to investigate the cure kinetics in glass fiber-BADGE epoxy systems.

In an earlier study, Sourour and Kamal (1976) assumed $m = n = 1$ and used

$$\frac{d\alpha}{dt} = (c_1 + c_2 \alpha)(1 - \alpha)(B - \alpha) \quad (2.4)$$

where B is the amine to epoxide equivalency ratio. The rate constants were determined using isothermal DSC experiments, and the activation energy constants were found assuming an Arrhenius relationship. This relationship followed for values of α up to 40 or 50%; at that time, the reaction rate decreased, indicating a diffusion controlled reaction for conversion rates greater than 50%. Likewise, Lee et al. (1982) used this model in studying Hercules 3501-6 resin and found that the reaction was diffusion controlled for $\alpha > 30\%$.

Prime (1973) implemented a simpler equation to describe curing in the BADGE/mPDA system incorporating both isothermal DSC experiments and dynamic DSC experiments which utilized the Borchardt and Daniels (1957) method. In this model, and nth order reaction is assumed with no autocatalyzation (c_2 is zero):

$$\frac{d\alpha}{dt} = c_1 (1 - \alpha)^n \quad (2.5)$$

Deviations from the
was assumed to be
investigation of the
model to investigate

Very few mod
analysis. Lee et al
than 50% in their s

$$\frac{da}{dt} =$$

where, c_1 was a
(1968) presented
an exponential te

$$\frac{da}{dt}$$

in this equation
assumed to follow

2.2.4 Cure Kinetics

There have been
studies reinforced
esters in a
sulphone (DDE)
only a very small
compared to the
found that the
the time required
differences
exist.

Deviations from this model were found for higher conversion rates, where the reaction was assumed to be diffusion controlled. Acitelli, et al. (1971) found similar results in an investigation of the cure of BADGE/mPDA epoxy. Pappalardo (1977) also used this model to investigate glass reinforced-BADGE epoxy prepreps.

Very few models have been developed which incorporate diffusion in the kinetic analysis. Lee et al. (1982) presented the following equation for extent of cure greater than 50% in their study of Hercules 3501-6 resin:

$$\frac{d\alpha}{dt} = c_1 (1 - \alpha) \quad (2.6)$$

where, c_1 was assumed to follow an Arrhenius relationship (eq. 2.3). Hawley et al. (1988) presented another model for conversion rates greater than 50%, which included an exponential term indicative of the diffusion phenomenon. This model is

$$\frac{d\alpha}{dt} = c_1 (1 - \alpha)e^{-D\alpha} \quad (2.7)$$

In this equation, D is a diffusion coefficient, and once again, the rate constant, c_1 , was assumed to follow an Arrhenius relationship.

2.2.4 Cure Kinetics of Neat vs. Carbon Fiber Reinforced Epoxy Systems

There have been a few studies on the comparison of the cure kinetics of neat versus reinforced epoxy systems. Mijović and Wang (1989) studied the effects of carbon fibers in a tetra-*N*-glycidyl-diaminodiphenylmethane (TGDDM)/dianisodiphenylsulphone (DDS) amine-epoxy system, and found that the presence of carbon fibers had only a very small initial effect on the kinetics of cure. In a related study, Mijović (1986) compared the cure kinetics of neat versus glass reinforced TGDDM/DDS epoxy. It was found that in the reinforced system, the reaction rate constants were slightly lower, and the time required to reach the maximum reaction rate was slightly longer. These minor differences were assumed to be the result of restricted mobility due to the reinforcement.

2.3 Estimation of Thermal Properties in Carbon/Epoxy Composite Systems during Curing

The estimation of thermal properties in composite materials during curing is complex due to the exothermic reactions which occur as the epoxy matrix cures. In order to estimate thermal properties during curing, the curing process itself must be first understood with regards to the heat transfer process. The mathematical models used to simulate heat transfer during the curing process are first reviewed. This is followed by a review of the previous work in the estimation of thermal properties during curing, which to date is quite limited.

2.3.1 Mathematical Models to Simulate Heat Transfer in Carbon/Epoxy Composite Materials during Curing

Several researchers have developed mathematical models to simulate heat transfer in cured composite materials (e.g. Golovchan and Artemenko, 1987), but few have developed models to describe heat transfer in composites during the curing process. Loos and Springer (1983) developed models to describe the curing process of composites constructed from continuous fiber-reinforced, thermosetting resin matrix prepreg materials. A computer program was developed which provides the temperature distribution, degree of cure of the resin, the resin viscosity inside the composite, the void sizes, and the residual stress distribution given a specific process for a flat plate composite. In the mathematical model for temperature, a term was added for the heat generated by chemical reactions which was proportional to the rate of degree of cure.

More commonly, researchers have focused on modelling another process which is mathematically related to the curing process, namely decomposition. Both processes have added terms in the energy equation which are proportional to the chemical reaction rate for the process (curing or decomposition). Tant et al. (1985) developed and tested a mathematical model including a decomposition term for the thermochemical expansion of polymer composites during pyrolysis. Henderson et al. (1985) developed a

model for the ther
tion assuming on
decomposition. U
and Wiecek (1987)
pansion. Griffis
response of carbo
decomposition.

2.3.2 Estimation of

While there
composites, there
properties of compo

Mijović and
conductivity of TG
paratus, a very th
plates, allowing fo
thickness of the sa
different isotherma
determined the de
posite during curi
temperatures for c
sny of the partial
column. The heat
tial scanning calo
substance of know

2.4 Minimization

One means
the function, such

model for the thermal response of a polymer composite material undergoing decomposition assuming one dimensional heat transfer and n th order kinetics for the rate of decomposition. Using a similar approach, Boyer and Thomas (1985) and Henderson and Wiecek (1987) investigated charring in composites in terms of thermochemical expansion. Griffis et al. (1981) developed a finite difference model for the thermal response of carbon epoxy composite subject to rapid heating, including the effects of decomposition.

2.3.2 Estimation of Thermal Properties in Composites during Curing

While there have been many studies on the estimation of thermal properties on composites, there have been relatively few studies on the estimation of thermal properties of composite materials during curing.

Mijović and Mei (1987) designed an apparatus for the measurement of thermal conductivity of TGDDM/DDS epoxy carbon fiber composite materials. Using this apparatus, a very thin section (1 mm) composite sample was cured between two parallel plates, allowing for the assumption of a linear temperature distribution across the thickness of the sample. Thermal conductivity was determined as a function of time for different isothermal curing temperatures. In a related study, Mijović and Wang (1988) determined the density and heat capacity (not thermal conductivity) of the same composite during curing. To measure density, samples were cured isothermally at different temperatures for different times and then quenched to prevent further curing. The density of the partially cured samples was then determined using a density gradient column. The heat capacity of the samples during curing was measured using differential scanning calorimetry (DSC). In this procedure, the reference DSC pan contains a substance of known specific heat (DuPont Company Instrument Systems, 1985).

2.4 Minimization Methods used for the Estimation of Thermal Properties

One means of estimating thermal properties involves the minimization of an objective function, such as a least squares function. This is a powerful estimation method,

but it has been
materials. There
mainly used meth
conjugate gradien
ing the appropriat
estimated. A brief

2.4.1 The Gauss Method

The Gauss method
Arnold (1977) desc
minima which are
the general region of

In this method
known parameters
Least squares func

$$S = \sum_{i=1}^n (y_i - \hat{y}_i)^2$$

where the vector \mathbf{y} of
or \mathbf{T} contained term
equation for the sys
this analysis that the
derivatives are bound

When the deriv
true minimum of the
minimizing $T(\hat{\beta})$ and the
 $\sum_{i=1}^n T'(\hat{\beta})^T$, which is de
First, $\mathbf{X}(\hat{\beta})$ is replaced
and secondly, $T(\hat{\beta})$ is

but it has been primarily used in the estimation of thermal properties in isotropic materials. There are several different minimization methods; three of the more commonly used methods are the Gauss method, the steepest descent method, and the conjugate gradient method. In each case, the objective function is minimized by selecting the appropriate direction and step size for perturbations in the parameters being estimated. A brief discussion of each of these methods is now presented.

2.4.1 The Gauss Method

The Gauss method is one of the more popular minimization methods. Beck and Arnold (1977) describe this method as being relatively simple and effective for seeking minima which are reasonably well-defined, assuming that the initial estimates are in the general region of the minimum.

In this method, a least squares function is minimized with respect to the unknown parameters (thermal properties) and the resulting expression is set equal to zero. A least squares function given by Beck and Arnold (1977) is

$$S = [\mathbf{Y} - \mathbf{T}(\underline{\beta})]^T \mathbf{W} [\mathbf{Y} - \mathbf{T}(\underline{\beta})] \quad (2.8)$$

where the vector \mathbf{Y} contains measured temperatures, $\underline{\beta}$ is the parameter vector, the vector \mathbf{T} contained temperatures as a function of $\underline{\beta}$, calculated from the appropriate energy equation for the system being studied, and \mathbf{W} is a weighting matrix. It is assumed in this analysis that the first derivatives of \mathbf{T} are continuous in $\underline{\beta}$ and that the higher derivatives are bounded.

When the derivative of the least squares function is set equal to zero, $\underline{\beta} = \hat{\underline{\beta}}$, the true minimum of the parameters. This minimization procedure results in terms containing $\mathbf{T}(\hat{\underline{\beta}})$ and the derivatives of $\mathbf{T}(\underline{\beta})$ with respect to the parameters in $\underline{\beta}$, namely, $[\nabla_{\underline{\beta}} \mathbf{T}^T(\hat{\underline{\beta}})]^T$, which is defined as $\mathbf{X}(\hat{\underline{\beta}})$; In the Gauss method, two approximations are made. First, $\mathbf{X}(\hat{\underline{\beta}})$ is replaced by $\mathbf{X}(\mathbf{b})$, where the \mathbf{b} vector contains the estimated parameters, and secondly, $\mathbf{T}(\hat{\underline{\beta}})$ is approximated by the first two terms of a Taylors series about \mathbf{b} .

These approxima

needed, given an

Beck (1966)

specific heat of n

used this method

2024-T351 alumin

2.4.2 The Steepest

The steepest

problem (Huang and

gradient of the obje

$$p^{(k)} =$$

and the magnitude

$$g^{(k+1)}$$

where $g^{(k)}$ is a weigh

$$g^{(k)} =$$

where $||\cdot||$ denotes

$$||f|| =$$

The superscript k , e

These approximations result in a linear equation in $\hat{\beta}$ which can be solved, iteratively if needed, given an initial estimate of the parameters in b .

Beck (1966) used this method in estimating the thermal conductivity and density-specific heat of nickel from transient temperature measurements, and Farnia (1976) used this method in estimating time and temperature dependent thermal properties of 2024-T351 aluminum alloy.

2.4.2 The Steepest Descent Method

The steepest descent method is an alternate approach to the minimization problem (Huag and Arora, 1979). Here, the marching direction is equal to the negative gradient of the objective or least squares function (Lamm, 1989)

$$P^{(k)} = -\nabla_{\beta} S(\beta^n) \quad (2.9)$$

and the magnitude of the change in β in is found from

$$\beta^{(k+1)} = \beta^{(k)} + \alpha^{(k)} P^{(k)} \quad (2.10)$$

where $\alpha^{(k)}$ is a weighting factor such that

$$\alpha^{(k)} = ||P^{(k)}||^2 / ||\partial T / \partial \beta||^2 \quad (2.11)$$

where $||\cdot||$ denotes the norm for a vector, f , with p components; it is defined by

$$||f|| = \left(\sum_{k=1}^p f_k^2 \right)^{1/2}$$

The superscript k , eq. (2.9), (2.10), and (2.11) indicates that this is an iterative process.

2.4.3 The Conjugate

The conjugate gradient method has been used to solve the problem (1981, and Tu, 1981, and Kerov (1981) proposed problems, and (1979) also used the thermal conductivity. In this method, the eigenvalues are found using an

$$p^{(k)} =$$

The magnitude of the

2.4.4 Methods of Derivatives

The minimization of the matrix derivative of the unknown parameters (or elements) in the direct method, and the differentiation, and the governing equations are solved analytically or numerically. The temperature derivative of the eigenvalues are discussed.

The adjoint method is the solution of the problem (1987). This method is used to solve the governing set of equations.

2.4.3 The Conjugate Gradient Method

The conjugate gradient method is similar to the steepest descent method, and it has been used to solve both inverse heat conduction problems (Alifanov and Kerov, 1981, and Tu, 1988) and optimal design problems (Huang and Arora, 1979). Alifanov and Kerov (1981) described the method as having good characteristics for solving ill-posed problems, compared with the method of steepest descent. Alifanov and Mikhailov (1979) also used the conjugate gradient method in the solution of the nonlinear inverse thermal conductivity problem.

In this method, the marching directions, $P(\beta)$, for the unknown parameters in β are found using an iterative sequence of the form (Huang and Arora, 1979)

$$P^{(k)} = P^{(k-1)} - \nabla_{\beta} S(\beta^n) \quad (2.12)$$

The magnitude of the change in $\beta^{(k)}$ is again found from eq. (2.10).

2.4.4 Methods of Determining the Matrix Derivatives

The minimization methods mentioned above involve the determination of the matrix derivative of the least squares function, S , or the temperature, T , with respect to the unknown parameters in β . These derivatives can be found directly, by using finite differences (or elements), or by using the adjoint method (Tu, 1988).

In the direct method, the matrix derivative of S is carried out through matrix differentiation, and the derivatives for T are found by differentiating the appropriate governing equations used to solve for temperature by β , and solving the resulting equation analytically or numerically. If finite differences are used to determine the temperature derivative, a simple forward difference expression can be used. These techniques are discussed in detail by Beck and Arnold (1977).

The adjoint method has been used in design analysis (Tortorelli et al., 1989) and in the solution of the inverse heat conduction problems (Alifanov and Rumyantsev, 1987). This method involves the solution of an adjoining set of equations, in addition to the governing set of equations. These adjoining equations or adjoint equations, as they

are sometimes ca

initial condition,

backwards in time

where temperature

are sometimes called, are solved backwards in time; that is, instead of requiring an initial condition, a terminal condition is required, and the adjoint solution marches backwards in time. Interface conditions, which guarantee continuity at the interfaces where temperature measurements are made, are also included in the adjoint equations.

Chapter 3

Theoretical Considerations

In this chapter, the theoretical development of the analysis used in estimating thermal and kinetic properties of continuous carbon-fiber/epoxy-matrix composite materials is presented. These materials are orthogonal due to the presence of the fibers, resulting in more than one component of thermal conductivity. Due to the complexity of this problem, this study is limited to the estimation of the thermal conductivity perpendicular to the fiber axis. The thermal properties estimated here are effective properties of the composite, and not of the individual fiber and matrix components.

In the first section of this chapter, the techniques used to estimate the thermal properties of cured composite specimens as functions of temperature are discussed. These techniques incorporate the Gauss minimization method (Section 3.4.1). The second section is devoted to theoretical considerations used in the estimation of kinetic properties which characterize the chemical reactions occurring during the curing process. The theoretical methods used in estimating thermal properties as functions of temperature and extent of cure during curing are outlined in the following section. These methods incorporate the techniques discussed in the first section and the results of the analysis presented in the second section. A final section is presented on the development of an optimum design criterion to maximize sensitivity in the estimation of the thermal properties.

3.1 Estimation

The direct p
heat transfer thro
estimation of the
problem is first de
thermal properties

3.1.1 Heat Conduc

One dimensi
fiber/amine-epoxy
imposed heat flux o
at the other surface

$$\frac{\partial}{\partial x} \left(k(T) \frac{\partial T}{\partial x} \right) =$$

with the boundary c

$$-k(T) \frac{\partial T}{\partial x}$$

$$T = T_L$$

and the initial condit

$$T = T_0$$

where x is the direct
thickness of the plate
conductivity of the co
the effective thermal

3.1 Estimation of Thermal Properties in Cured Composite Materials

The direct problem of determining the temperature field resulting from conduction heat transfer through a composite specimen is inherent in the procedure used for the estimation of the thermal properties of composite materials. In this section, the direct problem is first defined, and then the solution procedure used for the estimation of the thermal properties is discussed.

3.1.1 Heat Conduction in Cured Carbon-Fiber Reinforced Composites

One dimensional heat conduction was considered through a cured carbon-fiber / amine-epoxy composite flat plate. For the case where heat conduction due to an imposed heat flux on one surface is perpendicular to the fiber axis and the temperature at the other surface is known, the system can be expressed mathematically as

$$\frac{\partial}{\partial x} \left[k(T) \frac{\partial T}{\partial x} \right] = \rho c_p(T) \frac{\partial T}{\partial t} \quad 0 < x < L; \quad t > 0 \quad (3.1a)$$

with the boundary conditions,

$$-k(T) \frac{\partial T}{\partial x} = q(t) \quad x = 0; \quad t > 0 \quad (3.1b)$$

$$T = T_L(t) \quad x = L; \quad t > 0 \quad (3.1c)$$

and the initial condition,

$$T = T_0(x) \quad 0 \leq x \leq L; \quad t = 0 \quad (3.1d)$$

where x is the direction perpendicular to the fibers through the thickness, and L is the thickness of the plate. In this case, the thermal conductivity, k , is the effective thermal conductivity of the composite perpendicular to the fiber axis. It was assumed that both the effective thermal conductivity and the effective density specific heat product, ρc_p ,

were functions of
tions were known
of position.

The problem
ture distribution
properties, and th
described here is
in following section.

3.1.2 Estimation of

One method
imization method.
described in Section
composite specimen
which can be expressed

$$S = \sum$$

where the \mathbf{Y} vector
calculated temperature
thermal conductivity
conditions, the calculation

In the Gauss method
eq. (3.2) is minimized

$$\nabla_{\rho} S = 0$$

where the sensitivity
remains the estimated
using an iterative scheme

were functions of temperature; the heat flux, q , and temperature, T_L , boundary conditions were known functions of time; and, the initial condition, T_0 , was a known function of position.

The problem described in eqs. (3.1a-d) can be solved numerically for the temperature distribution using the Crank-Nicolson finite difference method, given the thermal properties, and the initial and boundary conditions. The solution of the direct problem described here is inherent in the estimation of the thermal properties discussed in the following section.

3.1.2 Estimation of Thermal Properties

One method of estimating thermal properties involves the use of the Gauss minimization method. This method requires the solution of the temperature distribution as described in Section 3.1.1 and experimental temperature measurements within the composite specimen. The estimation method is based on a least squares function, S , which can be expressed mathematically as (Beck and Arnold, 1977)

$$S = \sum [\mathbf{Y} - \mathbf{T}(\mathbf{b})]^T [\mathbf{Y} - \mathbf{T}(\mathbf{b})] \quad (3.2)$$

where the \mathbf{Y} vector contains the measured temperature values, the \mathbf{T} vector contains calculated temperature values, and the vector \mathbf{b} contains the 'true' parameter values of thermal conductivity and density-specific heat. Given the appropriate experimental conditions, the calculated temperatures can be found from the solution of eqs. (3.1a-d).

In the Gauss method, as discussed in Section 3.4.1, the least squares function in eq. (3.2) is minimized with respect to \mathbf{b} resulting in

$$\nabla_{\mathbf{b}} S = 2[-\mathbf{X}(\mathbf{b})][\mathbf{Y} - \mathbf{T}(\mathbf{b})] = 0 \quad (3.3a)$$

where the sensitivity coefficient matrix, $\mathbf{X}(\mathbf{b})$ is defined as $[\nabla_{\mathbf{b}} \mathbf{T}^T(\mathbf{b})]^T$, and the vector \mathbf{b} contains the estimated parameter values. This equation can be rearranged to solve for \mathbf{b} using an iterative scheme (Beck and Arnold, 1977), where

In this equation,
previous iteration
tains values of ten
found using a for
parameters is great
would be obtained
eq. (3.3b).)

An existing d
ture, PROPID (Be
carbon/epoxy com
estimation (Beck a
measurement) time
additional data on t
perimental design.
change in the para
effect the parameter

This program v
pendicular to the
m/epoxy composites
trained from exper
perimental procedure
properties at the diffe
ween the thermal pro

12 Estimation of KI

In order to estim
exothermic reaction

$$\mathbf{b}^{(i+1)} = \mathbf{b}^{(i)} + (\mathbf{X}^T \mathbf{X})^{-1} [\mathbf{X}^T (\mathbf{Y} - \mathbf{T}^{(i)})] \quad (3.3b)$$

In this equation, i indicates the iteration number, $\mathbf{b}^{(i)}$ contains the parameters at the previous iteration, $\mathbf{b}^{(i+1)}$ contains the new estimates for the parameters, and $\mathbf{T}^{(i)}$ contains values of temperature calculated from $\mathbf{b}^{(i)}$. The sensitivity coefficients in $\mathbf{X}^{(i)}$ are found using a forward difference approximation for $\mathbf{X}(\mathbf{b})$ about $\mathbf{b}^{(i)}$. (If the number of parameters is greater than about three, the solution of the normal equations, eq. (3.3a), would be obtained by solving eq. (3.3a) directly rather than using the inverse implied in eq. (3.3b).)

An existing one dimensional parameter estimation program based on this procedure, *PROP1D* (Beck, 1987), was used in the estimation of thermal properties in carbon/epoxy composite materials. This program utilizes the concept of sequential estimation (Beck and Arnold, 1977), in which the parameters are evaluated at each (measurement) time step. This has one advantage in that one can observe the effects of additional data on the estimates of the parameters to evaluate the adequacy of the experimental design. Ideally, at the conclusion of an experiment, there should be no change in the parameter estimates with time; that is, any additional data would not effect the parameter estimates.

This program was used specifically to estimate the effective thermal conductivity perpendicular to the fiber axis and the effective density-specific heat of cured carbon/epoxy composites at different temperatures. The measured temperatures, \mathbf{Y} , were obtained from experiments conducted at different temperatures as described in the experimental procedures in Chapter 4. The resulting estimates of these effective thermal properties at the different temperatures were then used to determine relationships between the thermal properties and temperature.

3.2 Estimation of Kinetic Parameters

In order to estimate thermal properties during curing, the heat generation due to the exothermic reaction of the epoxy must first be characterized. This analysis is based

on the assumption
rate, thus enabling
kinetic parameters
process, several
separated into two
cure less than 50%
greater than 50%).

12.1 Reaction Kinetics

The kinetic
system are present

$$\frac{d\alpha}{dt} =$$

$$\frac{d\alpha}{dt} =$$

$$\frac{d\alpha}{dt} =$$

In all cases, the rate
temperature:

$$c_i = A$$

where, in this case,

An autocatalytic
0.5), and an nth order
putting the exponential
implicitly assumed the
activation energy con
two exponents, m and

on the assumption that the heat of reaction rate is proportional to the degree of cure rate, thus enabling the use of differential scanning calorimetry (DSC) in determining the kinetic parameters which characterize the reaction. Due to the complexity of the curing process, several different kinetic models were investigated, these models can be separated into two groups: 1. limiting reaction rates due to autocatalyzation (degree of cure less than 50%); and, 2. limiting reaction rates due to diffusion (degree of cure greater than 50%).

3.2.1 Reaction Kinetics for Degree of Cure < 50%

The kinetic models investigated for the initial curing phase of an amine-epoxy system are presented in eqs. (2.2), (2.4), and (2.5), and are again listed below.

$$\frac{d\alpha}{dt} = (c_1 + c_2 \alpha^m)(1 - \alpha)^n \quad m + n = 2 \quad (3.4)$$

$$\frac{d\alpha}{dt} = (c_1 + c_2 \alpha)(1 - \alpha)(B - \alpha) \quad (3.5)$$

$$\frac{d\alpha}{dt} = c_1 (1 - \alpha)^n \quad (3.6)$$

In all cases, the rate constants, c_i , are assumed to follow an Arrhenius relationship with temperature:

$$c_i = A_i \exp(-E_i/R(T+273.15)) \quad i = 1, 2 \quad (3.7)$$

where, in this case, the temperature, T , is °C.

An autocatalyzed reaction was assumed in the models given by eqs. (3.4) and (3.5), and an n th order reaction was assumed in the model shown in eq. (3.6). By requiring the exponents m and n in eq. (3.4) to sum to two, a second order reaction is implicitly assumed in this model. The parameters to be estimated in each case are the activation energy constants, E_i , and the pre-exponential factors, A_i , and in addition, the two exponents, m and n , are to be determined for the models shown in eqs. (3.4) and

(3.6), respectively

typically measure

temperatures.

The underlying

the cumulative he

discussed above r

time (assuming a

data as follows:

$$\alpha =$$

where $H(t)$ is the

ments, and H_t is th

$$H_t =$$

where t_c is the to

temperature is incre

using this formula

perature, even the

achieved.

Kinetic param

ferent methods. In

$m + n = 2$, and the

method to be descr

constant, c_1 , was f

rate of cure, α , is as

(3.6), respectively. In the analysis of each of these models, the heat of reaction data are typically measured using differential scanning calorimetry (DSC) for several isothermal temperatures.

The underlying assumption in utilizing the DSC data for kinetic analysis, is that the cumulative heat of reaction is proportional to the reaction rate. The kinetic models discussed above require the fractional conversion (or degree of cure), α , as a function of time (assuming an isothermal cure), which can be obtained from the heat of reaction data as follows:

$$\alpha = \frac{\int_0^t H(t) dt}{H_t} \quad (3.8)$$

where $H(t)$ is the heat of reaction at time, t , measured during isothermal DSC experiments, and H_t is the total heat of reaction from dynamic DSC experiments, given by

$$H_t = \int_0^{t_0} H(t) dt \quad (3.9)$$

where t_0 is the total curing time. Dynamic DSC experiments are those in which the temperature is increased linearly with time throughout the entire cure. It is assumed in using this formulation that the total heat of reaction is independent of the curing temperature, even though at lower curing temperatures complete curing may not be achieved.

Kinetic parameters were determined for the first model (eq. 3.4) using two different methods. In both procedures, a second order reaction was assumed, so that $m + n = 2$, and the parameters estimated were A_1 , A_2 , E_1 , E_2 , and m . The first method to be described is that used by Ryan and Dutta (1979). In this case, the rate constant, c_1 , was found by the initial degree of cure data; at the initial time, t , the degree of cure, α , is assumed to be equal to zero, and eq. (3.4) reduces to

$$\frac{d\alpha}{dt}$$

The second
curve at the maximum

$$\frac{d^2\alpha}{dt^2}$$

The expression for
respect to time, and
low:

$$(2-m)$$

Solving eq. (3.11) for

$$c_1 =$$

By substituting eq.
Dutta obtained the

$$\ln(\alpha_p)$$

where α_p is $(d\alpha/dt)_p$
given values for c_1 .
Once the rate
curve temperatures,
found from eq. (3.7)

$$\left. \frac{d\alpha}{dt} \right|_{t=0} = c_1 \quad (3.10)$$

The second rate constant, c_2 , and the exponent, m , were found from the degree of cure at the maximum degree of cure rate, where the maximum is defined by

$$\frac{d^2\alpha}{dt^2} = 0$$

The expression for the degree of cure rate given in eq. (3.4) was differentiated with respect to time, and the resulting expression was set equal to zero, with $\alpha = \alpha_p$ as follows:

$$(2-m)c_1 \alpha_p^{1-m} + c_2 (2\alpha_p - m) = 0 \quad (3.11)$$

Solving eq. (3.11) for c_2 resulted in

$$c_2 = \frac{(2-m)c_1 \alpha_p^{1-m}}{m-2\alpha_p} \quad (3.12)$$

By substituting eq. (3.12) into eq. (3.14) with $\alpha = \alpha_p$ and rearranging terms, Ryan and Dutta obtained the following implicit relationship for m :

$$\ln(\alpha_p') = \ln \left[\frac{\alpha_p'}{(1-\alpha_p)^{2-m}} - c_1 \right] - \ln \left[\frac{(2-m)c_1 \alpha_p^{1-m}}{m-2\alpha_p} \right] \quad (3.13)$$

where α_p' is $(d\alpha/dt)$ evaluated at $\alpha = \alpha_p$. This equation was solved numerically for m , given values for c_1 , α_p , and α_p' from DSC experiments at different temperatures.

Once the rate constants, c_1 and c_2 were determined for a few different isothermal cure temperatures, the activation energy constants and pre-exponential factors were found from eq. (3.7) using linear regression.

Another method
here. The initial
estimated from c
cure rate data. E

$$\frac{da}{dt} = \frac{c}{(1-a)}$$

Equation (3.14) v
estimated values
eq. (3.13) using t
This procedure ha
has the disadvan
and a and da/dt a

In the second
A, A, E, and
described by Sich
a matter similar to

$$\frac{da}{dt} = \frac{c}{(1-a)}$$

and linear regress
stants and pre-exp
rate constants at d

In the third
parameters estima
were estimated by
rate constant, c, f
the rate constants

Another method of determining the kinetic parameters in eq. (3.4) is presented here. The initial procedure is the same as that used by Ryan and Dutta (1979): m was estimated from c_1 and α_p using the initial degree of cure and the maximum degree of cure rate data. Equation (3.4) was then rearranged as

$$\frac{d\alpha/dt}{(1-\alpha)^{2-m}} = c_1 + c_2 \alpha^m \quad (3.14)$$

Equation (3.14) was solved for c_1 and c_2 using linear regression and the previously estimated values for m . This is an iterative procedure where m was recalculated from eq. (3.13) using the new value for c_1 , and eq. (3.14) was again solved for c_1 and c_2 . This procedure has the advantage that it uses all of the degree of reaction data, but it has the disadvantages in that all the parameters are not determined simultaneously and α and $d\alpha/dt$ are treated as if they are independent of each other.

In the second kinetic model (eq. 3.5), there are four parameters to be determined: A_1 , A_2 , E_1 , and E_2 . The rate constants were first determined using the procedure described by Sichina (DuPont Publ. No. TA-93); the kinetic equation was rearranged in a manner similar to that shown in eq. (3.14),

$$\frac{d\alpha/dt}{(1-\alpha)^2} = c_1 + c_2 \alpha \quad (3.15)$$

and, linear regression was used to determine c_1 and c_2 . The activation energy constants and pre-exponential factors were then estimated using linear regression from the rate constants at different isothermal temperatures.

In the third model (eq. 3.6), an n th order reaction was assumed, and the parameters estimated were A_1 , E_1 , and the order of reaction, n . These parameters were estimated by first using linear regression to find the order of reaction, n , and the rate constant, c_1 , for each temperature investigated. Then, A_1 and E_1 were found from the rate constants at different temperatures using linear regression.

3.2.2 Reaction

Hawley et

fifty percent. Th

the number of c

fore, the reaction

in the model:

$$\frac{da}{dt}$$

where the diffus

using a nonlinear

follow an Arrheni

c_1

where A_1 and

Enterprises, 1987

A modificat

that diffusion bec

This value is desig

$$\frac{da}{dt} =$$

Again, the unknow

estimation schem

energy constant,

evaluated at differe

It should be

models, since by de

3.2.2 Reaction Models for Degree of Cure > 50%

Hawley et al. (1988) proposed the following model for a degree of cure greater than fifty percent. The basis of this model is the assumption that, as the epoxy cures and the number of cross-linkages increases, the flow of the molecules is restricted; therefore, the reaction is diffusion controlled. This is evident by the exponential decay term in the model:

$$\frac{d\alpha}{dt} = c_1 (1-\alpha)e^{-D\alpha} \quad (3.16)$$

where the diffusion coefficient, D , and the rate constant, c_1 , were found numerically using a nonlinear parameter estimation scheme. The rate constant was assumed to follow an Arrhenius relationship with temperature:

$$c_1 = A_3 e^{-E_3/RT} \quad (3.17)$$

where A_3 and E_3 were found using linear regression (Scientific Programming Enterprises, 1987).

A modification of eq. (3.17) is presented here. It was based on the assumption that diffusion becomes significant at some value of extent of cure, say α equal to 50%. This value is designed as α_D as shown in the equation below.

$$\frac{d\alpha}{dt} = \left(\frac{d\alpha}{dt} \right)_{\alpha=\alpha_D} + c_1 (\alpha_D - \alpha)e^{-D(\alpha_D - \alpha)} \quad (3.18)$$

Again, the unknown parameters, c_1 and D , were found using a nonlinear parameter estimation scheme (Scientific Programming Enterprises, 1987), and the activation energy constant, E_3 , and the pre-exponential factor, A_3 , were estimated from c_1 evaluated at different temperatures.

It should be noted that technically, neither of these models are true kinetic models, since by definition, diffusion is negligible in kinetic analysis; however, for these

purposes. It is
they were kinet

3.2.3 Selection

Since it w
reaction of the
ing the heat gen
following section
mal properties d

To determ
was selected from
model was selec
50%. The select
intervals of the e

3.3 Estimation

The estima
that described in
Several important
a result of an exo
equation shown
namely, the appr
energy equation.
well as temperatur

In this secti
resulting from hea
followed by a disc
ture for the estima

purposes, it is convenient to treat the reactions for degree of cure greater than 50% as if they were kinetic reactions.

3.2.3 Selection of Kinetic Models for the Determination of Thermal Properties

Since it was assumed that the degree of cure rate was proportional to the heat of reaction of the composite during curing, the kinetic parameters were used in determining the heat generation due to the exothermic reaction of the epoxy. As shown in the following section, the amount of heat generated is necessary for the estimation of thermal properties during curing.

To determine the degree of cure rate throughout the curing process, one model was selected from the three models given for degree of cure less than 50%, and a second model was selected from the two models were presented for degree of cure greater than 50%. The selection of the models was based on the minimization of the 95% confidence intervals of the estimated parameters.

3.3 Estimation of Thermal Properties during Curing

The estimation of thermal properties of a composite during curing is similar to that described in Section 3.1 for estimating the thermal properties of cured composites. Several important differences must be noted, however. First, since the curing process is a result of an exothermic reaction, a heat generation term must be added to the energy equation shown in eq. (3.1a). This results in an additional differential equation, namely, the appropriate kinetic model (eq. 3.4), which must be solved along with the energy equation. Also, the thermal properties may be a function of degree of cure as well as temperature.

In this section, the direct problem of determining the temperature distribution resulting from heat conduction through a composite specimen during curing is defined, followed by a discussion of the solution method for the direct problem and the procedure for the estimation of the thermal properties.

3.3.1 Heat Conduction

One dimension
epoxy reinforcement
boundary and
that the chemical
posite plate a
1983). A mathematical

$$\frac{\partial}{\partial x} (k(T, \alpha)$$

with the boundary

-k

T

and the initial condition

T =

where x is the thickness of the plate
effective thermal conductivity-specific heat
sur. α . Once agreed upon, we assumed to
selected for $\alpha < 50^\circ$
One method
the appropriate kinetic
hence approximate

3.3.1 Heat Conduction in Carbon Fiber Reinforced Composites during Curing

One dimensional heat transfer was considered through a flat carbon-fiber/amine-epoxy reinforced composite plate during curing, with an imposed heat flux on one boundary and a known temperature history on the other boundary. It was assumed that the chemical reactions due to the curing of the epoxy generate heat within the composite plate at a rate proportional to the rate of extent of cure (Loos and Springer, 1983). A mathematical statement of this problem is

$$\frac{\partial}{\partial x} \left(k(T, \alpha) \frac{\partial T}{\partial x} \right) + \rho H_t \frac{d\alpha}{dt} = \rho c_p(T, \alpha) \frac{\partial T}{\partial t} \quad 0 < x < L; \quad t > 0 \quad (3.19a)$$

with the boundary conditions,

$$-k(T, \alpha) \frac{\partial T}{\partial x} = q(t) \quad x = 0; \quad t > 0 \quad (3.19b)$$

$$T = T_L(t) \quad x = L; \quad t > 0 \quad (3.19c)$$

and the initial condition,

$$T = T_0(x) \quad 0 \leq x \leq L; \quad t = 0 \quad (3.19d)$$

where x is the direction perpendicular to the fibers through the thickness, L is the thickness of the plate, ρ is density, and H_t is the total heat of reaction. In this case, the effective thermal conductivity (perpendicular to the fiber direction), k , and the effective density-specific heat, ρc_p , were assumed to be functions of temperature, T , and extent of cure, α . Once again, the heat flux, q , temperature, T_L , and the initial condition, T_0 , were assumed to be known. The $\partial\alpha/\partial t$ term was obtained from the kinetic models selected for $\alpha < 50\%$ and $\alpha > 50\%$, as discussed in Section 3.2.3.

One method of solution involves the use of finite differences. At each time step, the appropriate kinetic equation (eq. 3.4 or eq. 3.18) can be solved using a forward difference approximation for the time derivative of α , and then the energy equation (eq.

3.19a-d) can be

derivatives. To

count for the term

A one dimen

solve the problem

above. In the so

both the kinetic

properties were a

cure for thermal

$$k = k_0 +$$

where k is contin

known values of

of cure, α_1 . Equa

follows

$$k = k(\alpha_1, T_1)$$

$$+ \left(\frac{k}{T} \right)$$

A similar express

quasi-linear appr

time step.

3.2.2 Parameter

The param

3.1.2 with the ex

3.19a-d) can be solved using Crank-Nicolson approximations for the temperature derivatives. To simplify the solution, a quasi-linear approximation can be used to account for the temperature and extent of cure dependence of the thermal properties.

A one dimensional finite difference program, *CURE1D* (Appendix A), was written to solve the problem described by eqs. (3.19a-d) using the solution method described above. In the solution, eq. (3.4) and eq. (3.18) were selected for the kinetic models, and both the kinetic and thermal properties were assumed to be known. The thermal properties were assumed to be piecewise linear functions of temperature and extent of cure, for thermal conductivity, k :

$$k = k_0 + k_1 T + k_2 \alpha \quad T_i < T < T_{i+1}, \quad \alpha_i < \alpha < \alpha_{i+1} \quad (3.20)$$

where k is continuous at T_i and α_i , and k_0 , k_1 , and k_2 are constants obtained from known values of the thermal conductivity for a given temperature, T_i , and a given extent of cure, α_i . Equation (3.20) was written in terms of $k(\alpha_i, T_i)$, $k(\alpha_{i+1}, T_i)$, and $k(\alpha_{i+1}, T_{i+1})$ as follows

$$k = k(\alpha_i, T_i) + [k(\alpha_{i+1}, T_i) - k(\alpha_i, T_i)](\alpha - \alpha_i) + \left[\frac{k(\alpha_{i+1}, T_{i+1}) - k(\alpha_{i+1}, T_i)}{T_{i+1} - T_i} \right] (T - T_i) \quad (3.21)$$

A similar expression was obtained for the density-specific heat product. Using the quasi-linear approach, these parameters (k and ρc_p) were assumed constant over each time step.

3.3.2 Parameter Estimation Method

The parameter estimation procedure was similar to that described in Section 3.1.2 with the exceptions that the calculated temperatures in eq. (3.3) were obtained

from the

tures w

PROPI

(3.19a

modifi

techni

peratu

3.4 Op

Pr

Th

tion of th

the optim

use of the

3.4.1 Ob

One

specific h

paramete

mal conc

condition

simplify

small tem

and exter

thermal p

number c

permeate

cut and

from the solution of eqs. (3.19a-d) instead of eqs. (3.1a-d), and the measured temperatures were obtained from a composite specimen during curing.

An updated version of the previously mentioned parameter estimation program, *PROP1DMA* (Beck, 1989), was modified to include the heat generation term shown in eq. (3.19a) due to the chemical reactions occurring during the curing of the epoxy. The modified program is called *PROP1D_CURE*. The same kinetic equations and solution technique used for the direct problem in *CURE1D* were also used in solving for the temperature distribution, T , in *PROP1D_CURE*.

3.4 Optimal Experimental Design Criterion for the Estimation of Thermal Properties

This section deals with the optimization of the experimental design for the estimation of the thermal properties of the composite material during curing. The objectives of the optimization are first presented, followed by a discussion of the development and use of the design criterion.

3.4.1 Objectives for the Experimental Design Optimization

One objective of this study was to estimate thermal conductivity and density-specific heat of carbon-epoxy composites during curing, with the assumption that these parameters are functions of temperature and extent of cure. In order to estimate thermal conductivity and density-specific heat independently, a heat flux boundary condition, such as that shown in eq. (3.19b), is required (Beck and Arnold, 1977). To simplify the estimation problem, it was desired to have short heat flux intervals with small temperature and extent of cure variations, compared to the overall temperature and extent of cure changes during the cure cycle, to justify the assumption of constant thermal properties over each heating interval. The objective here is to incorporate a number of these intervals at different degree of cure and temperature values in the experimental design so that a relationship between the thermal properties and degree of cure and temperature values can be obtained.

The recommended cure cycle for the AS4/EPON 828-mpDA composite system used in this study is for the specimen to be heated for two hours at 75°C and two hours at 125°C. Therefore, one objective for the experimental design was to have the heat flux interval be short compared to the overall curing time, and another was to have the temperature rise due to the heat flux be small compared to the temperature differentials in the curing cycle (e.g., 50°C). The third objective was that the heating interval be chosen to minimize the variance of the estimated thermal properties.

3.4.2 Optimal Experimental Design Criterion

The optimal experimental design criterion was based on the third objective listed above, with the first two objectives as constraints. In other words, a criterion was sought in which the heating interval duration time was optimized for the estimation of the thermal properties with the lowest variance, with the constraints that the interval be short compared to the total curing time and that the temperature rise during the heating time be small compared to temperature differentials in the recommended curing cycle. Practically, these constraints involved a fixed temperature rise and a fixed number of temperature measurements.

Many criteria have been proposed for the optimal design of experiments, and most of these involve the $\mathbf{X}^T\mathbf{X}$ matrix, where \mathbf{X} is the sensitivity matrix. The criterion used here is recommended by Beck and Arnold (1977) because it is equivalent to the minimization of the hypervolume of the confidence region (for more than one parameter and for the standard statistical assumptions, Beck and Arnold, 1977). This criterion is the maximization of the determinant of the $\mathbf{X}^T\mathbf{X}$ matrix,

$$\Delta = |\mathbf{X}^T\mathbf{X}| \quad (3.22)$$

Beck and Arnold (1977) presented an expression for Δ at time, t^n , where n is large and fixed, using uniformly spaced measurements, and two parameters. The expression for Δ for one sensor in dimensionless terms is

Δ^*

where,

$$C_{ij}^* = \frac{(\Gamma_m^* - \Gamma_{ij}^*)}{\Gamma_m^*}$$

and, Γ_m^*

in these equations

parameter to be

conductivity of the

The heat

curing was determined

dimensionless

periments:

$\frac{\partial^2}{\partial x^2}$

$\frac{\partial^2}{\partial x^2}$

with boundary

and initial conditions

$$\Delta^+ = C_{i1}^+ C_{i2}^+ - C_{i3}^+ \quad (3.23a)$$

where,

$$C_{ij}^+ = \frac{(T_{\max}^+)^2}{t_n} \int_0^{t^{(n)}} X_i^+(t) X_j^+(t) dt, \quad X_i^+(t) = \beta_i \frac{\partial T^+}{\partial \beta_i} \quad (3.23b,c)$$

$$\text{and,} \quad T_{\max}^+ = \frac{T_{\max}}{qL/k} \quad (3.23d)$$

In these equations, T_{\max} is the maximum temperature up to time, $t^{(n)}$, β_i is the i th parameter to be estimated, q is the heat flux, L is the thickness, and k is the thermal conductivity of the sample.

The heating time interval used in the transient temperature experiments during curing was determined using this criterion. The following hypothetical problem in dimensionless terms was formulated to simulate one heat flux interval during the experiments:

$$\frac{\partial^2 T^+}{\partial x^{+2}} + g^+ = \frac{\partial T^+}{\partial t^+} \quad 0 < x^+ < 1 \quad t^+ > 0; \quad (3.24a)$$

with boundary conditions,

$$-\frac{\partial T^+}{\partial x^+} = \begin{cases} 1 & 0 \leq t^+ \leq t_i^+ \\ 0 & t_i^+ < t^+ \end{cases} \quad x^+ = 0; \quad t^+ > 0; \quad (3.24b)$$

$$T^+ = 0 \quad x^+ = 1 \quad t^+ > 0; \quad (3.24c)$$

and initial condition,

$$T^+ = 0 \quad 0 \leq x^+ \leq 1 \quad t^+ > 0; \quad (3.24d)$$

where,

$$T^*$$

and

$$t^*$$

The heat gener

Note that the b

chosen because

approximate iso

the specimen to

thermal propert

such cases, the

and Arnold, 19

The temp

time, $t^* < t_1^*$, as

$$T^*(x^*, t^*)$$

and for $t^* > t_1^*$,

$$T^*(x^*, t^*)$$

The sen

respect to th

Differentiatin

$t^* < t_1^*$,

where,

$$T^+ = \frac{T - T_0}{qL/k}, \quad g^+ = gL/q, \quad x^+ = x/L,$$

and

$$t^+ = \alpha t / L^2. \quad (3.24e-h)$$

The heat generation term, g^+ , was assumed to be constant over the heating interval. Note that the boundary condition at $x^+ = 1$ is $T^+ = 0$. This isothermal condition was chosen because the tested composite materials have low thermal conductivity and an approximate isothermal condition is relatively easy to simulate; it is done by attaching the specimen to a high thermal conductivity material. This is in contrast to estimating thermal properties of metals, which have relatively high thermal conductivity values. In such cases, the case of an insulated boundary condition at $x = L$ has been used (Beck and Arnold, 1977).

The temperature solution for the conditions given in eqs. (3.24a-d) was found for time, $t^+ < t_1^+$, as,

$$T^+(x^+, t^+) = 0.5g^+(1-x^{+2}) + (1-x^+) - 2 \sum_{m=1}^{\infty} e^{-\beta_m^2 t^+} \cos(\beta_m x^+) (\beta_m - g^+(-1)^m) / \beta_m^3 \quad (3.25a)$$

and for $t^+ > t_1^+$,

$$T^+(x^+, t^+) = 0.5g^+(1-x^{+2}) - 2 \sum_{m=1}^{\infty} \cos(\beta_m x^+) \left[(\beta_m - g^+(-1)^m) e^{-\beta_m^2 t^+} - \beta_m e^{-\beta_m^2 (t^+ - t_1^+)} \right] / \beta_m^3 \quad (3.25b)$$

The sensitivity terms in eq. (3.23b) were found by differentiating eqs (3.25a,b) with respect to the parameters thermal conductivity, k , and density-specific heat, ρc_p . Differentiating eq. (3.25a) first with respect to k resulted in the following expression for $t^+ < t_1^+$,

$$X_t^* = k \frac{\partial^2}{\partial t^2}$$

and for $t > t_1^*$,

$$X_t^* = -0.5$$

Equations (3.25a)

X_t^* . For $t < t_1^*$,

$$X_t^*$$

and for $t > t_1^*$,

$$X_t^* = -2$$

To calculate

was first determined

were then found

X_t^* and X_t^* , calculated

found and compared

unless heat generated

Results for

heating times

$$X_1^* = k \frac{\partial T^*}{\partial k} = -0.5g^*(1-x^*) - (1-x^*) + 2 \sum_{m=1}^{\infty} e^{-\beta_m^2 t^*} \cos(\beta_m x^*) \times (\beta_m - g^*(-1)^m)(1+\beta_m^2 t^*)/\beta_m^3 \quad (3.26a)$$

and for $t^* > t_i^*$,

$$X_1^* = -0.5g^*(1-x^*) + 2 \sum_{m=1}^{\infty} \cos(\beta_m x^*) \left[(1+\beta_m^2 t^*)(1-g^*(-1)^m/\beta_m) e^{-\beta_m^2 t^*} - (1+\beta_m^2 (t^*-t_i^*)) e^{-\beta_m^2 (t^*-t_i^*)} \right] / \beta_m^3 \quad (3.26b)$$

Equations (3.25a,b) were then differentiated with respect to ρc_p to obtain expressions for X_2^* . For $t^* < t_i^*$,

$$X_2^* = \rho c_p \frac{\partial T^*}{\partial k} = -2 \sum_{m=1}^{\infty} t^* e^{-\beta_m^2 t^*} \cos(\beta_m x^*) (\beta_m - g^*(-1)^m) / \beta_m^3 \quad (3.27a)$$

and for $t^* > t_i^*$,

$$X_2^* = -2 \sum_{m=1}^{\infty} t^* \cos(\beta_m x^*) \left[(1-g^*(-1)^m/\beta_m) e^{-\beta_m^2 t^*} - (t^*-t_i^*)(e^{-\beta_m^2 (t^*-t_i^*)}) \right] \quad (3.27b)$$

To calculate the criterion Δ^* in eq. (3.23a), the maximum temperature rise, T_{\max}^* , was first determined from eqs. (3.25a,b) at $x^* = 0$. The C_{ij} components in eq. (3.23b) were then found using numerical integration from T_{\max}^* , and the sensitivity coefficients, X_1^* and X_2^* , calculated using eqs. (3.26a,b) and (3.27a,b). Finally, the criterion, Δ^* , was found and compared for different heating intervals. Two different values of the dimensionless heat generation term, g^* , were used in analysis.

Results for the criterion of Δ^* as a function of time for six different dimensionless heating times are shown in Figure 3.1 for $g^* = 0.1$ and in Figure 3.2 for $g^* = 1.0$. The

Experimental Design Criterion, Δ^*
(dimensionless)

0.02
0.01
0.005
0.002
0.001
0.000

Figure
Dimens

Experimental Design Criterion, Δ^*
(dimensionless)

0.02
0.01
0.005
0.002
0.001
0.000

Fig
Dime

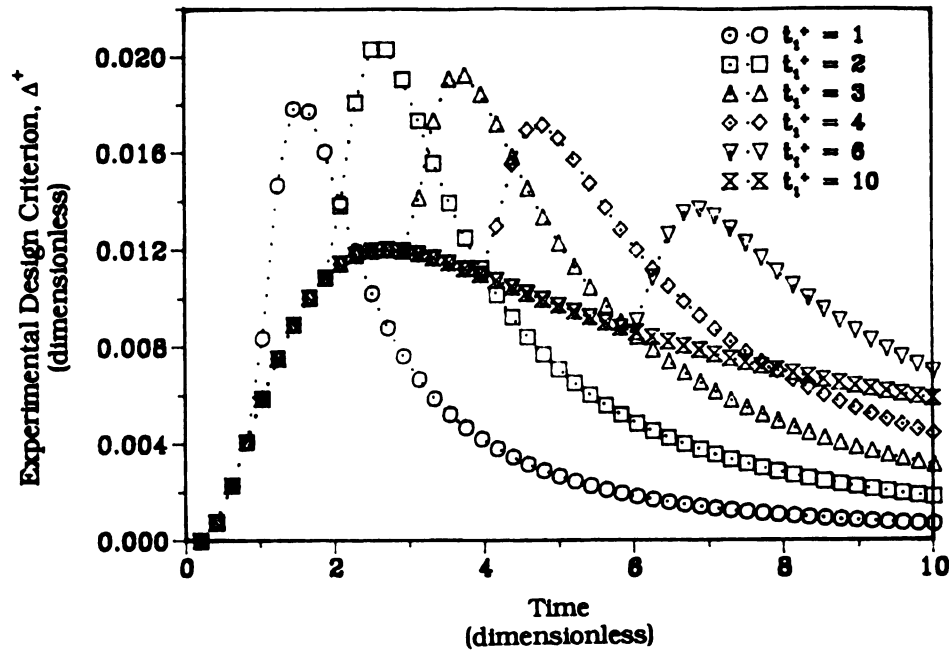


Figure 3.1 Dimensionless Experimental Design Criterion, Δ^+ , for Different Dimensionless Heating Times, t_1^+ , and a Dimensionless Heat Generation Term, g^+ , equal to 0.1.

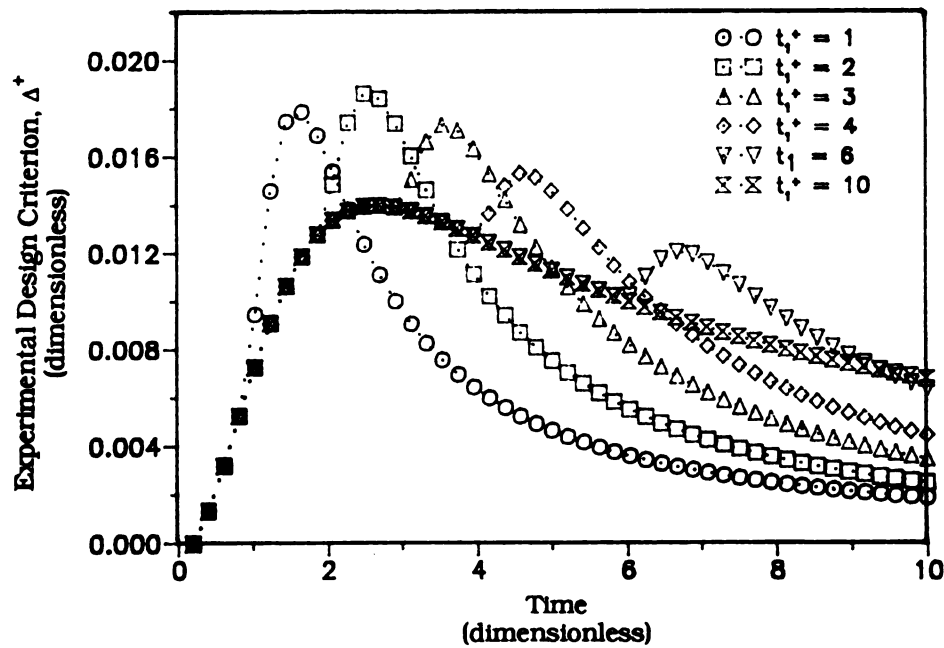


Figure 3.2 Dimensionless Experimental Design Criterion, Δ^+ , for Different Dimensionless Heating Times, t_1^+ , and a Dimensionless Heat Generation Term, g^+ , equal to 1.0.

optimum heating

both figures, the

ing time, t^* , of

heating time was

the optimum h

resulted in only

= 0.

The dimen

values based on

presented in Sec

heat flux was th

of no more than

optimum heating interval was chosen from the curve with the highest value of Δ^+ . In both figures, the curves with the highest value of Δ^+ resulted from a dimensionless heating time, t^+ , of 2. Further analysis of the case with $g^+ = 0.1$, revealed that the optimum heating time was closer to 2.125. An analysis of the case with $g^+ = 0.0$ indicated that the optimum heating time was approximately 2.25; therefore, the case for $g^+ = 1$, resulted in only a 10% decrease in the optimum heating time, compared to that with $g^+ = 0$.

The dimensional optimum heating time was determined from thermal property values based on results obtained for the cured composite samples from the analysis presented in Section 3.1 and a fixed thickness for the composite sample. The required heat flux was then calculated from eq. (3.23d), assuming a maximum temperature rise of no more than 5°C.

Chapter 4

Experimental Procedures

The focus of this chapter is on the experimental procedures used in the experiments used to estimate thermal and kinetic properties in carbon/epoxy composite materials. The first section is devoted to the procedures used in the transient temperature experiments for the estimation of thermal properties in cured composite materials (Section 4.1), and the second section is concentrated on the differential scanning calorimetry experiments used to estimate kinetic properties during curing (Section 4.2). In the final section, an outline of the methodology used in the transient experiments for the estimation of thermal properties during curing (Section 4.3) is given.

4.1 Experiments for the Estimation of Thermal Properties in Cured Composites

The experiments conducted for the estimation of thermal properties of cured composites involved temperature measurements within carbon/epoxy composite samples subject to an imposed heat flux at one boundary. These experiments are described in the following subsections. Included in these descriptions are the sample preparation techniques, the experimental set-up design, the data acquisition system, the procedures for the transient temperature experiments, and finally, a discussion of the experimental parameters.

4.1.1 Preparation

The composite was suspended in an aqueous solution of the M.S.C. Compound. The composite was divided into four parts and 4. consolidated. The carbon fibers were divided into two phases, stacked and cured. The fabrication of the composite is described in detail.

4.1.1.1 Epoxy Preparation

The same composite materials were used in the transient experiments with 1.3 Phenylglycidyl ether. The composite was a priority in the critical with regard to the curing of the epoxy. Therefore, a resin was used. The gloves were worn. The composite also served to result in perfect epoxy is given.

1. The composite was cured for 24 hours before use.
2. Two samples were prepared with a

4.1.1 Preparation of the Composite Samples

The composite samples used in this study were composed of carbon fibers suspended in an epoxy matrix. All of the samples were prepared using the facilities in the M.S.U. Composite Materials and Structures Center. The preparation procedure can be divided into four phases: 1. epoxy preparation; 2. prepreg preparation; 3. stacking; and, 4. consolidation. In the first two phases, the two part epoxy was mixed, and then the carbon fibers were impregnated with epoxy (prepreg preparation). During the final two phases, stacking and consolidation, the prepreg plies or impregnated fibers were stacked and cured to form a composite plate. Each experimental set-up required the fabrication of four composite plates. The phases of the preparation procedure are described in detail in the following subsections.

4.1.1.1 Epoxy Preparation

The same type of epoxy was used in the transient experiments with cured composite materials, in the differential scanning calorimetry (DSC) experiments, and in the transient experiments during curing. The epoxy consisted of Shell's EPON 828 Resin with 1,3 Phenylenediamine (mPDA) as the curing agent, mixed in a one to one equivalency. The curing agent is a suspected carcinogen, so safety was a number one priority in the preparation procedures. The crystalline form of the mPDA is the most critical with regards to safety. Extreme caution was taken so that the crystalline form of the curing agent was not inhaled, and all skin contact with the mPDA was avoided. Therefore, a respirator, protective clothing, such as a laboratory coat, and disposable gloves were worn at all times during the preparation procedure. The protective clothing also served to protect one's personal clothing, since contact with the curing agent resulted in permanent stains. The detailed step by step procedure used to prepare the epoxy is given below.

1. The mPDA was set out at room temperature from cold storage at least one half hour before use.
2. Two large disposable beakers were cleaned with acetone, and then wiped dry with a disposable tissue.

3. One of

poured into

0.050 kg of

4. The res

5. In the

of mPDA

alency. O

measure of

the lid on

The jar w

scoped ou

6. The be

agent wa

odically.

7. While

scale, th

cleaned

placed

9. The

minute

prehe

the m

The e

1410

The

dimi

rem

10.

or t

3. One of the beakers was tared on a scale; the appropriate amount of resin was poured into the beaker (approximately 0.200 kg resin for prepreg preparation or 0.050 kg for DSC experiments); and, the weight of the resin was recorded.
4. The resin was then heated in an oven to approximately 70°C.
5. In the mean time, the second beaker was tared, and the appropriate amount of mPDA was determined from the weight of the resin. For one to one equivalency, 0.0145 kg mPDA are required for every 0.100 kg epoxy (Rich, 1987). To measure out the appropriate amount of mPDA, the jar of mPDA was shaken with the lid on and placed on its side on some foil that was spread out in a fume hood. The jar was then opened, and the appropriate amount of mPDA was carefully scoped out into the second beaker using a clean spatula.
6. The beaker with mPDA was placed into the oven with the resin until the curing agent was completely melted (about 40 minutes). The mPDA was checked periodically, and stirred with a clean glass stirring rod if needed.
7. While mPDA was melting, the foil in the fume hood was removed, and the scale, the spatula, and the surfaces around where the curing agent was used were cleaned thoroughly with acetone. Both the foil and the cleaning cloths were placed in a sealed plastic bag for disposal.
9. The beaker with the resin was removed from the oven approximately five minutes before the mPDA was completely melted, and a vacuum oven was preheated to 60°C. Once the curing agent was melted, the resin was poured into the mPDA beaker, and the mixture was stirred until it appeared homogeneous. The epoxy mixture was placed into the vacuum oven (VWR Scientific, Inc. Model 1410), and the pressure was reduced to the limits of the instrument (-99 kPa). The mixture was held under a vacuum until bubbles on the side of the beaker had diminished (approximately 5 to 10 minutes); at that time, the epoxy mixture was removed, and the oven was turned off.
10. The epoxy mixture was then ready for immediate use in prepreg preparation or in DSC experiments.

4.1.1.2 Prepreg

A prepreg

this study, the

aneous AS4 car

the prepregs were

40). A hot-melt

the resin to form

through a small

impregnated with

The epoxy resin

detailed procedu

Tool Corporation

indicating the p

exam. protective

1. While

prepared

mount a

bracket.

screws.

Figures

2. A tow

the furn

Figures

3. The

was the

spool w

prior to

4. The

the res

prepre

4.1.1.2 Prepreg Preparation

A prepreg consists of a single layer of fibers impregnated with uncured resin. In this study, the prepregs were prepared from EPON 828/mPDA epoxy resin and continuous AS4 carbon fibers with 12,000 fibers per tow (Hercules Aerospace Corp.); all of the prepregs were prepared using carbon fibers from the same lot number (Lot No. 708-4C). A hot-melt prepregger (Research Tool Co.) was used to impregnate the fibers with the resin to form a prepreg. In this procedure, a tow of continuous fibers was fed through a small vat of epoxy and then through a die, so that the tow was completely impregnated with fibers. The tow was then wrapped around a drum to form a prepreg. The epoxy resin was prepared using the procedure described in Section 4.1.1.1, and the detailed procedure to impregnate the fibers with the resin is given below. The Research Tool Corporation Prepregger is shown in Figure 4.1. Additional views of the prepregger, indicating the parts referenced in this section, are shown in Figures 4.2-4.6. Once again, protective clothing and disposable gloves were worn.

1. While the mPDA was melting (step 7., Section 4.1.1.1), the prepregger was prepared. First, a spool of AS4 carbon fibers was placed on the single spool mount and secured in place using the large spool holder, the side mounting bracket, and the end nut. The side bracket was held in place with two thumb screws. The single spool mount with the spool of fibers in place is shown in Figures 4.2a,b.
2. A tow, or strand of fibers, was then fed up over the first guide roller, through the furnace (which was not used), and around the tension rollers, as shown in Figures 4.3a,b.
3. The resin pot chamber was fastened in place with two thumb screws. The tow was then guided through the resin pot, and the exposed layer of the fiber on the spool was pulled off and thrown away. Masking tape was used around the ends prior to cutting.
4. The large end of the die appropriate for this fiber (die A-A) was placed under the resin pot, and secured in place with a thumb screw. The control panel of the prepregger was then turned on, and full tension was applied to the fiber. The tow

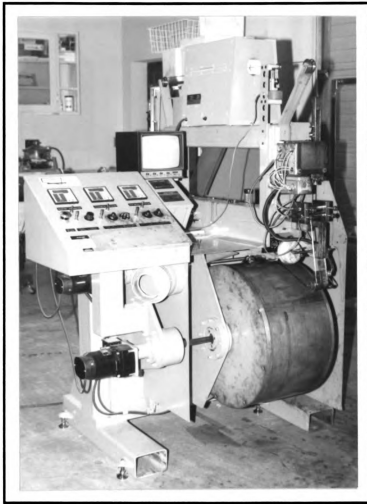


Figure 4.1 Hot Melt Prepregger (Research Tools Corporation).

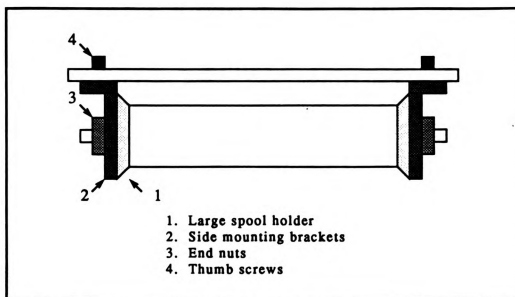


Figure 4.2a Schematic of Single Spool Mount on Hot-Melt Prepregger.

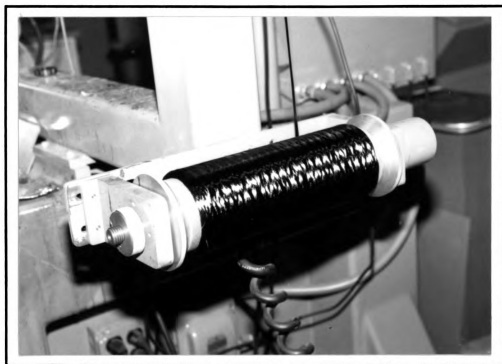


Figure 4.2b Photograph of Single Spool Mount.

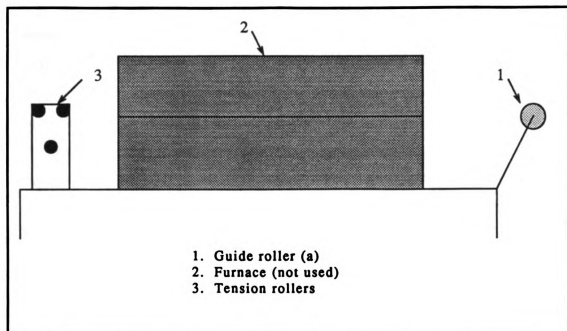


Figure 4.3a Schematic of Guide Roller, Furnace, and Tension Rollers on Hot Melt Prepregger.

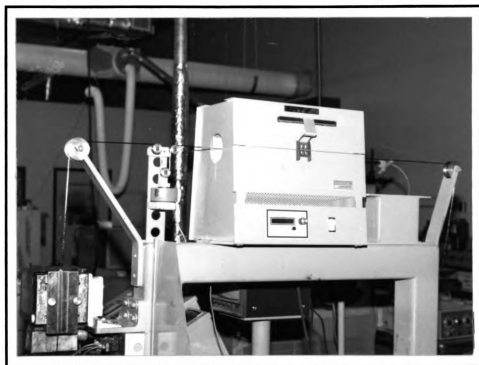


Figure 4.3b Photograph of Fibers Through Guide Roller, Furnace, and Tension Rollers.

was pulled
opening
taking of
secure by
once the
the resin
view of the
5. The resin
then turned
follows:

6. Two
prevent
side cover
(Figure
drum.
thorough
7. On
was pulled
was
guided
pin.
so that
in place
8. Cover
with
9. Cover
pulled

was pulled taut against the die opening so that all of the fibers were in the die opening. The small end of the die was then put in place with a thumb screw, taking care to keep the tow taut. Two large thumb screws were then used to secure both ends of the die. Extreme care was taken not to pull on the dry tow once the die was in place, since this would break the fibers. The die, mounted on the resin pot, with the fibers in place is shown in Figures 4.4a,b, and a close-up view of the resin pot, die and pin guide (step 7) is shown in Figure 4.5.

5. The resin pot, flattening pin, and guide roller heaters (Figures 4.4a,b) were then turned using the control panel (Figure 4.6). The set points were adjusted as follows:

Resin pot = 125°F (69.4°C)

Flattening pin = 95°F (52.8°C)

Guide roller = 95°F (52.8°C)

6. Two sheets of plastic, 193 cm by 33 cm, were cut. The plastic was used to prevent the impregnated tow from sticking to the drum and to protect it from outside contamination. One end of one sheet was taped to the prepregger drum (Figures 4.4a,b), and the drum was rotated so that the plastic lay smoothly on the drum. The remaining end was then taped down, and then the plastic was cleaned thoroughly with acetone.

7. Once the epoxy mixture was ready (see step 10, Section 4.1.1.1), the mixture was poured into the resin chamber until it was about two-thirds full. Some epoxy was poured over the fibers above the resin pot to ease the placement of the pin guide. The pin guide was then inserted so that the fibers ran in front of the top pin, behind the second, and in front of the bottom two pins. The guide was placed so that the top pin lay just below the surface of the resin pot, and it was secured in place with a side mount and two thumb screws (Figure 4.4a,b).

8. Once the pin guide was set in place, the resin chamber was filled up to the rim with epoxy.

9. The tension on the fibers was released, and the wetted tow of fibers were pulled down through the die, between the flattening pins, and around the guide

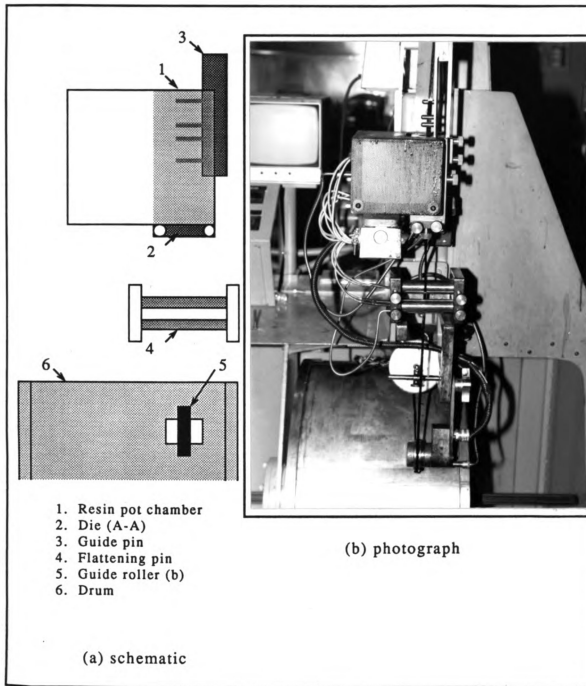


Figure 4.4a,b Schematic (left) and Photograph (right) of Resin Pot Assembly on Hot Melt Prepregger.

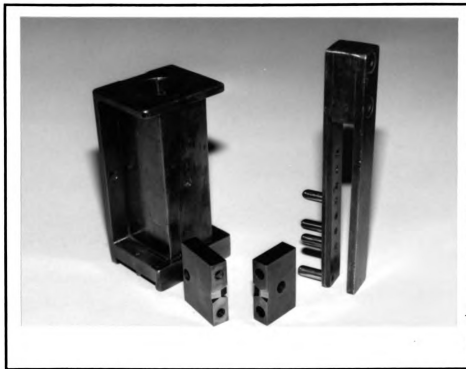


Figure 4.5 Detailed View of Resin Pot, Die (A-A), and Pin Guide (from left to right).



Figure 4.6 Hot-Melt Prepregger Control Panel.

roller.

one ha.

10. The

adjuste

The fibre

carriage

previou

11. The

restri le

12. W

tion a

to the

13. T

place

plas

the

14.

bag

15.

ca

g

roller. The tow was then taped to the drum, and the drum was rotated at least one half revolution to ensure that the tow stayed in place.

10. The drum rotation, fiber tension, and drum carriage movement controls were adjusted as follows:

Drum rotation - 1.0 rpm

Fiber tension - 0.5 to 1.0

Drum carriage movement - approximately 23 (scale: 0 to 100)

The fibers were watched carefully for the first three to four revolutions, and the carriage movement was adjusted so that in each rotation, the tow lined up the previous rotation with no gaps between the two lines.

11. The resin pot was checked and refilled every five to ten minutes to keep the resin level above the top guide pin.

12. When the fiber had wound to the left hand side of the drum, the drum rotation and drum carriage movement were turned off, and the fiber was cut off close to the drum.

13. The remaining sheet of plastic was cleaned with acetone, and one end was placed on the surface of the exposed fibers. The drum was rotated slowly, and the plastic was wrapped smoothly around the drum. The prepreg was cut away from the drum along a grooved cutting line using a utility knife with a new blade.

14. The prepreg was then carefully rolled or folded, and placed in a sealed plastic bag in a freezer until needed.

15. The clean up process was critical in this procedure since the epoxy mixture can eventually cure and harden at room temperature. The clean up procedure is given below.

a. The fiber around the resin pot was cut off and discarded. The resin pot was then removed by unscrewing the two thumb screws on the side of the pot, and the remaining resin in the pot was drained into the resin beaker under the fume hood.

b. The prepregger was cleaned thoroughly with acetone, especially around the resin pot chamber. The flattening pins were cleaned in place, but the

guide roller was removed and cleaned under the hood. The drum was also cleaned with acetone, and excess tape was removed.

- c. All switches on the control panel were turned off, along with the power switch to the control panel.
- d. The spool of fiber was wrapped in foil, labeled, and put away.
- e. The screws, pin guide, and die were removed from the resin pot under a fume hood. All pieces were carefully washed twice with acetone, and placed back on the prepregger.
- f. Finally, the fume hood area was checked and cleaned with acetone, and the soiled cleaning cloths and empty beakers were sealed in a plastic bag and disposed of properly. The epoxy in the resin beaker was allowed to cure in the hood at room temperature before discarding.

4.1.1.3 Stacking Procedure

The prepreg plies were stacked and prepared for curing in this phase. Twenty-four pieces or plies were cut from the prepreg and stacked for each composite plate. In stacking the prepreg plies, two fiber orientations were used: $[0^\circ]_{24}$ (parallel fibers) and $[0, 30, -30, 60, -60, 90^\circ]_{2(\text{sym})}$ (quasi-isotropic laminate). The two stacking orientations are shown in Figure 4.7. One prepreg was required for each of the $[0^\circ]_{24}$ composite plates, and one and a half prepregs were required for each of the quasi-isotropic plates. A total of eight $[0^\circ]_{24}$ and four $[0, 30, -30, 60, -60, 90^\circ]_{2(\text{sym})}$ plates were prepared. After stacking, the prepreg laminates were placed on an aluminum plate covered with a piece of release ply, which is a plastic sheet used to protect the aluminum plate from the epoxy. A dam was built up around the composite using a gummy tape or a cork tape to maintain the shape of the laminate during consolidation. Pieces of porous Teflon^R cloth and bleeder cloth were then placed on top of the composite. The bleeder cloth is an absorbent material used to absorb the excess epoxy during consolidation, and the porous Teflon^R cloth was placed between the prepreg laminate and the bleeder cloth to protect the surface of the composite. A second aluminum plate, covered with a release ply was laid on top of the bleeder cloth, and then the entire assembly was sealed in a

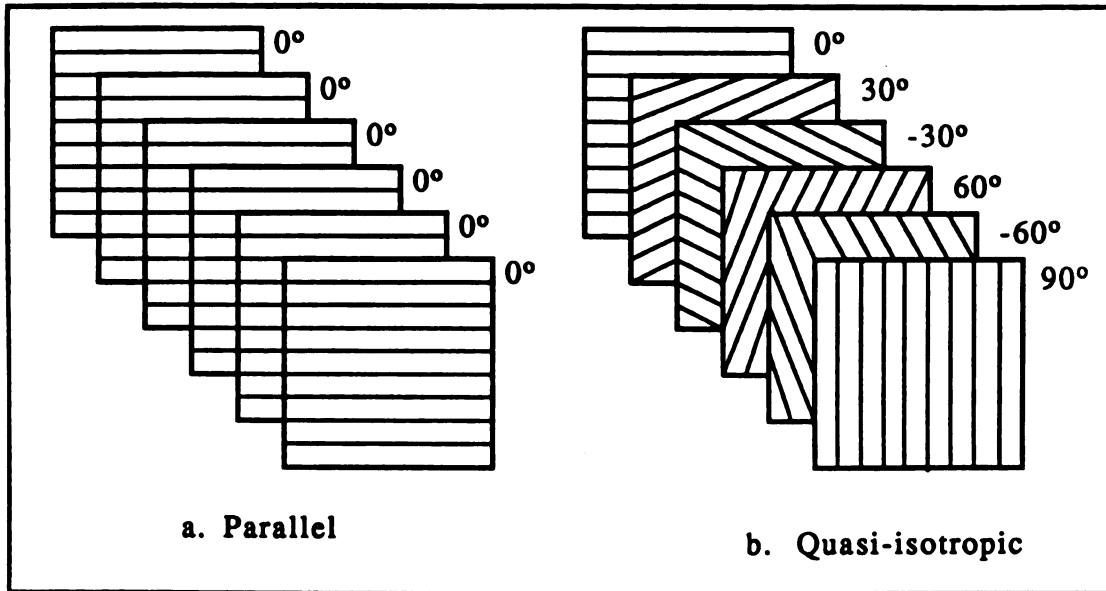


Figure 4.7 Stacking for Orientation for the First Six Parallel and the First Six Quasi-isotropic Laminates for the $[0^\circ]_{24}$ and the $[0^\circ, 30^\circ, -30^\circ, -60^\circ, 60^\circ, 90^\circ]_{2(\text{sym})}$ Composite Disks.

vacuum bag

lows.

1. One

from th

release

by 10 c

2. The

become

dry ice w

3. The p

of foil, a

a carper

15.2 cm

the prep

a half p

4. One

square

Inc.) at

5. The

prepre,

were p

was sp

were p

tion w

frost o

togethe

A rolle

betwee

6. Step

release

vacuum bag for curing. The steps used in the stacking process for one plate are as follows.

1. One 23 cm by 23 cm square piece was cut from the porous Teflon^R cloth and from the bleeder cloth, and two 23 cm by 23 cm squares pieces were cut from the release ply. In addition, a small piece of thick bleeder cloth (approximately 8 cm by 10 cm) and sheet of vacuum bag material at least 40 cm by 70 cm were cut.
2. The prepreg was taken out of the freezer and allowed to cool just enough to become pliable (approximately 5 minutes); during this time, approximately 3 kg of dry ice was obtained and chopped into small chunks.
3. The prepreg, which measured 193 cm by 30.5 cm, was spread out on a sheet of foil, and a piece of poster board was placed under the section to be cut. Using a carpenter's square as a guide and a sharp utility knife, twenty-four 15.2 cm by 15.2 cm plies were cut from each prepreg for the $[0^\circ]_{24}$ composite plates. Since the prepreg had to be cut at different angles for the quasi-isotropic plates, one and a half prepregs were required for each of these plates.
4. One piece of the release ply was secured using to a smooth 23 cm by 23 cm square aluminum plate using small amounts of Tacky Tape^R (Schnee-Morehead, Inc.) at the corners.
5. The dry ice was used to facilitate the removal of the release ply from the prepreg. Several prepreg plies were laid out on the foil, and the remainder plies were placed back in the freezer until needed. Using thermal gloves, the dry ice was spread over the prepreg plies, and the release plies on one side of each ply were peeled off as they stiffened and separated from the prepreg. Particular attention was taken not to peel off any fibers with the plastic. After any accumulated frost on the exposed surface had evaporated off, two prepreg plies were stacked together with the desired fiber orientation ($[0^\circ]_{24}$ or $[0, 30, -30, 60, -60, 90^\circ]_{2 (sym)}$). A roller was used to press the plies together in an effort to remove air trapped between the plies.
6. Step 5. was repeated with all 24 plies, resulting in a 24 ply laminate with two release plies still in tack.

7. One

placed for

8. Either

2.54 cm

Sales, In

it was lev

9. The l

was cover

second a

10. The

material

vacuum

tube tow

folded ov

the bag.

where ne

pregreg

solidatio

4.1.1.4 Cons

The pr

platens (Fre

autoclave (U

isotropic pla

cured in the

samples were

applied so tha

and the lamina

vacuum bag w

reduced to -99

7. One of the last two release plies was then removed, and the laminate was placed face down on one of the aluminum plates covered with release ply.
8. Either gummy tape (Air Dam I, General Sealants) or 0.32 cm (or 0.16 cm) by 2.54 cm cork tape (Pressure Sensitive Backed Cork Dam, Northern Fiber Glass Sales, Inc.) was used to as a dam around the sample. The dam was built up until it was level with the laminate thickness.
9. The last release ply was removed from the sample, and the exposed surface was covered with the porous Teflon^R cloth, followed by the bleeder cloth and the second aluminum plate protected with release ply.
10. The entire assembly was centered on one half of the sheet of vacuum bag material. A rubber hose was held in place with Tacky Tape^R at one end of the vacuum bag, with the piece of thick bleeder cloth placed over the mouth of the tube towards the inside of the bag. The remaining vacuum bag material was folded over the assembly, and then Tacky Tape^R was used around the edges to seal the bag. The assembly was checked visibly for leaks, and extra tape was added where needed, especially around the rubber tube. A diagram of the stacked prepreg is shown in Figure 4.8. The prepreg laminate was then ready for consolidation.

4.1.1.4 Consolidation

The prepreg laminates were consolidated either in an hydraulic press with heated platens (Fred S. Carver, Inc., Hydraulic Equipment, Model SP-F-6030) or in an autoclave (United McGill Corporation). The eight $[0^\circ]_{24}$ plates and two of the quasi-isotropic plates were cured in the press; the remaining two quasi-isotropic plates were cured in the autoclave. (The autoclave was not available at the time the first ten samples were made.) The same curing cycle was used in both cases. Pressure was applied so that the pressure over the surface of the laminate equaled 689 kPa (100 psi), and the laminate was heated to 75°C at 5°C/min. During this time, the hose on the vacuum bag was attached to a vacuum pump, and pressure inside the base was reduced to -99 kPa. This was done to further remove any air which might have been

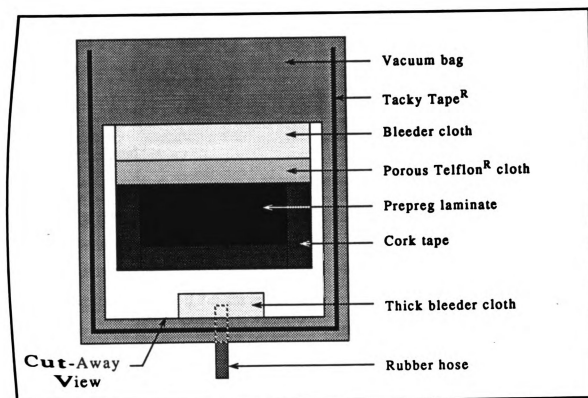


Figure 4.8 Cut-Away View of Stacked Prepreg Laminate.

trapped betw

it was heated

the recommen

After c

down to room

autoclave, r

At this time

thickness, w

4.1.2 Exper

Two e

and a third

90°/ _{22.5mm} dis

composite pl

The dis

to avoid any

disk was me

average thick

Table 4.1. T

were most li

trolled accu

maintained

was initially

the samples

damming m

talement m

cork tape w

The r

Thermofoil[®]

boundary co

trapped between the prepreg plies. The laminate was held at 75°C for two hours, then it was heated to 125°C at 5°C and held at 125°C for another two hours, according to the recommended curing cycle for this composite (Rich, 1987).

After completion of the cure cycle, the composite laminate plates were cooled down to room temperature, and then they were taken out of either the press or the autoclave, removed from the vacuum bag, and separated from the stacking materials. At this time the plates, measuring approximately 15.2 cm by 15.2 cm by 3 to 4 mm in thickness, were ready for use in the experimental set-ups, described in the next section.

4.1.2 Experimental Set-up

Two experimental set-ups were assembled using the eight $[0^\circ]_{24}$ composite disks, and a third experimental set-up was assembled using the four $[0, 30, -30, 60, -60, 90^\circ]_{2(\text{sym})}$ disks. Each experimental set-up was composed of four disks cut from the composite plates, a resistance heater, thermocouples, and two aluminum cylinders.

The disks, measuring 7.6 cm in diameter, were cut from the center of each plate to avoid any end effects resulting from the stacking process. The thickness of each disk was measured at various locations around the disk and recorded; a record of the average thickness, consolidation method, and fiber orientation for each disk is given in Table 4.1. The variations in the thicknesses between disks cured in the hydraulic press were most likely a result of differences in the applied pressure, which could not be controlled accurately. (Due to the hydraulic control on the press, the pressure was maintained at a constant value throughout the curing process; however, the pressure was initially set with an accuracy of only ± 2 kPa.) The greater thicknesses reported for the samples cured in the autoclave were most likely due to the use of the cork tape as a damming material instead of the gummy tape. The cork tape proved to be a better containment material for the epoxy than the gummy tape due to its more rigid form. (The cork tape was not available at the time the first eight samples were fabricated.)

The resistance heaters were thin (0.25 mm), 7.6 cm diameter, 9.4 ohm Thermofoil^R heaters (Minco Products, Inc.) and were used to provide the heat flux boundary condition shown in eq. (3.1b). The thermocouples were fabricated from

Table 4.1 F.
Experiments.

Disk No.	Time min
1	2
2	3
3	3.
4	4.
5	3.
6	3.
7	3.
8	3.
9	3.
10	3.
11	4.
12	4.

1. Clock tape

Table 4.1 Fabrication Parameters for Cured Composite Disks used in Transient Experiments.

Disk No.	Thickness (mm)		Consolidation Method	Fiber Orientation
	mean	st.d.		
1	2.96	0.04	hydraulic press	$[0^\circ]_{24}$
2	3.32	0.05	hydraulic press	$[0^\circ]_{24}$
3	3.56	0.02	hydraulic press	$[0^\circ]_{24}$
4	4.17	0.10	hydraulic press	$[0^\circ]_{24}$
5	3.02	0.11	hydraulic press	$[0^\circ]_{24}$
6	3.01	0.11	hydraulic press	$[0^\circ]_{24}$
7	3.68	0.08	hydraulic press	$[0^\circ]_{24}$
8	3.66	0.03	hydraulic press	$[0^\circ]_{24}$
9	3.14	0.07	hydraulic press	$[0, 30, -30, 60, -60, 90^\circ]_{2(sym)}$
10	3.56	0.09	hydraulic press	$[0, 30, -30, 60, -60, 90^\circ]_{2(sym)}$
11	4.61	0.04	autoclave ^a	$[0, 30, -30, 60, -60, 90^\circ]_{2(sym)}$
12	4.93	0.02	autoclave ^a	$[0, 30, -30, 60, -60, 90^\circ]_{2(sym)}$

a. Cork tape used as a dam instead of gummy tape.

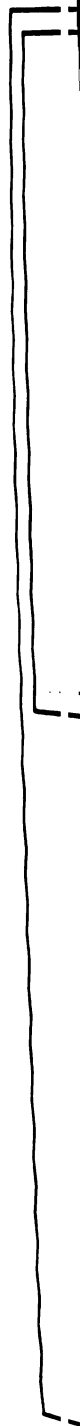
chromel and constantan wires (ANSI Type E). The two aluminum cylinders, each with a diameter of 7.6 cm and a height of 3.7 cm, were used to as heat sinks to approach a constant temperature for the boundary condition shown in eq. (3.1c). The procedures used in fabricating the thermocouples and in assembling the experimental set-up are given in the following subsections.

4.1.2.1 Thermocouple Fabrication

Fine thermocouples were used in both the transient temperature experiments on cured composite samples and the experiments on composite samples during curing. The thermocouples were prepared from 0.08 mm (AWG 40), chromel/constantan (ANSI Type E), Teflon^R/Neoflon^R duplex insulated wires from Omega Engineering, Inc. The duplex insulation consisted of an inner insulation layer around each individual wire, plus an outer insulation layer around both wires.

To prepare each thermocouple, the thermocouple wire was cut into pieces approximately 94 cm long, and the outer insulation layer was stripped off 40 cm from one end. The inner insulation layer around each wire was stripped off about 8 cm from the same end, and pieces of overbraid insulation, approximately 32 cm long, were slipped over each wire to cover the portion of the wire with only one layer of insulation. The exposed wires were flattened to approximately 0.05 mm by placing them between smooth, flat, steel dies and applying pressure using a hydraulic press. The flattened ends of the wires were over-laid and welded using a portable welder (Black & Webber, Model 848). The other end of the thermocouple was stripped about 1 cm from the end, and instrumented with a male, Type E, subminiature thermocouple connector from Omega Engineering, Inc. A prepared thermocouple with a close up view of the thermocouple junction is shown in Figure 4.9.

In addition, extension thermocouple wires were used to connect the instrumentation thermocouples to the data acquisition system. PFA Teflon^R Coated ANSI Type EX extension grade wires with 304 stainless steel shielding (Omega Engineering, Inc.) were used for this purpose. Female subminiature connectors were placed on one end for connection with the instrumentation wire, and the other end was either stripped for



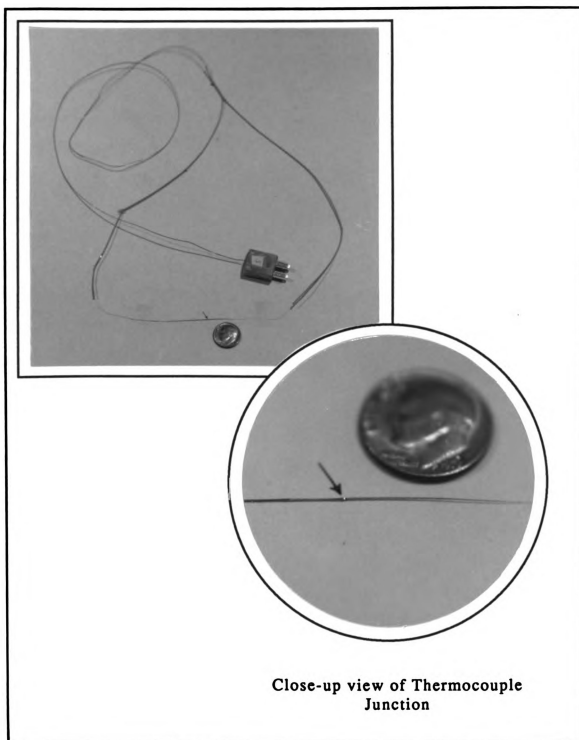


Figure 4.9 Prepared Thermocouple (ANSI Type E) with Close-up View of Thermocouple Junction.

direct con

nectors.

4.1.2.2 Exp

The c

plate. The t

center line o

the center-li

ment on on

disks were p

on the adjac

-60, 90°]

adjacent sur

Compound,

plates and b

side of each

silicon was

clumps.

A resis

thermocoupl

between the

thickness on

disks instrum

between the t

composite dis

together betw

through thre

photograph of

direct connection to the data acquisition system or fitted with male subminiature connectors.

4.1.2.2 Experimental Set-up Assembly

The composite disks were stacked with two thermocouples laid in between each plate. The thermocouples were placed across the disk about 6 mm on either side of the center line of the disk perpendicular to the fibers, with the thermocouple junction on the center-line of the disk parallel to the fibers. A diagram of the thermocouple placement on one disk is shown in Figure 4.10. For the set-ups with parallel fibers, the disks were placed on top of one another with the fibers on one disk parallel to the fibers on the adjacent disk. In the case of the set-up using the disks with the $[0, 30, -30, 60, -60, 90^\circ]_{2(\text{sym})}$ fiber orientation, the disks were arranged so that the fibers on the two adjacent surfaces were parallel to provide symmetry. Silicon grease (Silicon Heat Sink Compound, Dow Corning Corp.) was used to provide good thermal contact between the plates and between the thermocouples and the plates. This grease was applied to one side of each disk before placing the thermocouples using a small, thin, flat board. The silicon was spread out down until its thickness appeared uniform, with no gaps or clumps.

A resistance heater was placed between the middle two disks, and two additional thermocouples were placed on each side of the heater, again using the silicon grease between the heater and the composite plates. The disks were stacked so that the total thickness on either side of the heater was approximately equal. The stacked composite disks instrumented with thermocouples and the resistance heater, were then placed between the two aluminum cylinders, and two thermocouples were placed at each of the composite disk-aluminum cylinder interfaces. The entire assembly was then pressed together between two 14 cm by 14 cm by 4 mm aluminum plates. Pressure was applied through threaded rods which ran through the corners of the aluminum plates. A photograph of the experimental set-up is shown in Figure 4.11.



Fig

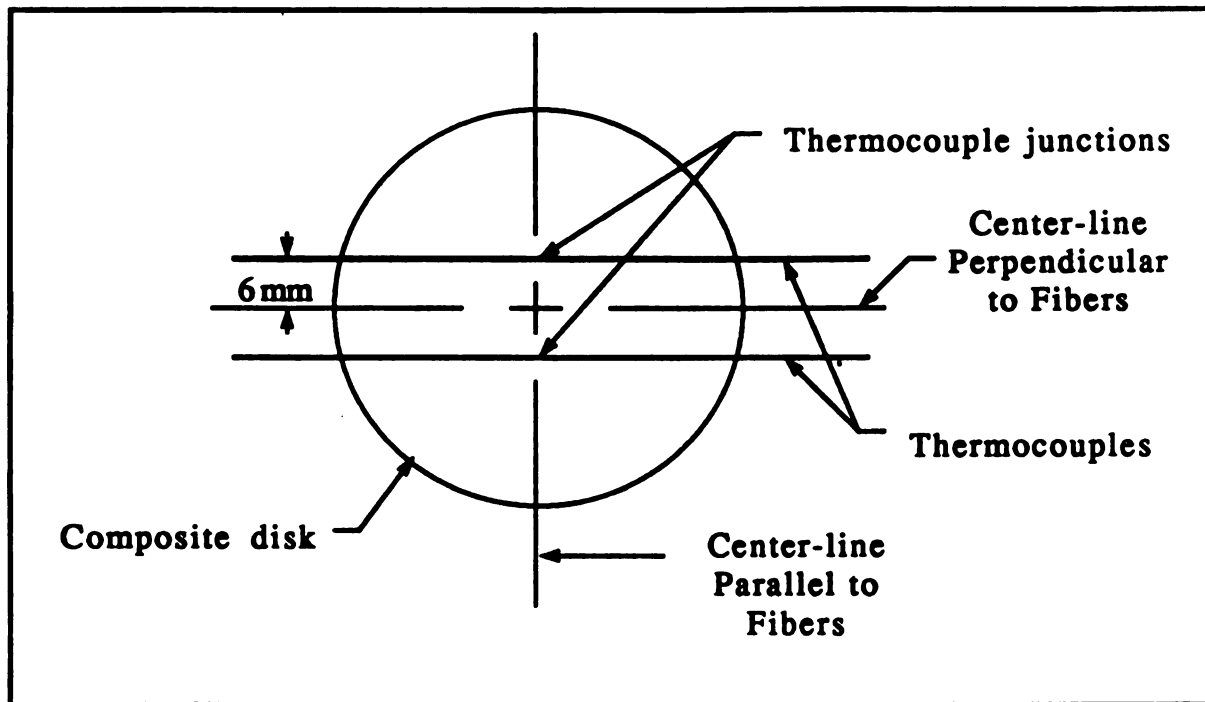


Figure 4.10 Thermocouple Placements on Composite Disks Used in Transient Temperature Experiments.

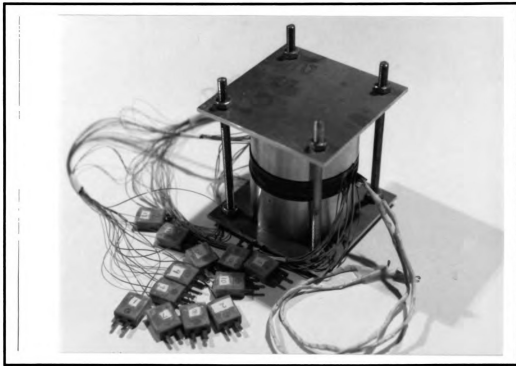


Figure 4.11 An Experimental Set-up for Transient Temperature Measurements using Cured Composite Samples.

4.1

11/

ing

amp

sign

tion

hea

4.1

DT

sup

wa

enc

int

4.

th

ar

al

D

f

c

a

J

4.1.3 Data Acquisition System and Controlled Heat Flux

Temperature measurements from the thermocouples were recorded using a PDP 11/05 microcomputer (Plessey Peripheral Systems) running under an RT-11/V4 operating system. The signal from the thermocouples was conditioned through the use of amplifiers prior to being read by the RT-11/V4 system. The data acquisition hardware, signal conditioning, and data acquisition software are described in the following sections. A schematic of the data acquisition system and power supply for the controlled heat flux is shown in Figure 4.12.

4.1.3.1 Data Acquisition Hardware

The PDP 11/05 was equipped with an analog-to-digital (A/D) converter (Model DT2764) and a real-time clock/counter unit (Model DT2769). Both of these units were supplied by Data Translation, Inc. The full scale input voltage on the A/D converter was configured to operate from 0 to 10 V, with a gain of one and with eight differential ended input channels. The clock unit was a programmable unit which determined the intervals of count events. Details of these devices are given by Osman (1987).

4.1.3.2 Signal Conditioning

Since the signal produced by the thermocouples was on the order of millivolts and the A/D operated on a scale from 0 to 10 V, a signal conditioning unit was required to amplify the thermocouple signals prior to processing by the A/D converter. This unit, also supplied by Data Translation, Inc., consisted of a ± 15 V power supply (Model DT7692), a backplane board (Model DT750), and eight amplifiers (Model DT6705E).

Each amplifier was instrumented with an electronic cold junction compensation for ANSI Type E thermocouples. In this case, the extension thermocouple wires were connected directly to the channel trip on the DT750 backplane. The gain of the amplifiers was set at 1000, and before each experiment, the zero calibration was adjusted using the calibration screws on the front panel of each amplifier.

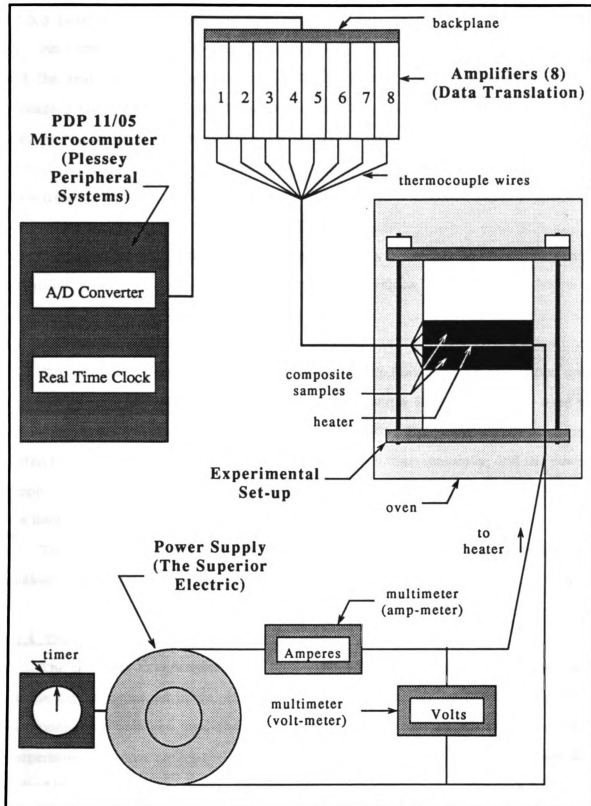


Figure 4.12 Schematic of Data Acquisition for Transient Experiments using Cured Composite Samples.

4.1.3.3

A

and the

package

used to

'sweep'

clock in

1987).

Ar

output f

4.1.3.4

Th

tem. A

supply t

ected to

supply w

was limit

To

measure

4.1.4. The

Th

ing the e

condition

tempera

each of t

1.

4.1.3.3 Data Acquisition Programs

An existing program, *DATAcq* (Osman, 1987), was used for controlling the A/D and the real-time clock-counter units. The program utilizes a real-time software package, *DTLIB/RT*, provided by Data Translation, Inc. (1981). The real-time clock was used to trigger the A/D converter at user designated intervals. The A/D operated in a 'sweep' mode, in which the input channels 0 through 7 were read sequentially on each clock trigger. The time required for each sweep was less than 0.002 seconds (Osman, 1987).

An adjoining program, *DATFIT* (Osman, 1987), was used to convert the binary output from the thermocouple readings to temperature values.

4.1.3.4 Controlled Heat Flux

The resistance heater was controlled independently from the data acquisition system. A Powerstat^R Variable Autotransformer (The Superior Electric, Co.) was used to supply the power requirements for the resistance heater. The power supply was connected to a timer; during operation, the timer was switched on manually, and the power supply was activated for a preset interval on the timer. The maximum heating interval was limited to 60 seconds using this timer.

To measure the applied heat flux, two multimeters (Keithley Co.) were used to measure the current to the heater and the voltage drop across the heater (Figure 4.12).

4.1.4 Transient Temperature Experiments

The transient experiments using the cured composite samples consisted of placing the experimental set-up in an oven at the desired temperature until steady-state conditions were obtained, and then activating the heater and recording the resulting temperature response using the data acquisition program. The procedures used for each of these experiments were as follows:

1. The experimental assembly was placed in an oven; then the thermocouples

w
t
h
2
s
w
s
3
P
t
b
f
a

4.1.5

7

cured
ambie:
heat fl
total n

pling
tempe
peratu

4.1.4.
resiste

Power
about
to 20:

were connected to the extension cables wired to the backplane of the data acquisition system; the heater was wired to the power supply; and, the assembly was heated to the desired testing temperature (this usually took two to three hours).

2. The data acquisition program was started, and the experimental parameters, such as sampling rate, total experimental time, and number of thermocouples, were entered. The total heating time was set on the timer connected to the power supply.

3. Data acquisition commenced upon an external input to the data acquisition program. At the same time the data collection was started, a stop watch was activated. The heater was manually started 20 seconds after each experiment was begun, and the voltage and amperage readings were recorded every five seconds for the duration of the heating interval. Data collection continued on the data acquisition program until the end of the total experimental time.

4.1.5 Experimental Parameters

The experimental parameters in the transient temperature experiments using cured composite materials included total experimental time, data sampling interval, ambient temperature, heating time interval for the resistance heater, magnitude of the heat flux, fiber orientation with respect to heat flux, number of thermocouples and the total number of repetitive experiments for each set of parameters.

The total experimental time was set at 200 seconds, with a one second data sampling interval for all cases. The experiments were conducted at five different ambient temperatures: 25 (or room temperature), 50, 75, 100, and 125°C. The ambient temperature conditions above 25°C were conducted using the oven as described in Section 4.1.4. These temperatures served as the initial temperatures for each run since the resistance heater heated the composite samples above these temperatures.

The heating time interval was set at 40 seconds, using the timer connected to the Powerstat^R power supply, and the output power from the power supply was adjusted to about 28-29 watts. This resulted in a maximum temperature rise of approximately 15 to 20°C above the initial temperature.

as dis
propo
perpe
result
noted
the e
volum

moco
the o
there
ones
moco
very

paran
stack
show

4:6

meas
Optim
1988
sign
perpe
micro
the dig
After a

The fiber stacking angles investigated were $[0^\circ]_{24}$ and $[0, 30, -30, 60, -60, 90^\circ]_{2(\text{sym})}$, as discussed previously. This study was limited to the estimation of the thermal properties transverse to the fiber direction, so in all cases the heat flux was assumed perpendicular to the fiber axis. Therefore, it was anticipated in this case that similar results would be obtained for the two different fiber stacking angles. It should also be noted that the orientation of the fibers is only pertinent with respect to the estimation of the effective thermal conductivity, since the density-specific heat product is a volumetric term, and should not depend on fiber orientation.

Twelve thermocouples were used in each experimental set-up, with two thermocouples at each disk interface with the aluminum cylinders, the heaters, and with the other disks. Only six amplifiers were available on the data acquisition system; therefore, only six thermocouples were actually used for data collection, the remaining ones were installed as a precautionary measure in case one or more of the other thermocouples broke. (Due to the small diameters of these thermocouple wires, they broke very easily.)

Each experiment was repeated at least six times using the same experimental parameters. The experimental parameters for each set of experiments, including fiber stacking angle, stacking order for the disks, temperature, and number of repetitions are shown in Table 4.2.

4.1.6 Fiber Volume Fraction

The fiber volume fractions of disk numbers 5, 6, and 8 (in Table 4.1) were measured by personal at the Composite Materials and Structures Center using an Optimal Numerical Volumetric Analysis (ONVfA) technique developed by Waterbury (1988). In this technique, the density of the samples were first measured by an immersion weighing technique. The samples were then cut through the thickness perpendicular to the fibers and polished. The polished surface was placed under a microscope, and the image was digitized. The fiber volume fraction was calculated from the digitized image, the measured density, and the published densities of the individual fiber and epoxy components, using the ONVfA software developed by Waterbury. These

Ex
1

2

3

4

5

6

7

8

9

10

11

12

13

14

15

16

17

18

Table 4.2 Experimental Parameters for Transient Experiments using Cured Composite Samples.

Exper. No.	Initial ^a Temp. (°C)	Fiber Orientation	Disk Numbers ^b	No. of Repetitions
1.1	29 - 32	$[0^\circ]_{24}$	3,2,1,4	9
1.2	53 - 54	$[0^\circ]_{24}$	3,2,1,4	6
1.3	76 - 78	$[0^\circ]_{24}$	3,2,1,4	6
1.4	101 - 103	$[0^\circ]_{24}$	3,2,1,4	6
1.5	126 - 128	$[0^\circ]_{24}$	3,2,1,4	9
1.6	25 - 29	$[0^\circ]_{24}$	1,4,3,2	6
1.7	49 - 52	$[0^\circ]_{24}$	1,4,3,2	12
1.8	75	$[0^\circ]_{24}$	1,4,3,2	6
1.9	100	$[0^\circ]_{24}$	1,4,3,2	6
1.10	126	$[0^\circ]_{24}$	1,4,3,2	6
1.11	26 - 27	$[0^\circ]_{24}$	5,8,7,6	6
1.12	52 - 53	$[0^\circ]_{24}$	5,8,7,6	6
1.13	75 - 77	$[0^\circ]_{24}$	5,8,7,6	6
1.14	100	$[0^\circ]_{24}$	5,8,7,6	6
1.15	125	$[0^\circ]_{24}$	5,8,7,6	6
1.16	25 - 29	$[0,\pm30,\pm60,90^\circ]_{2(sym)}$	10,11,12,9	12
1.17	52 - 53	$[0,\pm30,\pm60,90^\circ]_{2(sym)}$	10,11,12,9	6
1.18	78	$[0,\pm30,\pm60,90^\circ]_{2(sym)}$	10,11,12,9	6
1.19	25 - 31	$[0,\pm30,\pm60,90^\circ]_{2(sym)}$	11,10,9,12	6
1.20	49 - 53	$[0,\pm30,\pm60,90^\circ]_{2(sym)}$	11,10,9,12	6
1.21	76 - 77	$[0,\pm30,\pm60,90^\circ]_{2(sym)}$	11,10,9,12	6

a. Initial laminate temperatures in experiments.

b. Disk numbers refer to Table 4.1. They are listed in stacking order, from top to bottom.

results were
the matrix
results for
volume fraction

4.2 Differences

Differences
estimate the
resin. The
3.2. The es
obtain the
periments to
calculate the
parameters

Sample

cause the re
and it would
inhomogeneous
presence of t
by the obser
fibers had on

The sam
tal parameter

4.2.1 Sample

Sample
epoxy resin, t
pans with lid
equipment op

results were compared with those obtained using an acid digestion technique, in which the matrix material is dissolved away, so that the remaining fibers can be weighed. The results for both the ONVfA analysis and the acid digestion analysis, including the fiber volume fraction, the void volume fraction, and the density, are shown in Table 4.3.

4.2 Differential Scanning Calorimetry Experiments

Differential scanning calorimetry (DSC) experiments were conducted in order to estimate the kinetic parameters associated with the curing of EPON 828/MPDA epoxy resin. These parameters are those shown in the kinetic models described in Section 3.2. The estimation of the parameters required several isothermal DSC experiments to obtain the heat of reaction at different temperatures, and dynamic or ramped DSC experiments to determine the total heat of reaction. The heat of reaction data was used to calculate the total heat of reaction and the degree of cure, from which the kinetic parameters were estimated as described in Section 3.2.

Samples of neat resin rather than prepreg were used in these experiments, because the required sample size for DSC experiments was small (on the order of 10 mg), and it would have been very difficult to insure consistent sample composition due to the inhomogeneous nature of the prepreg. In using the neat resin, it was assumed that the presence of the fibers had no effect on the cure kinetics. This assumption was justified by the observations of Mijović and Wang (1989) who found that the presence of carbon fibers had only a very small initial effect on the cure kinetics.

The sample preparation method, the experimental procedures and the experimental parameters for the DSC experiments are presented in the following sections.

4.2.1 Sample Preparation for DSC Experiments

Sample preparation for the DSC experiments involved the preparation of the epoxy resin, the placement of the resin in small special pans, and the closure of the pans with lids. These lids and pans were especially designed for use with the DSC equipment operated in this study.

Table 4.3
Numerical

Plate No. ^a	De (x)
5	1
6	1
8	1
10 ^b	1

a. Plate

b. CNVFA

Table 4.3 Fiber Volume Fractions using Acid Digestion Analysis and Optical Numerical Volumetric Analysis (ONVfA).

Plate No. ^a	Density (kg/m ³)	Acid Digestion			ONVfA		
		Fiber Vol. Fr.	Matrix Vol. Fr.	Void Vol. Fr.	Fiber Vol. Fr.	Matrix Vol. Fr.	Void Vol. Fr.
5	1,538.	66.2%	28.6%	5.1%	65.7%	29.3%	5.0%
6	1,531.	64.9%	30.2%	5.0%	66.4%	29.4%	4.2%
8	1,563.	64.7%	32.9%	2.4%	68.5%	28.0%	3.5%
10 ^b	1,570.	64.3%	32.4%	3.3%	--	--	--

a. Plate number corresponds to disk number in Table 4.1.

b. ONVfA analysis not appropriate for the quasi-isotropic plates.

The pans and lids designated for use with liquid samples were initially weighed and separated according to weight, and the epoxy was prepared according to the procedures in Section 4.1. Once the epoxy was mixed, several 3cc Becton Dickson single use syringes were filled with the epoxy and placed in a freezer until needed. To prepare a sample for a DSC experiment, approximately 10 mg of epoxy was placed in the center of a tarred pan using the syringe. The weight of the epoxy was then measured and recorded. A lid was placed on the pan, and the pan and the lid were crimped and hermetically sealed together using a crimper for liquid DSC pans (DuPont Instruments, Inc.). Each experiment required a reference pan containing no resin, so a second pan and lid of approximately the same weight as the empty sample pan and lid were also crimped and sealed together. The syringe was placed back in the freezer until further use.

4.2.2 Differential Scanning Calorimeter Operation

A DuPont Instruments Thermal Analyzer System 9900 coupled with a 910 Differential Scanning Calorimeter were used for these experiments. The DuPont 910 Calorimeter is shown in Figure 4.13. The operation procedure consisted of a set up procedure, in which the experimental parameters for each experiment were entered, an initialization procedure, in which the experiment was begun, and after the experiment was completed, a post-processing procedure. These procedures are discussed in the following sections.

4.2.2.1 Differential Scanning Calorimeter Set Up Procedure

The DuPont System 9900 software is menu driven, and the experimental parameters for each experiment were entered using two of these menus: the Sample Info menu and the Select Method menu.

The Select Method menu contains a number of different time-temperature profiles which can be edited to fit the users needs. (The program stores approximately 17 different methods, and each of these methods is designated by a number.) In the Sample



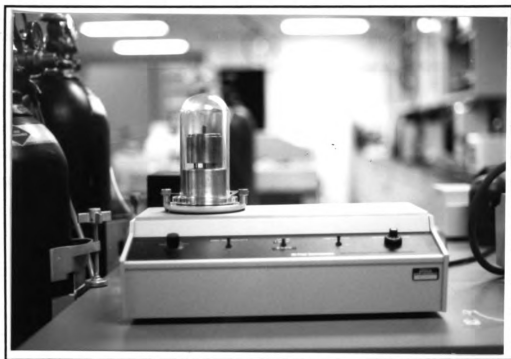


Figure 4.13 DuPont Instruments 910 Differential Scanning Calorimeter.

Info menu, the output data file name is entered, along with the sample weight, the user name, and the method number from the Select Method menu.

In setting up a method in the Select Method menu, several different segments for the time-temperature histories were used. These included INITIAL, ISOTHERMAL, SAMPLING INTERVAL, and RAMP. In the INITIAL segment, the calorimeter cell is heated rapidly to some designated temperature, and it is held at that temperature until prompted by an external trigger by the user to the thermal analysis program; at which time the program proceeds to the next segment. In the ISOTHERMAL segment, the cell is held at its existing temperature for a designated time. The SAMPLING INTERVAL segment is used to set the sampling rate for data collection. In the last segment, RAMP, the cell was heated at a designated rate (i.e., 5°C/min) to a designated temperature.

Using these different segments, the method for the dynamic or ramped temperature experiments was set up as follows:

1. INITIAL: 25°C
2. SAMPLING INTERVAL: 1.0 second
3. ISOTHERMAL: 1 minute
4. RAMP: 5°C/minute to 220°C

In this case, the DSC cell was first initialized at 25°C, and the sampling interval was set to collect data at one second intervals. Upon external trigger to the thermal analysis program, the cell was held at 25°C for one minute, then the temperature was increased linearly at a rate of 5°C/minute until it reached 220°C, at which time the experiment was completed and the cell cooled down to the room temperature.

Similarly, the isothermal experiments were set up using the INITIAL, SAMPLING INTERVAL, and ISOTHERMAL segments to define the time-temperature history.

4.2.2.2 Initialization Procedure for the DuPont 910 Calorimeter

The dynamic experiments were begun after all the necessary parameters had been entered in the Thermal Analysis program. To start the initialization procedure, the bell jar, the cell cover, and the ceramic lid were removed from the DSC cell, and the sample pan and the reference pan were placed on the calorimeter cell as shown in Figures

4.14a.b. The

were replaced

cc/minute.

through the

The

achieve is

mize the

preheated

for the nit

started, and

and sample

were replaced

after the IS

4.2.2.3 Po

After

sociated w

In e

reaction r

of reaction

The heat

were ther

for one re

In e

the heat

routine.

fully cur

of reacti

off, the

format f

4.14a,b. The pans were covered by the ceramic lid, then the cell cover and the bell jar were replaced, and a nitrogen atmosphere was induced into the bell jar at a rate of 50 cc/minute. The data acquisition and controlled heating cycle was then initiated through the thermal analysis program.

The isothermal experiments were initiated differently. Since it was desired to achieve isothermal conditions throughout these experiments, it was important to minimize the heating time for the sample. To do this, the calorimeter cell was first preheated to the desired temperature using the INITIAL segment, and the rate was set for the nitrogen atmosphere into the bell jar. The ISOTHERMAL segment was then started, and the bell jar, the cell cover, and the ceramic lid were removed. The reference and samples pans were then placed in the calorimeter cell, and the jar, cover, and lid were replaced as quickly as possible. The time required to complete these maneuvers after the ISOTHERMAL segment was started was approximately 30 to 40 seconds.

4.2.2.3 Post-Processing Procedure

After the completion of each experiment, several post-processing programs associated with the Thermal Analysis System were utilized.

In each repetition of the dynamic DSC experiment, the area under the heat of reaction rate curve was integrated, and the total area under each curve or the total heat of reaction for that experiment, was determined using the Thermal Analysis software. The heat of reaction rate data and the integrated data (the cumulative heat of reaction) were then plotted using the Thermal Analysis plotting subroutines. The resulting plot for one repetition of the dynamic DSC experiment is shown in Figure 4.15.

In each of the isothermal experiments, the associated baseline was subtracted off the heat of reaction rate curve, and the results were plotted using the plotting subroutine. A baseline consists of the heat of reaction data for a sample after it has been fully cured, assuming the same curing method; it serves as a reference line for the heat of reaction rate data of the samples during curing. After the baseline was subtracted off, the modified heat of reaction rate data was then transferred to a floppy disk in ASC format for later processing.



Figure 4.14a DuPont Instruments 910 Differential Scanning Calorimeter Cell (left), Showing Bell Jar (right), Cell Cover (center), and Ceramic Lid (on cell)



Figure 4.14b Close-up View of Sample Pan (right) and Reference Pan (left) in Calorimeter Cell Shown Above.

Sample: TMA25.220.01
Size: 19.0000 mg
Method: 25 C-220 C 5 /C/MIN
Comment: 25°C-220C AT 5C/MIN

DSC

File: A: THREEPS.02
Operator: SCOTT
Run Date: 05/09/89 14:02

Sample: THR25_220.01
 Size: 19.0000 mg
 Method: 25 C-220 C 5 C/MIN
 Comment: 25°C-220C AT 5C/MIN

DSC

File: A:THREPS.02
 Operator: SCOTT
 Run Date: 05/09/89 14:02

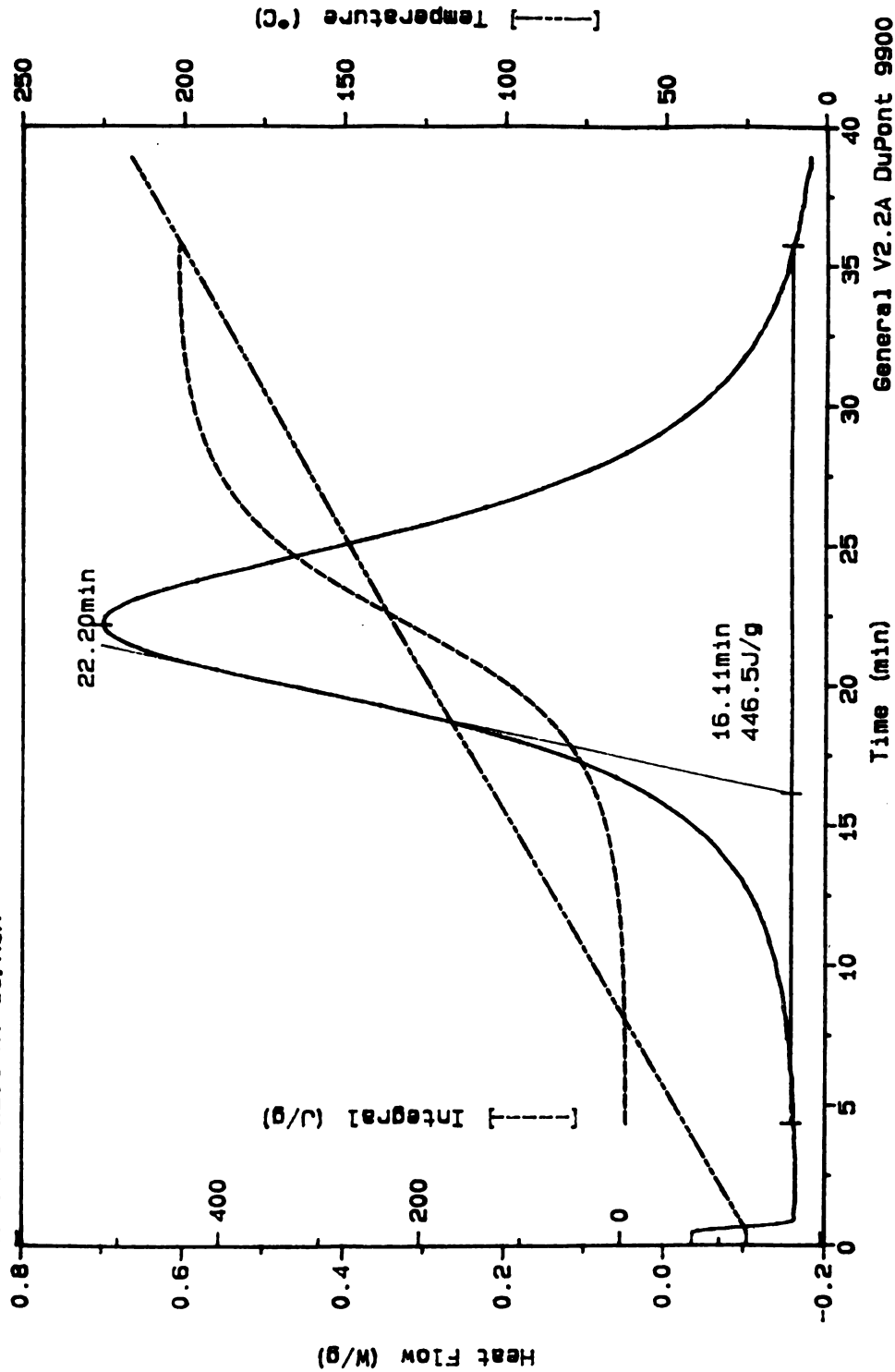


Figure 4.15 Heat of Reaction Data from One Repetition of the Dynamic DSC Experiment using DuPont Thermal Analysis Plotting Subroutines

4.2.3. Experiments

Four

were conducted

experiments were

experimental

minutes.

The

procedure described

procedure

10°C below

heated at

the temperature

selected is

reaction conditions

isothermal

were conducted

temperature.

Preliminary

temperature

experiments

4.2.3 Experimental Parameters

Four different sets of isothermal experiments and one set of dynamic experiments were conducted using the DuPont Thermal Analyzer System 9900. The dynamic experiments were conducted using the segment methods discussed in Section 4.2.2. These experiments were repeated eight times, with each experiment running for about 40 minutes.

The four temperatures for the isothermal experiments were chosen using the procedure described by Sichnetz (DuPont Applications Brief No. TA-93). Using this procedure, the isothermal temperatures were chosen from an interval defined between 10°C below the onset of cure and a point midway to the peak maximum of a thermoset heated at a rate of 5°C/min. Since the dynamic experiments followed this heating rate, the temperatures were selected using these thermosets. Sichnetz recommended that the selected isothermal temperatures be 5°C to 10°C apart. Figure 4.16 shows a heat of reaction curve from one of the dynamic DSC experiments with the interval for the isothermal temperatures indicated. Based on this interval, the isothermal experiments were conducted at 60°C, 70°C, 100°C, and 110°C, with three repetitions at each temperature.

Preliminary experiments were run to establish the required curing time at each temperature. The resulting time-temperature segments used for each set of isothermal experiments are given below.

60°C: INITIAL: 60°C

SAMPLING RATE: 2 seconds

ISOTHERMAL: 300 minutes

70°C: INITIAL: 70°C

SAMPLING RATE: 2 seconds

ISOTHERMAL: 240 minutes

100°C: INITIAL: 100°C

SAMPLING RATE: 1 second

ISOTHERMAL: 90 minutes

110°C: INITIAL: 110°C

Sample: THA25_220.01
Size: 19.0000 mg
Method: 25 C--220 C 5 /C/MIN
Comment: 25°C--220C AT 5C/MIN

DSC

File: A: THREPS.02
Operator: SCOTT
Run Date: 05/09/89 14:02

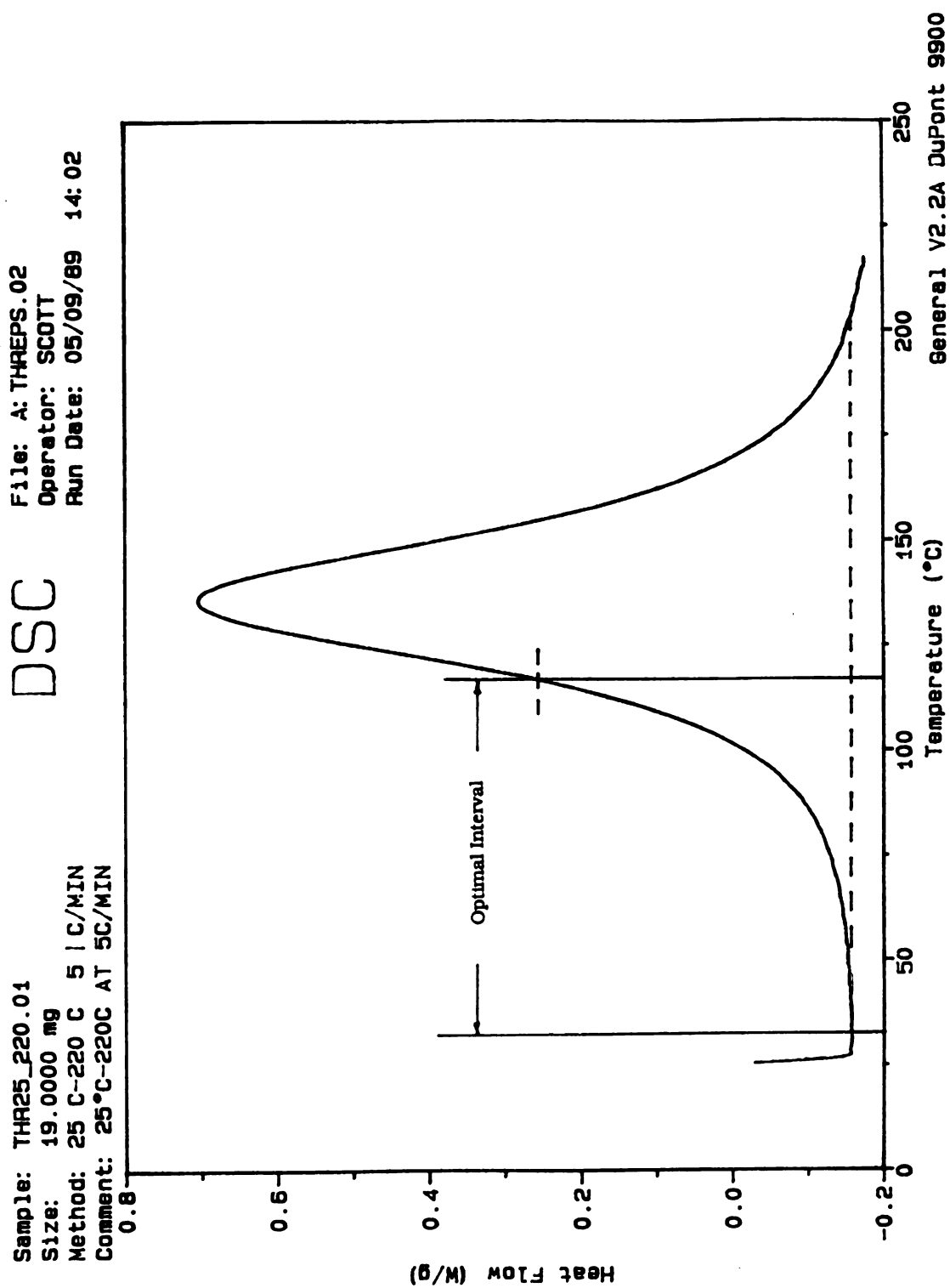


Figure 4.16 Determination of Temperatures for Isothermal DSC Experiments from a Dynamic DSC Experiment

Each of the

sample pa

A su

ber of repe

4.3 Trans

The

those desc

composite

were taken

with therm

conducted

data acquis

VAXstation

acquisition

amplifiers a

periments w

one addition

3.2 under six

In each

curing proce

so that each

shorter exper

ing sub-secti

SAMPLING RATE: 1 second

ISOTHERMAL: 60 minutes

Each of the above isothermal segments was also repeated once using a previously cured sample pan to establish a baseline for each temperature regime.

A summary of the DSC experiments, including the time, temperature, and number of repetitions is shown in Table 4.4.

4.3 Transient Temperature Measurements during Curing

The transient temperature experiments discussed in this section were similar to those described in Section 4.1 for the transient temperature experiments using cured composite samples; however, in these experiments, the temperature measurements were taken during the curing process; therefore, the prepreg laminate was instrumented with thermocouples and heaters during the stacking process. Two experiments were conducted using the procedures described in this section. In the first experiment, the data acquisition procedure was similar to that described in Section 4.1.3, except that a VAXstationII/GPX microcomputer was used instead of the Plessey system. A new data acquisition procedure was developed for the second experiment which included new amplifiers and a new computer controlled power supply for the heaters. These two experiments will be referred to as Exp. 3.1 and Exp. 3.2 in subsequent chapters. Finally, one additional experiment (Exp. 3.3) was conducted using the cured samples from Exp 3.2 under similar experimental conditions.

In each experiment, the heaters were activated at regular intervals throughout the curing process. In the analysis, procedure, these intervals were considered separately, so that each curing experiment could be considered as a combination of 15 to 20 shorter experiments. The procedures used for these experiments are given in the following sub-sections.

Table 4
Experiments

Expe No
2.1
2.2
2.3
2.4
2.5

- a. For
- b. Dec

Table 4.4 Experimental Parameters for Differential Scanning Calorimetry Experiments.

Exper. No.	Experiment Type	Temperature (°C) (Heating Rate) ^a	Time (min)	No. of Repetitions ^b
2.1	Dynamic	25°C-220°C (5°C/min)	39	8
2.2	Isothermal	60°C	300	3
2.3	Isothermal	70°C	240	3
2.4	Isothermal	100°C	90	3
2.5	Isothermal	110°C	60	3

a. For dynamic experiments only.

b. Does not include experiments to establish baselines.

4.3.1.1

P

fibers.

proceed

outlined

heaters

the pro

and the

4.3.1.1

The

tion in t

Inc.) we

and hel

Coming

sheet of

compound

distribut

4.3.1.2

The

during th

and then

mented s

prepreg

smooth a

placed in

described

tion of t

4.3.1 Sample Preparation

Prepregs, composed of EPON 828/mDPA epoxy and continuous AS4 carbon fibers, were also used in these experiments. The epoxy was prepared according to the procedures in Section 4.1.1.1, and the prepregs were prepared following the procedures outlined in Section 4.1.1.2. The prepreg plies were stacked with thermocouples and heaters embedded between the plies; these thermocouples were prepared according to the procedure given in Section 4.1.2.1. The preparation procedure for the heaters and the stacking process are discussed in the following sub-sections.

4.3.1.1 Heater Preparation

Thin, flat, resistance heaters were used to supply the heat flux boundary condition in the transient experiments. Two 7.6 ohm Thermofoil[®] heaters (Minco Products, Inc.) were laid on top of each other so that the heating elements were not overlapping and held in place using a very thin layer of the Silicon Heat Sink Compound (Dow Corning Corp.). The heated surface of the heaters measured 12.4 cm by 9.8 cm. A sheet of aluminum foil was cut and adhered to each side of the heaters using the silicon compound to protect the heaters from the epoxy resin and to insure a uniform heat distribution.

4.3.1.2 Stacking Procedure

The prepreg was instrumented with the thermocouples and the resistance heaters during the stacking procedure. Forty-four plies were cut from each prepared prepreg, and then they were stacked with the fibers parallel to each other ($[0^\circ]_{44}$) and instrumented symmetrically with the thermocouples and the heaters. The instrumented prepreg laminate was set between porous Teflon[®] cloths, bleeder cloths, and flat, smooth aluminum plates covered with release ply, and then the entire assembly was placed in a vacuum bag for curing. This procedure is very similar to the procedure described in Section 4.1.1.3, with some important differences, such as the instrumentation of the laminate with the thermocouples during the stacking process, and the

includ:

this pr

1.

b

b

le

2.

be

in

3.

pl

for

a s

4.

alu

5.

pla

sp

wa

6.

off

Th

me

of

7.

jur

the

des

hea

to

inclusion of the bleeder and Teflon^R cloths on both sides of the laminate. An outline of this process follows.

1. Two 15.2 cm by 17.8 cm pieces were cut from the porous Teflon^R cloth, the bleeder cloth, and the release ply plastic. In addition, a small piece of thick bleeder cloth (approximately 8 cm by 10 cm) and piece of vacuum bag material at least 40 cm by 66 cm were cut.
2. The prepreg was taken out of the freezer, and allowed to cool just enough to become pliable (approximately 5 minutes), and dry ice was obtained and chopped into small chunks.
3. The prepreg was spread out on a sheet of foil, and a piece of poster board was placed under the section to be cut. Using a carpenters square as a guide, forty-four 10.2 cm by 12.7 cm plies were cut from the prepreg using a utility knife with a sharp blade.
4. One piece of the release ply was adhered to a smooth 23 cm by 23 cm aluminum plate, using small amounts of Tacky Tape^R at the corners.
5. Several prepreg plies were laid out on the foil, and the remaining pieces were placed back in the freezer until needed. Using thermal gloves, the dry ice was spread over the pieces of prepreg, and one of the release plies on each prepreg ply was removed, taking care not to peel off any fibers with the plastic.
6. After any frost which had accumulated on the exposed surface had evaporated off, two prepreg plies were stacked together with the fibers parallel to each other. This process was repeated with the other plies, except that some plies were instrumented with thermocouples, and a resistance heater was placed at the mid-plane of the plies (step 7.).
7. The plies were instrumented with thermocouples by placing the thermocouple junction at the center of the exposed prepreg surface, with the exposed portion of the wires oriented perpendicular to the fibers. A second ply was stacked as described above, taking care to keep the thermocouple in place. The resistance heater was placed in between the middle two plies. A roller was used in an effort to remove air trapped between the plies or between the prepreg and the heater.

8. Once the prepreg laminate had been stacked and instrumented, one of the last two release plies was removed, and a piece of porous Teflon^R cloth was centered on the exposed surface. The sample was then placed on top of one of the bleeder cloths placed on the aluminum plate covered with release ply.
9. Cork tape was used to as a dam around the sample. The dam was built up until it was level to the sample thickness; special care was taken not to disturb the thermocouple wires and the heater connectors.
10. The last release ply was removed from the sample, and the exposed surface was covered with the second pieces of porous Teflon^R and bleeder cloth. Finally, the aluminum plate covered with release ply was placed on top of the bleeder cloth. A stacked composite laminate, with the porous Teflon^R and bleeders cloths cut away to expose the thermocouples at the surface, is shown in Figure 4.17. (This photograph was taken after curing.)
11. The entire assembly was placed on one half of the vacuum bag material and the other half of the sheet was folded over the assembly. Tacky Tape^R was used to seal the bag, and a short rubber hose (approximately 12 cm long) was placed at one end. The remaining piece of thick bleeder cloth was placed over the mouth of the tube and held in place with Tacky Tape^R. The assembly was checked visibly for leaks, and extra tape was added where needed, especially around the rubber tube. A stacked and instrumented laminate, sealed in a vacuum bag is shown in Figure 4.18.
12. The vacuum bag with sample enclosed was placed in the freezer until ready for curing.

4.3.2 Experimental Set-up

The curing process for thermoset epoxy composites requires both elevated temperatures and applied pressure. The required temperature regime was obtained by curing the stacked prepreg laminate in a laboratory oven (Matheson Scientific), and a mechanical press was designed and built to fulfill the pressure requirements. The required pressure for the type of epoxy used is 689 kPa (100 psi), and the composite

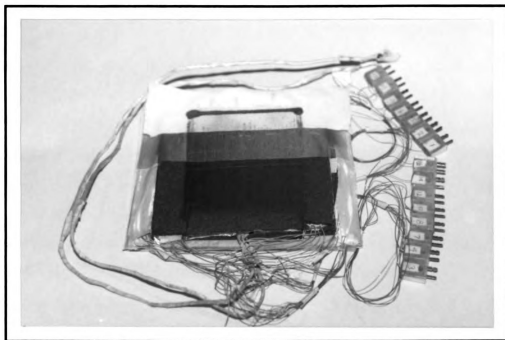


Figure 4.17 Stacked Composite Prepreg, Instrumented with Thermocouples and Heaters. (Photograph taken after curing.)

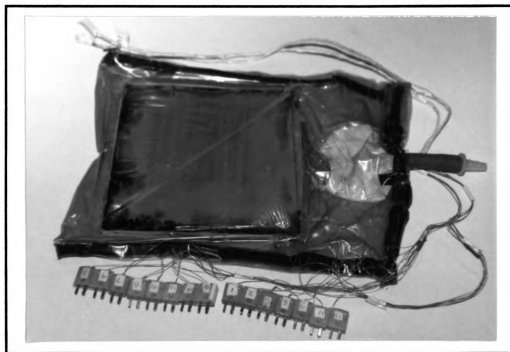


Figure 4.18 Stacked and Instrumented Composite Prepreg Sealed in a Vacuum Bag.

samp

quire

and e

called

the m

held b

nuts.

vacuu

spring

spring

weight

quired

lamina

of Eng

I

in Sec

devices

sides o

hydrau

equipm

4.3.3

ture d

one a

A/D c

conve

posite

samples were approximately 12.7 cm by 10.2 cm (see Section 4.3.3), resulting in a required load on the sample of 890 N.

The press was designed using two 28 cm by 28 cm by 1.2 cm thick steel plates and eight 5 cm compression springs with springs constants of 175 N/cm. The design called for eight 1.3 cm holes to be drilled in each plate, four at each corner, and four at the midplane of each edge, at a location 1.9 cm from each edge. The springs were to be held in place at these locations using 1.3 cm by 12.7 cm long bolts with the appropriate nuts. The press was designed such that the stacked prepreg laminate sealed in the vacuum bag lay between the plates, and the bolts fastened the plates together with the springs on top of the plates. Pressure was applied through the deflection of each spring 0.75 cm, which resulted in a total force from the eight springs of 890 N. (The weight of the upper plate was subtracted from the required load in determining the required deflection for each spring.) A photograph of the press design with the composite laminate in place is shown in Figure 4.19. The press was machined at the MSU College of Engineering Machinery Shop.

It should be noted that preferably the autoclave or the hydraulic press discussed in Section 4.1.1.4 would have also been used in this consolidation process. These devices are preferable because they allow for uniform pressure and temperature on both sides of the composite throughout the curing process. Neither the autoclave or the hydraulic press could be used, however, because the data acquisition system and this equipment were situated in different locations, and none of these could be moved easily.

4.3.3 Data Acquisition and Controlled Heat Flux

The VAXlab system (Digital Equipment Corporation) was used to record temperature data during both the transient temperature experiments. In the first experiment, one analog-to-digital (A/D) converter was utilized, and in the second experiment, two A/D converters and one digital-to-analog (D/A) converter were incorporated. The A/D converters were used to record temperature data from the thermocouples in the composite sample, and in the second experiment, the D/A converter was used to control a

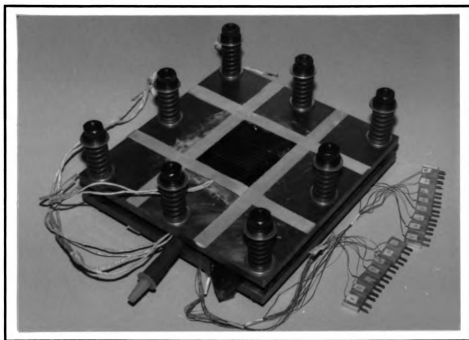


Figure 4.19 Mechanical Press with Composite Laminate in Place.

pow

mod

amp

men

expe

the

to ru

secon

in th

exper

4.3.3.

Equip

board

verter

AXV1

(conti

only t

the fi

which

be us

tache

signal

D/A c

power supply which supplied the heat flux for the resistance heater. The thermocouples produced a signal on the order of millivolts, and amplifiers were used to amplify the signal for the A/D input. New amplifiers were used in the second experiment, while the Data Translation amplifiers (Section 4.1.3.2) were used in the first experiment. Two different computer programs were employed for these experiments. In the first case, the programs used on the Plessey system (Section 4.1.3.3) were modified to run using the VAXlab system subroutines. A new program was developed for the second experiment, using both the A/D and D/A converters.

The details of the data acquisition systems used for the two experiments are given in the following sub-sections. Schematics of the data acquisition systems for the two experiments are given in Figures 4.20 and 4.21.

4.3.3.1 The VAXlab Data Acquisition Hardware

The VAXlab system was run on a VAXstationII/GPX microcomputer (Digital Equipment Corporation). The system hardware included a KWV11-C real time clock board and two AXV11-C combination boards with one A/D converter and two D/A converters each. Each A/D converter was set for a maximum of eight channels. The AXV11-C boards were equipped to run using synchronous (sequential) or asynchronous (continuous) input/output (I/O), however the asynchronous I/O was limited to using only the A/D or the D/A, but not both. Therefore, the asynchronous I/O was used in the first experiment, and the synchronous I/O was used in the second experiment which included a controlled power supply. The KWV11-C is a clock module which can be used to trigger the AXV11-C devices. In the second experiment, the clock was attached to both boards so that there was a total of sixteen available A/D channels. The signal range for the A/D converters was set from 0 to 10 volts, and the range for the D/A converter used in the second experiment was set from -10 to 10 volts.



0

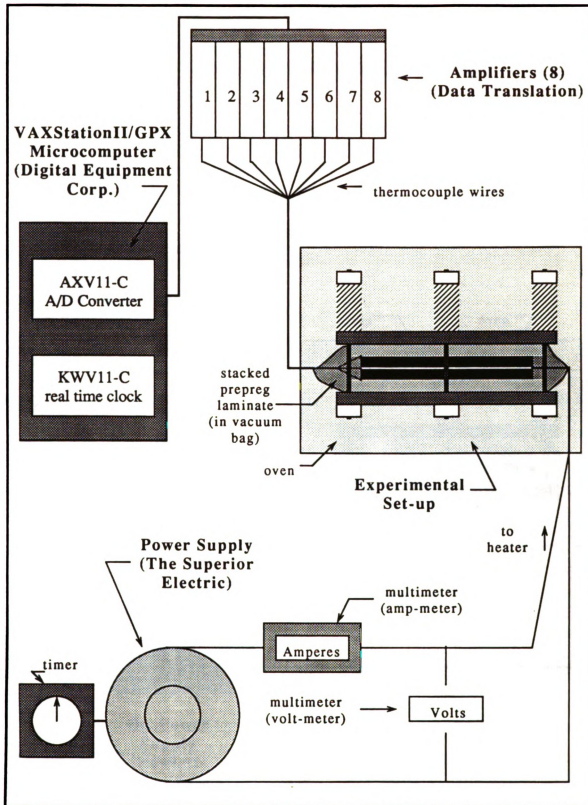


Figure 4.20 Schematic of Data Acquisition for First Transient Experiment during Curing.

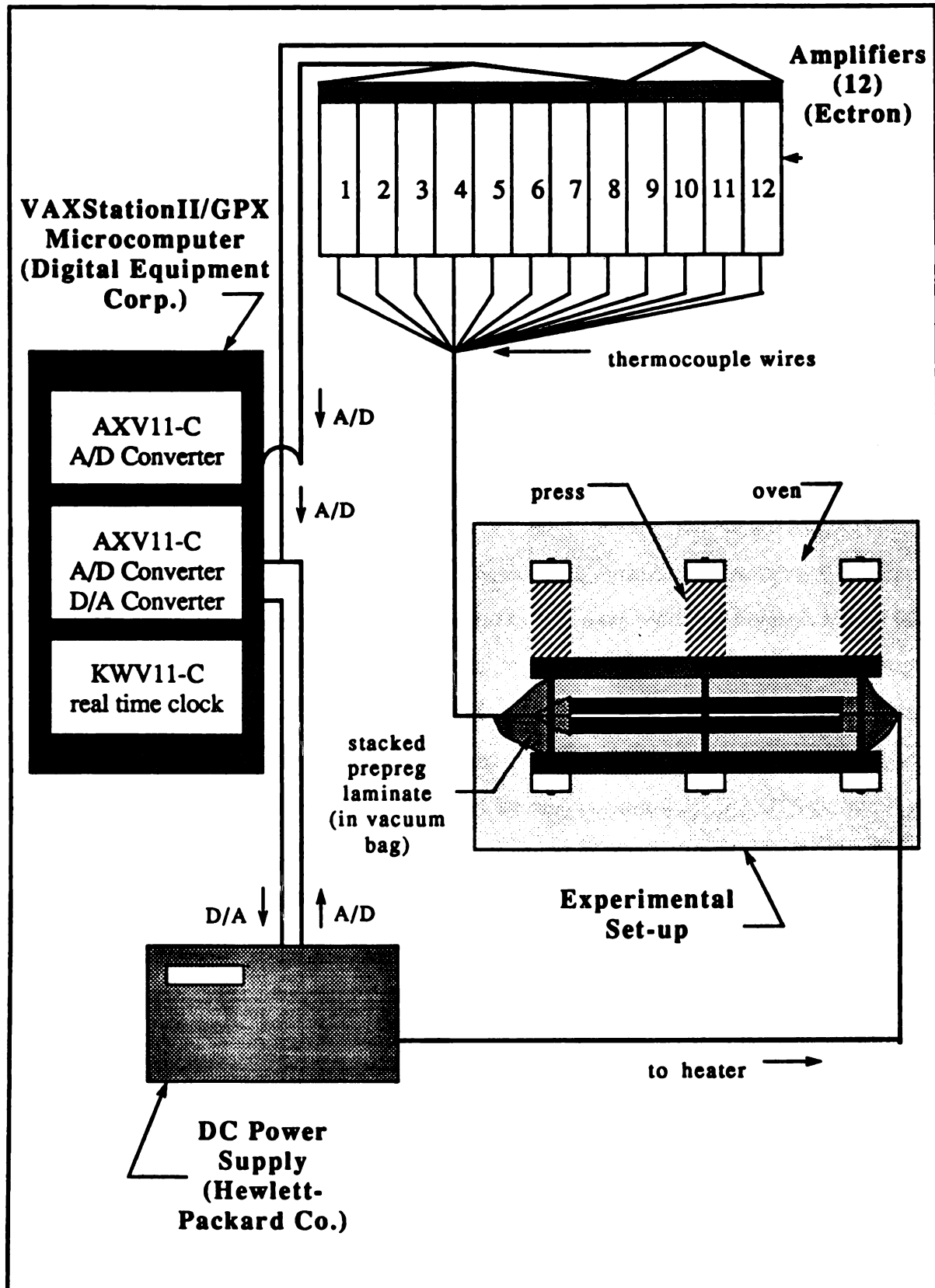


Figure 4.21 Schematic of Data Acquisition for Second Transient Experiment during Curing.

4.3.

rang

sign

for th

687

Model

1000.

quenc

used

amplif

7

Model

amplifi

Adapto

served

attache

an ice p

In this c

Pr

instruct

gain of e

amplifier

amplifier

readings

mined.

The

on the an

potention

4.3.3.2 Signal Amplification

Since the signal from the thermocouples was on the order of millivolts and the range of the A/D converters was from 0 to 10 volts, amplifiers were used to amplify the signals.

The eight Data Translation amplifiers discussed in Section 4.1.3.2 were also used for the first experiment on the composite samples during curing, and twelve new Model 687 DC Amplifiers (Ectron Corporation) were used in the second experiment. These Model 687 amplifiers were equipped with set gains of 10, 20, 50, 100, 200, 500, and 1000, with a vernier adjustment to obtain values between the set points, and the frequency response of these amplifiers was on the order of 3 kHz. A gain of 1000 was used in this case. The remainder of this sub-section focuses on the Model 687 amplifiers.

Two optional accessories, Model 683, Universal Thermocouple Adaptor (UTA), and Model 684, Ambient Temperature Compensator (ATC), were installed on each Model 687 amplifier for operation with thermocouple inputs. The Universal Thermocouple Adaptors were attached to the input connector at the rear of each amplifier, which served as the reference junctions for the thermocouples. The ATC is a card which was attached to the amplifier board and operated in conjunction with the UTA to simulate an ice point reference junction for the particular type of thermocouple used, which was in this case Type E, chromel-constantan.

Prior to use, the gains and zeros of the amplifiers were checked according to the instruction manual for the amplifiers (Ectron Corporation, 1982). To check the actual gain of each amplifier, a power supply with set voltage outputs was connected to each amplifier, bypassing the UTA. Then, one and ten millivolt signals were sent to the amplifier, and the output signals were recorded with the set gain at 1000. From these readings, the fractional differences between the set gain and the actual gain were determined.

The amplifiers were zeroed with the UTA switched off. There are two zero controls on the amplifiers: a referred to input (RTI) potentiometer and a referred to output (RTO) potentiometer. To zero the amplifiers, a jumper was first connected across the signal

input

rem

was

tained

adjust

were

0°C

adjust

4.3.3.

the fir

regula

heater

I

led us

The M

to 60 v

supply

source

The ac

source

was re

the D/

the pow

was sca

input terminals, then the gain was adjusted to 10, and any offset (from zero) was removed using the RTO potentiometer. Then the gain was set to 1000, and any offset was removed using the RTI. This process was repeated until a zero reading was obtained from both RTO and RTI potentiometers.

The actual reference junction temperature was also measured and adjusted. After adjusting the RTO and RTI potentiometers, the UTA was turned on, and thermocouples were connected to the amplifiers. The junctions of the thermocouples were placed in a 0°C electronic ice bath (Omega, Inc.), and the output signals from the amplifiers were adjusted to read 0.0 mvolts using the potentiometer on the UTA card.

4.3.3.3 Controlled Heat Flux

The same power supply apparatus described in Section 4.1.3.4 was also used in the first transient experiment during curing. The timer was operated manually at regular intervals throughout the curing cycle to provide the required heat flux to the heaters.

In the second experiment, the input voltage to the resistance heaters were controlled using a DC power supply (Model 6024A, DC Power Supply, Hewlett-Packard Co.). The Model 6024A is an autoranging 200 W power supply, with an operating range of 0 to 60 volts and 0 to 10 amps, and with remote programming capabilities. The power supply was operated in a constant voltage, voltage control mode, where an input voltage source from 0 to 5 volts produced a proportional output voltage from zero to full scale. The actual output voltage of the power was measured remotely. The input voltage source was obtained from the VaxStationII/GPX D/A converter, and the output voltage was read by one of the A/D converters. Since the voltage ranges for both the A/D and the D/A on the VaxStationII/GPX were set at 0 to 10 volts, the input voltage source to the power supply was scaled to 0 to 5 volts using a 2:1 divider, and the output voltage was scaled from 0 to 60 volts to 0 to 10 volts using a 6:1 divider.

4.3.1

bine

This

Equi

ers.

DATA

a ne

secon

moco

to th

opera

age

Proce

binar

data

the p

the p

routh

SETU

(max

addi

that

ente

heat

tran

pow

desi

4.3.3.4 Data Acquisition Program

The data acquisition programs, *DATAQ* and *DATFIT* (Osman, 1987), were combined and modified to run on the VaxLab system for the first experiment during curing. This new program, *DATAAQ*, utilized the Vaxlab LabStar I/O Routines (LIO) (Digital Equipment Corporation, 1986) to read thermocouple data using one of the A/D converters. The operating mode of this program was similar to that described for *DATAQ* and *DATFIT* in Section 4.1.3.3. The remainder of this section is devoted to the discussion of a new data acquisition program, *DATA_DA_AD* (Appendix B), which was used in the second curing experiment.

DATA_DA_AD was written for the VaxStationII/GPX to read from the thermocouples and the power supply using the two AXV11-C A/D converters, while writing to the power supply using an D/A converter on one of the AXV11-C devices. These operations required the use of the LIO routines. The program converts the binary voltage readings from the thermocouples to temperature using the LabStar Signal-Processing Routines (LSP) (Digital Equipment Corporation, 1986), and it converts the binary voltage readings from the power supply to heat flux. The program also sets up a data file for use in the parameter estimation program, *PROP1D_CURE*. A schematic of the program and its subroutines is shown in Figure 4.22, and a detailed description of the program is now presented.

The parameters required for data acquisition are first entered using the subroutines *SETUP_DATA*, *SETUP_POWER*, and *SETUP_AMP*. In the first subroutine, *SETUP_DATA*, the user enters the sampling interval, the total number of A/D channels (maximum of twelve), and the total number of data points for each channel. In addition, the program allows the user to average data within each sampling interval, so that the number of data points to be averaged over each sampling interval is also entered. In the second subroutine, *SETUP_POWER*, the parameters for the controlled heat flux are entered. These values include the surface heated area of the sample in the transient experiments, the resistance of the heater, and the input voltage data for the power supply, namely, the times at which the power supply is activated, and the desired voltage input corresponding to that time. The D/A is set up in such a way that

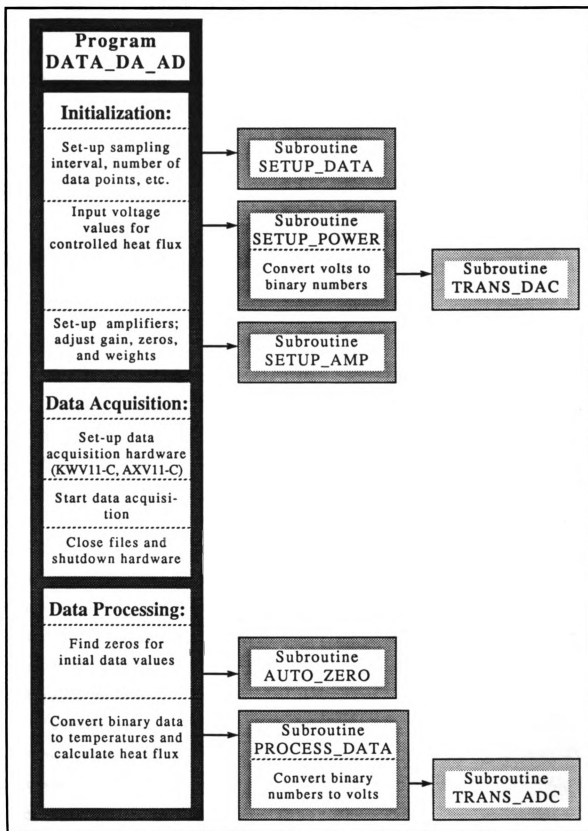


Figure 4.22 Schematic of Data Acquisition Program *DATA_DA_AD*.



once it was activated, it continued to send the same signal until the signal was changed. These data are converted to binary format in subroutine *TRANS_DAC*, where the input 0 to 10 volts are scaled to approximately 0 to 2048 in binary format.

Finally, the 0°C reference junctions, the gains and the weights of the amplifiers can be adjusted in subroutine *SETUP_AMP*. The 0°C reference junctions may be adjusted by the user, or the program will calculate the 'zeros' by averaging the first few data points over a time in which no heat flux is applied, assuming the conditions are isothermal. The gains of the amplifiers can also be adjusted, and a weighting factor is assigned to each amplifier. These values are either set to one or to zero, for the case of a 'bad' amplifier or a broken thermocouple.

Once the initial set up procedure has been completed, the program begins the data acquisition hardware setup, which utilizes the LIO routines. First the devices are attached, including the KWV11-C clock, and the two AXV11-C boards (AXV11-Ca and AXV11-Cb). The clock is then set up to read data at the desired rate, and both AXV11-C devices are set up to read the desired number of channels from the A/D converters. The AXV11-Ca device is set up to sweep through all channels on each clock trigger, while the AXV11-Cb device is set up to trigger on the 'READ' statement of the AXV11-Ca device. The AXV11-Cb is also set to write to the power supply using the D/A converter.

The clock is started by a trigger from the user, and data is read from the A/D converters and written to the D/A converters synchronously. The data is immediately written to a file after it is read, in case of unexpected program interruption. Once the desired number of data points have been read, the program begins the shut down procedure, in which a terminating zero voltage is sent to the power supply, and the clock is stopped, and the devices are detached.

The analysis portion of the program then begins. If indicated, the 0°C reference junctions are calculated in subroutine *AUTO_ZERO*. Here the binary reading from the thermocouples are averaged over the first few time step, and the 'zeros' for each channel are calculated from

$$z_i = (B^{avg} - B_i^{avg}g_i)/n_i$$

where z_i is the 'zero' adjustment for the i th channel, B^{avg} is the average of the binary data over all the channels and over n_t time steps, B_i^{avg} is the same average, but just for the i th channel, and g_i is the gain for the i th channel.

The subroutine *PROCESS_DATA* is used in the rest of the analysis. The data are first converted to voltages using *TRANS_ADC* (0 to 4095 = 0 to 10 volts), and the data from the power supply are adjusted to the actual range of the power supply (0 to 60 volts). The data readings from the thermocouples are then adjusted to account for the gains and the 0°C reference junctions as follows:

$$V_i^* = V_i g_i + z_i$$

where V_i^* is the adjusted voltage for the i th channel and V_i is the unadjusted voltage. These values are converted to °C using one of the signal processing subroutines, *LSP\$THERMOCOUPLE_E*, in the Vax LabStar system, which is specifically for Type E, chromel-constantan, thermocouples. The heat flux associated with the resistance heaters is calculated from the heated area, the resistance of heater, and the voltage measurements. Finally, the time, heat flux, and thermocouple readings in °C are written to a file for use in the parameter estimation program, *PROP1D_CURE*.

4.3.4 Experimental Procedure for Transient Temperature Measurements during Curing

The procedures for the two experiments to measure temperature in the carbon/epoxy composite during curing were similar, except that some of the procedures used in the first experiment were modified in the second experiment due to the purchase of new amplifiers and a new powers supply. In both experiments, the stacked prepreg laminate (Section 4.3.1.2) was cured in the press as described in Section 4.3.2, using the standard cure cycle recommended for this type of composite (Rich, 1987). This cycle included a heating up period from room temperature to 75°C, a two hour isothermal period at 75°C, a second heating period to 125°C, and a two hour isothermal period at 125°C. (This is the same cure cycle used for the disks prepared for the transient experiments using cured composite samples, described in Section 4.1.1.) The

heaters embedded in the laminate were activated at regular intervals throughout the curing cycle. The data acquisition programs were set up to record temperature data continuously throughout the entire cure cycle.

At the beginning of each experiment, the laboratory oven (Section 4.3.2) was first preheated to 75°C, and the appropriate data acquisition program for each experiment was set up. The prepreg laminate, sealed in a vacuum bag, was then taken from the freezer in the Composite Materials and Structures Center and set out at room temperature for about five minutes. A valve was attached to the rubber hose on the vacuum bag, and then it was connected to a vacuum pump. Pressure was reduced in the bag to -99 kPa for ten minutes. At this time the valve was closed, and the vacuum bag, including the short hose and valve, was disconnected from the vacuum pump and transported to Rm. A-32, Research Complex / Engineering as quickly as possible. The vacuum bag was placed in the press, then the press was assembled, and pressure was applied to the laminate through the depression of the springs on the press. Due to the large mass of the press, extra heaters were attached to the top and bottom extremities of the press to reduce the heating time required to heat the press from 25°C to 75°C and from 75°C to 125°C. (These heaters were disconnected during the short heating intervals throughout the isothermal periods.)

The press was then placed in the preheated oven, and the thermocouples were connected to the extension thermocouple cables, and the heaters were connected in parallel to the power supply as quickly as possible. The oven door was closed, and the data acquisition program was started, along with a separate stop watch.

In the first experiment, the same power supply discussed in Section 4.1.3.4 was used. The power supply was disconnected from the timer during the initial heat up period in the curing cycle and during the heat up period from 75°C to 125°C. During these periods, power was continuously supplied to the internal heaters in the stacked laminate and to the heaters fixed on the surface of the press in order to reduce the time required to heat the sample and the press. At the end of the first heat up period, when the laminate temperature was close to 75°C, the power supply was disconnected from the heaters on the press and reconnected to the timer. Using the stop watch to record

events with respect to overall experimental time. The heaters embedded in the laminate were activated at regular intervals using the timer, throughout the isothermal curing period at 75°C. At the end of the first isothermal period, the timer was disconnected, and the oven temperature was set at 125°C. The heaters on the press were reconnected, and power was supplied to the heaters in the same manner as in the first heating up period. Once the laminate was close to 125°C, the heaters on the press were disconnected, and the timer was reconnected, and the heater embedded in the laminate was activated at regular intervals as before. The output temperature responses resulting from the imposed heat fluxes were recorded continuously throughout the whole experiment using the data acquisition program, *DATAAQ*.

In the second experiment, the power supply was computer controlled so that the complete history, including the heating up periods and heating intervals during the isothermal portions of the cure cycle, for the power supply output was entered through the data acquisition program at the beginning of the experiment. The stop watch was activated at the time the sample was placed in the oven, in case of an unplanned interruption in the data acquisition program, and the external heaters on the press were connected during the initial heating up period to 75°C. At the end of the first isothermal period, the oven temperature was increased to 125°C, and the external heaters on the press were once again connected during the heating up period from 75°C to 125°C. The output responses from the thermocouples and from the power supply were read continuously using the data acquisition program, *DATA_DA_AD*.

In both experiments, after the curing cycle was completed, the oven was turned off, and the data processing portions of the data acquisition programs were completed. Once the cured samples were completely cooled, they were cut apart at the thermocouple junctions, perpendicular to the thermocouples, using a diamond circular saw, and then the exact thermocouple locations at the cut surfaces were measured.

4.3.5 Experimental Parameters

The experimental parameters in the transient temperature experiments on the carbon/epoxy composite materials during curing included the curing cycle, the data

sampling interval, the heating interval for the embedded heaters during the isothermal curing periods, the frequency of the heating intervals, the magnitude of the heat flux, fiber orientation with respect to the heat flux, the number of plies in the laminate, and the position and number of thermocouples.

In both experiments, the recommended curing cycle discussed previously was followed. Due to the mass of the press, the heating up periods took much longer than the usual 20 minutes recommended. Therefore, the isothermal periods were shortened slightly to account for the longer heat up time. The fibers were oriented perpendicular to the heat flux, and forty-four plies were used in both experiments, resulting in two cured laminate plates approximately 4 mm thick for each experiment. (There was one plate on either side of the heater.) Due to the type of press used in the experiments, it was felt that an attempt to cure a thicker sample might result in an increased number of voids.

In Exp. 3.2, which was the first experiment, the data sampling interval was limited to six seconds, due the data acquisition program used. The heating interval was set at forty seconds, consistent with that used in the experiments with the cured composite samples. The heating intervals were repeated every ten minutes with the exception of the first two which were repeated at six minute intervals. This resulted in a total of fifteen heating intervals throughout the curing cycle. The output power from the power supply was adjusted to approximately 50 watts for the first half of the heating intervals and 100 watts for the second half. A total of twelve thermocouples were embedded in the laminate during the stacking process, but only four of the data translation amplifiers were working at the time of the experiment; therefore, two thermocouples on either side of the heater, and the two thermocouples next to the top and bottom plates of the press were used for data acquisition, as shown in Figure 4.23.

In the second experiment, the data acquisition program was adjusted so that data was recorded every second. The duration of the heating intervals was determined using the optimal experimental criterion discussed in Section 3.4. First, the dimensional heating time was determined from eq. (3.24h), using the optimal dimensionless heating time of 2 based on the assumption that the dimensionless heat generation term in eq.

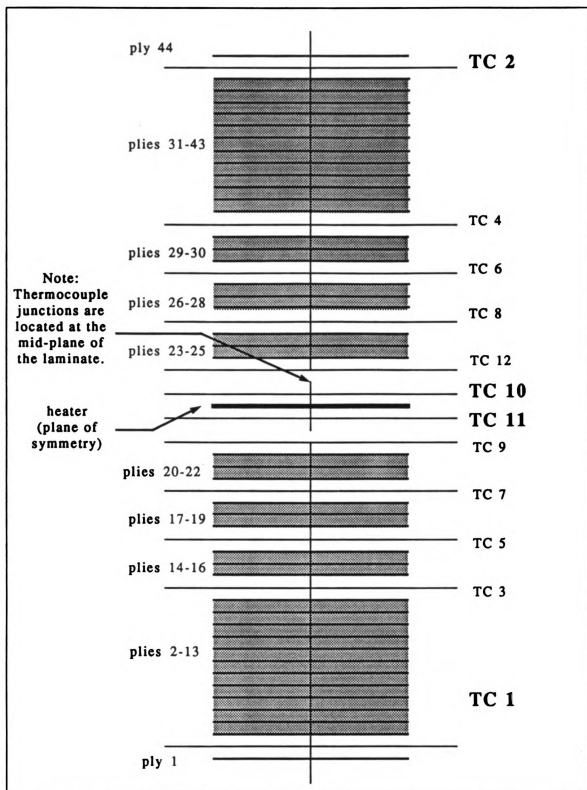


Figure 4.23 Thermocouple (TC) Locations in Prepreg Laminate for the First Transient Experiment during Curing. Plies are Numbered from Bottom to Top, and the Thermocouples used in Data Acquisition are Numbers 1, 2, 10, and 11 (shown in boldface type).

(3.24f), g^* , was equal to 1, a thermal diffusivity value determined from the cured composite at 100°C, and the thickness was chosen as a fixed value equal to the maximum of the values shown in Table 4.1. This resulted in an optimum heating interval of approximately 135 seconds. (Alternatively, one could also optimize the thickness of the sample for a given heating rate.) In order to reach steady state conditions after each heating interval, 500 seconds were required between each interval.

The heat flux used in this experiment was determined from eq. (3.24e), with a maximum temperature rise of 5°C. The dimensionless temperature, T^* , in eq. (3.24e) was determined from eq. (3.25a) using the optimum heat time, t_1^* , and g^* equal to 0.1. This resulted in a value of T^* equal to 1.045, and the required heat flux was calculated to be approximately 800 W/m². The results of the DSC experiments (Section 4.2) were used to justify the assumption of g^* equal to 0.1. The heat generation term in eq. (3.19a) is proportional to the heat of reaction rate ($H_r d\alpha/dt$), and the heat of reaction rate was determined from the maximum heat of reaction rate data from the DSC experiments conducted at 70°C. The maximum heat of reaction was approximately 50 W/kg at this temperature. Using this value as the heat of reaction rate, and the density values shown in Table 4.3, the calculated dimensionless heat generation term was approximately 0.4, which is on the order of 0.1, supporting the assumption of g^* equal to 0.1. (Note that there was very little difference (<6%) between the optimal heating times reported Section 3.4.2 for $g^* = 0.1$ and $g^* = 1.0$.)

A total of sixteen thermocouples were embedded in the laminate during stacking, but since there were only twelve Ectron amplifiers, only twelve thermocouples were actually used for data acquisition. The locations of these thermocouples are shown in Figure 4.24.

One additional experiment was conducted using the cured samples from Exp. 3.2 under similar experimental conditions; however, the heat flux during the heating intervals was increased from 800 W/m² to 1500 W/m². This experiment is referred to as Exp. 3.3 in Chapter 5. The purpose of this experiment was to provide a means of evaluating the experimental procedures using during the curing experiments, since

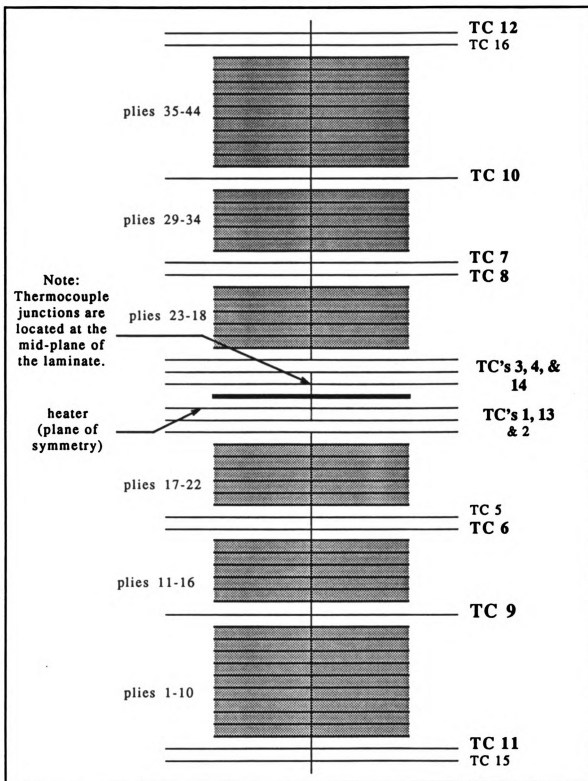


Figure 4.24 Thermocouple (TC) Locations in Prepreg Laminate for the Second Transient Experiment during Curing. Plies are Numbered from Bottom to Top, and the Thermocouples used in Data Acquisition are Numbers 1, 3, 4, 6, 7, 8, 9, 10, 11, 12, 13, and 14 (shown in boldface type).

properties evaluated from this data could directly be compared with the results from the experiments discussed in Section 4.1.

Chapter 5

Results and Discussion

The results of the analysis for the estimation of thermal and kinetic properties are presented and discussed in this chapter. In the first section, the results for the estimation of thermal properties in cured composites from the experiments discussed in Section 4.1 are given. These results include estimates of thermal conductivity perpendicular to the fiber direction and density-specific heat as functions of temperature for two different fiber orientations. The results for the estimation of kinetic properties of the EPON 828 epoxy are presented and discussed in Section 5.2. Section 5.3 is devoted to an analysis of the estimation procedure and experimental design used in the estimation of thermal properties during curing.

5.1 Estimation of Thermal Properties of Cured AS4/EPON 828-mpDA Composite Materials

The thermal properties, effective thermal conductivity perpendicular to the fiber axis and effective density-specific heat, were estimated using the parameter estimation program *PROP1D* from the transient experiments using the cured AS4/EPON 828 composite samples (Section 4.1). Three different aspects of the estimation process were first analyzed to provide insight into the experimental and analytical procedures. These results are presented in Section 5.1.1. The parameter estimates for the experiments

shown in Table 4.2, in which $[0^\circ]_{24}$ and $[0^\circ, \pm 30^\circ, \pm 60^\circ, 90^\circ]_{2(\text{sym})}$ composite samples were tested, are presented and discussed in Section 5.1.2.

5.1.1 Analysis of the Estimation Procedure

Three important aspects of the estimation procedure were analyzed in detail in this section. The first of these pertains to the residuals, which give insight into experimental errors. This analysis is presented in Section 5.1.1.1. The second aspect of the estimation procedure investigated here relates to the sensitivity coefficients; these results are presented in Section 5.1.1.2. Finally, a discussion is presented on the sequential estimation of the parameters in Section 5.1.1.3.

5.1.1.1 The Residuals

The residuals are defined as the differences between the experimental temperatures and the calculated temperatures using the estimated parameters at corresponding times and locations. Close examination of the residuals can give insight into the adequacy of the experimental design.

The residuals for one typical experiment are presented and discussed here. These results correspond to the second repetition of Exp. 1.9, shown in Table 4.2. In this particular experiment, six thermocouples were used. Three were located at the heated surface (TC #1, TC #2, and TC #3); the fourth and fifth thermocouples (TC #4 and TC #5) were located 3.0 mm and 3.3 mm from the heated surface, respectively, and the sixth thermocouple was used to determine the second boundary condition, which was 7.1 mm from the heated surface. The heat flux was activated ten seconds after the initialization of the experiment. The duration of the heat flux interval was approximately 40 seconds, and the total experimental time was 200 seconds. The residuals of the first two thermocouples, TC #1 and TC #2, and the fifth thermocouple, TC #5, along with the time interval in which the heat flux was activated, are shown in Figure 5.1.

Several observations can be made from this figure. First, the magnitude of the residuals associated with the thermocouples located at the heated surface (TC #1 and TC #2) are highest at the beginning and end of the heat flux interval. The maximum

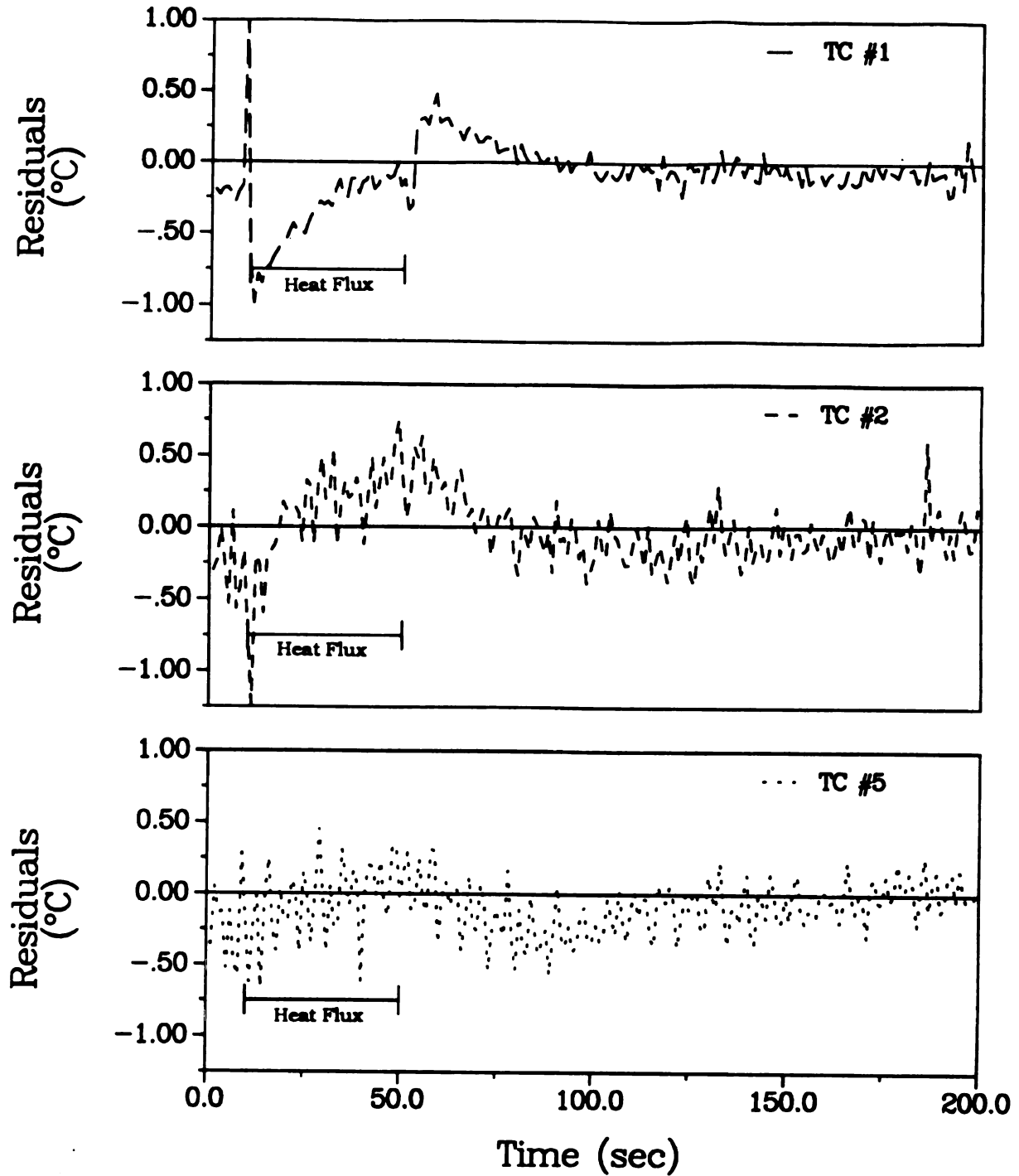


Figure 5.1. Residuals (°C) for Two Thermocouples Located at the Heated Surface (TC #1 and TC #2) and One Thermocouple Located 3.3 mm from the Heated Surface (TC #5) for the Second Repetition of Experiment No. 9 (initial temperature = 100°C).

residual is approximately 1°C , which is approximately 5% of the maximum temperature rise during the experiments. The increase in the magnitude of the residuals at the beginning and end of the heat flux interval was not as pronounced for TC #5, which was located away from the heated surface. Second, the residuals for TC #1 and TC #2 were both biased, but opposite in sign during and immediately after the heating interval. (The residuals for TC #1 are predominantly negative, and the residuals for TC #2 are predominantly positive over this time period.) Also, small biases were observed for the residuals associated with all three thermocouples shown in Figure 5.1 (TC #1, TC #2, and TC #5) and for the two thermocouples not shown in this figure (TC #3 and TC #4) during the second half of the experiment. In all three cases shown in Figure 5.1, these biases were negative, but the biases were observed to be positive for the residuals associated with TC #3 and TC #4.

The high residuals at the beginning and end of the heat flux interval could have resulted from errors in determining the exact time in which the heat flux was activated. As discussed in Section 4.1.3.4, the heater in this experiment was activated manually through use of a timer. Due to the diffusive nature of heat conduction, these errors were not as pronounced for the thermocouple located some distance from the heater (TC#5). Also, finite difference errors tend to be the greatest during step changes in the boundary condition.

The residual bias over the heat flux interval for the heaters located near the surface was most likely due to the placement of the thermocouples with respect to the heater. The heating element in each of the heaters used in these experiments traced back and forth across the heater in rows, leaving a small gap between each row. Therefore, a thermocouple placed directly beneath the heating element would be expected to read higher than the average surface temperature, and a thermocouple placed between the element rows would be expected to read lower than the average surface temperature. This would result in biased residuals, depending on where the thermocouples were located.

The small biases observed for each thermocouple towards the end of the experiment may have been due to improper zeroing of the thermocouples. These experiments

were completed using the Data Translation amplifiers (Section 4.1.3.2) which were very difficult to zero accurately.

Two important points from these observations are that the thermocouples next to the heated surface were the most susceptible to measurement errors and that one major source of errors appeared to be related to the heat flux initialization time.

5.1.1.2 The Sensitivity Coefficients of the Estimated Parameters

The sensitivity coefficients are defined in this case as

$$X_1 = k \left(\frac{\partial T}{\partial k} \right) \quad \text{and} \quad X_2 = \rho c_p \left(\frac{\partial T}{\partial \rho c_p} \right)$$

Monitoring each of these values as a function of time can also provide insightful information regarding to the experimental design and the estimated parameters. These sensitivity coefficients are shown in Figure 5.2 for the first and fifth thermocouple locations for the experiment discussed in Section 5.1.1. The first thermocouple location corresponds to TC #1, which was located at the heated surface, and the fifth thermocouple location corresponds to TC #5, which was located 3.3 mm from the heated surface.

The sensitivity coefficients are useful in determining whether or not the estimated parameters are correlated; if the parameters had been correlated, the sensitivity coefficients would have been proportional to each other. From Figure 5.2, the two curves for X_1 and the two curves for X_2 cross over each other and change signs at different times, indicating that the curves are not proportional, and thus implying that the parameters are not correlated.

By definition, the sensitivity coefficients indicate the sensitivity of temperature with respect to small changes in the thermal property values. Thus, relatively higher values of the sensitivity coefficients are desired for parameter estimation. From Figure 5.2, the sensitivity coefficients are approximately zero for the first ten seconds of the

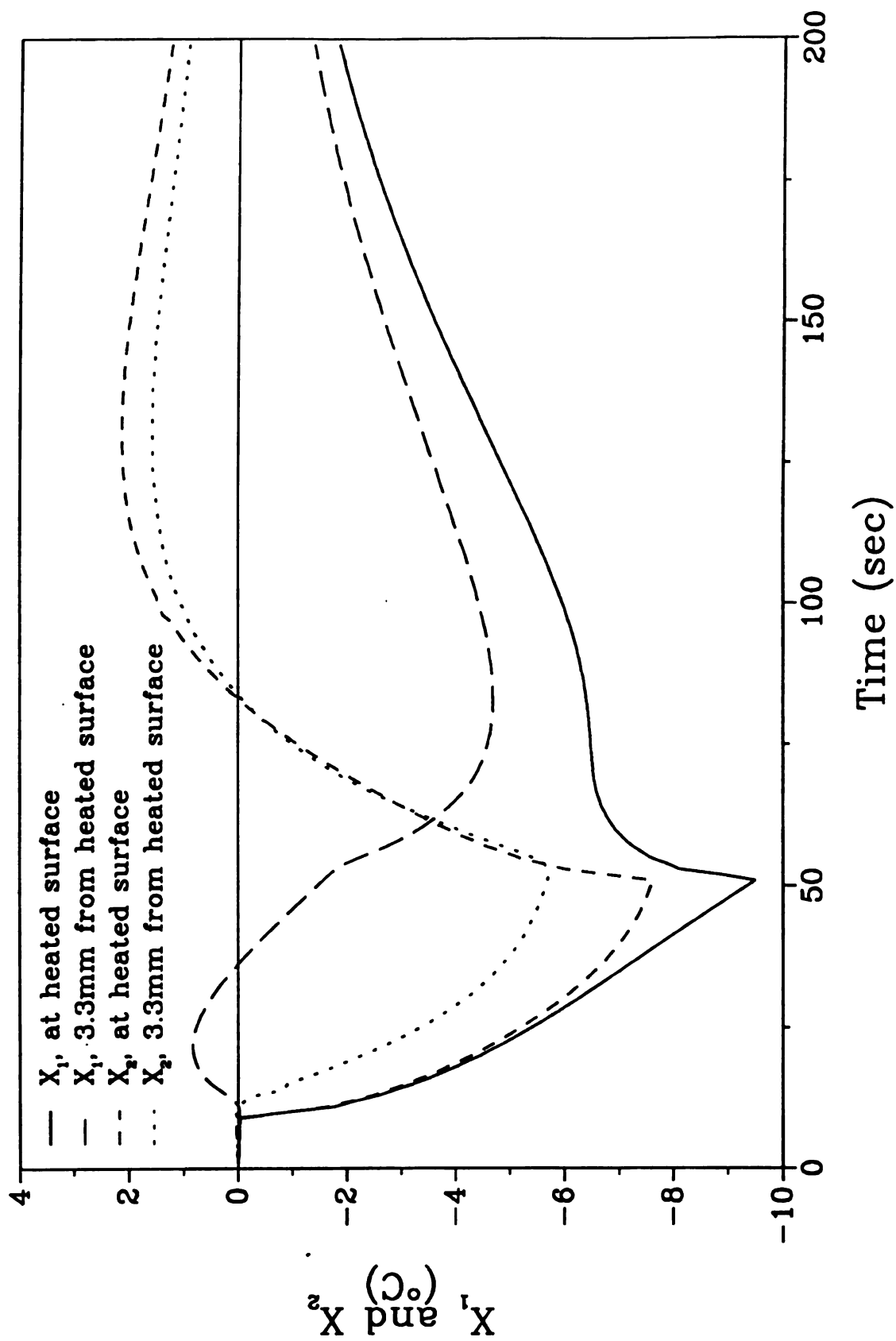


Figure 5.2. Sensitivity Coefficients, X_1 ($k\partial T/\partial k$) and X_2 ($\rho c_p \partial T/\partial \rho c_p$), at the Heated Surface and 3.3 mm from the Heated Surface for Second Repetition of Experiment No. 9.

experiment since there was no heat flux over this period. The sensitivity coefficients corresponding to TC #1 (at heated surface) increased in magnitude immediately with the onset of the heat flux, while the responses of the sensitivity coefficients associated with the interior thermocouple (TC #5) were dampened due to the diffusive effects of conduction heat transfer. The magnitudes of the sensitivity coefficients at the heated surface were higher throughout the heating interval (from 10 to 50 seconds), at which time they experienced a sharp decrease in magnitude. The sensitivity coefficients at the interior location also diminished after the heating interval, but in this case, the response was delayed.

From these observations, the sensitivity coefficients at the heated surface provided the most information with regards to the estimation of the parameters.

5.1.1.3 The Sequential Estimates of the Estimated Parameters

Investigation of the sequential parameter estimates is also useful in evaluating an experimental design. The sequential estimates of thermal conductivity, k , and density-specific heat, ρc_p , for the experiment discussed in Section 5.1.1 are shown in Figure 5.3. The heat flux was activated ten seconds after the beginning of the experiment. The estimated parameters fluctuated greatly over this period, with some values off the scale shown in Figure 5.3. These values can be disregarded since no information was available from the measurements. (As discussed in the the previous section, the sensitivity coefficients equaled zero during the first ten seconds.) The estimates for both thermal conductivity and density-specific heat were constant after approximately 130 seconds, indicating that additional data would have provided little additional information for the estimation of the parameters; also it indicates that the heat conduction model is satisfactory.

5.1.1.4 Insights into the Experimental Design

The observations discussed in Sections 5.1.1.1, 5.1.1.2, and 5.1.1.3 are summarized here. One important observation was that the thermocouples closest to the heated surface provided the most information for parameter estimation, however, these

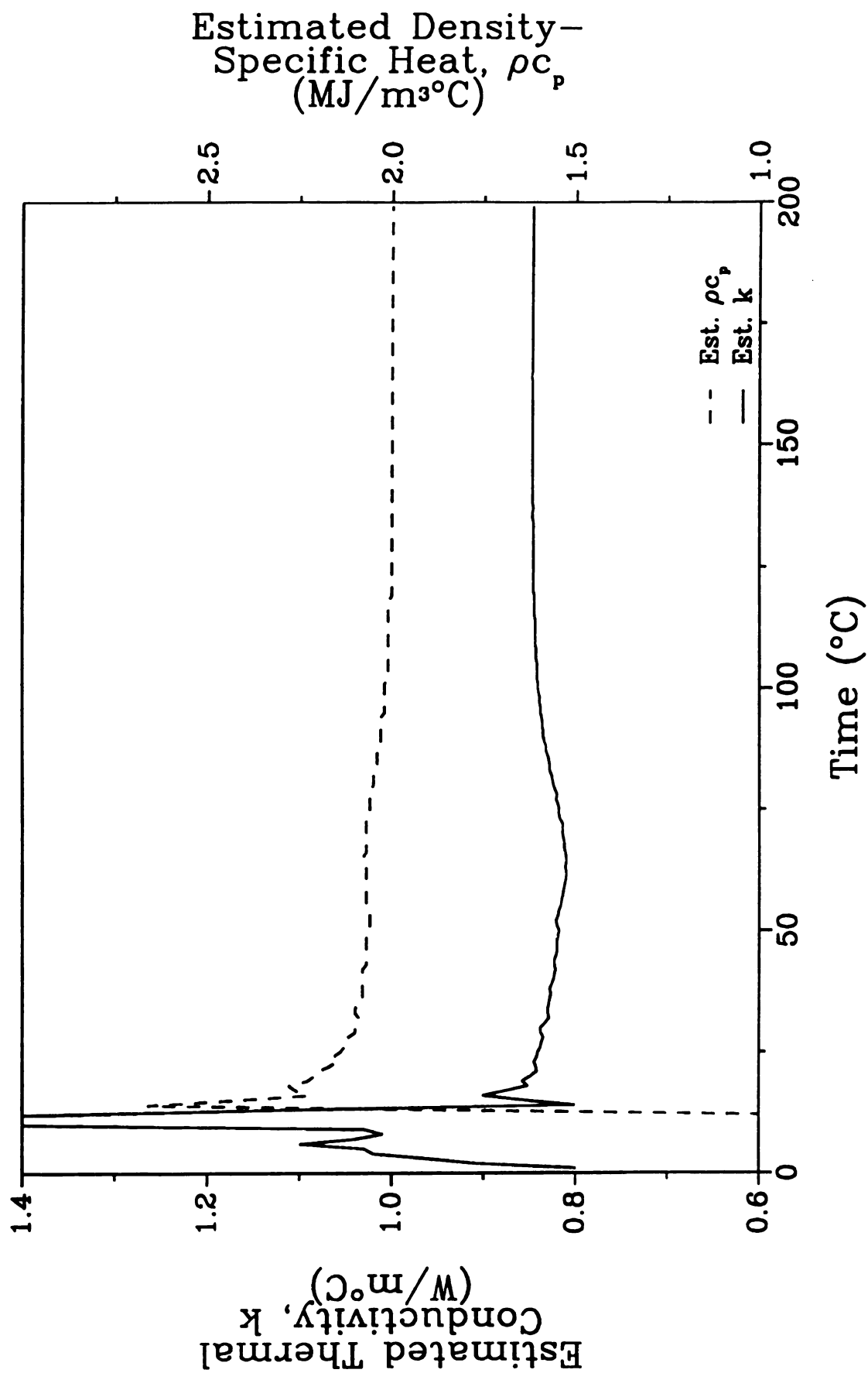


Figure 5.3. Sequential Estimation of Thermal Conductivity, k , and Density Specific Heat, ρc_p , from the Second Repetition of Experiment No. 9 (initial temperature $\sim 100^{\circ}C$).

thermocouples were also the most sensitive to experimental errors. In addition, at least two thermocouples were required at the heated surface to account for the variations in temperature due to the location of the heating element within the heater. Finally from the analysis of the sequential parameter estimates, the total experimental time of 200 seconds appeared to be satisfactory.

5.1.2 Estimation of Thermal Conductivity and Density-Specific Heat of Cured AS4/EPON 828 Composite Materials

The thermal properties, thermal conductivity and density-specific heat were estimated using the procedures presented in Section 3.1 for each repetition of the experiments discussed in Section 4.1.5 and shown in Table 4.2. The results of this estimation procedure are presented in this section. First, results for the experiments using the $[0^\circ]_{24}$ samples are given and discussed in Section 5.1.2.1, and then the results for the experiments using the $[0^\circ, \pm 30^\circ, \pm 60^\circ, 90^\circ]_{2(\text{sym})}$ samples are presented and discussed in Section 5.1.2.2. A comparison of these results is given in Section 5.1.2.3, and finally, the results from this study are compared to previously published data in Section 5.1.2.4.

5.1.2.1 Experiments using $[0^\circ]_{24}$ Samples

The results for the thermal properties, namely the estimated effective thermal conductivity perpendicular to the fiber axis and the estimated effective density-specific heat product, of the cured $[0^\circ]_{24}$ AS4/EPON 828 composite samples are given for the experiments with approximate initial temperatures of 25°C, 50°C, 75°C, 100°C, and 125°C in Tables C.1-C.5 (Appendix C), respectively. These results include the root mean squared errors, which were based on the difference between the experimental and calculated temperatures using the estimated thermal properties. In each of these experiments, five or six thermocouples were used, and at least two were located at the heated surface.

The results from each repetition of each experiment were averaged, and the averaged property estimates are given in Table 5.1. In each case, the total number of

Table 5.1. Averaged Estimated Values and 95% Confidence Intervals for Effective Thermal Conductivity, k , Perpendicular to the Fiber Axis and Effective Density-Specific Heat, ρc_p , of Cured $[0^\circ]_2$, AS4/EPON 828-mPDA Composites.

Exper. No. ^a	No. of Repet.	Avg. Temp. Range (°C)	\bar{k} (W/m°C)	$\overline{\rho c_p}$ (kJ/m ³ °C)
1.1	9	25 - 52	0.797±0.014	1,580±10
1.6	6	27 - 46	0.797±0.007	1,570±30
1.11	6	26 - 46	0.745±0.014	1,560±10
1.1, 1.6 1.11	21	26 - 48	0.782±0.013	1,570±10
1.2	6	53 - 75	0.793±0.006	1,650±20
1.7 ^b	12	50 - 68	0.868±0.010	1,680±20
1.12	6	52 - 72	0.790±0.021	1,600±30
1.2, 1.12	12	52 - 72	0.791±0.009	1,630±20
1.3	6	78 - 98	0.810±0.012	1,690±20
1.8 ^b	6	75 - 91	0.918±0.009	1,810±30
1.13	6	77 - 95	0.797±0.020	1,760±15
1.3, 1.13	12	77 - 95	0.803±0.010	1,730±30
1.4	12	102 - 120	0.832±0.015	1,900±50
1.9 ^b	6	100 - 115	0.971±0.015	1,960±30
1.14	6	100 - 115	0.816±0.008	1,830±30
1.4, 1.14	18	101 - 117	0.826±0.010	1,880±40
1.5	9	127 - 145	0.880±0.040	2,050±80
1.10 ^b	6	126 - 141	1.011±0.010	2,090±30
1.15	6	126 - 140	0.874±0.007	1,930±30
1.5, 1.15	15	126 - 142	0.877±0.020	2,000±50

a. Experiment numbers refer to those in Table 4.2.

b. Samples preheated to 150°C; not used in boldface average values.

repetitions, the average temperature range of the experiments, the average effective thermal conductivity perpendicular to the fiber axis, and the average effective density-specific heat are given, along with the 95% confidence intervals of the estimated parameters. The 95% confidence intervals were calculated using the estimated standard deviation of the averaged values and the t-distribution (Walpole and Meyers, 1978).

The averaged parameter estimates within the different temperature levels were then compared. In the experiments initially at approximately 25°C (Exp. 1.1, 1.6, and 1.11 in Table 5.1), the 95% confidence intervals for the estimated thermal conductivities of Exp. 1.1 and 1.6 overlapped one another, but the 95% confidence interval for Exp. 1.11 was slightly lower. The 95% confidence intervals for density-specific heat overlapped each other for all three cases, indicating that statistically, the means were equivalent.

The composite samples in Exp. 1.7, 1.8, 1.9, and 1.10, with corresponding initial temperatures of approximately 50°C, 75°C, 100°C and 125°C, were accidentally heated to 150°C for two hours prior to the experiments. This is above the glass transition temperature of the epoxy, which is approximately 135°C to 150°C, depending on the heating rate. (The glass transition temperature increases with increased heating rates.) The glass transition temperature is the temperature at which the molecules in the amorphous phase (epoxy) begin to rotate, and at this temperature, the material begins to change from a glassy structure to a rubbery structure (Sichina, 1989). (There is, however, no visible change in the epoxy.) It is evident that these changes effected the epoxy even after the samples were cooled, when comparing the 95% confidence intervals of the estimated parameters at each temperature interval. In all cases, the 95% confidence intervals of the effective thermal conductivities estimated for Exp. 1.7, 1.8, 1.9, and 1.10 were higher than the other two corresponding experiments at each temperature interval. One explanation for the increased thermal conductivity is that the rotation of the molecules facilitated better bonding along the matrix fiber interface after the composite had cooled, and therefore, increased the contact conductance between

the fiber and the epoxy matrix. Although the mean estimates of the effective density-specific values were higher for Exp. 1.7, 1.8, 1.9, and 1.10, than for the other experiments at the same temperature intervals, the 95% confidence intervals were higher only for Exp. 1.8, in which the initial temperature was approximately 75°C.

Comparing the parameter estimates for the experiments not preheated to 150°C at each of the four temperature levels above 25°C (50°C, 75°C, 100°C, and 125°C), the 95% confidence intervals of the estimated thermal conductivity values overlapped one another within each temperature level. The 95% confidence intervals of the density-specific heat estimates did not overlap, however, for the experiments with initial temperatures at 75°C and 125°C.

The estimated thermal properties for Exp. 1.1, 1.6, and 1.11 (~25°C), Exp. 1.2 and 1.12 (~50°C), Exp. 1.3 and 1.13 (~75°C), Exp. 1.4 and 1.14 (~100°C), and Exp. 1.5 and 1.15 (~125°C) were combined at each temperature level, and the combined results, along with their respective confidence intervals are indicated by the boldface type in Table 5.1. Note that the results from the samples preheated to 150°C were not included in these values. The combined results clearly indicate that both thermal conductivity and density-specific heat estimates increase with temperature.

The experiments conducted above 125°C approached the glass transition temperature, which may have affected some of the estimated parameters, even though the sample achieved these temperatures for only a few seconds near the surface of the sample. From Table C.5 (Appendix C), the estimates for thermal conductivity perpendicular to the fibers increased with each successive repetition in Exp. 1.5; however, this did not hold true for the repetitions in Exp. 1.15. Therefore, it is difficult to conclude whether or not the glass transition temperature had any effect on the parameter estimates based on these observations.

It was desired to associate the estimated parameters values with discrete temperature values, but this was difficult since each experiment was conducted over a temperature range rather than at single temperature, and because of the temperature variation within the experimental samples. For convenience, the estimated parameters

were associated with the average surface temperature next to the heater from each experiment, and the estimated thermal conductivity and density-specific heat values given in Tables C.1-C.5 are plotted against these temperatures in Figures 5.4 and 5.5, respectively.

A linear regression curve was fit through the estimated thermal conductivity values from Exp. 1.1-1.6, shown in Figure 5.4. The regression line and the 95% confidence band of this curve are indicated by the solid lines. A second regression curve was determined for the estimated thermal conductivity values from Exp. 1.7-1.10 in which samples were preheated to 150°C for two hours; this regression line and the associated confidence band are indicated by the medium dashed lines. These two regression lines are independent of one another since their respective confidence bands do not overlap one another. A third regression line (short dashed line) is shown for the data from Exp. 1.1-1.4, 1.6, and 1.11-1.15; this curve does not include data from the experiments initializing at approximately 125°C, in which the sample may have exceeded the glass transition temperature for a few seconds in each experiment. The confidence band for this curve overlaps the confidence band for the first regression line which included the experiments above 125°C, indicating that there is no significant difference between these two curves.

The parameter estimates for density-specific heat were analyzed and plotted in a similar manner, and the results from the linear regression analysis are also shown in Figure 5.5. The 95% confidence bands of the linear regression curves associated with Exp. 1.1-1.6 and 1.11-1.15 (solid lines) and Exp. 1.7-1.10 (medium dashed lines) did not overlap, indicating that these regression lines are independent, as was found for the thermal conductivity curves. The confidence bands for the regression line which did not incorporate the data above 125°C (short dashed lines) overlapped the bands which did include this data (solid lines), indicating that, as for the case for thermal conductivity, the regression lines were the statistically the same.

The estimated effective thermal conductivity perpendicular to the fiber axis and the effective density-specific heat values can be expressed as functions of temperature from the linear regression curves in Figures 5.4 and 5.5 as:

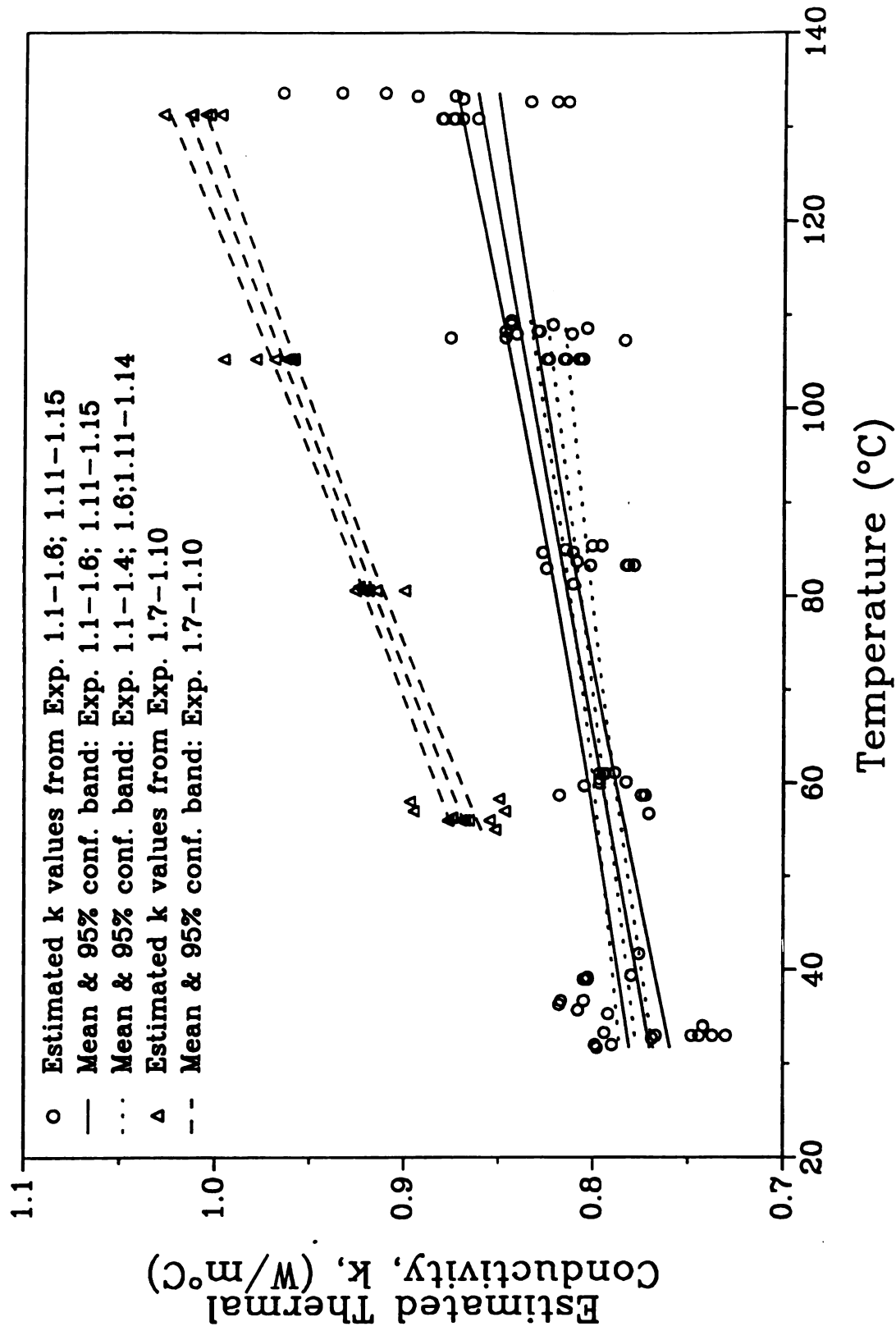


Figure 5.4. Estimation of Effective Thermal Conductivity Perpendicular to the Fiber Axis, k , of Cured $[0^{\circ}]_{24}$ AS4/EPON 828-mPDA Composites.

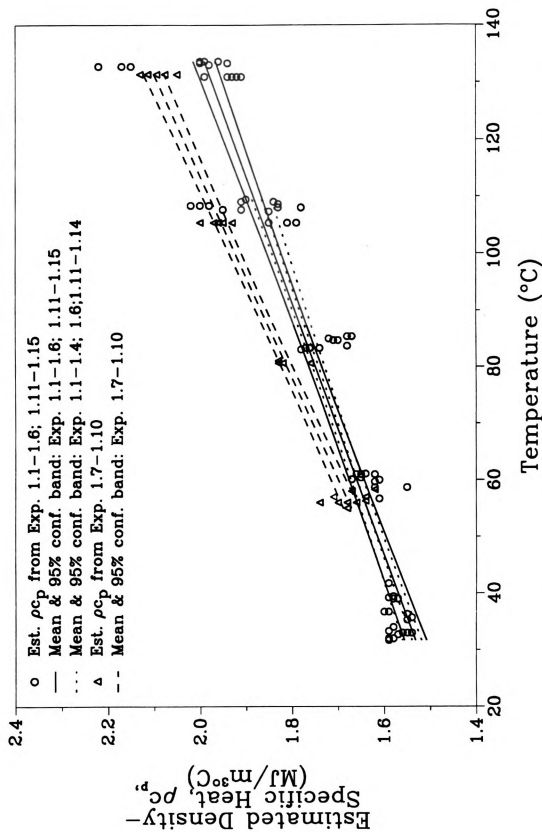


Figure 5.5. Estimation of Effective Density-Specific Heat, $\rho_c \bar{c}_p$, of Cured [0°] ₂₄ AS4/EPON 828-mPDA Composites.

$$k(T) = k_0 + k_1 T \quad (5.1a)$$

for thermal conductivity, and,

$$\rho c_p(T) = (\rho c_p)_0 + (\rho c_p)_1 T \quad (5.1b)$$

for density-specific heat. The regression parameters (k_0 , k_1 , $(\rho c_p)_0$ and $(\rho c_p)_1$) and their associated 95% confidence intervals are given in Table 5.2.

5.1.2.2 Experiments using $[0^\circ, \pm 30^\circ, \pm 60^\circ, 90^\circ]_{2(\text{sym})}$ Samples

Results, including the estimated effective thermal conductivity values perpendicular to the fibers and the estimated effective density-specific heat values, for each repetition of the experiments using cured $[0^\circ, \pm 30^\circ, \pm 60^\circ, 90^\circ]_{2(\text{sym})}$ samples with initial temperatures of approximately 25°C, 50°C, and 75°C are given in Tables C.6-C.8 (Appendix C), respectively.

Averaged repetition values for each experiment are given in Table 5.3. In each case, the average thermal conductivity and density-specific heat values are given, along with the 95% confidence intervals of the averaged parameters, the total number of repetitions averaged, and the average temperature range of the experiments.

The average parameter estimates for each experiment within each different temperature level were again compared. At each temperature interval, the confidence intervals of the density-specific heat overlapped one another, but the confidence intervals of the thermal conductivity values did not. The differences in the values for thermal conductivity may have been the result of the different processing methods used to cure the samples. Since, from Figure 5.2, the sensitivity coefficients evaluated closest to the heater were the highest in magnitude, the thermocouples at these locations had the greatest influence on the estimates of the thermal conductivity. Therefore, in Exp. 1.16, 1.17, 1.18, the estimates of the parameters had the greatest influence from the samples cured in the hydraulic press, since these sample plates were closest to the heated surface. Likewise, the samples cured in the autoclave had the

Table 5.2. Estimated Parameters and 95% Confidence Intervals for the Linear Regression of Both Effective Thermal Conductivity, k , Perpendicular to the Fibers and Effective Density-Specific Heat, c , with Temperature of Cured $[0^\circ]_{24}$ AS4/EPON 828-mPDA Composites.

Thermal Conductivity		$k = k_0 + k_1 T$	
Figure Number	Experiment Numbers	k_0 (W/m°C)	k_1 (W/m(°C) ²)
5.4	1.1-1.6; 1.11-1.15	0.742±0.015	(0.902±0.173) 10 ⁻³
5.4	1.1-1.4; 1.6; 1.11-1.15	0.758±0.014	(0.615±0.183) 10 ⁻³
5.4	1.7-1.10	0.760±0.016	(1.943±0.175) 10 ⁻³
5.6	1.16-1.21	0.689±0.038	(0.877±0.642) 10 ⁻³
Density-Specific Heat		$\rho c_p = (\rho c_p)_0 + (\rho c_p)_1 T$	
Figure Number	Experiment Numbers	$(\rho c_p)_0$ (MJ/m ³ °C)	$(\rho c_p)_1$ (MJ/m ³ (°C) ²)
5.5	1.1-1.6; 1.11-1.15	1.390±0.034	(0.450±0.039) 10 ⁻²
5.5	1.1-1.4; 1.6; 1.11-1.15	1.407±0.033	(0.419±0.043) 10 ⁻²
5.5	1.7-1.10	1.362±0.038	(0.562±0.042) 10 ⁻²
5.7	1.16-1.21	1.588±0.092	(0.187±0.154) 10 ⁻²

Table 5.3. Averaged Estimated Values and 95% Confidence Intervals for Effective Thermal Conductivity, \bar{k} , Perpendicular to the Fiber Axis and Effective Density-Specific Heat, $\bar{\rho c}_p$, of Cured $[0^\circ, \pm 30^\circ, \pm 60^\circ, 90^\circ]_2$ AS4/EPON 828-mPDA Composites.

Exper. No. ^a	No. of Repeti.	Avg. Temp. Range (°C)	\bar{k} (W/m°C)	$\bar{\rho c}_p$ (kJ/m ³ °C)
1.16	11	27 - 41	0.687±0.017	1,680±70
1.19	6	28 - 51	0.767±0.037	1,600±40
1.16, 1.19	17	27 - 46	0.715±0.025	1,660±50
1.17	6	53 - 71	0.716±0.009	1,650±20
1.20	6	52 - 75	0.786±0.020	1,690±20
1.17, 1.20	12	52 - 74	0.751±0.025	1,670±20
1.18	6	76 - 97	0.744±0.008	1,710±20
1.21	6	78 - 97	0.767±0.061	1,820±220
1.18, 1.21	12	77 - 97	0.756±0.026	1,770±90

a. Experiment numbers refer to those in Table 4.2.

greatest influence on the parameters estimates for Exp. 1.19, 1.20, and 1.21. At each temperature level, the estimated thermal conductivities which had the greatest influence from the autoclave cured samples were higher than the estimated parameters which had the greatest influence from the samples cured in the press. One explanation for the higher thermal conductivity values is that the autoclave provided a more uniform pressure distribution with time throughout the curing process, thus providing better bonding between the epoxy matrix and the fibers. It is expected that these differences would be greater when the fibers are multi-directional, as they were in this case, since during the experimental stacking procedure, it was observed that the fibers tended to slide over each other when they were stacked at different angles.

The average results for each experiment were combined at each temperatures interval. These values, along with the associated 95% confidence intervals are indicated by the boldface type in Table 5.3. As was observed for the results using the $[0^\circ]_{2,4}$, both the estimated thermal conductivity and density specific heat values increased with temperature. The estimated thermal conductivity and density-specific heat values are shown versus the average surface temperature in each experiment in Figure 5.6 and 5.7, respectively. A linear regression curve was fit through the estimates in each of these figures using PLOTIt^R (1989) software, and these curves, along with their associated 95% confidence bands are indicated by the solid lines. The estimated parameters associated with these linear regression curves (see eq. 5.1a,b) are also shown in Table 5.2.

5.1.5.3 Comparison of Results from $[0^\circ]_{2,4}$ and $[0^\circ, \pm 30^\circ, \pm 60^\circ, 90^\circ]_{2(\text{sym})}$ Samples

The linear regression curves indicated by the solid lines in Figures 5.4 and 5.6 for thermal conductivity, and by the solid lines in Figures 5.5 and 5.7 for density-specific heat are compared in Figures 5.8 and 5.9, respectively. The curves in Figure 5.8 for thermal conductivity are clearly independent; one explanation for these differences is that there is better bonding between the laminates stacked with the plies oriented in the same direction than when the ply angle is changed. Poorer bonding would decrease the

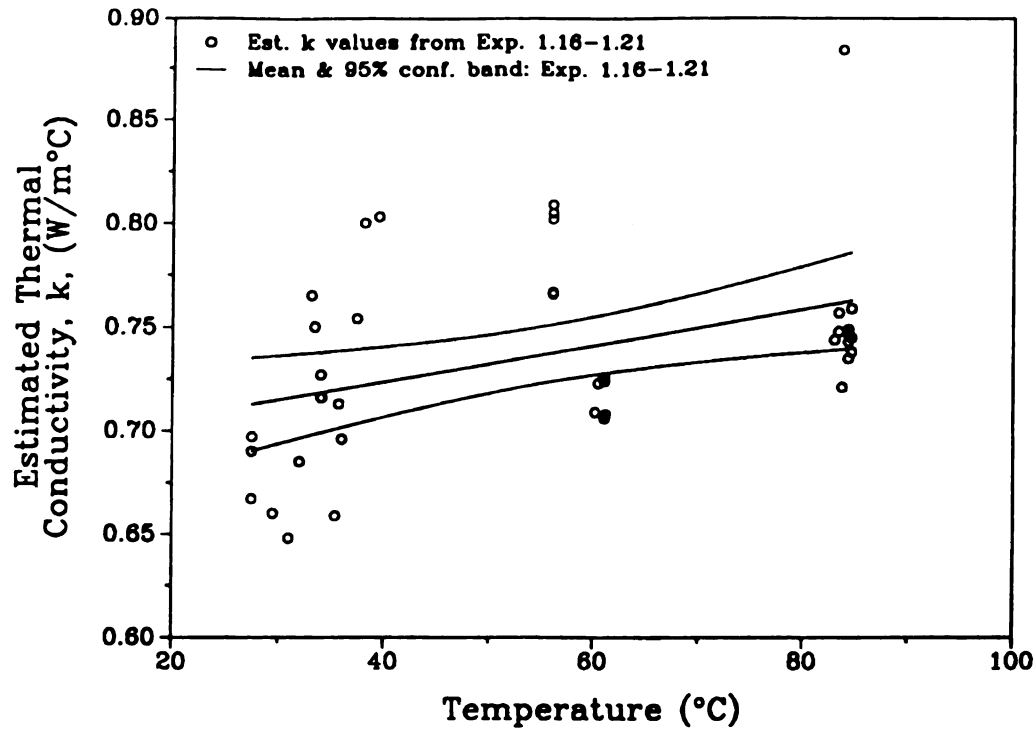


Figure 5.6. Estimation of Effective Thermal Conductivity Perpendicular to the Fiber Axis, k , of Cured $[0^\circ, \pm 30^\circ, \pm 60^\circ, 90^\circ]_{2(sym)}$ AS4/EPON 828-mPDA Composites.

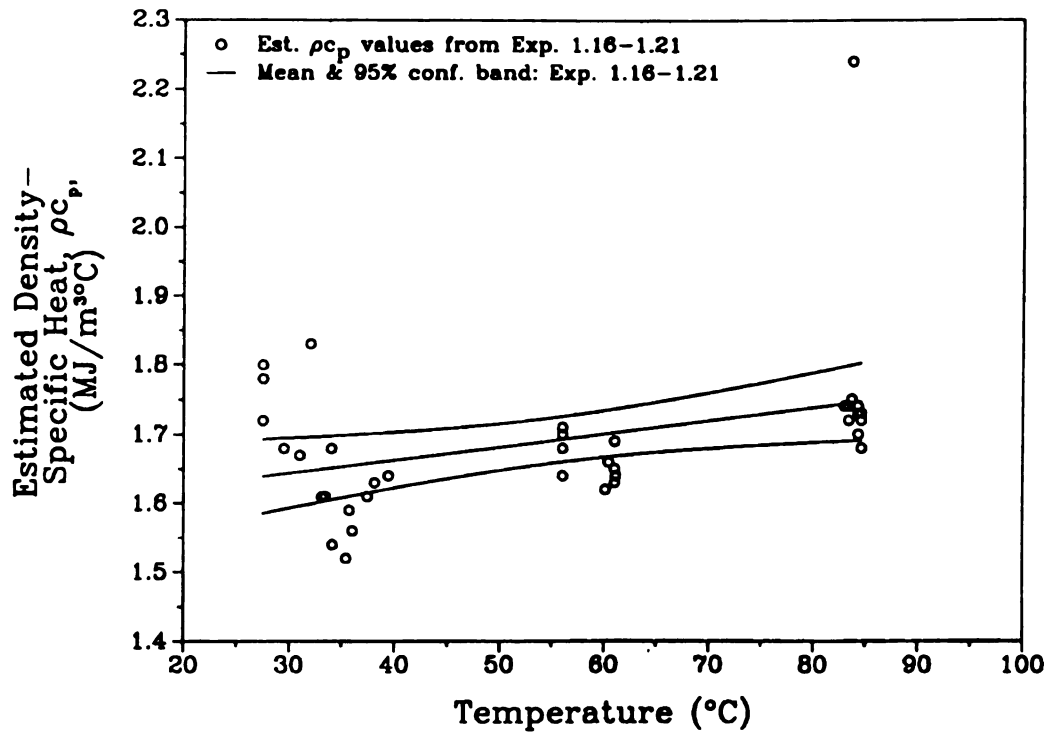


Figure 5.7. Estimation of Effective Density-Specific Heat, ρc_p , of Cured $[0^\circ, \pm 30^\circ, \pm 60^\circ, 90^\circ]_{2(sym)}$ AS4/EPON 828-mPDA Composites.

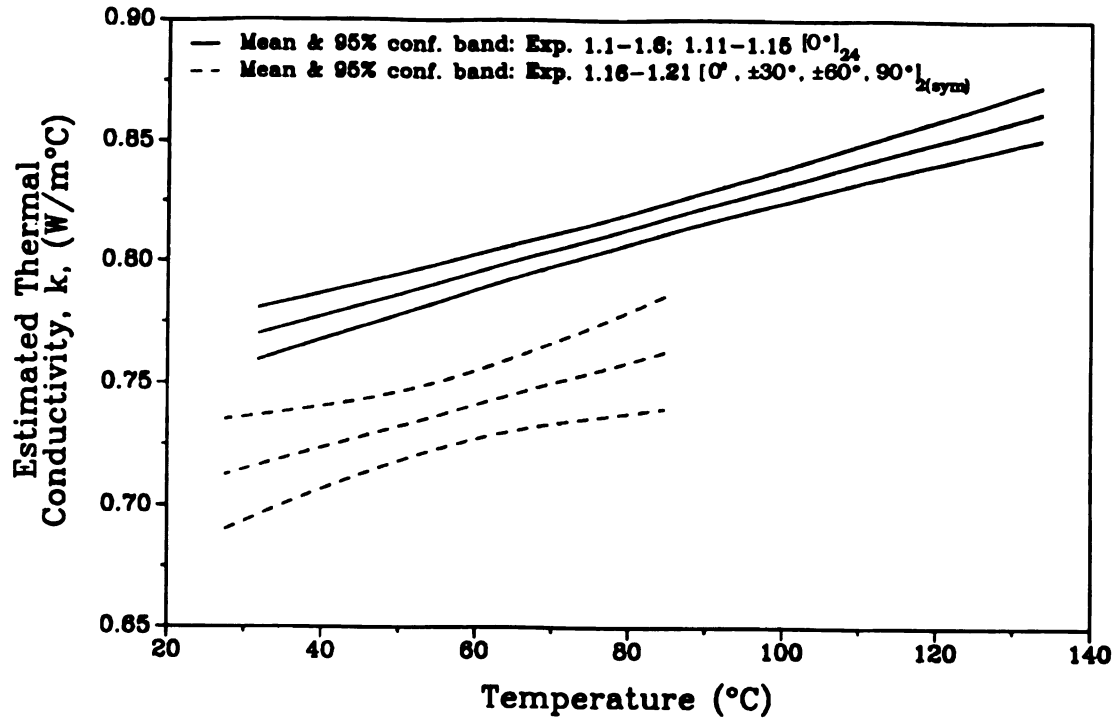


Figure 5.8. Comparison of Linear Regression Curves for Effective Thermal Conductivity Perpendicular to the Fiber Axis, k , of Cured $[0^\circ]_{24}$ and Cured $[0^\circ, \pm 30^\circ, \pm 60^\circ, 90^\circ]_{2(sym)}$ AS4/EPON 828-mPDA Composites.

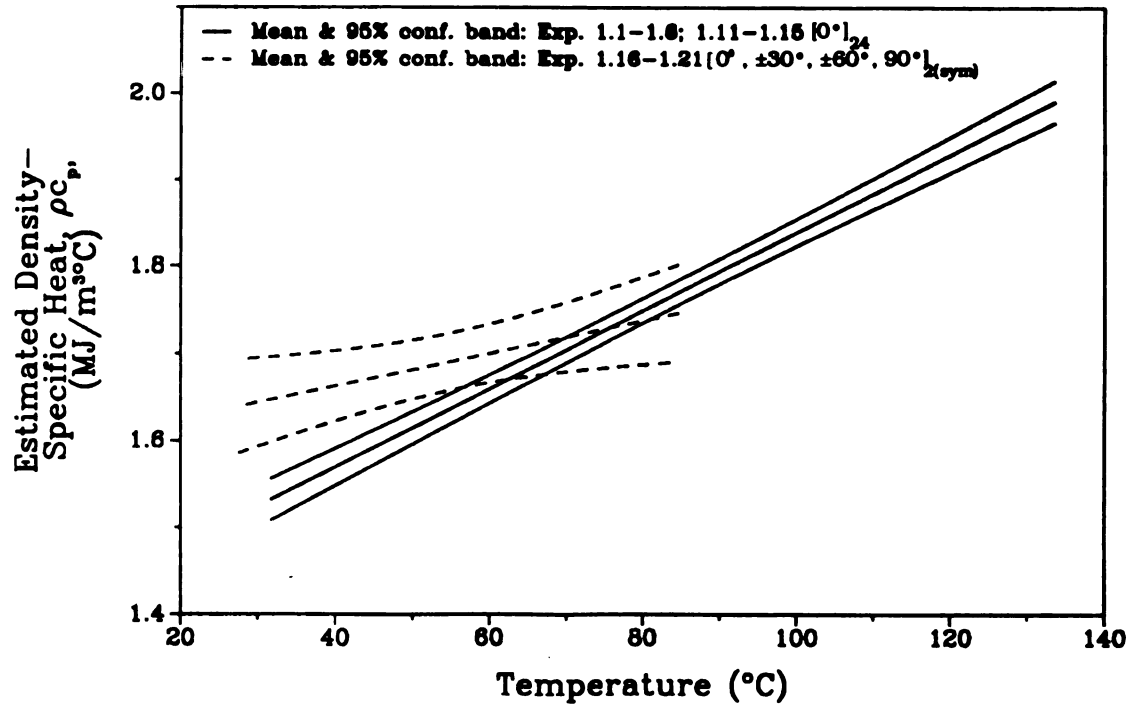


Figure 5.9. Comparison of Linear Regression Curves for Effective Density-Specific Heat, ρc_p , of Cured $[0^\circ]_{24}$ and Cured $[0^\circ, \pm 30^\circ, \pm 60^\circ, 90^\circ]_{2(sym)}$ AS4/EPON 828-mPDA Composites.

thermal contact conductance between the ply interfaces and reduce the resulting effective thermal conductivity perpendicular to the fiber direction. The differences between the density specific heat curves in Figure 5.9 are not as evident since the two curves overlap one another from approximately 55°C to 85°C. It was not expected that the stacking sequence would alter the density-specific heat values.

5.1.5.4 Comparison with Previously Published Results

The estimated thermal conductivity values perpendicular to the fiber axis using [0°] oriented samples are compared to previously published results on comparable fiber-epoxy systems in Table 5.4. At 20°C, the results in this study were within the 95% confidence interval of the results presented by Loh (1989), and since the confidence interval for the results by Ishikawa (1980) are not given, it can not be said with any certainty whether or not these estimates are comparable. The results of Loh (1989) at 100°C were 12% higher than those found in this study.

5.2 Estimation of Kinetic Parameters Associated with the Curing of EPON 828/mPDA Epoxy

In this section, the results from the differential scanning calorimetry (DSC) experiments used to characterize the curing of an EPON 828/mPDA epoxy system are given. The total heat of reaction was first found from the dynamic DSC experiments, and then the degree of cure was calculated for each isothermal DSC experiment shown in Table 4.4; these results are presented and discussed in Section 5.2.1. The first half of the cure was evaluated with the assumption that the reaction rate was limited by autocatalyzation, and the second half of the cure was analyzed with the assumption that the reaction rate was controlled by diffusion. Three different models were evaluated for the first half of the cure; estimates for the kinetic parameters using these models are presented and compared with previously published results on similar epoxy systems in Section 5.2.2. In addition, estimates are given for the parameters associated with the model shown in eq. (3.18) for the last half of the cure in Section 5.2.3. Finally,

Table 5.4. Comparison of Estimated Effective Thermal Conductivity Perpendicular to the Fiber Axis, k , with Previously Published Results.

Composite Material	Temp. (°C)	k (W/m°C)	Estimation Method	Reference
Carbon/3130 Epoxy ^a	20	0.72	Infrared Radiation Method	Ishikawa (1980)
AS4 Carbon/Epon 828	20 100	0.80±0.02 0.93±0.02	Gauss Minimization	Loh (1989)
AS4 Carbon/Epon 828	20 100	0.76±0.02 0.83±0.03	Gauss Minimization	present study Exp. 1.1-1.6; 1.11-1.15

a. Similar in structure to Epon 828 epoxy, with similar thermal conductivity (Ishikawa (1980)).

the models and the associated parameters estimates selected for use in procedures for the estimation of thermal properties during curing are presented in Section 5.2.4.

5.2.1 Determination of the Total Heat of Reaction and Degree of Cure

The total heat of reaction (eq. 3.9) was required to determine the degree of cure (eq. 3.8) from the isothermal differential scanning calorimetry (DSC) experiments. The total heat of reaction was first determined from the dynamic DSC experiments as described in Section 4.2. In each of these experiments, a constant base-line was established, and the magnitude of the baseline was subtracted from the experimental data. The modified data was integrated over time using the DuPont Thermal Analysis System 9900 software to determine the total heat of reaction. The total heat of reaction values calculated for the eight dynamic experiments shown in Table 4.4, along with the average heat of reaction from all the experiments, are shown in Table 5.5.

The degree of cure was then determined for each isothermal experiment conducted at 60°C, 70°C, 100°C, and 110°C (Table 4.4). The isothermal DSC data was post processed as discussed in Section 4.2.2.3 to obtain heat of reaction rate values for each isothermal experiment. These values were then transferred to a VAXstationII/GPX microcomputer, where the cumulative heat of reaction was determined as a function of time through numerical integration of the heat of reaction rates with time, and the degree of cure was calculated by dividing the cumulative heat of reaction values by the average total heat of reaction shown in Table 5.5.

These degree of cure values, which vary with time, for the various isothermal experiments were then used to estimate the kinetic parameters in the kinetic models shown in eqs. (3.4-6).

5.2.2 Parameter Estimation for Autocatalyzed Cure Kinetics (no Diffusion)

The degree of cure data less than 0.50 were assumed to follow an autocatalyzed kinetic reaction without any influence from decreased molecular mobility. The use of 0.50 as a limit for the autocatalyzed controlled reactions is based on the observations

Table 5.5. Total Heat of Reaction Calculated from Dynamic Differential Scanning Calorimetry Experiments (Exp. 2.1) using EPON 828/mPDA Epoxy.

Repetition No.	Heat of Reaction (J/kg)
1	0.459
2	0.444
3	0.468
4	0.452
5	0.432
6	0.451
7	0.439
8	0.447
Average	0.449 ± 0.009

by Sourour and Kamal (1976) as discussed in Section 2.2.3, and on similar observations in this study. The degree of cure data was first used to determine the kinetic parameters (i.e. rate constants) at the different experimental temperatures associated with the kinetic models shown in eqs. (3.4-3.6), and then the estimated parameters were used to determine the activation energy constants and the pre-exponential factors in eq. (3.7).

5.2.2.1 Estimation of Rate Constants and Exponents

The rate constants and exponents in each of the kinetic models shown in eqs. (3.4-3.6) were first determined for each of the isothermal DSC experiments shown in Table 4.4. These experiments were conducted at 60°C, 70°C, 100°C, and 110°C, with three repetitions at each temperature. In these analyses, all linear regression calculations were performed using PLOTit^R (1989) software.

In eq. (3.4), the parameters to be estimated were the rate constants, c_1 and c_2 , and the exponential, m . These parameters were estimated from the initial and maximum degree of cure rate data from each experiment, using the method given by Ryan and Dutta (1979) and outlined in eqs. (3.10-3.13). The least squares method discussed in Section 3.2.1 and shown in eq. (3.14), was also used to determine these parameters. In this method, the parameters were estimated from all of the degree of cure data in each experiment through the minimization of a least squares function. The estimated values for c_1 , c_2 , and m , using the Ryan and Dutta method and the least squares method are shown in Tables 5.6 and 5.7, respectively. In addition, 95% confidence intervals are given for the rate constants estimated using the alternate approach.

The isothermal DSC data were then used to determine the rate constants, c_1 and c_2 in eq. (3.5), using the method given by Sourour and Kamal (1976) and discussed in Section 3.2.1. The estimated rate constants and their respective 95% confidence intervals are shown in Table 5.8 for each isothermal DSC experiment shown in Table 4.4.

The rate constant, c_1 , and the exponential, n , from the model shown in eq. (3.6) were also evaluated from the isothermal DSC data. These parameters were determined

Table 5.6. Rate Constants, c_1 and c_2 , and Exponent, m , Determined from eq. (3.4) and Degree of Cure Values, α , Less than 50% for EPON 828/mPDA Epoxy, using the Ryan and Dutta (1979) Method.

Exper. No.	Rep. No.	Temp. (°C)	Ryan and Dutta Method		
			c_1 (s^{-1})	c_2 (s^{-1})	m
2.2	1	60	3.06E-5	3.70E-4	0.809
	2	60	3.04E-5	3.43E-4	0.817
	3	60	1.86E-5	3.51E-4	0.777
2.3	1	70	4.27E-5	6.01E-4	0.797
	2	70	5.33E-5	6.05E-4	0.815
	3	70	6.02E-5	5.29E-4	0.848
2.4	1	100	2.40E-4	2.36E-3	0.757
	2	100	2.92E-4	2.37E-3	0.749
	3	100	2.60E-4	2.12E-3	0.727
2.5	1	110	3.97E-4	3.81E-3	0.793
	2	110	4.56E-4	3.65E-3	0.705
	3	110	3.02E-4	3.61E-3	0.668

a. Experiment numbers and repetition numbers refer to those in Table 4.4

Table 5.7. Rate Constants, c_1 and c_2 , and Exponent, m , and Associated 95% Confidence Intervals, Determined from eq. (3.4) and Degree of Cure Values, α , less than 50% for EPON 828/MPDA Epoxy, using a Least Squares Method.

Exper. No. ^a	Rep. No. ^a	Temp. (°C)	Alternate Method		
			c_1 (s^{-1})	c_2 (s^{-1})	m
2.2	1	60	(2.22±0.12)E-5	(2.46±0.05)E-4	0.832
	2	60	(2.31±0.08)E-5	(2.27±0.02)E-4	0.834
	3	60	(1.55±0.08)E-5	(2.30±0.03)E-4	0.781
2.3	1	70	(3.46±0.17)E-5	(3.92±0.06)E-4	0.816
	2	70	(4.06±0.22)E-5	(4.02±0.08)E-4	0.847
	3	70	(5.33±0.40)E-5	(3.36±0.16)E-4	0.880
2.4	1	100	(1.76±0.20)E-4	(1.59±0.07)E-3	0.765
	2	100	(1.59±0.36)E-4	(1.57±0.12)E-3	0.691
	3	100	(1.58±0.22)E-4	(1.45±0.07)E-3	0.731
2.5	1	110	(3.38±0.19)E-4	(2.49±0.08)E-3	0.809
	2	110	(3.09±0.18)E-4	(2.39±0.09)E-3	0.713
	3	110	(2.98±0.17)E-4	(2.18±0.07)E-3	0.665

a. Experiment and repetition numbers refer to those in Table 4.4.

Table 5.8. Rate Constants, c_1 and c_2 , and Associated 95% Confidence Intervals Determined from eq. (3.5) and Degree of Cure Values, α , less than 50% for Epon 828/mDPA Epoxy, using the Sourour and Kamal (1976) Method.

Exper. No. ^a	Rep. No. ^a	Temp. (°C)	Sourour and Kamal Method	
			c_1 (s^{-1})	c_2 (s^{-1})
2.2	1	60	(1.22±0.49)E-5	(5.04±0.19)E-4
	2	60	(1.52±0.34)E-5	(4.57±0.13)E-4
	3	60	(1.35±0.21)E-5	(4.42±0.08)E-4
2.3	1	70	(2.17±0.61)E-5	(7.93±0.23)E-4
	2	70	(2.15±1.10)E-5	(8.31±0.41)E-4
	3	70	(3.60±1.53)E-5	(7.17±0.59)E-4
2.4	1	100	(1.56±0.31)E-4	(3.22±0.11)E-3
	2	100	(1.58±0.61)E-4	(3.34±0.23)E-3
	3	100	(1.51±0.41)E-4	(2.96±0.15)E-3
2.5	1	110	(2.70±0.37)E-4	(5.16±0.15)E-3
	2	110	(2.83±0.44)E-4	(5.30±0.18)E-3
	3	110	(3.08±0.35)E-4	(4.97±0.14)E-3

a. Experiment and repetition numbers refer to those in Table 4.4.

using linear regression (PLOTIT^R, 1989), and they are shown, along with their respective 95% confidence intervals, in Table 5.9.

5.2.2.2 Estimation of the Activation Energy Constants and the Pre-Exponential Factors

Each of the rate constants shown in the kinetic models in eqs. (3.4-3.6) was assumed to follow an Arrhenius relationship with temperature. The activation energy constants and the pre-exponential factors associated with the Arrhenius relationship in eq. (3.7) were estimated using linear regression (PLOTIT^R, 1989) from the rate constants, c_1 and c_2 , shown in Tables 5.6-5.9. These rate constants are shown along with their associated linear regression curves in Figures 5.10 and 5.11, respectively. Also, the exponential values for m , in Tables 5.6 and 5.7, and n , in Table 5.9, indicated some temperature dependence; this dependence was assumed to linear. Thus, for eq. (3.4),

$$m = m_0 + m_1 T \quad (5.3)$$

and for eq. (3.6),

$$n = n_0 + n_1 T \quad (5.4)$$

where m_0 , m_1 , n_0 , and n_1 are estimated constants using linear regression. The estimated values for the activation energy constants, the pre-exponential factors, and the exponential constants and their respective 95% confidence intervals are compared with values obtained by Sourour and Kamal (1976), Kamal et al. (1973), Ryan and Dutta (1979), and Prime (1970, 1973) for bisphenol-A-diglycidylether (BADGE-DER332)/mPDA systems in Table 5.10. The DER332 BADGE resin has approximately the same structure as the EPON 828 system used here.

In comparing the kinetic parameters estimated in this study with those estimated in the other studies, the parameters characterizing the second rate constant, namely A_2 and E_2 , are very similar for the models shown in eqs. (3.4) and (3.5). (It is difficult to

Table 5.9. Rate Constant, c_1 , and Exponential, n , and Associated 95% Confidence Intervals Determined from eq. (3.6) and Degree of Cure Values, α , less than 50% for EPON 828/MPDA Epoxy.

Exper. No. ^a	Rep. No. ^a	Temp. (°C)	c_1 (s^{-1})	n
2.2	1	60	(1.85±0.12)E-2	-1.25±0.18
	2	60	(1.84±0.22)E-2	-1.11±0.18
	3	60	(1.49±0.14)E-2	-1.45±0.29
2.3	1	70	(3.01±0.17)E-2	-1.22±0.17
	2	70	(3.23±0.24)E-2	-1.12±0.22
	3	70	(3.32±0.35)E-2	-0.85±0.32
2.4	1	100	0.141±0.023	-1.00±0.46
	2	100	0.161±0.017	-0.84±0.31
	3	100	0.145±0.016	-0.83±0.32
2.5	1	110	0.238±0.023	-0.85±0.29
	2	110	0.254±0.017	-0.79±0.21
	3	110	0.251±0.017	-0.71±0.22

a. Experiment and repetition numbers refer to those in Table 4.4.

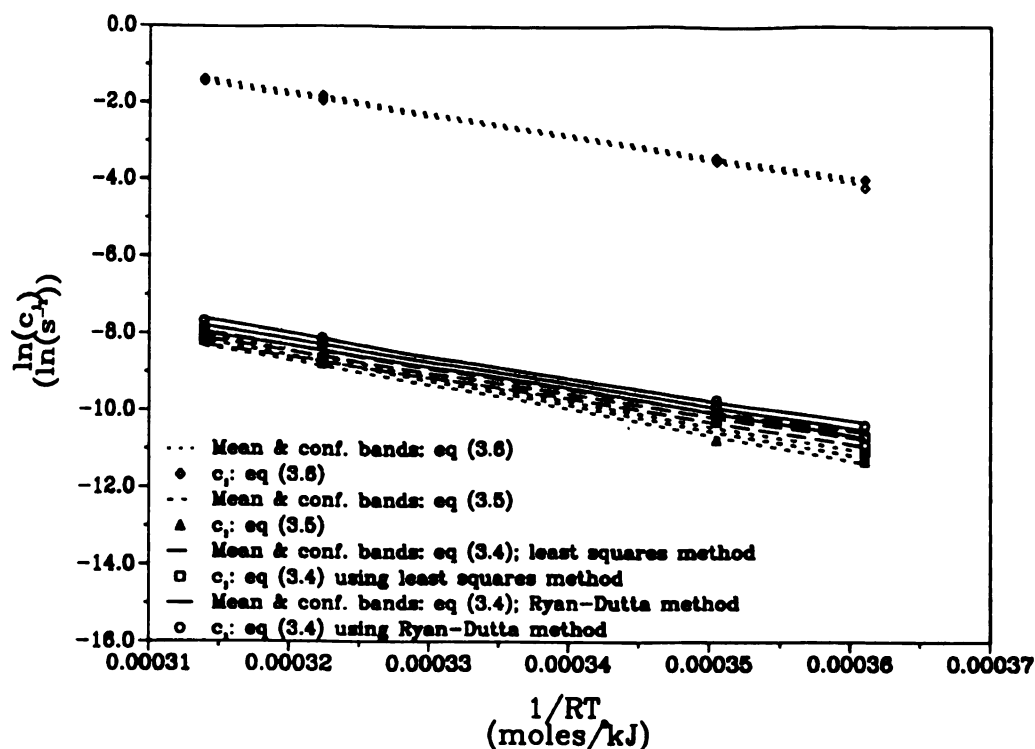


Figure 5.10 Arrhenius Relationship for the First Rate Constant, c_1 in eq. (3.4), (3.5), and (3.6): $\ln(c_1)$ versus $1/RT$ (R = Gas Const. (kJ/mole \cdot K); T_a = Abs. Temp. ($^{\circ}$ K)).

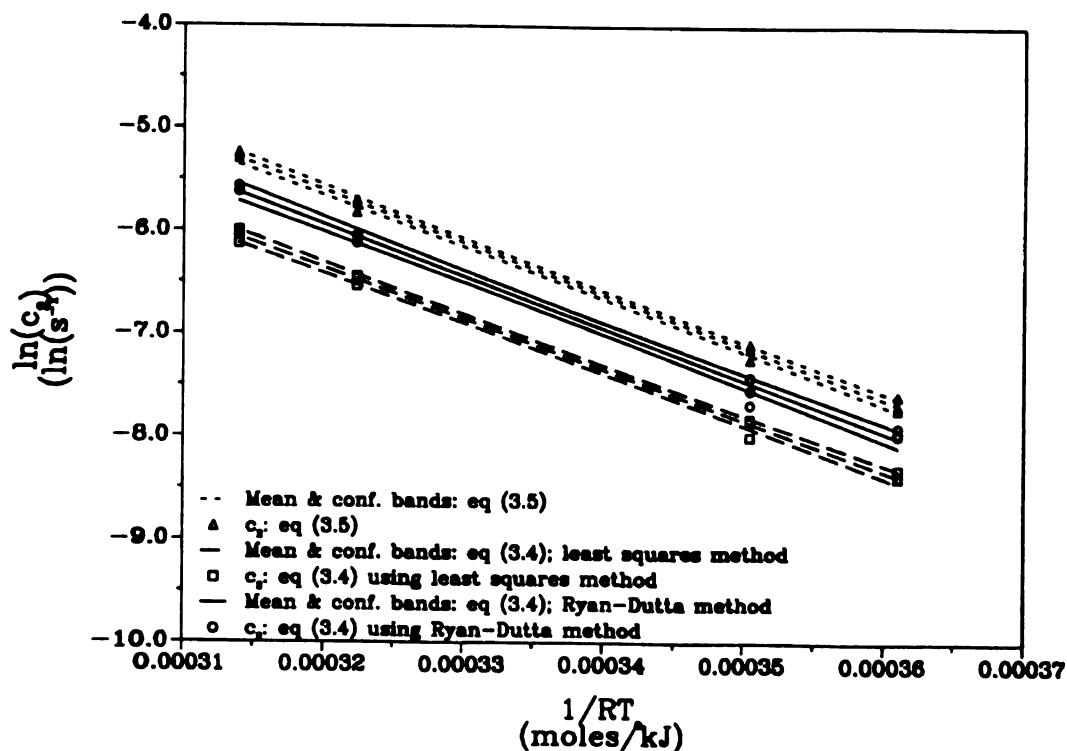


Figure 5.11 Arrhenius Relationship for the Second Rate Constant, c_2 in eq. (3.4), (3.5), and (3.6): $\ln(c_2)$ versus $1/RT$ (R = Gas Const. (kJ/mole \cdot K); T_a = Abs. Temp. ($^{\circ}$ K)).

Table 5.10. Activation Energy Constants, E_a and E_p , and Pre-Exponential Factors, A_p and A_s , Determined from the Arrhenius Relationship (eq. 3.7) and Estimated Rate Constants Estimated from eqs. (3.4), (3.5), and (3.6), for Degree of Cure Values, α , Less than 50% for EPON 828/MPDA Epoxy.

Model	DSC Exp. (temp., °C)	E_a , (kJ/mole)	E_a , (kJ/mole)	$\ln(A_p)$ $\ln(s^{-1})$	$\ln(A_s)$ $\ln(s^{-1})$	Exponential Constants	Reference (Method)
(3.4)	Isothermal (60-110)	57.4±6.3	50.4±2.9	10.2±2.1	10.2±0.9	$m = m_0 + m_1 T$ $m_0 = 0.98 \pm 0.13$ $m_1 = -(2.0 \pm 1.5)E-3$	this study (Ryan and Dutta, 1979, Method)
(3.4)	Isothermal (60-110)	55.8±5.8	49.2±2.1	9.4±2.0	9.4±0.7	$m = m_0 + m_1 T$ $m_0 = 0.98 \pm 0.13$ $m_1 = -(2.3 \pm 1.5)E-3$	this study (least squares method)
(3.4)	Isothermal (70-140)	62	48	10.6	9.1	$m = 1$	Kamal et al. (1973)
(3.4)	Isothermal (90-170)	65	46	11.8	not given	$m = 1.06$	Ryan and Dutta (1979)
(3.5)	Isothermal (60-110)	64.5±4.9	50.6±2.0	12.1±1.7	10.6±0.7		this study (linear regres.)
(3.5)	Isothermal (60-130)	81	48	16.0	9.5		Sourour and Kamal (1976)
(3.6)	Isothermal (60-110)	56.1±4.9		16.2±0.8		$n = n_0 + n_1 T$ $n_0 = -1.74 \pm 0.36$ $n_1 = (8.7 \pm 2.1)E-3$	this study (linear regression)
(3.6)	Dynamic (115-130)	50-63		8-12		$n = 0.9-1.3$ $n_0 = -1.74 \pm 0.36$	Prime (1970, 1973) (Borchardt and Daniels Method)

a. Model refers to equation numbers.

determine whether or not the parameters are statistically equivalent, since the confidence intervals of the parameters estimated in the previous studies were not given, and calculations of the confidence intervals for the activation energy constants and the pre-exponential factors shown for this study did not include the confidence intervals from the rate constants.) The parameters associated with the first rate constant differ by a wider margin. This is to be expected, however, since the first rate constant represents the initial portion of the cure, which is difficult to measure using the DSC, and therefore it is more susceptible to errors. This is evident by the larger confidence intervals for E_1 and A_1 , compared with E_2 and A_2 . Fortunately, since the second rate constant, c_2 , is approximately one order of magnitude greater than the first rate constant, c_1 , as shown in Tables 5.6-5.9, the first rate constant is only dominant during the initial stages of the cure when the degree of cure rate is small.

5.2.3 Diffusion Controlled Reactions and Parameter Estimation

There have been relatively few studies to characterize the cure of an amine-epoxy resin for diffusion controlled reactions (Section 2.2.3). The model presented by Hawley et al. (1988) and shown in eq. (3.16) was first investigated to simulate the curing of the EPON 828/mPDA resin for degrees of cure greater than 0.5. To check the validity of the model, a natural logarithm was applied to eq. (3.16), and then the equation was rearranged as follows,

$$\ln \left(\frac{d\alpha/dt}{1-\alpha} \right) = \ln(c_2) - D\alpha$$

A preliminary analysis indicated that the left hand side of the above equation was highly nonlinear, and so this model was deemed to be inappropriate for this analysis.

The alternate model shown in eq. (3.18) was then used to characterize the curing reaction for α greater than 0.50. This model is similar that shown in eq. (3.16) in that the reaction rate was assumed to follow an exponential decay, however, this model is inherently coupled to the kinetic model used for the degree of cure less than 0.50, in which diffusion was assumed to be negligible through the α_D terms in the equation.

The rate constant, c , and the diffusion constant, D , were evaluated from the degree of cure rate at the time the reaction became diffusion controlled, which was assumed to be at $\alpha_D = 0.50$, and the degree of cure and associated degree of cure rate values greater α_D , using the nonlinear parameter estimation scheme discussed in Section 3.2.2. Once again it is noted that the selection of α_D was based on the results of the studies discussed in Section 2.2.3 and on visual observation of plots of the degree of cure rate data versus the degree of cure. The estimated parameters, c , and D , are shown, along with their 95% confidence intervals, in Table 5.11 for each isothermal DSC experiment. The rate constant was assumed to follow an Arrhenius relationship with temperature (eq. 3.7) and the diffusion constant was assumed to vary linearly with temperature as follows

$$D = D_0 + D_1 T \quad (5.5)$$

The parameters, E_a , A , D_0 , and D_1 , were estimated using linear regression (PLOTIT^R, 1989) from these relationships; the estimated parameters are also shown in Table 5.11.

5.2.4 Selection of Kinetic Parameters for use in the Estimation of Thermal Properties during Curing

In order to estimate the thermal properties during the curing of the carbon/epoxy system discussed in Section 4.3, degree of cure rate values were required throughout the cure cycle, as discussed in Section 3.2. The degree of cure rate was found from one of the three kinetic models characterizing the autocatalyzed reaction discussed in Section 3.2.1, and from the diffusion controlled models presented in Section 3.2.2. The selection of the models was based on the confidence intervals of the estimated rate constants, activation energy constants, and pre-exponential values.

For the parameters estimated assuming an autocatalyzed controlled reaction rate (Tables 5.6-5.8), the rate constants estimated using eq. (3.4) for the kinetic model had the lowest confidence intervals, and from Table 5.10, the confidence intervals of the activation energy constants and the pre-exponential factors estimated using eq. (3.4)

Table 5.11. Rate Constant, c_s , and Diffusion Constant, D , and Associated 95% Confidence Intervals Determined from eq. (3.16) and Degree of Cure Values, α , Greater than 50% for EPON 828/mPDA Epoxy.

Exper. No. ^a	Rep. No. ^a	Temp. (°C)	c_s^b (s ⁻¹)	D^b
2.2	1	60	(2.33±0.10)E-2	6.51±0.18
	2	60	(4.47±0.17)E-2	6.55±0.22
	3	60	(4.94±0.29)E-2	7.42±0.38
2.3	1	70	(4.19±0.18)E-2	4.76±0.16
	2	70	(4.03±0.25)E-2	4.89±0.21
	3	70	(5.57±0.57)E-2	5.71±0.46
2.4	1	100	0.265±0.006	1.87±0.07
	2	100	0.276±0.013	1.68±0.12
	3	100	0.311±0.013	1.52±0.12
2.5	1	110	0.496±0.009	0.94±0.05
	2	110	0.477±0.010	0.96±0.05
	3	110	0.493±0.011	0.97±0.06
E_a , (kJ/mole)		$\ln(A_s)$ $\ln(s^{-1})$	Diffusion Constants	
56.9±8.5		17.1±2.9	$D = D_0 + D_1 T$ $D_0 = 13.4 \pm 1.2$ $D_1 = -0.117 \pm 0.013$	

a. Experiment and repetitions numbers refer to those in Table 4.4.

were slightly higher than those found using eq. (3.5). Since eq. (3.4) resulted in the lowest confidence intervals for the estimated rate constants, and since the confidence intervals for the activation energy constants did not incorporate the variability of the rate constants, eq. (3.4) was determined to be the best model for the EPON 828/MPDA system studied here. The parameters estimated using eq. (3.4) with the least squares method were used in the estimation procedure for the thermal properties during curing because it incorporated all of the kinetic DSC data in the analysis, instead of relying on just a few points.

The parameters estimated using the alternate diffusion model (eq. 3.18) presented in Section 3.2.2 were used in the estimation of the thermal properties during the second half of the curing reaction. The degree of cure rates estimated using eq. (3.4) at $\alpha_D = 0.50$ were included in the procedure. The first model presented in Section 3.2.2 by Hawley et al. (1988) was determined to be inappropriate, as discussed in Section 5.2.3.

The kinetic models used in the estimation of the thermal properties during curing are summarized below.

Degree of cure less than 0.50 (autocatalyzed controlled reaction):

$$\frac{d\alpha}{dt} = (c_1 + c_2 \alpha^m)(1 - \alpha)^n \quad m + n = 2$$

where $c_1 = A_1 \exp(-E_1 / R(T+273.15));$

$c_2 = A_2 \exp(-E_2 / R(T+273.15));$

and, $m = m_0 + m_1 T.$

The estimated parameters are:

$E_1 = 55.8 \text{ kJ/mole},$

$E_2 = 49.2 \text{ kJ/mole},$

$A_1 = 1.21 \times 10^4 \text{ s}^{-1},$

$A_2 = 1.21 \times 10^4 \text{ s}^{-1},$

$m_0 = 0.98,$

and, $m_1 = -0.0023.$

Degree of cure greater than 0.50 (diffusion controlled reaction):

$$\frac{d\alpha}{dt} = \left(\frac{d\alpha}{dt} \right)_{\alpha=\alpha_D} + c_3 (\alpha_D - \alpha) e^{-D(\alpha_D - \alpha)}$$

where $c_3 = A_3 \exp(-E_3 / R(T+273.15))$,

$$\alpha_D = 0.5$$

and $D = D_0 + D_1 T$.

The estimated parameters are:

$$E_3 = 56.9 \text{ kJ/mole,}$$

$$A_3 = 2.75 \times 10^7 \text{ s}^{-1},$$

$$D_0 = 13.4,$$

and, $D_1 = -0.117$.

These models and associated parameters were incorporated into the computer programs *CURE1D* and *PROP1D_CURE* for the estimation of the thermal properties during curing.

5.3 Estimation of the Thermal Properties of Composite Materials during Curing

The estimation of thermal properties of AS4/EPON 828 composite materials during curing is the focal point of this section. First, an analysis of the estimation procedure through the use of simulated data is given in Section 5.3.1. The second section (5.3.2) is devoted to the analysis of the results for the estimated properties from experimental data. The estimated thermal properties are presented and discussed, and improvements for the experimental apparatus and design are proposed. It is emphasized that this is an introductory investigation into this problem, and that the objective here is to establish the procedures and experimental design for the estimation of thermal properties during curing, rather than to determine specific numerical values.

5.3.1. Analysis of the Estimation Procedure using Simulated Data

The procedure for the estimation of thermal properties during the curing of carbon /epoxy composite materials described in Section 3.3 was first implemented and analyzed using simulated temperature data. This simulated temperature data was generated through the use of the computer program *CURE1D*, described in Section 3.3.1, and the resulting temperatures were used as input for the program *PROP1D_CURE* (Section 3.3.2) for the estimation of the thermal properties. A description of the test cases used in the analysis of the estimation procedure is first given, followed by the results of the estimated thermal properties using the simulated data as input.

5.3.1.1 Description of Test Cases

The computer program, *CURE1D*, was used to generate temperature data as input for the program *PROP1D_CURE*. Several different test cases, involving different input conditions for the program *CURE1D* and added random errors, were used in this analysis. The input conditions for *CURE1D* were designed to simulate one of the heat flux pulses in Exp. 3.2, which corresponds to the second experiment during curing described in Section 4.3. The thermo-kinetic problem defined by these parameters can be mathematically described as

$$\frac{\partial}{\partial x} \left[k(T, \alpha) \frac{\partial T}{\partial x} \right] + \rho H_t \frac{d\alpha}{dt} = \rho c_p(T, \alpha) \frac{\partial T}{\partial t} \quad 0 \leq x \leq L; \quad t > 0$$

with the boundary conditions,

$$-k(T, \alpha) \frac{\partial T}{\partial x} = q(t) = \begin{cases} 0 & ; 0 < t \leq t_1 \\ q_0 & ; t_1 < t \leq t_2 \\ 0 & ; t_2 < t \leq t_3 \end{cases} \quad x = 0$$

$$T = T_L(t) \quad x = L; \quad t > 0$$

and the initial condition,

$$T = T_0(x) \quad 0 \leq x \leq L; \quad t = 0$$

where,

$$\frac{d\alpha}{dt} = (c_1 + c_2 \alpha^m)(1 - \alpha)^n \quad m + n = 2 \quad \alpha \leq 0.5$$

$$c_1 = A_1 \exp(-E_1 / R(T+273.15));$$

$$c_2 = A_2 \exp(-E_2 / R(T+273.15));$$

$$m = m_0 + m_1 T.$$

with the initial condition,

$$\alpha = 0.0 \quad t = 0$$

and for $\alpha > 0$,

$$\frac{d\alpha}{dt} = \left(\frac{d\alpha}{dt} \right)_{\alpha=\alpha_D} + c_3 (\alpha_D - \alpha) e^{-D(\alpha_D - \alpha)} \quad \alpha > 0.5$$

$$c_3 = A_3 \exp(-E_3 / R(T+273.15)),$$

$$D = D_0 + D_1 T.$$

with the initial condition,

$$\alpha = \alpha_D \quad t = t_{\alpha=\alpha_D}$$

where T is °C.

The kinetic parameters presented in Section 5.4.2 were used in the analysis of the kinetic equations shown above. The total heating time ($t_2 - t_1$) was set equal to 135

seconds and the input heat flux, q_0 , was set equal to 800 W/m^2 ; these values are consistent with the values used in the experimental procedures. A total time, t_0 , of 300 seconds was used in this analysis. Based on the measured thicknesses of the experimental composite samples, the hypothetical composite thickness, L , was taken to be 4.5 mm. All of these parameters mentioned thus far were identical in all of the case tests studied. The temperature boundary condition at $x = L$, $T_L(t)$, and the initial condition, $T_0(x)$, were both taken to be constant and equal to one another in each test case studied. Two different values were used for these parameters; one set of test cases was evaluated at 75°C and a second set was evaluated at 125°C . The analysis also required the initial degree of cure; in all cases it was assumed that the initial degree of cure was uniformly constant. For the test cases at 75°C , a value of 0.40 was used, and for the test cases at 125°C , a initial degree of cure of 0.80 was used.

Two different conditions were used for the thermal properties, in one instance the properties were taken to be constant, and in the second instance, the properties were taken to vary linearly with both temperature and degree of cure. For the first instance, the constant properties were evaluated at 100°C using the equations shown in Table 5.2:

$$k(T) = 0.742 + 9.02 \times 10^{-4} T;$$

$$\text{for } T = 100^\circ\text{C}, k = 0.83 \text{ W/m}^\circ\text{C};$$

$$\rho c_p(T) = 1.39 + 4.5 \times 10^{-3} T;$$

$$\text{for } T = 100^\circ\text{C}, \rho c_p = 1.84 \text{ MJ/m}^3 \text{ }^\circ\text{C}.$$

and for the case where the properties were assumed to vary linearly with temperature and degree of cure, the following hypothetical relationship was assumed:

$$k(T, \alpha) = 0.9k_0 + k_1 T + 0.1k_2 \alpha,$$

and,

$$\rho c_p(T, \alpha) = 0.9(\rho c_p)_0 + (\rho c_p)_1 T + 0.10(\rho c_p)_2 \alpha$$

(Note that when α equals 1.0, these equations reduce to those shown in Table 5.2.)

Using the values for k_0 , k_1 , $(\rho c_p)_0$ and $(\rho c_p)_1$ given in Table 5.2, one obtains

$$k(T, \alpha) = 0.6678 + 9.02 \times 10^{-4} T + 0.0742 \alpha, \quad (\text{W/m}^\circ\text{C}) \quad (5.6)$$

and,

$$\rho c_p(T, \alpha) = 1.251 + 4.5 \times 10^{-3} T + 0.139 \alpha, \quad (\text{MJ/m}^3 \text{ }^\circ\text{C}) \quad (5.7)$$

The program *CURE1D* requires input values for k and ρc_p at two different temperatures and two different degree of cure values for the case where the thermal properties vary linearly with both temperature and degree of cure (see eq. 3.21). Therefore, using eqs. (5.6) and (5.7) with temperature values of 75°C and 100°C, and degree of cure values of 0.4 and 0.8, the input property values for *CURE1D* were as follows:

For thermal conductivity, k , (W/m°C)

$$\begin{aligned} k(75, 0.4) &= 0.765; & k(75, 0.8) &= 0.795; \\ k(100, 0.4) &= 0.810; \text{ and} & k(100, 0.8) &= 0.840. \end{aligned}$$

For density-specific heat, ρc_p , (MJ/m³ °C)

$$\begin{aligned} \rho c_p(75, 0.4) &= 1.644; & \rho c_p(75, 0.8) &= 1.700; \\ \rho c_p(100, 0.4) &= 1.869; & \rho c_p(100, 0.8) &= 1.925. \end{aligned}$$

The temperatures were calculated using *CURE1D* and the various input parameters described in this section at the locations for $x = 0.0$ mm, $x = 2.25$ mm, $x = 3.375$, and $x = 4.5$ mm. Normally distributed random temperature errors (Abramowitz and Stegun, 1970) were added to the results from *CURE1D* prior to use in the parameter estimation program *PROP1D_CURE*. Two thermocouples were simulated at each of the above locations by adding two different sets of normally distributed random errors to the temperatures calculated using *CURE1D*. Three different values for the standard deviations of the temperature errors, σ_T , were used: $\sigma_T = 0.0$ (no errors); $\sigma_T = 0.10^\circ\text{C}$; and, $\sigma_T = 0.25^\circ\text{C}$.

The input parameters for the test cases used in this analysis are summarized in Table 5.12. A total of eleven different test cases were studied, each with different combinations of initial temperature, thermal property, and standard deviation for temperature errors values. The cases with the standard deviation, σ_T , not equal to zero were repeated six times using a different set of random errors with the same standard deviation for each repetition. The temperature change associated with each case was approximately 5°C, and the degree of cure change was approximately 5%.

5.3.1.2 Results from Test Cases

Each of the test cases shown in Table 5.12 was analyzed using *PROP1D_CURE* for the estimation of thermal conductivity and density-specific heat. In each case, the 95% confidence intervals of the estimated parameters were calculated within the program *PROP1D_CURE* assuming that the errors associated with the temperature measurements are correlated and autoregressive (Beck, 1989). These conditions are typically associated with actual temperature measurements, however, the errors in this case were calculated as normally distributed and independent. The differences between these types of errors can be seen through the comparison of the residuals from actual experiments (see Figure 5.1) and the residuals from the hypothetical cases. The residuals from the hypothetical thermocouples at $x = 0.$, $x = 1.125$ mm, $x = 2.25$ mm, and $x = 3.375$ for one test case with $\sigma_T = 0.25$ are shown in Figure 5.12. These errors, unlike those shown in Figure 5.1, are uncorrelated and unbiased, with a constant variance throughout the time period. Despite these differences in the types of errors, the use of hypothetical data in the parameter estimation procedure provides an excellent means of testing and evaluating the process.

The estimated thermal conductivity and density-specific heat values for cases 1.1, 2.1-2.6, and 3.1-3.6, involving an initial temperature of 75°C and constant thermal properties are given in Table 5.13. Similarly, results for cases 4.1, 5.1-5.6, and 6.1-6.6, involving an initial temperature of 125°C and constant thermal properties are given in Table 5.14. The percent errors given in both of these tables represent the differences between calculated properties and the input properties values to *CURE1D*. Since the

Table 5.12. Test Cases for the Estimation of Thermal Conductivity, k , and Density-Specific Heat, ρc_p , from Simulated Data for Composite Materials during Curing.

Case No.	T_L, T_o^a (°C)	α^b	σ_T^c (°C)	k (W/m°C)	ρc_p (MJ/m ³ °C)
1.1	75	0.40	0.00	0.83	1.84
2.1-2.6	75	0.40	0.10	0.83	1.84
3.1-3.6	75	0.40	0.25	0.83	1.84
4.1	125	0.80	0.00	0.83	1.84
5.1-5.6	125	0.80	0.10	0.83	1.84
6.1-6.6	125	0.80	0.25	0.83	1.84
7.1	75	0.40	0.00	linear ^c k	linear ^c ρc_p
8.1-8.6	75	0.40	0.10	linear ^c k	linear ^c ρc_p
9.1-9.6	75	0.40	0.25	linear ^c k	linear ^c ρc_p
10.1	125	0.80	0.00	linear ^c k	linear ^c ρc_p
11.1-11.6	125	0.80	0.10	linear ^c k	linear ^c ρc_p
12.1-12.6	125	0.80	0.25	linear ^c k	linear ^c ρc_p

- a. Temperature boundary condition and initial temperature (constant).
b. Degree of cure.
c. Standard deviation of temperature errors.

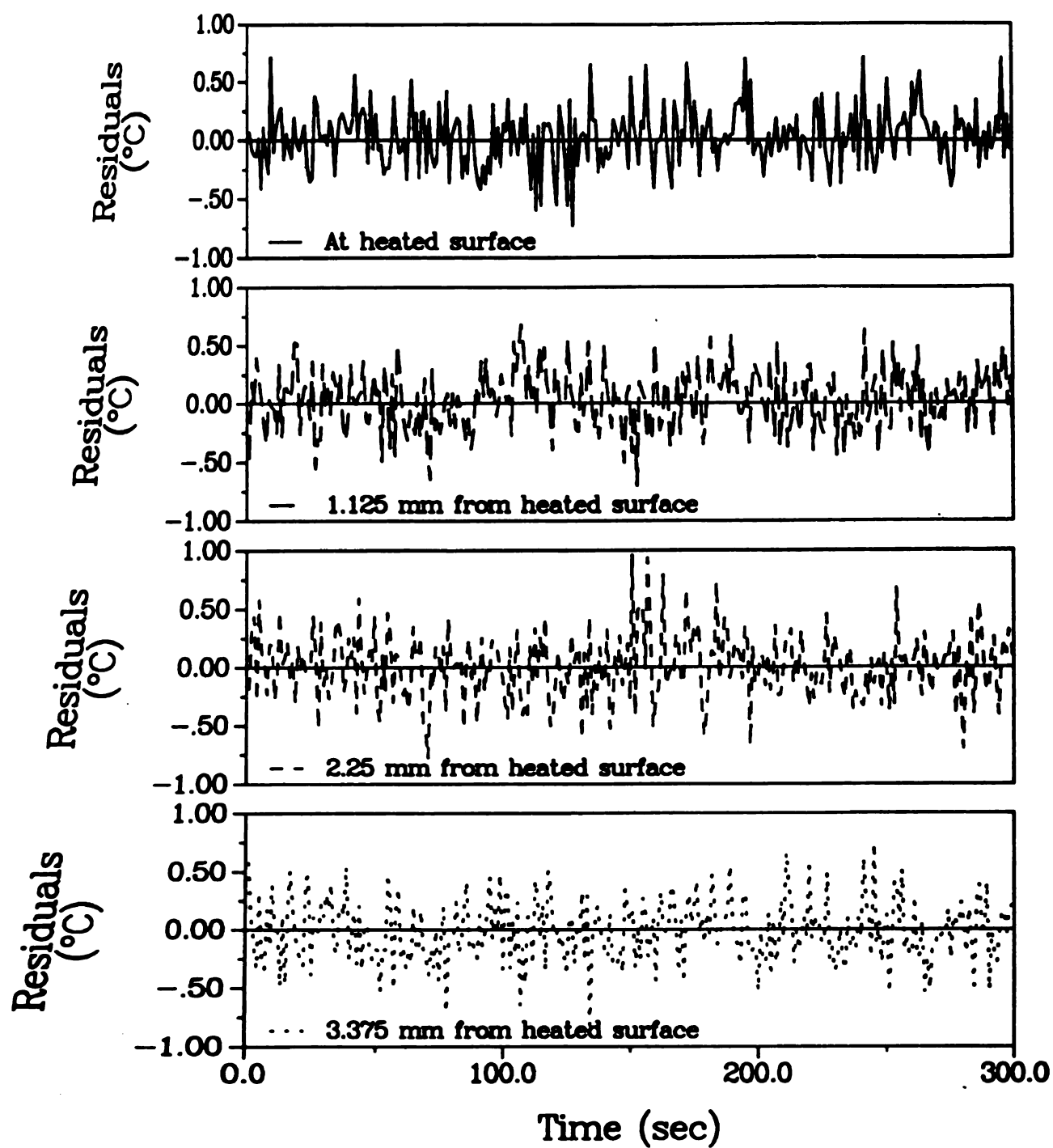


Figure 5.12 Residuals for a Simulated Test Case, using Input Temperature Errors with a Standard Deviation of 0.25°C , at Four Different Locations (total thickness equal to 4.5 mm).

Table 5.13. Estimated Effective Thermal Conductivity, k , Perpendicular to the Fibers and Density-Specific Heat, ρc_p , and the Associated 95% Confidence Intervals for a Simulated Composite with an Initial Temperature of 75°C, an Initial Degree of Cure of 0.40, and Thermal Properties: $k = 0.83 \text{ W/m}^\circ\text{C}$ and $\rho c_p = 1.84 \text{ MJ/m}^3 \text{ }^\circ\text{C}$.

Case No.	σ_T^a (°C)	RMS ^b (°C)	Estimated Thermal Conductivity		Estimated Density-Specific Heat	
			k (W/m°C)	Error ^c (%)	ρc_p (MJ/m ³ °C)	Error ^c (%)
1.1	0.00	0.003	0.8299	0.01	1.840	0.00
2.1	0.10	0.100	0.8218±0.0063	0.99	1.821±0.034	1.03
2.2	0.10	0.101	0.8315±0.0022	0.18	1.846±0.025	0.60
2.3	0.10	0.098	0.8268±0.0021	0.39	1.865±0.019	1.35
2.4	0.10	0.100	0.8294±0.0021	0.12	1.827±0.039	0.71
2.5	0.10	0.103	0.8291±0.0025	0.11	1.824±0.021	0.87
2.6	0.10	0.101	0.8267±0.0020	0.40	1.852±0.018	0.65
3.1	0.25	0.248	0.8312±0.0051	0.15	1.843±0.045	0.08
3.2	0.25	0.253	0.8217±0.0054	1.00	1.940±0.049	5.44
3.3	0.25	0.248	0.8389±0.0059	1.07	1.841±0.050	0.05
3.4	0.25	0.252	0.8234±0.0056	0.79	1.882±0.049	2.28
3.5	0.25	0.258	0.8373±0.0056	0.70	1.882±0.048	2.28
3.6	0.25	0.256	0.8294±0.0052	0.07	1.820±0.045	1.09

a. Standard deviation of temperature errors.

b. Root mean squared error between calculated and input temperatures in PROP1D_CURE.

c. % difference between input and estimated thermal properties.

Table 5.14. Estimated Effective Thermal Conductivity, k , Perpendicular to the Fibers and Density-Specific Heat, ρc_p , and the Associated 95% Confidence Intervals for a Simulated Composite with an Initial Temperature of 125°C, an Initial Degree of Cure of 0.80, and Thermal Properties: $k = 0.83 \text{ W/m}^\circ\text{C}$ and $\rho c_p = 1.84 \text{ MJ/m}^3 \text{ }^\circ\text{C}$.

Case No.	σ_T^a (°C)	RMS ^b (°C)	Estimated Thermal Conductivity		Estimated Density-Specific Heat	
			k (W/m°C)	Error ^c (%)	ρc_p (MJ/m ³ °C)	Error ^c (%)
4.1	0.00	0.003	0.8296	0.05	1.839	0.05
5.1	0.10	0.100	0.8274±0.0019	0.31	1.808±0.017	1.74
5.2	0.10	0.101	0.8286±0.0019	0.17	1.832±0.017	0.43
5.3	0.10	0.100	0.8297±0.0020	0.04	1.866±0.018	1.41
5.4	0.10	0.100	0.8313±0.0018	0.16	1.847±0.016	0.38
5.5	0.10	0.103	0.8321±0.0018	0.25	1.874±0.016	1.85
5.6	0.10	0.101	0.8309±0.0019	0.11	1.816±0.017	1.30
6.1	0.25	0.251	0.8107±0.0126	2.33	1.801±0.073	2.12
6.2	0.25	0.261	0.8261±0.0043	0.47	1.795±0.039	2.45
6.3	0.25	0.249	0.8336±0.0048	0.43	1.866±0.043	1.41
6.4	0.25	0.250	0.8389±0.0049	1.07	1.880±0.044	2.17
6.5	0.25	0.248	0.8373±0.0044	0.88	1.833±0.039	0.38
6.6	0.25	0.255	0.8357±0.0049	0.69	1.896±0.044	3.04

a. Standard deviation of temperature errors.

b. Root mean squared error between calculated and input temperatures in PROP1D_CURE.

c. % difference between input and estimated thermal properties.

two programs (*CURE1D* and *PROP1D_CURE*) utilize similar numerical methods, the errors associated with the case of $\sigma_T = 0.0$ were very small ($<0.05\%$), as expected, and these errors are assumed to be numerical round-off errors. In all cases, the root mean squared errors (RMS) are close in magnitude to the standard deviation of the input temperature errors, σ_T , as expected. The estimated thermal conductivity values associated with initial temperatures equal to 75°C and 125°C , and σ_T equal to 0.10°C all had errors less than 1% of the input thermal properties used in *CURE1D*. The errors associated with the estimated thermal conductivity values with σ_T equal to 0.25°C were all less than 2.5%. The errors associated with the estimated density-specific heat were typically higher; errors with $\sigma_T = 0.10^\circ\text{C}$ were less than 2%, while the errors in the estimated density-specific heat values with $\sigma_T = 0.25^\circ\text{C}$ were less than 2.5%, with the exception of one case for which the error was over 5%. It should be noted that in many cases, the confidence intervals calculated using *PROP1D_CURE* of estimated thermal properties with $\sigma_T > 0.0^\circ\text{C}$ did not include the thermal properties determined with $\sigma_T = 0.0^\circ\text{C}$, as expected.

The results for the cases in which the properties were taken to be linear functions of temperature and degree of cure are given in Table 5.15 for Cases 7.1, 8.1-8.6, and 9.1-9.6, for which the initial temperatures were all equal to 75°C , and in Table 5.16 for Cases 10.1, 11.1-11.6, and 12.1-12.6, in which the initial temperatures are all were equal to 125°C . In these tables, the percent errors given were calculated from the differences between the estimated properties with $\sigma_T = 0.0$ and the estimated properties with $\sigma_T \neq 0.0$. Exact property values were not used in the error analysis in these cases since the properties were assumed to be linear with temperature and degree of cure, and these values varied slightly over each run. However, if the estimated parameters are associated with the average surface temperature over each run and the average degree of cure, one can compare these estimated values with using the same temperature and degree of cure values in eqs. (5.6) and (5.7). The average surface temperatures and degree of cure values were calculated from the cases with $\sigma_T = 0.0$. For the case with an initial temperature of 75°C and initial degree of cure of 0.40,

Table 5.15. Estimated Effective Thermal Conductivity, k , Perpendicular to the Fibers and Density-Specific Heat, ρc_p , and the associated 95% Confidence Intervals for a Simulated Composite with an Initial Temperature of 75°C, an Initial Degree of Cure of 0.40, and Thermal Properties: k (W/m°C) = $0.6678 + 9.03 \times 10^{-4}T + 0.0742\alpha$, and ρc_p (MJ/m³ °C) = $1.251 + 0.0045T + 0.139\alpha$.

Case No.	σ_T^a (°C)	RMS ^b (°C)	Estimated Thermal Conductivity		Estimated Density-Specific Heat	
			k (W/m°C)	Error ^c (%)	ρc_p (MJ/m ³ °C)	Error ^c (%)
7.1	0.00	0.003	0.7678±0.0003	-	1.653±0.002	-
8.1	0.10	0.102	0.7680±0.0019	0.03	1.654±0.016	0.06
8.2	0.10	0.103	0.7663±0.0019	0.20	1.629±0.015	1.45
8.3	0.10	0.100	0.7664±0.0018	0.18	1.668±0.015	0.91
8.4	0.10	0.100	0.7700±0.0019	0.29	1.653±0.015	0.00
8.5	0.10	0.104	0.7697±0.0018	0.25	1.650±0.018	0.18
8.6	0.10	0.098	0.7683±0.0017	0.07	1.657±0.016	0.24
9.1	0.25	0.253	0.7646±0.0050	0.42	1.610±0.042	2.60
9.2	0.25	0.252	0.7652±0.0043	0.34	1.691±0.038	2.30
9.3	0.25	0.255	0.7732±0.0052	0.70	1.706±0.044	3.21
9.4	0.25	0.255	0.7678±0.0047	0.00	1.664±0.041	0.67
9.5	0.25	0.262	0.7672±0.0051	0.08	1.608±0.043	2.72
9.6	0.25	0.251	0.7658±0.0047	0.26	1.649±0.040	0.24

a. Standard deviation of temperature errors.

b. Root mean squared error between calculated and input temperatures in PROP1D_CURE.

c. % difference between test cases with $\sigma_T > 0$ and $\sigma_T = 0$.

Table 5.16. Estimated Effective Thermal Conductivity, k , Perpendicular to the Fibers and Density-Specific Heat, ρc_p , and the Associated 95% Confidence Intervals for a Simulated Composite with an Initial Temperature of 125°C, an Initial Degree of Cure of 0.80, and Thermal Properties: k (W/m°C) = $0.6678 + 9.03 \times 10^{-4}T + 0.0742\alpha$ and ρc_p (MJ/m³ °C) = $1.251 + 0.0045T + 0.139\alpha$.

Case No.	σ_T^a (°C)	RMS ^b (°C)	Estimated Thermal Conductivity		Estimated Density-Specific Heat	
			k (W/m°C)	Error ^c (%)	ρc_p (MJ/m³ °C)	Error ^c (%)
10.1	0.00	0.004	0.8443±0.0000	-	1.930±0.000	-
11.1	0.10	0.101	0.8446±0.0009	0.04	1.919±0.017	0.57
11.2	0.10	0.104	0.8442±0.0019	0.01	1.921±0.017	0.47
11.3	0.10	0.100	0.8452±0.0019	1.65	1.948±0.018	0.93
11.4	0.10	0.105	0.8451±0.0021	0.10	1.933±0.019	0.16
11.5	0.10	0.105	0.8469±0.0021	0.31	1.933±0.019	0.16
11.6	0.10	0.099	0.8434±0.0019	0.11	1.938±0.017	0.42
12.1	0.25	0.252	0.8451±0.0051	0.10	1.937±0.046	0.36
12.2	0.25	0.255	0.8479±0.0054	0.43	1.926±0.049	0.21
12.3	0.25	0.250	0.8568±0.0048	1.48	1.962±0.004	1.66
12.4	0.25	0.254	0.8407±0.0055	0.43	1.928±0.051	0.10
12.5	0.25	0.248	0.8436±0.0045	0.08	1.926±0.041	0.21
12.6	0.25	0.259	0.8459±0.0052	0.08	1.972±0.047	2.18

a. Standard deviation of temperature errors.

b. Root mean squared error between calculated and input temperatures in PROP1D_CURE.

c. % difference between test cases with $\sigma_T > 0$ and $\sigma_T = 0$.

$$\bar{T} = 76.8^{\circ}\text{C}$$

and, $\bar{\alpha} = 0.425;$

for the case with an initial temperature of 125°C and initial degree of cure of 0.80,

$$\hat{T} = 126.8^{\circ}\text{C}$$

and, $\bar{\alpha} = 0.856.$

Substituting the above values into eqs. (5.6) and (5.7), the thermal conductivity and density-specific heat values are:

$$k(76.8, 0.425) = 0.7686 \text{ W/m}^{\circ}\text{C} \quad (5.8a)$$

$$\rho c_p(76.8, 0.425) = 1.656 \text{ MJ/m}^3 \text{ }^{\circ}\text{C} \quad (5.8b)$$

$$k(126.8, 0.856) = 0.8457 \text{ W/m}^{\circ}\text{C} \quad (5.8c)$$

$$\rho c_p(76.8, 0.425) = 1.940 \text{ MJ/m}^3 \text{ }^{\circ}\text{C} \quad (5.8d)$$

The the parameters estimates resulting from six repetitions in each of the test cases in Tables 5.15 and 5.16 were averaged and compared with the values shown in eqs. (5.8a-d). The average parameter estimates, along with the percent error, based on the difference between these averaged parameter values and those shown in eqs. (5.8a-d) are shown in Table 5.17. In all cases the percent errors are less than 1%, and due to the uncertainty of the temperature and degree of cure values, the estimates from the cases with the lowest variance in the 'measured' temperature values do not necessarily have the lowest percent error.

5.3.2 Analysis of the Estimation of Thermal Properties from Experimental Data

This section involves the analysis of the temperature data from the experiments discussed in Section 4.3 for the estimation of thermal properties during the curing of AS4/EPON 828-mPDA composite samples. The results from this estimation procedure

Table 5.17. Comparison of Averaged Estimated Thermal Conductivity, \bar{k} , and Density-Specific Heat, $\overline{\rho c_p}$. Values with Values Calculated Using eqs. (5.6) and (5.7).

Case No.	σ_T^a (°C)	T_L, T_0^b (°C)	\bar{k} (W/m°C)	Error ^c (%)	$\overline{\rho c_p}$ (MJ/m ³ °C)	Error ^c (%)
7.1	0.00	75	0.7678	0.10	1.653	0.16
8.1-8.6	0.10	75	0.7681	0.06	1.652	0.25
9.1-9.6	0.25	75	0.7673	0.17	1.655	0.08
10.1	0.00	125	0.8443	0.17	1.930	0.52
11.1-11.6	0.15	125	0.8449	0.10	1.932	0.41
12.1-12.6	0.25	125	0.8467	0.11	1.942	0.10

a. Standard deviation of temperature errors.

b. Temperature boundary condition and initial temperature (constant).

c. % difference between estimated parameters and parameters calculated using eqs. (5.6) and 5.7).

are first presented in Section 5.3.2.1, followed by analysis of the parameter estimates with regards to errors in Section 5.3.2.2. In the last sub-section, suggestions for improvements in the experimental design are presented.

5.3.2.1 Results from Experimental Data

The thermal properties, effective thermal conductivity perpendicular to the fiber axis and effective density-specific heat, were estimated using the temperature measurements from the three experiments discussed in Section 4.3. The first two of these experiments were conducted during the curing process, and the third experiment was conducted after curing. The third experiment was used as a basis for comparison with the results previously presented for cured composite samples in Section 5.1. The temperature measurements from the first experiment (Exp. 3.1), along with the associated heat flux measurements are shown in Figure 5.13, and temperature measurements from six of the twelve thermocouples in the second experiment (Exp. 3.2) are shown in Figure 5.14. The break in the temperature data at approximately 140 minutes was due to an unexpected abort of the data acquisition program. The calculated temperatures resulting from a simulated experiment, using similar experimental conditions as those used in Exp. 3.2 and thermal properties evaluated at 100°C from the results shown in Table 5.1, are shown in Figure 5.15. Exp. 3.2 and 3.3 were conducted using the new Ectron amplifiers and the computer controlled power supply, while Exp. 3.1 was conducted using the Data Translation amplifiers and the manually controlled power supply.

In estimating the thermal properties as functions of temperature and degree of cure, the series of heat flux pulses associated with each experiment were evaluated independently. There were a total of 15 heat flux pulses associated with Exp. 3.1, 16 pulses were associated with Exp. 3.2, and 18 pulses were associated with Exp. 3.3. The average magnitude of the heat flux pulses in Exp. 3.1 was approximately 2000 W/m², and the duration time of each of the pulses was 40 seconds. The average magnitudes of the heat flux pulses in Exps. 3.2 and 3.3 were approximately 800 W/m² and 1500 W/m², respectively, and the duration of each pulse was 135 seconds in both cases.

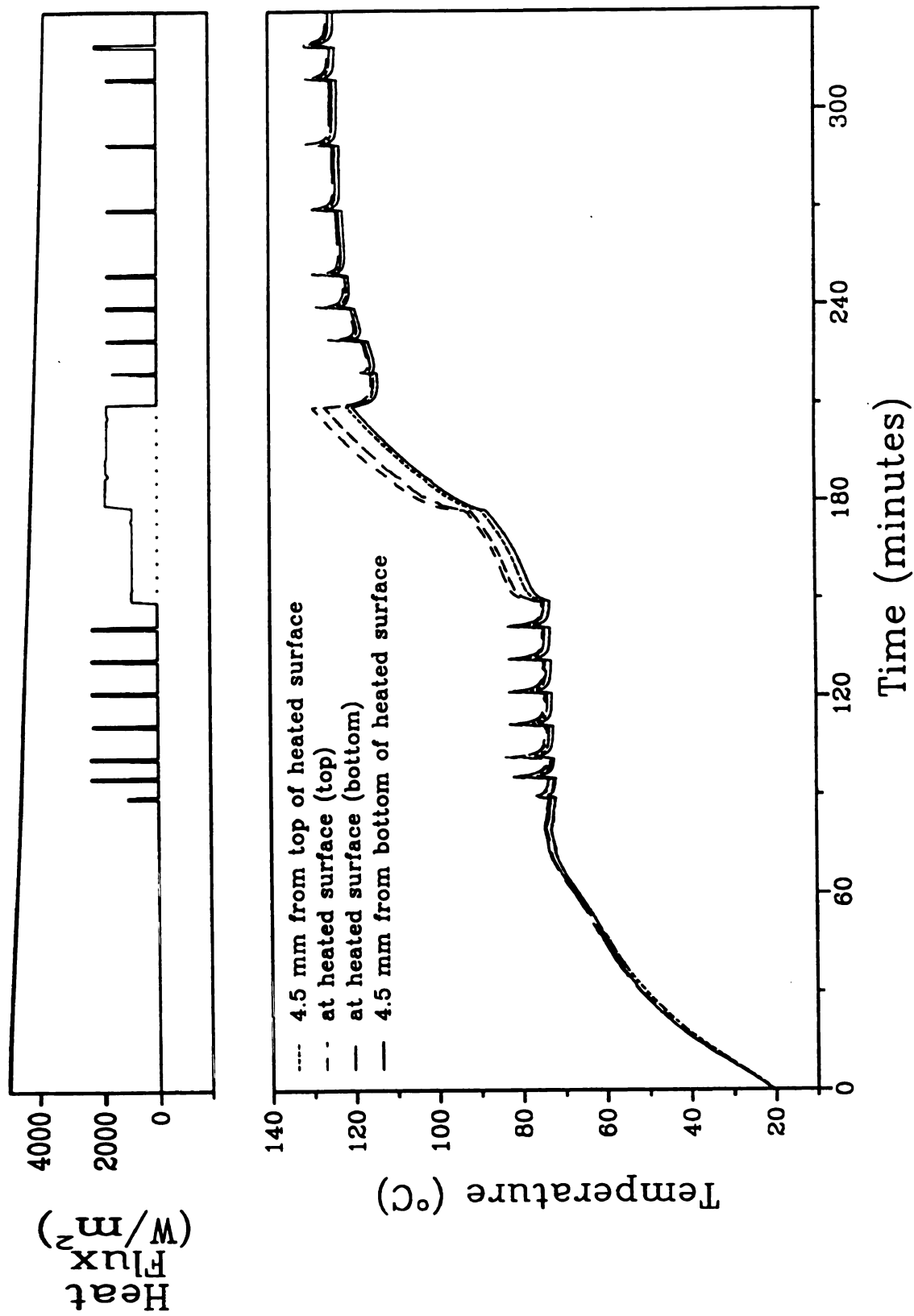


Figure 5.13 Temperature Measurements and Applied Heat Flux from Four Thermocouples in the First Transient Temperature Experiment during Curing (Exp. 3.1).

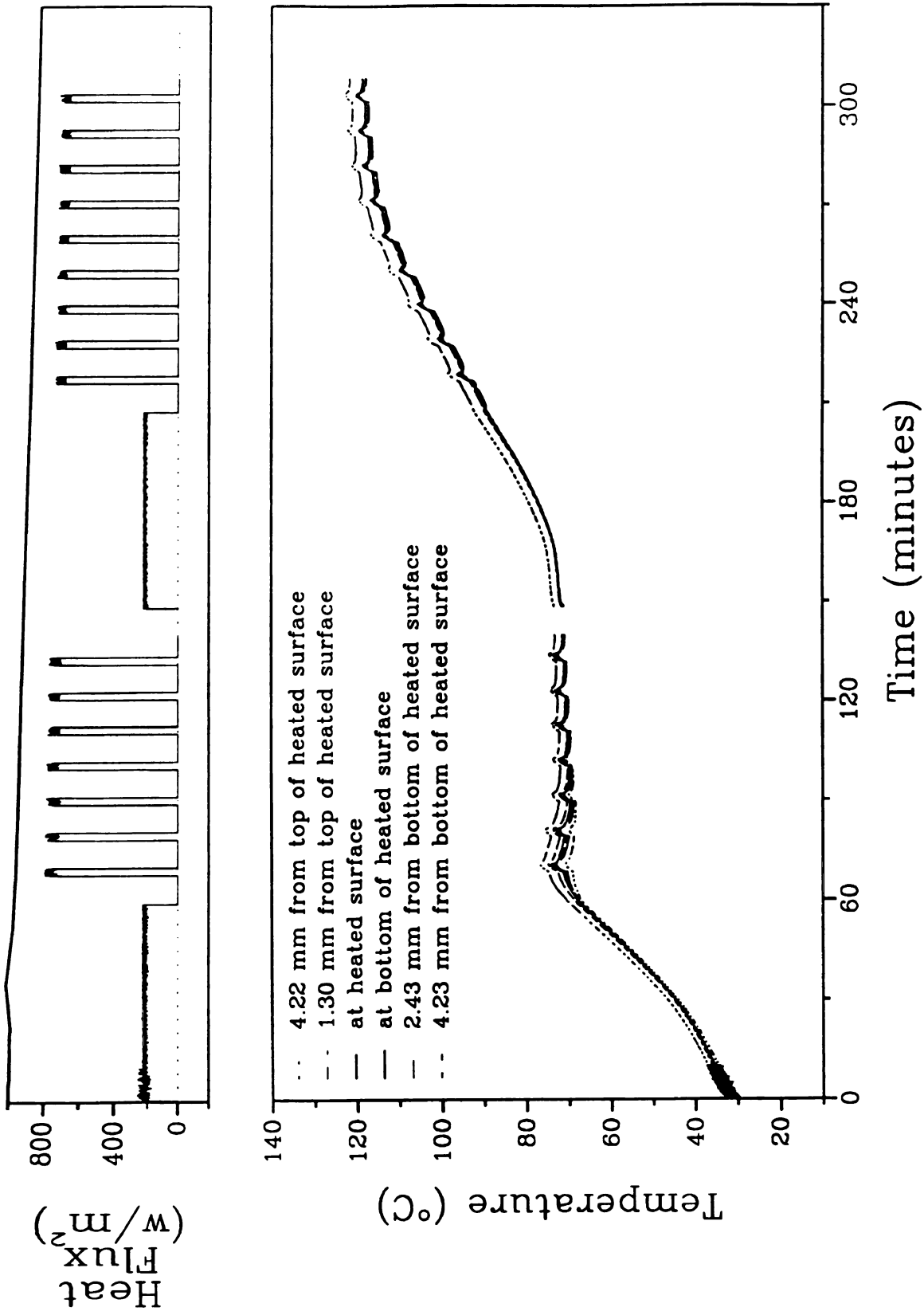


Figure 5.14 Temperature Measurements and Applied Heat Flux from Six Thermocouples in the Second Transient Temperature Experiment during Curing (Exp. 3.2).

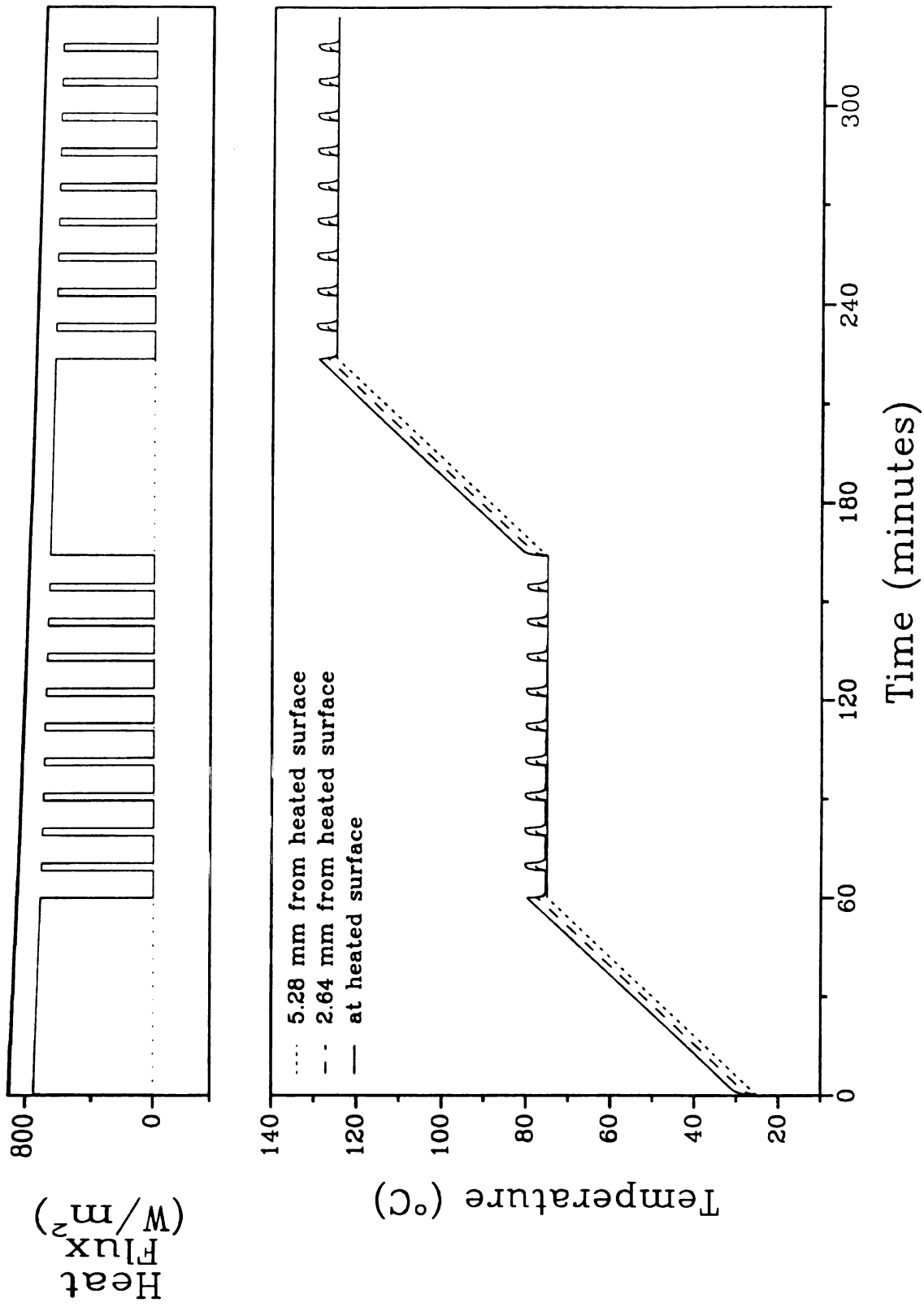


Figure 5.15 Temperatures Resulting from the Simulation of the Second Transient Experiment (3.2) using Thermal Properties Estimated from Cured Composite at 100°C .

Also, the steady state temperatures evident in Figures 5.13 and 5.14 between the heat flux intervals were removed by determining the average temperature from the all of the thermocouple measurements prior to the onset of each heat flux, and subtracting the difference between each thermocouple measurement and the overall average temperature from each thermocouple measurement. Each analysis for the estimation of thermal properties included temperatures from ten seconds prior to the onset of each heat flux interval to at least 150 seconds after the end of each heat flux interval, over which time the thermal properties were assumed constant.

In the experimental design, the heater was placed in the center of the laminate, separating the laminate into two sections, top and bottom, and in using this design, it was assumed that the heat flow was symmetric on either side of the heater. In the estimation of thermal properties, the top and bottom sections were first analyzed separately, assuming half of the measured heat flux was applied to the top section and the other half was applied to the bottom section.

The top and bottom sections associated with the eighteen heat flux pulses in the experiment after curing (Exp. 3.3) were first analyzed for the estimation of the thermal properties, effective thermal conductivity perpendicular to the fiber axis and effective density-specific heat, using *PROPID_CURE*. The estimated thermal conductivity and density-specific heat values for the top and bottom sections, along with the temperature range over each heat flux pulse and the root mean squared error between the calculated and measured temperatures, are shown in Tables 5.18 and 5.19, respectively. The temperature data from the second experiment during curing (Exp. 3.2) was analyzed in a similar manner, and parameter estimates for the top and bottom sections are given in Tables 5.20 and 5.21, respectively. These tables also include the average degree of cure values at the beginning and end of each analysis interval. In both experiments, during and after curing, the estimated thermal conductivity and density-specific heat values for the bottom section were higher than those estimated for the top section.

The differences in the parameter estimates between the top and bottom sections suggested that, even though the steady state temperatures were subtracted from the data, there was uneven heat flow within the top and bottom sections of the sample. To

Table 5.18. Estimation of Thermal Conductivity, k , Perpendicular to the Fiber Direction and Density-Specific Heat, ρc_p , of Cured AS4/EPON 828-mPDA Composites using Temperature Data from the Top Composite Section Only in Exp. 3.3.

Pulse No.	Temperature Range ($^{\circ}\text{C}$)	k ($\text{W}/\text{m}^{\circ}\text{C}$)	ρc_p ($\text{MJ}/\text{m}^3\ ^{\circ}\text{C}$)	RMS ^a ($^{\circ}\text{C}$)
1	51-57	0.493	0.855	0.147
2	54-60	0.504	0.906	0.142
3	57-63	0.480	0.903	0.168
4	60-65	0.508	0.919	0.153
5	62-68	0.499	0.951	0.153
6	63-69	0.516	0.923	0.143
7	65-70	0.506	0.970	0.148
8	66-71	0.546	0.993	0.149
9	67-71	0.573	0.963	0.219
10	78-84	0.532	1.053	0.180
11	81-86	0.499	0.980	0.220
12	85-91	0.518	1.021	0.149
13	90-96	0.499	1.012	0.187
14	94-100	0.519	1.051	0.164
15	99-105	0.506	1.055	0.211
16	104-110	0.516	1.063	0.160
17	109-114	0.515	1.075	0.167
18	112-117	0.501	1.120	0.182

a. Root mean squared error determined from the differences between calculated and experimental temperatures.

Table 5.19. Estimation of Thermal Conductivity, k , Perpendicular to the Fiber Direction and Density-Specific Heat, ρc_p , of Cured AS4/EPON 828-mPDA Composites using Temperature Data from the Bottom Composite Section Only in Exp. 3.3.

Pulse No.	Temperature Range ($^{\circ}\text{C}$)	k ($\text{W/m}^{\circ}\text{C}$)	ρc_p ($\text{MJ/m}^3\ ^{\circ}\text{C}$)	RMS ^a ($^{\circ}\text{C}$)
1	51-57	1.762	1.535	0.136
2	54-60	1.655	1.664	0.139
3	57-63	1.677	1.695	0.127
4	60-65	1.862	1.705	0.151
5	62-68	1.589	2.030	0.176
6	63-69	1.796	1.792	0.138
7	65-70	1.564	1.977	0.144
8	66-71	1.912	1.755	0.155
9	67-71	1.751	1.950	0.171
10	78-84	1.533	1.917	0.160
11	81-86	1.533	1.681	0.163
12	85-91	1.643	1.784	0.156
13	90-96	1.476	1.682	0.137
14	94-100	1.526	1.606	0.144
15	99-105	1.304	1.475	0.157
16	104-110	1.143	1.412	0.175
17	109-114	1.205	1.320	0.167
18	112-117	1.084	1.455	0.178

a. Root mean squared error determined from the differences between calculated and experimental temperatures.

Table 5.20. Estimation of Thermal Conductivity, k , Perpendicular to the Fiber Direction and Density-Specific Heat, ρc_p , of AS4/EPON 828-mPDA Composites during Curing using Temperature Data from the Top Composite Section Only in Exp. 3.2.

Pulse No.	Temperature Range ($^{\circ}\text{C}$)	Degree of Cure	k ($\text{W/m}^{\circ}\text{C}$)	ρc_p ($\text{MJ/m}^3 \cdot ^{\circ}\text{C}$)	RMS ^a ($^{\circ}\text{C}$)
1	71-73	0.11-0.15	0.761	1.409	0.161
2	70-72	0.19-0.23	0.806	0.686	0.364
3	70-72	0.27-0.31	0.837	0.702	0.345
4	70-72	0.35-0.39	0.781	0.708	0.287
5	70-73	0.43-0.47	0.870	0.784	0.300
6	70-73	0.51-0.55	0.794	0.720	0.256
7	71-74	0.58-0.62	0.737	0.853	0.195
8	92-96	0.82-0.84	0.590	1.041	0.131
9	97-100	0.85-0.87	0.646	1.122	0.140
10	102-105	0.88-0.90	0.573	1.140	0.116
11	107-110	0.91-0.93	0.564	1.040	0.148
12	111-114	0.94-0.96	0.567	1.119	0.139
13	114-117	0.96-0.98	0.674	1.045	0.114
14	116-118	0.99-1.00	0.661	1.157	0.152
15	116-119	1.00	0.578	1.087	0.119
16	117-120	1.00	0.583	1.166	0.120

a. Root mean squared error determined from the differences between calculated and experimental temperatures.

Table 5.21. Estimation of Thermal Conductivity, k , Perpendicular to the Fiber Direction and Density-Specific Heat, ρc_p , of AS4/EPON 828-mPDA Composites during Curing using Temperature Data from the Bottom Composite Section Only in Exp. 3.2.

Pulse No.	Temperature Range ($^{\circ}\text{C}$)	Degree of Cure	k ($\text{W/m}^{\circ}\text{C}$)	ρc_p ($\text{MJ/m}^3 \text{ }^{\circ}\text{C}$)	RMS ^a ($^{\circ}\text{C}$)
1	71-73	0.11-0.15	5.665	5.168	0.124
2	70-72	0.19-0.23	1.279	2.700	0.104
3	70-72	0.27-0.31	1.533	2.793	0.112
4	70-72	0.35-0.39	1.762	1.515	0.162
5	70-73	0.43-0.47	1.808	2.018	0.116
6	70-73	0.51-0.55	1.786	1.717	0.139
7	71-74	0.58-0.62	1.762	1.762	0.145
8	92-96	0.82-0.84	3.662	2.024	0.143
9	97-100	0.85-0.87	3.205	1.842	0.138
10	102-105	0.88-0.90	3.152	1.590	0.145
11	107-110	0.91-0.93	4.419	1.921	0.143
12	111-114	0.94-0.96	3.651	1.561	0.155
13	114-117	0.96-0.98	3.543	1.721	0.168
14	116-118	0.99-1.00	2.860	1.840	0.147
15	116-119	1.00	2.501	1.453	0.133
16	117-120	1.00	2.845	1.583	0.136

- a. Root mean squared error determined from the differences between calculated and experimental temperatures.

eliminate the need for the assumption of symmetrical heat flow, the temperature distributions in the top and bottom sections were averaged. The basis for this averaging can be expressed mathematically as follows:

From eqs. (3.19a-d) and the assumption of constant thermal properties over each analysis interval, the governing equations for the top section can be expressed as,

$$k \frac{\partial}{\partial x} \left(\frac{\partial T}{\partial x} \right) + \rho H_t \frac{d\alpha}{dt} = \rho c_p \frac{\partial T}{\partial t} \quad 0 < x < L_T; \quad t > 0 \quad (5.9a)$$

with the boundary conditions,

$$-k \frac{\partial T}{\partial x} = q_T(t) \quad x = 0; \quad t > 0 \quad (5.9b)$$

$$T = T_{LT}(t) \quad x = L_T; \quad t > 0 \quad (5.9c)$$

and the initial condition,

$$T = T_0(x) \quad 0 \leq x \leq L_T; \quad t = 0 \quad (5.9d)$$

where $T_T(x,t)$ represents the temperatures associated with the top section, $q_T(t)$ represents the heat flux boundary condition due to the heater, and L_T is the thickness of the top section.

Likewise, for the bottom section,

$$k \frac{\partial}{\partial x} \left(\frac{\partial T}{\partial x} \right) + \rho H_t \frac{d\alpha}{dt} = \rho c_p \frac{\partial T}{\partial t} \quad 0 < x < L_B; \quad t > 0 \quad (5.10a)$$

with the boundary conditions,

$$-k \frac{\partial T}{\partial x} = q_B(t) \quad x = 0; \quad t > 0 \quad (5.10b)$$

$$T = T_{LB}(t) \quad x = L_B; \quad t > 0 \quad (5.10c)$$

and the initial condition,

$$T = T_0(x) \quad 0 \leq x \leq L_B; \quad t = 0 \quad (5.10d)$$

where $T_B(x,t)$, $q_B(t)$, and L_B are the temperatures, heat fluxes and thickness associated with the bottom section. By assuming that bottom thicknesses of the top and bottom sections are similar, and substituting the average of these thickness, $L = (L_T + L_B)/2$, for L_T and L_B , eqs. (5.9a) and (5.10a); (5.9b) and (5.10b); (5.9c) and (5.10c); and, (5.9d) and (5.10d) can be added together and averaged as follows:

$$k \frac{\partial}{\partial x} \left(\frac{\partial T}{\partial x} \right) + \rho H_t \frac{d\alpha}{dt} = \rho c_p \frac{\partial T}{\partial t} \quad 0 < x < L; \quad t > 0 \quad (5.11a)$$

with the boundary conditions,

$$-k \frac{\partial T}{\partial x} = q(t) \quad x = 0; \quad t > 0 \quad (5.11b)$$

$$T = T_L(t) \quad x = L; \quad t > 0 \quad (5.11c)$$

and the initial condition,

$$T = T_0(x) \quad 0 \leq x \leq L; \quad t = 0 \quad (5.11d)$$

where, $T = (T_T + T_B)/2,$

$$T = (q_T + q_B)/2,$$

and, $T = (T_{LT} + T_{LB})/2$

Therefore, the temperature data from both top and bottom sections of the composite can be used by using the average heat flux (which was used when the sections were analyzed separately) for the first boundary condition and the average temperature for the second boundary.

The heat flux intervals in the experiment during curing and the two experiments after curing were then analyzed using temperature measurements from both top and bottom sections. The results for the estimated thermal properties for some of the heat flux pulses in Exp. 3.3, the experiment after curing; Exp. 3.2, the second experiment during curing; and, Exp. 3.1, the first experiment during curing, are shown in Tables 5.22, 5.23, and 5.24, respectively. The 95% confidence intervals shown for these values were determined in the program *PROP1D_CURE* (Beck, 1989).

The results from the experiment after curing were first compared with the previous estimates of the thermal properties shown in Table 5.1. All of the estimated thermal conductivity values shown in Table 5.22 were approximately 90% higher than the values at corresponding temperature ranges in Table 5.1, and the density-specific heat values in Table 5.22 were approximately 150% higher than the density-specific heat estimates at corresponding temperature ranges in Table 5.1. In addition, the parameter estimates for both thermal conductivity and density-specific heat indicated no significant temperature dependence, since all of the confidence intervals for each parameter were overlapping. The temperature rises for each heat flux pulse were also compared with the temperature rises for the heat flux pulses resulting from the simulated experiments discussed in Section 5.3.1. The heat fluxes in the simulated experiments were 800 W/m^2 , and the resulting temperature rises were approximately 5°C , using thermal properties based on the values shown in Table 5.1. However, the temperature rises shown in Table 5.22 for Exp. 3.3 were only 5°C to 6°C for a heat flux of approximately 1500 W/m^2 .

The results from the second experiment during curing (Exp. 3.2) in Table 5.23 were then compared to the results from Exp. 3.3 shown in Table 5.22. As was found for Exp. 3.3, both the estimated thermal conductivity and density-specific heat values in

Table 5.22. Estimation of Thermal Conductivity, k , Perpendicular to the Fiber Direction and Density-Specific Heat, ρc_p , of Cured AS4/EPON 828-mPDA Composites using Temperature Data from Both Top and Bottom Composite Sections in Exp. 3.3.

Pulse No.	Temperature Range ($^{\circ}\text{C}$)	k ($\text{W/m}^{\circ}\text{C}$)	ρc_p ($\text{MJ/m}^3 \text{ }^{\circ}\text{C}$)	RMS ^a ($^{\circ}\text{C}$)
2	54-60	1.44 ± 0.10	3.86 ± 0.46	0.330
5	54-60	1.54 ± 0.17	4.25 ± 0.68	0.397
8	66-71	1.47 ± 0.06	3.83 ± 0.31	0.282
11	81-86	1.51 ± 0.14	4.33 ± 0.60	0.340
14	94-100	1.52 ± 0.16	4.47 ± 0.66	0.359
17	109-114	1.56 ± 0.19	4.75 ± 0.79	0.416

a. Root mean squared error determined from the differences between calculated and experimental temperatures.

Table 5.23. Estimation of Thermal Conductivity, k , Perpendicular to the Fiber Direction and Density-Specific Heat, ρc_p , of AS4/EPON 828-mPDA Composites during Curing using Temperature Data from both Top and Bottom Composite Sections in Exp. 3.2.

Pulse No.	Temperature Range ($^{\circ}\text{C}$)	Degree of Cure	k ($\text{W/m}^{\circ}\text{C}$)	ρc_p ($\text{MJ/m}^3 \text{ }^{\circ}\text{C}$)	RMS ^a ($^{\circ}\text{C}$)
2	70-72	0.19-0.23	1.67 ± 0.09	3.90 ± 0.56	0.258
4	70-72	0.35-0.39	1.73 ± 0.10	3.80 ± 0.61	0.223
6	70-73	0.51-0.55	1.77 ± 0.08	3.73 ± 0.48	0.205
9	97-100	0.85-0.87	1.65 ± 0.10	4.60 ± 0.57	0.216
12	111-114	0.94-0.96	1.62 ± 0.19	5.24 ± 0.96	0.267
15	116-119	1.00	1.60 ± 0.12	4.62 ± 0.70	0.256

a. Root mean squared error determined from differences between calculated and experimental temperatures.

Table 5.24. Estimation of Thermal Conductivity, k , Perpendicular to the Fiber Direction and Density-Specific Heat, ρc_p , of AS4/EPON 828-mPDA Composites during Curing using Temperature Data from Both Top and Bottom Composite Sections in Exp. 3.1.

Pulse No.	Temperature Range ($^{\circ}\text{C}$)	Degree of Cure	k ($\text{W/m}^{\circ}\text{C}$)	ρc_p ($\text{MJ/m}^3\ ^{\circ}\text{C}$)	RMS ^a ($^{\circ}\text{C}$)
2	73-81	0.34-0.38	1.20 ± 0.11	2.60 ± 0.45	0.356
4	74-81	0.49-0.54	1.24 ± 0.20	2.95 ± 0.91	0.415
6	74-81	0.65-0.68	1.24 ± 0.13	2.95 ± 0.60	0.351
9	117-123	0.98-0.99	1.52 ± 0.37	2.50 ± 1.16	0.441
11	121-129	0.99	1.13 ± 0.10	2.71 ± 0.50	0.275
14	123-131	1.00	1.60 ± 0.23	3.40 ± 0.77	0.168

a. Root mean squared error determined from differences between calculated and experimental temperatures.

Table 5.23 are statistically independent of temperature. The estimated thermal conductivity values from Exp. 3.3 were approximately 10% higher than those estimated for Exp. 3.2, and the estimated density-specific heat values were statistically equivalent in both experiments. Also, the temperature rise during this experiment was expected to be on the order of 5°C to 6°C, as discussed in Section 4.3; however, the observed temperature rise was only 2°C to 3°C. This is consistent with the results shown for Exp. 3.3, for which the temperature rise was much less than anticipated.

Finally, the results from the two experiments during curing (Exp. 3.1 and Exp. 3.2) were compared. Both the thermal conductivity and density-specific heat estimates shown in Table 5.23 for Exp. 3.2 were significantly higher than the values shown in Table 5.24 for Exp. 3.1.

Due to the discrepancies between the results from the experiment after curing (Exp. 3.3) and those shown in Table 5.1, the difference in the required heat flux for a given temperature rise between the simulated experiments discussed in Section 5.3.1 and Exp. 3.3, and the differences between the results for the two curing experiments (Exps. 3.1 and 3.2), the parameter estimates from these three experiments were taken to be unreasonable, and additional efforts were concentrated on finding the reasons for the discrepancies listed above with the goal of providing improvements for the experimental design.

5.3.2.2 Investigation of Possible Errors in the Estimation of Thermal Properties during Curing

The residuals, as discussed previously, are useful in gaining insight into possible errors in the experimental design and estimation procedure. The residuals for three of the five thermocouples at the heated surface during the fifth heat flux pulse for Exp. 3.3, conducted after curing, are shown in Figure 5.16. These values are typical of the residuals for all the heat flux pulses in Exp. 3.3. The temperature rise at the heated surface in Exp. 3.3 was approximately 6°C, and the magnitude of the maximum residuals of the three thermocouples shown in this figure were approximately 3.0°C.

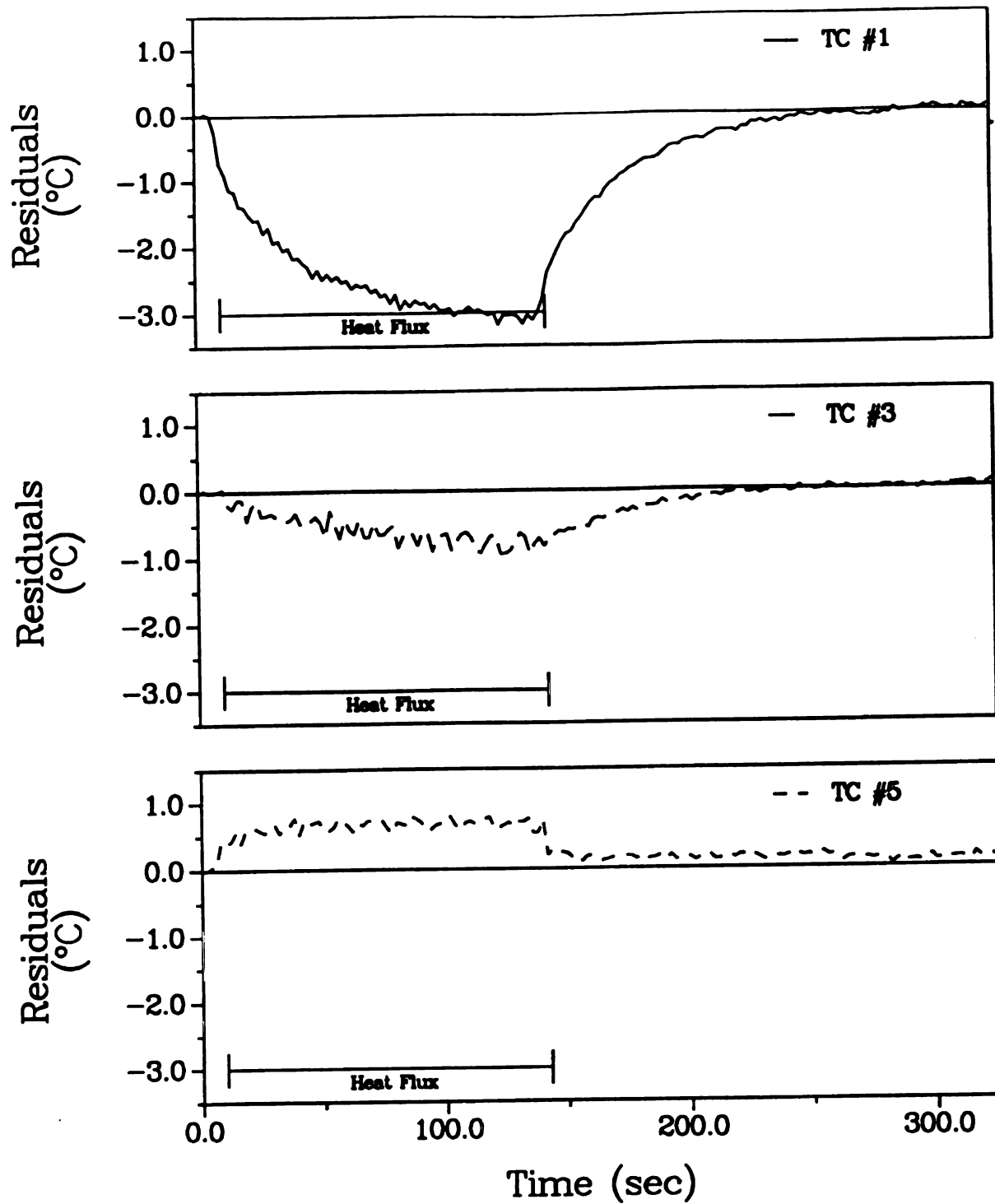


Figure 5.16 Residuals Associated with Three of the Five Thermocouples (TC#1, TC#2, and TC#3) Located at the Heated Surface for the Fifth Heat Flux Pulse in Exp. 3.3.

0.9°C, and 0.8°C, and the magnitude of the maximum residuals for the two thermocouples at the heated surface not shown in this figure were 2.8°C and 1.5°C. These residuals were from 12% to 50% of the maximum temperature rise, which suggests significant errors could be associated with these measurements. The residuals are also very biased, suggesting that the heat flux distribution across the heater was extremely nonuniform; this is especially evident for the first thermocouple.

To further investigate other possible sources of error, the temperatures measurements at the end of the heat flux pulses shown in Tables 5.22, 5.23, and 5.24 were plotted as functions of location with respect to the heated surface in Figures 5.17, 5.18, and 5.19, respectively. The 95% confidence bands shown in each figure were found from the linear regression of temperatures with respect to location using PLOTIT^R (1989). In all of these figures, the temperature differences across the composite samples were within the error limits of the thermocouples. This is evident by comparing the confidence bands near the heated surface with the confidence bands of the corresponding regions farthest from the heated surface. In each of the heat flux pulses shown in each figure, the confidence intervals overlapped one another, signifying that the temperatures were statistically equivalent. This also indicated that the temperatures at the boundary away from the heated surface increased, which is illustrated by comparing the measured temperatures farthest from the heated surface in Figures 5.13 and 5.14 with the calculated temperatures farthest from the heat flux boundary condition in the simulated experiment shown in Figure 5.15. The experimental temperatures farthest from the heated surface were shown to increase significantly during the heat flux intervals, while ideally they would remain constant, as shown by the calculated temperatures farthest from the heated surface in Figure 5.15. This suggests that the mechanical press and oven apparatus used in these experiments were inappropriate due to lack of a means to control the temperature at the boundaries of the composite away from the heated surface.

Another point of question is the degree of temperature rise resulting from the applied heat flux. As noted previously, the temperature rises in both Exp. 3.2 and Exp. 3.3 were much less than expected. One possible explanation for this is that the thin

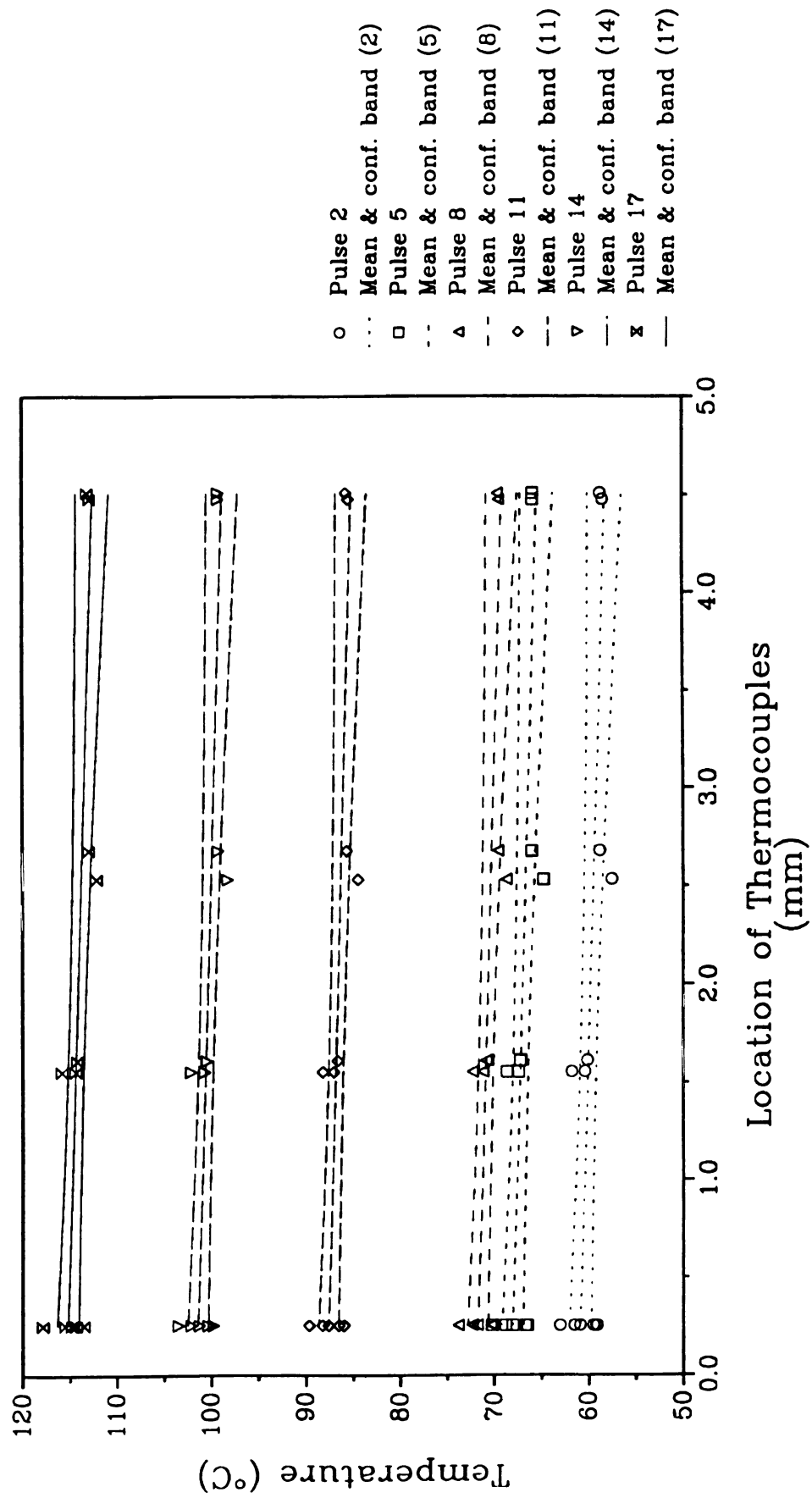


Figure 5.17 Temperature Measurements at the End of the 2nd, 5th, 8th, 11th, 14th, and 17th Heat Flux Pulses in Exp. 3.3 (cured composites) as Functions of Thermocouple Location from the Midsection of the Heater.

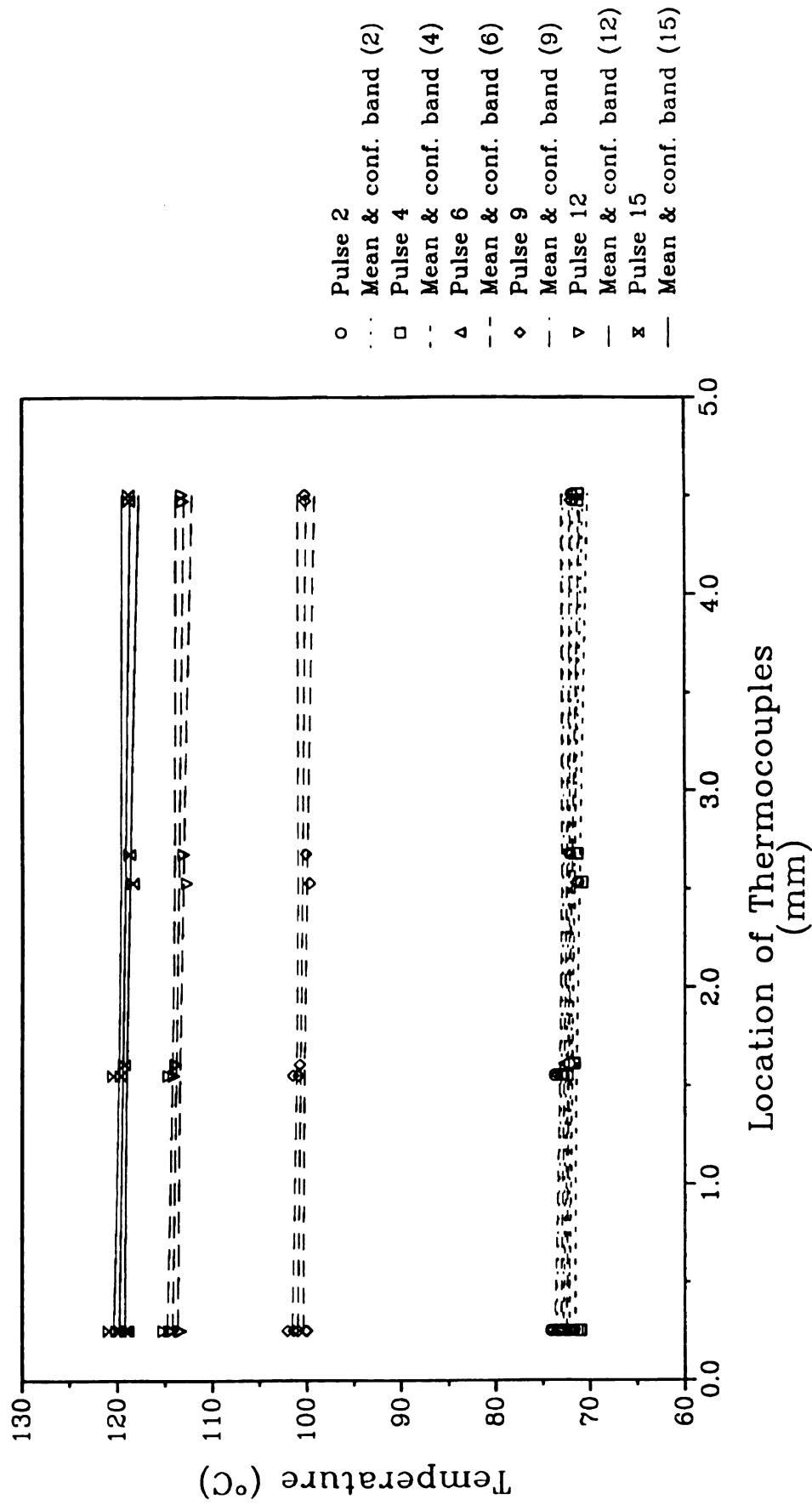


Figure 5.18 Temperature Measurements at the End of the 2nd, 4th, 6th, 9th, 12th, and 15th Heat Flux Pulses in Exp. 3.2 (uncured composites; second experiment) as Functions of Thermocouple Location from the Midsection of the Heater.

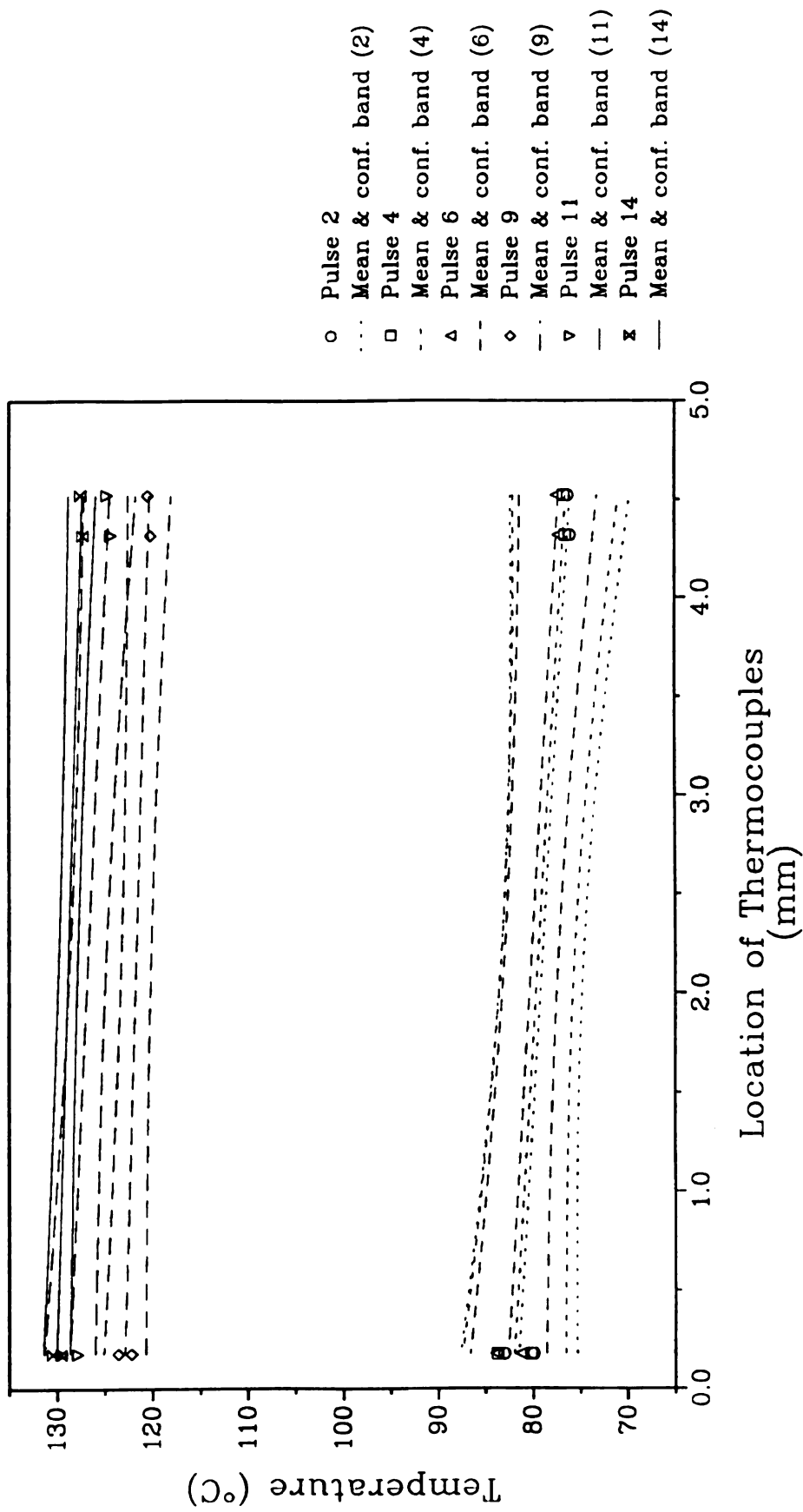


Figure 5.19 Temperature Measurements at the End of the 2nd, 4th, 6th, 9th, 11th, and 14th Heat Flux Pulses in Exp. 3.1 (uncured composites; first experiment) as Functions of Thermocouple Location from the Midsection of the Heater.

sheets of aluminum foil placed on either side of the heater extended past the heater on all sides, acting as a fin around the heater. Due to the low thermal conductivity of the composite compared to that of the heater, it is possible that some of the heat was dissipated through the fin area, reducing the effective heat flux. If the heat flux is calculated using the foil surface area instead of the heater surface area, the resulting heat flux is 65% less than the heat flux calculated from the heater surface area. The cases shown in Table 5.22 for the cured composite were re-evaluated using the adjusted heat flux. The resulting parameter estimates are shown in Table 5.25. Comparing these values to those shown in Table 5.1, the confidence intervals of the density-specific heat values overlapped one another at corresponding temperature levels. The confidence intervals of the thermal conductivity values did not all overlap, and the results from Exp. 3.3 were approximately 5 - 8% higher than those shown in Table 5.1. However, due to the uncertainties discussed in the previous paragraphs, these estimates were still regarded as unreliable.

5.3.2.3 Improvements in the Experimental Design for the Estimation of Thermal Properties in Composite Materials during Curing

From the investigation of possible sources for error presented in the previous section, several suggestions for improvement in the experimental design are presented.

1. Due to the difficulties of maintaining the proper temperature boundary conditions, it is recommended that the samples be cured in an autoclave or a hydraulic press with heated platens. While the autoclave is generally more effective, the hydraulic press is practically preferred, because the thermocouple wires and the heater connections would not interfere with its operation, while special ports for these wires would be required to use the autoclave. This would also reduce the heating times between room temperature and 75°C, and from 75°C and 125°C. Ideally, the composite would be heated at approximately 2.5°C/minute; however, as shown in Figures 5.13 and 5.14, the samples were heated at a rate less than 1°C/minute.

Table 5.25. Estimation of Thermal Conductivity, k , Perpendicular to the Fiber Direction and Density-Specific Heat, ρc_p , of Cured AS4/EPON 828-mpDA Composites using Temperature Data from both Top and Bottom Composite Sections in Exp. (3.3), with the Applied Heat Flux Calculated from the Measured Power Input and the Surface Area of the Aluminum Foil Protection Layer.

Pulse No.	Temperature Range ($^{\circ}\text{C}$)	k ($\text{W}/\text{m}^{\circ}\text{C}$)	ρc_p ($\text{MJ}/\text{m}^3\ ^{\circ}\text{C}$)	RMS ^a ($^{\circ}\text{C}$)
2	54-60	0.86 ± 0.02	1.61 ± 0.07	0.144
5	54-60	0.84 ± 0.04	1.71 ± 0.17	0.205
8	66-71	0.90 ± 0.02	1.64 ± 0.07	0.133
11	81-86	0.84 ± 0.04	1.89 ± 0.15	0.195
14	94-100	0.89 ± 0.03	1.82 ± 0.11	0.152
17	109-114	0.88 ± 0.05	1.81 ± 0.18	0.192

a. Root mean squared error determined from the differences between calculated and experimental temperatures.

2. In order to increase the temperature difference across the samples, it is recommended that sample thickness be doubled; this would result in a total thickness of eighty-eight plies, which would require the fabrication of two prepregs for each experiment.
3. Because of the high variations between the thermocouples at the heated surface, it is recommended that a heater with a more uniform heat distribution across the surface be used.
4. In addition, it is recommended that the thermocouples closest to the heated surface be placed one ply away from the heated surface, instead of directly next to the heater.
5. Finally, due to the possible dissipation of heat due to the increased surface area of the foil, the foil should only be applied to the surface area of the heater.

Chapter 6

Summary and Conclusions

The focus of this study was on the estimation of thermal properties for cured carbon/epoxy composites and on the estimation of both thermal and kinetic properties for these composites during curing. Although much attention has been devoted to the determination of the mechanical properties of these materials, relatively little effort has been given to the determination of thermal properties, especially during the curing process.

The first overall objective was related to the estimation of thermal properties of cured carbon/epoxy composites as functions of temperature. Experimental set-ups were designed using AS4/EPON 828 composite samples with the fibers oriented in two different directions: $[0^\circ]_{24}$ and $[0^\circ, \pm 30^\circ, \pm 60^\circ, 90^\circ]_{2(\text{sym})}$. These experiments were conducted at different initial temperatures ranging from 25°C to 125°C, and the thermal response of the composite to an applied heat flux was measured using thermocouples embedded between composite samples. The thermal conductivity perpendicular to the fiber direction, k , and the density-specific heat, ρc_p , were estimated using an established parameter estimation program, *PROP1D* (Beck, 1989), which utilizes a Gauss minimization procedure. From this analysis, both k and ρc_p were found as functions of temperature. This analysis differs from previous studies in that the experiments were transient, resulting in the simultaneous estimation of both k and ρc_p , and the properties were estimated as a function of temperature.

The estimation of the kinetic properties associated with the curing of the EPON 828/mPDA epoxy matrix was the second overall objective of this investigation. Isothermal experiments were performed at four different temperatures using differential scanning calorimetry, and the heat of reaction rate was recorded as a function of time. Rate constants were estimated from this data using three different kinetic models for the first half of the curing process, and two different models for the second half of the curing process in which diffusion was assumed to be significant. The kinetic parameters, including activation energy constants and pre-exponential factors, were determined from the estimated rate constants, assuming an Arrhenius relationship with temperature. The most appropriate model was then selected for the first half of the cure, based on the confidence intervals of the estimated kinetic parameters, and a new model was proposed for the diffusion-controlled, second half of the cure cycle.

The last overall objective was related to the estimation of thermal properties as functions of temperature and degree of cure. A new and potentially powerful estimation procedure was proposed for the simultaneous estimation of k and ρc_p throughout the curing process. This procedure was once again based on the minimization of a least squares function. In this case, the parameter estimation program, *PROP1D* (Beck, 1989), was modified to account for the heat of reaction of the epoxy during curing. This required the solution of an additional differential equation for the kinetic reaction rate in the computations. The estimation procedure was tested and verified using simulated data from the one dimensional curing program, *CURE1D*, with added normally distributed independent errors. Experiments using AS4/EPON 828 composites, conducted both during and after the curing process, were used in conjunction with the modified parameter estimation program, *PROP1D_CURE*, for the estimation of thermal properties. Unrealistic estimates of the thermal properties from the experimental data led to the conclusion that the experimental design and equipment used in this study were insufficient for the estimation of the thermal properties. Proposed improvements for the experimental design included curing the samples in a hydraulic press with heated platens and doubling the sample thickness.

The following conclusions were drawn from this study. (All references to thermal conductivity are perpendicular to the fiber axis.)

1. Both the thermal conductivity and the density-specific heat of cured AS4/EPON 828 composite materials were found to increase with temperature from 25°C to 145°C.

2. The estimates of the thermal conductivity of AS4/EPON 828 composite samples with an orientation of $[0^\circ]$ were significantly higher than the thermal conductivities estimated for the same material with an orientation of $[0^\circ, \pm 30^\circ, \pm 60^\circ, 90^\circ]$, based on a comparison of the estimated linear regression curves given in Table 5.2. For example, at 100°C, the thermal conductivity estimated for the $[0^\circ]$ samples was 7% higher than the thermal conductivity estimated for the $[0^\circ, \pm 30^\circ, \pm 60^\circ, 90^\circ]$ samples.

3. The estimates for thermal conductivity with an orientation of $[0^\circ]$ were within 5% of previously published values (Table 5.4) for the same or similar materials at 25°C.

4. The thermal history above the glass transition temperature of the epoxy had a significant effect both on the thermal conductivity and density-specific heat of AS4/EPON 828 composite materials; heating a sample for two hours at 150°C increased the thermal conductivity 15% and the density-specific heat 5%, again based on a comparison of the estimated linear regression curves given in Table 5.2 at 100°C.

5. For the EPON 828/MPDA epoxy system used in this study and degree of cure values less than 50%, the kinetic model used by Ryan and Dutta (1979) was shown to be the most appropriate model of the three kinetic models investigated based on the confidence intervals of the estimated parameters and assuming an autocatalyzed second order reaction.

6. A new model for the degree of cure rate was presented for degree of cure greater than 50%. In this model, the rate of reaction is assumed to be diffusion-controlled and to follow an exponential decay with the degree of cure.

7. The procedure for the estimation of the thermal properties during the curing process was verified using the program *PROP1D_CURE* with simulated data plus normally distributed independent errors of 0.25°C (5% of the maximum temperature rise).

The estimated parameters were found to be within 5% of the input parameters used to generate the simulated temperature data.

8. The experimental design and equipment used for the estimation of thermal properties during curing, which included a unheated mechanical press, were not adequate to provide accurate estimates of these parameters. It is recommended that a hydraulic press with heated platens be used in place of the mechanical press and that thicker composite samples be used in the experiments.

9. In the experiments conducted during curing, the thermocouples located at the heated surface had the highest residuals; to reduce these errors it was recommended that these thermocouples be placed at least one ply layer away from the surface of the heater.

APPENDIX A

APPENDIX A

ONE DIMENSIONAL CURING PROGRAM, *CURE1D*

A.1 Summary of Program

The one dimensional curing program, *CURE1D*, discussed in Chapter 3, is presented in this appendix. An outline of the program is given in Table A.1, and a listing of the program, written in Fortran 77 for a VaxstationII/GPX microcomputer is given in Table A.1.

Table A.1 Description of the One Dimensional Curing Program, *CURE1D*.

<u>Subroutine Title</u>	<u>Description</u>
PROGRAM CURE1D	Main program; contains program menu.
SUBROUTINE PROPER	Allows interactive input of thermal properties. Writes data to a file.
SUBROUTINE INPUT1	Allows interactive input of ambient conditions and product geometry. Writes data to a file.
SUBROUTINE INPUT2	Allows interactive input of kinetic properties. Writes data to a file.
SUBROUTINE SOLN	Computes temperature distribution and quality retention as a function of temperature. Calls output subroutine.
SUBROUTINE COEFF	Determines matrix coefficients used in finite difference algorithm.
SUBROUTINE HEAT	Determines heat generation term from kinetic equations.
SUBROUTINE BCFIND	Interpolates boundary conditions.
SUBROUTINE PFIND	Interpolates thermal property values required for the finite difference solution.
SUBROUTINE OUTPUT	Writes input data and resulting temperature and degree of cure values to an output file.

A.2 Program Listing for CURE1D.FOR

```

      PROGRAM CURE1D
C*****
C*****

c              One Dimensional

c              Curing Program for Composite Materials

c              by

c              Elaine Scott, Ph.D.

c              1989

c              Copyright (c) 1989 Michigan State University

c              All rights reserved.

C*****

c  Note: this program was adapted from program 'FREEZE1D.FOR', by
c  E.P. Scott, 1987.

c  This program calculates temperature and extent of cure as a
c  function of time and location in composite materials during
c  curing. It is assumed that one dimensional heat transfer and a
c  second order autocatalyzed chemical reaction occurs with an
c  Arrhenius relationship with temperature.

c  Input parameters include the effective composite density,
c  thermal conductivity, and specific heat. The kinetic properties,
c  including rate constants and activation energy constants are
c  required to determine the extent of cure.

c  Boundary conditions are assumed to be in the form of a known
c  heat flux or temperature as a function of time. The initial
c  condition must be a known function of position.

C*****

      parameter(maxp=100,maxm=101)

      integer model

      character title*20,t1lfil*4,filyn1*1,filyn2*1,filyn*1,
&t1lprp*4,t1lkin*4,fildat*12,inpdatt*12,kindat*12

      logical itmode

      common/mod/model,/itm/itmode,/t1l/title,t1lfil,t1lprp,t1lkin,
&/datfil/fildat,inpdatt,kindat

C  Set ITMODE = .FALSE. if running batch.
      ITMODE = .TRUE.

      IF(ITMODE) THEN

      write(5,1000)

```

```

1000 format('1',72('*')) ,/, '0',t21,'One Dimensional Curing Program',
      &/, '0',t35,'by',/, '0',t27,'Elaine Scott, Ph.D.',
      &/, '0',t14,'Copyright (c) 1987 Michigan State',
      &' University',/, ' ',t26,'All rights reserved.',/, '0',72('*'))
      WRITE(5,100)
100 FORMAT('0','Program Menu:',/
      &/, ' ', '1. Temperature only (no chemical reactions)',
      &/, ' ', '2. Temperature & extent of cure: exact kinetic prop.',
      &/, ' ', '3. Temp. & extent of cure: kinetic prop. with variance',
      &/, ' ', 'Selection?')
      ENDIF
      READ(5,10)model
10 FORMAT(I1)
      IF(ITMODE) write(5,200)
200 format(' ',/, ' ', 'Title: ')
      READ(5,20)TITLE
      IF(ITMODE)then
        write(5,300)
300 format(' ',/, ' ', 'Key word for input boundary conditions ',/
      &' ',2x,'and geometry data file; 4 Characters: ')
      READ(5,20)TTLFIL
      endif
      IF(ITMODE) write(5,320)
320 format(' ',/, ' ', 'Key word for thermal property data ',
      &' file; 4 Char.: ')
      READ(5,20)TTLprp
      IF(ITMODE.and.model.ne.1)then
        write(5,340)
340 format(' ',/, ' ', 'Key word for kinetic property data ',
      &' file; 4 Char.: ')
      READ(5,20)TTLkin
      endif
20 FORMAT(A)
      if(itmode) write(5,400)
400 format(' ',/, ' ', 'Are thermal properties approximations',/, ' ',2x,
      &'with temperature stored on file? (y/n) ')
      read(5,20)filyn1
      if(itmode)then
        write(5,500)
500 format(' ',/, ' ', 'Are input initial and boundary conditions',/, ' ',
      &' ',2x,'and geometrical dimensions stored on file? (y/n) ')
      read(5,20)filyn2
      endif
      if(model.ne.1) then
        if(itmode) write(5,600)
600 format(' ',/, ' ', 'Are the kinetic properties stored on file? ',
      &' (y/n) ')
      read(5,20)filyn3
      endif
      if(filyn1.eq.'n'.or.filyn1.eq.'N')then
        call proper
      endif
      if(filyn2.eq.'n'.or.filyn2.eq.'N')then
        call input1
      endif
      if(model.ne.1)then
        if(filyn3.eq.'n'.or.filyn3.eq.'N')then
          call input2
        endif
      endif
      call soln
      end

```

SUBROUTINE PROPER

c This subroutine provides the input for the property functions.
c Input values include effective product thermal conductivities and the
c density-specific heat products at given temperatures and/or extent of
c cure values.

c Output includes a printout of thermal conductivity and density-
c specific heat products as functions of temperature.

c The variables used in this subroutine are:

c Constants-

c Input Variables-

c Ntemp = number of temperatures at which properties are given

c Kp(I) = Effective thermal conductivity (W/mK) at Ith temp.

c DCp(I) = Density-specific heat product (kJ/m3K) at Ith temp.

c Misc. Variables-

c Tc = Temperature for printout.

c Yn = Character- Y or N

integer ntemp,prpscr

double precision dcp(10,10),kp(10,10),tdc(10),tk(10),aldc(10),
&alk(10)

character yn*1,title*20,ttlfil*4,ttlprp*4,ttlkin*4,fildat*12,
&inpdat*12,kindat*12

logical itmode

SAVE

common /ITM/ITMODE,
&/ttl/title,ttlfil,ttlprp,ttlkin,/datfil/fildat,inpdat,kindat,
&/mod/model

```

IF(.NOT.ITMODE) THEN
  READ(10,*) NTK,NTDC
  IF (MODEL.NE.1) THEN
    READ(10,*) NALK,NALDC
  ELSE
    NALK = 1
    NALDC = 1
  ENDIF
  READ(10,*) (TK(I),I = 1,NTK)
  IF (MODEL.NE.1) THEN
    READ(10,*) (ALK(I),I = 1,NALK)
  ELSE
    ALK(1) = 1.0D0
  ENDIF
  DO I = 1,NTK
    READ(10,*) (KP(I,J),J = 1,NALK)
  ENDDO
  READ(10,*) (TDC(I),I = 1,NTDC)
  IF (MODEL.NE.1) THEN

```

```

        READ(10,*) (ALDC(I), I = 1, NALDC)
    ELSE
        ALDC(1) = 1.0D0
    ENDIF
    DO I = 1, NTDC
        READ(10,*) (DCP(I,J), J = 1, NALDC)
    ENDDO
    GO TO 20
ENDIF
5   write(5,2000)
2000 format('1',72('-'),/, '0',t27,'Thermal Properties',/, '0',72('-'))
    write(5,600)'Enter number of temperatures for thermal ',
&'conductivity, k, values:'
600 format(' ',/, ' ',A,A)
    READ(5,*) NTK
    IF(MODEL.NE.1) THEN
        write(5,600)'Enter number of extent of cure values for k:'
605 format(' ',/, ' ',A)
        READ(5,*) NALK
    ELSE
        NALK = 1
    ENDIF
    WRITE(5,610)'Enter temperatures (C) for k (' ,NTK,') :'
610 FORMAT(1X,/, 1X,A, I2,A)
    READ(5,*) (TK(I), I = 1, NTK)
    IF(MODEL.NE.1) THEN
        WRITE(5,610)'Enter extent of cures for k (' ,NALK,') :'
        READ(5,*) (ALK(I), I = 1, NALK)
    ELSE
        ALK(1) = 1.0D0
    ENDIF
    WRITE(5,620)'Enter k (W/mC) values: '
620 FORMAT(1X,/, 1X,A,/)
    DO I = 1, NTK
        IF(MODEL.NE.1) THEN
            WRITE(5,630)'Enter k at ', TK(I), 'C for ', NALK,
&' extent of cure value(s):'
630 FORMAT(1X,A,F6.2,A, I2,A)
        ELSE
            WRITE(5,640)'Enter k at ', TK(I), 'C :'
640 FORMAT(1X,A,F6.2,A)
        ENDIF
        READ(5,*) (KP(I,J), J = 1, NALK)
    ENDDO

c End of thermal conductivity input

    WRITE(5,900)
900 FORMAT(' ',/, ' ',72('-'),/, ' ', 'Are these values correct? (y/n) ')
    read(5,200) yn
200 FORMAT(A)
    if(yn.ne.'y'.and.YN.NE.'Y') goto 5

c Start density-specific heat input

6   write(5,600)'Enter number of temperatures for density-',
&'specific heat, d-Cp, values:'
    READ(5,*) NTDC
    IF(MODEL.NE.1) THEN
        write(5,605)'Enter number of extent of cure values for d-Cp'
        READ(5,*) NALDC
    ELSE
        NALDC = 1

```

```

ENDIF
WRITE(5,610)'Enter temperatures (C) for d-Cp (' ,NTDC,') : '
READ(5,*) (TDC(I),I = 1,NTDC)
IF(MODEL.NE.1)THEN
  WRITE(5,610)'Enter extent of cures for d-Cp (' ,NALDC,') : '
  READ(5,*) (ALDC(I),I = 1,NALDC)
ELSE
  ALDC(1) = 1.0D0
ENDIF
WRITE(5,620)'Enter d-Cp values: '
DO I = 1,NTDC
  IF(MODEL.NE.1)THEN
    WRITE(5,630)'Enter d-Cp at ',TDC(I),'C for ',NALDC,
&  ' extent of cure value(s)'
  ELSE
    WRITE(5,640)'Enter d-Cp at ',TDC(I),'C '
  ENDIF
  READ(5,*) (DCP(I,J),J = 1,NALDC)
ENDDO

  WRITE(5,900)
  read(5,200)yn
  if(yn.ne.'y'.and.YN.NE.'Y')goto 6
20 CONTINUE

  IF(ITMODE)THEN
    write(6,908)
908  format(' ',72('-'),// ' ','END OF PROPERTY DATA INPUT')
  ENDIF

C
C Convert C temperatures to K temperatures:
C
  DO I = 1,NTK
    TK(I) = TK(I)+273.15D0
  ENDDO
  DO I = 1,NTDC
    TDC(I)= TDC(I)+273.15D0
  ENDDO

C
C Write thermal property data to file
C
  WRITE(FILDAT,1000)TTLPRP,'PRP.DAT'
1000 FORMAT(' ',A,A)
  OPEN(UNIT=12,NAME=FILDAT(1:12),TYPE='NEW',CARRIAGECONTROL='LIST')
  WRITE(12,*)NTK,NTDC
  WRITE(12,*)NALK,NALDC
  WRITE(12,*) (TK(I),I = 1,NTK)
  WRITE(12,*) (ALK(I),I = 1,NALK)
  DO I = 1,NTK
    WRITE(12,*) (KP(I,J),J = 1,NALK)
  ENDDO
  WRITE(12,*) (TDC(I),I = 1,NTDC)
  WRITE(12,*) (ALDC(I),I = 1,NALDC)
  DO I = 1,NTDC
    WRITE(12,*) (DCP(I,J),J = 1,NALDC)
  ENDDO

  return
END

```

-----C-----

```
subroutine input1
```

```
c This subroutine provides the input for the boundary condi-
c tions assuming a known heat flux or temperature at the boundary.
c The boundary conditions may be constant, a linear function of
c time, or a combination of the two.
```

```
c Input variables include initial temperature, type of boundary
c condition, and time and temperature and/or heat flux at each
c boundary.
```

```
parameter(maxp=100)
```

```
integer Isym, ISTEP, Ishape, m, nbc1, nbc2, ibc1, ibc2
```

```
double precision TI, TQ1(maxp), TQ2(maxp), time1(maxp),
&time2(maxp), H, L, DZ, DT, PDT
```

```
character yn*1, title*20, ttlfil*4, ttlprp*4, ttlkin*4, fildat*12,
&inpdatt*12, kindat*12
```

```
logical itmode
```

```
common /ttl/title, ttlfil, ttlprp, ttlkin, /mod/model,
&/itm/itmode, /datfil/fildat, inpdatt, kindat
```

```
save
```

```
c IBC1 and IBC2 indicate type of boundary condition at each surface.
c IBC1, IBC2 = 1 indicates temperature boundary condition, and
c IBC1, IBC2 = 2 indicates heat flux boundary condition.
c NTBC1 and NTBC2 indicates the number of temperature and/or heat flux
c values given for each boundary.
```

```
if(itmode)go to 3
read*, ti, ibc1, nbc1, ibc2, nbc2, ttime, DT, PDT
do i = 1, nbc1
  read*, time1(i), TQ1(i)
enddo
do i = 1, nbc2
  read*, time2(i), TQ2(i)
enddo
read Ishape
if(Ishape.lt.3)then
  read*, l
  h = 1.0d0
else
  read*, l
  h = 0.0d0
endif
go to 500
```

```
3  write(5,1)
1  format('1',72('-'),/, '0',27x, 'Boundary Conditions',/, '0',72('-'))
5  write(6,10) 'Initial product temperature (C): '
10 format(' ',/, ' ',A)
  read*, ti
  write(6,20)
20 format(' ',/, ' ', 'Are the boundary conditions symmetrical? ',
&'(y/n) ',/, ' ', ' (Enter ''y'' for solid cylindrical & spherical ',
&'geometries) ')
  read(5,2) yn
  if(yn.eq.'y'.or.yn.eq.'Y') Isym = 1
```

```

write(6,30)
30  format(' ','/',' ','Enter type of boundary condition for IBC1:',
&/,5x,'1 = temperature boundary','/,5x,'2 = heat flux boundary')
read*,Ibc1
if(Ibc1.eq.1)then
write(6,15)'Enter number of temperatures given at IBC1 ',
&' (include values at time = 0, and at time = tmax):'
15  format(/,1x,A,/,1X,A)
read*,nbcl
else
write(6,15)'Enter number of heat fluxes given at IBC1',
&' (include values at time = 0, and at time = tmax):'
read*,nbcl
endif
if(Isym.ne.1)then
write(6,32)
32  format(/,1x,'Enter type of boundary condition for IBC2:',
&/,5x,'1 = temperature boundary','/,5x,'2 = heat flux boundary')
read*,Ibc2
if(Ibc2.eq.1)then
write(6,15)'Enter number of temperatures given at IBC2 ',
&' (include values at time = 0, and at time = tmax):'
read*,nbc2
else
write(6,15)'Enter number of heat fluxes given at IBC2 ',
&' (include values at time = 0, and at time = tmax):'
read*,nbc2
endif
endif
write(6,10)'Enter total time (s):'
read*,ttime
write(6,10)'Are these values correct? (y/n) '
read(5,2)yn
2  format(a)
if(yn.ne.'y'.and.yn.ne.'Y')goto 5
write(6,106)

```

c input boundary conditions: time and temperature and/or heat flux

```

100  if(ibc1.eq.1)then
write(6,10)'Enter time (s) and temperatures (C) for IBC1:'
do i=1,nbcl
write(6,120)i
120  format(6X,i2,': ')
read*,time1(i),TQ1(i)
enddo
else
write(6,10)'Enter time (s) and heat flux (W/m2) for IBC1:'
do i=1,nbcl
write(6,120)i
read*,time1(i),TQ1(i)
enddo
endif
if(ibc2.eq.1)then
write(6,10)'Enter time (s) and temperatures (C) for IBC2:'
do i=1,nbc2
write(6,120)i
read*,time2(i),TQ2(i)
enddo
else
write(6,10)'Enter time (s) and heat flux (W/m2) for IBC2:'
do i=1,nbc2
write(6,120)i

```

```

        read*,time2(i),TQ2(i)
    enddo
endif

write(6,10)'Are these values correct? (y/n) '
read(5,2)yn
if(yn.ne.'y'.and.yn.ne.'Y')goto 100
write(6,106)
106  format(' ', ' ', 72('-'))

c input geometry and size

140  write(6,150)
150  format('0','Enter product geometry: ',/, ' ',5x,'1 = slab',/, ' ',5x
+,'2 = cylinder',/, ' ',5x,'3 = sphere')
    read*,Ishape
    if(Ishape.gt.1.and.Isym.eq.0)then
        print*,'Boundary conditions must be symmetrical for cylinder and',
&' sphere; try again!!'
        go to 3
    endif
    if(Ishape.eq.1)then
        write(6,160)
160  format(' ',/, ' ', 'Enter dimensions for slab:',/, ' ',5x,
&'thickness in direction of heat transfer (m) = ')
        read*,l
        h = 1.0d0
    else
        if(Ishape.eq.2)then
            write(6,180)
180  format(' ',/, ' ', 'Enter dimensions for cylinder:',/,
+ ' ',5x,'radius (m) = ')
            read *,l
            h = 1.0d0
        else
            write(6,200)
200  format(' ',/, ' ', 'Enter dimensions for sphere (m):',/,
+ ' ',5x,'radius (m) = ')
            read *,l
            h=0.0d0
        endif
    endif
500  ti = ti+273.150d0
    if(Isym.eq.1.and.Ishape.eq.1)L = L*0.50d0
    do i = 1,nbcl
        if(ibcl.eq.1)TQ1(i) = TQ1(i)+273.150d0
        if(Isym.eq.1.or.Ishape.ne.1)then
            if(Ishape.eq.1)then
                TQ2(i) = 0.0d0
                ibc2 = 2
            else
                TQ2(i) = TQ1(i)
                TQ1(i) = 0.0d0
            endif
        endif
    enddo
    do i = 1,nbcl
        if(ibc2.eq.1)TQ2(i) = TQ2(i)+273.150d0
    enddo
    write(6,220)
220  format(' ',/, ' ', 'Enter total number of spatial increments:',/
&' ', ' (Must be a multiple of four.)')
    read*,m

```

```

      ISTEP = m/4
      write(6,230)
230  format(1x,/,1x,'Enter time step for finite difference ',
      &'calculations:')
      read*,dt
      write(6,240)
240  format(1x,/,1x,'Enter time step for print out:',/
      &' ',(Must be a multiple of the time step.))
      read*,pdt

c Check input values

      write(6,10)'Are these values correct? (y/n) '
      read(5,2)yn
      if(yn.ne.'y'.and.yn.ne.'Y')goto 140
      write(6,106)
      write(6,580)
580  format(' ',//,' ',END OF BOUNDARY CONDITIONS AND GEOMETRY INPUT')

c Write data to file.

590  write(inpdat,600)ttlfil,'inp.dat'
600  format(' ',a,a)
      open(unit=12,name=inpdat(1:12),type='new',carriagecontrol='list')
      write(12,700)ibc1,ibc2,nbc1,nbc2,Isym,ti,ttime
700  format(' ',5(i2,2x),2(2x,E11.5))
      do i = 1,nbc1
         write(12,800)TQ1(i),time1(i)
800  format(' ',2x,E11.5,2x,f18.2)
      enddo
      do i = 1,nbc2
         write(12,800)TQ2(i),time2(i)
      enddo
      write(12,900)ISHAPE,L,H,M,ISTEP,DT,PDT
900  format(' ',i1,2(2x,E10.4),2x,i3,2x,i2,2x,E12.5)
      close(unit=12)
      return
      end

c-----

      subroutine input2

c      Kinetic properties to determine extent of cure in a composite
c      during curing are entered in this subroutine. A file titled
c      'TTLFILkin.dat' containing the kinetic properties is created. This
c      file is reopened in the solution subroutine, so that it may be reused
c      again in subsequent runs.
c
c      The extent of cure is determined assuming an autocatalyzed, second
c      order reaction exists for extent of cure < 0.5, and a diffusion control-
c      led reaction for extent of cure > 0.5. Nine parameters are required:
c      a) for extent of cure < 0.5; the activation energy constants, EA1 and
c      EA2, the pre-exponential factors, A1 and A2, and the exponent, MEXP;
c      for extent of cure > 0.5; the activation energy constant, EA3, the pre-
c      exponential factor, A3, and the diffusion constant, D3; and for all
c      extent of cure; the density, DENS, and the total heat of reaction, HT.
c      In addition the variances associated with A1, A2, EA1, and EA2 are
c      included in model 3.

```

```

integer model

double precision LNA1,LNA2,EA1,EA2,M0,M1,DENS,HT,VA1,VA2,VEA1,
1      VEA2,LNA3,EA3,D0,D1,D2,A1,A2,A3

character title*20,t1lfil*4,t1lprp*4,t1lkin*4,fildat*12,
&inpdatt*12,kindat*12

logical itmode

common /t1l/title,t1lfil,t1lprp,t1lkin,
&/mod/model,/itm/itmode,
&/datfil/fildat,inpdatt,kindat

c Read batch file data (if itmode = .false.)

      if(itmode)go to 1
c
c Read in values for extent of cure < 0.5
c
      read*,LNA1,LNA2,EA1,EA2,M0,M1
c
c Read in values for extent of cure < 0.5
c
      read*,LNA3,EA3,D0,D1,D2,DENS,HT
      if(model.eq.3)then
        read*,VA1,VA2,VEA1,VEA2
      endif
      go to 30

c Read interactive input

      1 write(5,2)
      2 format('1',72('-'),/, '0',t40,'Kinetic Data',/, '0',
&72('-'))
      10 write(5,100)
      100 format(' ',/, ' ', 'Enter parameters for extent of cure < 0.5 :',/,
& ' ',4x,'Pre-exponential factor, LN(A1) LN(1/s) : ')
      read*,LNA1
      write(5,110)'Pre-exponential factor, LN(A2) LN(1/s) : '
      110 format(5x,A)
      read*,LNA2
      write(5,200)'Activation Energy Constant, EA1, (kJ/mole) : '
      200 format(' ',/,5x,A)
      read*,EA1
      write(5,110)'Activation Energy Constant, EA2, (kJ/mole) : '
      read*,EA2
      write(5,200)'Exponent, M = M0 + M1*T(C) : '
      WRITE(5,110)'      M0 = '
      read*,M0
      WRITE(5,110)'      M1 = '
      read*,M1
      write(5,210)
      210 format(' ',/, ' ', 'Enter parameters for extent of cure > 0.5 :',/,
& ' ',4x,'Pre-exponential factor, LN(A3) LN(1/s) : ')
      read*,LNA3
      write(5,110)'Activation Energy Constant, EA3, (kJ/mole) : '
      read*,EA3
      write(5,200)'Diffusion coefficient, D = D0 + D1*T + D2*T*T (T=C):'
      WRITE(5,110)'      D0 = '
      read*,D0
      WRITE(5,110)'      D1 = '
      read*,D1

```

```

WRITE(5,110)'      D2 = '
read*,D2
write(5,200)'Density (kg/m3) : '
read*,DENS
write(5,200)'Total heat of reaction, Ht, (J/kg) : '
read*,HT
if(model.eq.3)then
  write(5,200)'Standard deviation of LN(A1) LN(1/s) : '
  read*,VA1
  write(5,110)'Standard deviation of LN(A2) LN(1/s) : '
  read*,VA2
  write(5,200)'Standard deviation of EA1 (kJ/mole) : '
  read*,VEA1
  write(5,110)'Standard deviation of EA2 (kJ/mole) : '
  read*,VEA2
endif
write(5,550)
550 format(' ',/, ' ', 'Are these values correct? (y/n) ')
read(5,20)yn
20 format(a)
if(yn.eq.'n'.or.yn.eq.'N')go to 10

WRITE(6,560)
560 FORMAT(' ',/, ' ', 'END OF KINETIC DATA INPUT')
30 A1 = EXP(LNA1)
A2 = EXP(LNA2)
A3 = EXP(LNA3)
EA1 = EA1*1000.0d0
EA2 = EA2*1000.0d0
EA3 = EA3*1000.0d0
if(model.eq.3)then
  vea1 = (vea1*1000.0d0)**2.0d0
  vea2 = (vea2*1000.0d0)**2.0d0
  vA1 = (vA1)**2.0d0
  vA2 = (vA2)**2.0d0
endif

c Write kinetic data to file.

write(kindat,600)ttlkin,'kin.dat'
600 format(' ',a,a)
open(unit=12,name=kindat(1:12),type='new',carriagecontrol='list')
write(12,*)A1,A2,EA1
write(12,*)EA2,M0,M1
write(12,*)A3,EA3,D0
write(12,*)D1,D2,DENS
write(12,*)HT
if(model.eq.3)then
  write(12,800)VA1,VA2,VEA1,VEA2
800 format(' ',4(2x,e11.5))
endif
close(unit=12)
return
end

c *****

SUBROUTINE soln

parameter(maxm=101,maxp=100,tol=0.10d0,r=8.3140d0)

IMPLICIT DOUBLE PRECISION(A-H,P-Z)

```

```

double precision BCTQ(2,2),TAVG,cc(maxm),dd(maxm),a(maxm),
1      b(maxm),c(maxm),d(maxm),t(maxm,2),pi,pr,AL(MAXM),ALAVG,
1      ABC(5),AL_5(MAXM),DAL_5(MAXM),TC(12),SIGMA,ALPHA

character fildat*12,inpdat*12,kindat*12,OUTFIL2*12,OUTFIL3*12

logical itmode

C Declare variables in common statements

C Common block /ttl/
character title*20,ttlfil*4,ttlprp*4,ttlkin*4

C Common block /kin/
DOUBLE PRECISION A1,A2,EA1,EA2,M0,M1,DENS,HT,VA1,VA2,VEA1,
1      VEA2,A3,EA3,D0,D1,D2

C Common block /prop/
INTEGER NTDC,NALDC,NTK,NALK
DOUBLE PRECISION dcp(10,10),tdc(10),aldc(10),kp(10,10),tk(10),
&alk(10)

C Common block /bound/
INTEGER IBC1,IBC2,NBC1,NBC2
DOUBLE PRECISION TI,TQ1(MAXP),TQ2(MAXP),TIME1(MAXP),TIME2(MAXP)

C Common block /geom/
INTEGER ISHAPE,ISYM,M,MP1,ISTEP
DOUBLE PRECISION H,L,DZ

C Common block /tim/
DOUBLE PRECISION DT,TTIME,PDT

c Common blocks.
common/bound/ibc1,ibc2,nbc1,nbc2,ti,TQ1,TQ2,time1,time2,
&/ttl/title,ttlfil,ttlprp,ttlkin,
&/geom/ISHAPE,ISYM,M,MP1,ISTEP,H,L,DZ,
&/mod/model,/itm/itmode,
&/datfil/fildat,inpdat,kindat,
&/prop/dcp,tdc,aldc,kp,tk,alk,ntdc,naldc,ntk,nalk,
&/KIN/A1,A2,EA1,EA2,M0,M1,DENS,HT,VA1,VA2,VEA1,VEA2,A3,EA3,D0,D1,D2
&/TIM/TTIME,DT,PDT

save

c Read in boundary and initial conditions

write(inpdat,600)ttlfil,'inp.dat'
600 format(' ',a,a)
open(unit=12,name=inpdat(1:12),type='old',carriagecontrol='list')

read(12,*)ibc1,ibc2,nbc1,nbc2,Isym,ti,ttime
do i = 1,nbc1
  read(12,*)TQ1(i),time1(i)
enddo
do i = 1,nbc2
  read(12,*)TQ2(i),time2(i)
enddo

C Input geometry and dimensions

read(12,*)Ishape,L,h,m,ISTEP,dt,PDT
close(unit=12)

```

c Read in constant property assumptions

```

WRITE(FILDAT,310)TTLprp,'PRP.DAT'
310 FORMAT(' ',A,A)
OPEN(UNIT=12,NAME=FILDAT(1:12),TYPE='OLD',CARRIAGECONTROL='LIST')
READ(12,*)NTK,NTDC
READ(12,*)NALK,NALDC
READ(12,*)(TK(I),I = 1,NTK)
READ(12,*)(ALK(I),I = 1,NALK)
DO I = 1,NTK
  READ(12,*)(KP(I,J),J = 1,NALK)
ENDDO
READ(12,*)(TDC(I),I = 1,NTDC)
READ(12,*)(ALDC(I),I = 1,NALDC)
DO I = 1,NTDC
  READ(12,*)(DCP(I,J),J = 1,NALDC)
ENDDO
CLOSE(UNIT=12)

```

c Read in kinetic data

```

if(model.ne.1)then
  write(kindat,600)ttlkin,'kin.dat'
open(unit=12,name=kindat(1:12),type='old',carriagecontrol='list')
READ(12,*)A1,A2,EA1
READ(12,*)EA2,M0,M1
READ(12,*)A3,EA3,D0
READ(12,*)D1,D2,DENS
READ(12,*)HT
  if(model.eq.3)READ(12,*)VA1,VA2,VEA1,VEA2
  close(unit=12)
endif

```

C Read standard deviation for errors added to TC for PROP1D

```

WRITE(*,110)'Enter standard deviation (C) for TC errors:'
READ(*,*)SIGMA

WRITE(*,110)'Enter seed for random numbers:'
READ(*,*)IAR

```

c Read in initial extent of cure values

```

IF(MODEL.NE.1)THEN
  WRITE(*,110)'Enter initial extent of cure (alpha) values:'
110  FORMAT(' ',5X,A)
  WRITE(*,120)'Alpha (constant) = '
120  FORMAT(' ',10X,A)
  READ(*,*)ALPHA
  DO I = 1,M+1
    AL(I) = ALPHA
  ENDDO
ENDIF

if(itmode)write(6,1)
1 format(' ','PROGRAM IS RUNNING!')
ntime = int(ttime/dt)

pi = dacos(-1.0d0)
dz = L/m
mpl = m+1

```

C Initialize temperature

```

DO I = 1,mp1
  DO K = 1,2
    t(I,k)=ti
  enddo
enddo

tavg = ti
time=0.0D0
BCTQ(1,1) = TQ1(1)
BCTQ(1,2) = TQ2(1)
BCTQ(2,1) = TQ1(1)
BCTQ(2,2) = TQ2(1)

Ncount=0
NPR = PDT/DT
nprint = 0
IF (MODEL.eq.1) THEN
  HEADTQ=1
else
  headtq=2
endif
call output(nprint,headtq,t,tavg,time,al,alavg,al_5,dal_5,val)
c
c Write temperatures to file for PROP1DMA.FOR
c
  write(outfil2,1000)ttlfil,'OUT.TEM'
1000 format(' ',a,a)
  open(unit=13,name=outfil2(1:12),type='new',carriagecontrol='list')
  DO I = 1,5
    ABC(I) = T((I-1)*ISTEP+1,2)
  ENDDO
  WRITE(13,1010)TIME,BCTQ(2,1),t(1,2),t(1,2),t(3,2),t(3,2),
  1      t(5,2),t(5,2),t(7,2),t(7,2),t(9,2),t(9,2)
1010 FORMAT(1X,F8.2,1X,F10.2,12(1X,F7.2))

  write(outfil3,1000)ttlfil,'OUT.ALP'
  open(unit=14,name=outfil3(1:12),type='new',carriagecontrol='list')
  DO I = 1,5
    ABC(I) = AL((I-1)*ISTEP+1)
  ENDDO
  WRITE(14,1020)TIME,(ABC(I),I=1,5)
1020 FORMAT(1X,F8.2,5(1X,F7.4))

  j=1

c finite difference solution

  do 160 III=1,ntime

    time = III*dt

c Find boundary conditions for each time step

    CALL BCFIND(TIME,BCTQ)
c
c
c thomas algorithm

c find coefficients for thomas algorithm

  call coeff(III,BCTQ,T,A,B,C,D,AL,ALAVG,AL_5,DAL_5)

  cc(1)=c(1)/b(1)

```

```

dd(1)=d(1)/b(1)
do k=2,mp1
  kk=k-1
  cc(k)=c(k)/(b(k)-a(k)*cc(kk))
  dd(k)=(d(k)-a(k)*dd(kk))/(b(k)-a(k)*cc(kk))
enddo
t(mp1,2)=dd(mp1)
tavg = t(mp1,2)
do k=2,mp1
  kk=m-k+2
  t(kk,2)=dd(kk)-cc(kk)*t(kk+1,2)
  tavg = tavg+t(kk,2)
enddo
tavg = tavg/mp1

c
c find quality distribution and adjust time step

c find mass average quality

c
Ncount=Ncount+1

c printout

IF(NCOUNT.EQ.NPR) THEN
  nprint = 1
  call output(nprint,headtq,t,tavg,time,al,alavg,al_5,dal_5,val)
  DO I = 1,5
    ABC(I) = T((I-1)*ISTEP+1,2)
  ENDDO
  tc(1)=t(1,2)
  tc(2)=TC(1)
  tc(3)=t(3,2)
  tc(4)=TC(3)
  tc(5)=t(5,2)
  tc(6)=TC(5)
  tc(7)=t(7,2)
  tc(8)=TC(7)
  tc(9)=t(9,2)
  tc(10)=TC(9)
  CALL RANDNU(tc,10,iii,sigma,IAR)
  WRITE(13,1010)TIME,BCTQ(2,1),(TC(I),I = 1,10)
  DO I = 1,5
    ABC(I) = AL((I-1)*ISTEP+1)
  ENDDO
  WRITE(14,1020)TIME,(ABC(I),I=1,5)
  NCOUNT = 0
ENDIF

c
c initial t for next time step

do 100 i=1,mp1
100 t(i,1)=t(i,2)

c end of finite difference calculations

c *****

BCTQ(1,1) = BCTQ(2,1)
BCTQ(1,2) = BCTQ(2,2)

```

```

160  continue
      NPRINT=2
      call output(nprint,headtq,t,tavg,time,al,alavg,al_5,dal_5,val)
      close(13)
      CLOSE(14)
      return
      end

c *****

      subroutine coeff(III,BCTQ,T,A,B,C,D,AL,ALAVG,AL_5,DAL_5)

      parameter(maxm=101,maxp=100,r=8.3140d0)

      IMPLICIT DOUBLE PRECISION(A-H,P-Z)

      double precision beta,nu,omega,gama,BCTQ(2,2),aar,ar(maxm),
&arl(maxm),area,avg1,avg2,da,db,dc,ddd(MAXM),ck(maxm),csd(maxm,2),
&a(maxm),b(maxm),c(maxm),d(maxm),t(maxm,2),AL(MAXM),
&DAL(MAXM),ALAVG,pi,dzz,HDEN,AL_5(MAXM),DAL_5(MAXM)

c Declare variables in common statements

c Common block /kin/

      DOUBLE PRECISION A1,A2,EA1,EA2,M0,M1,DENS,HT,VA1,VA2,VEA1,
1      VEA2,A3,EA3,D0,D1,D2

c Common block /prop/

      INTEGER NTDC,NALDC,NTK,NALK
      DOUBLE PRECISION dcp(10,10),tdc(10),aldc(10),kp(10,10),tk(10),
&alk(10)

c Common block /bound/

      INTEGER IBC1,IBC2,NBC1,NBC2
      DOUBLE PRECISION TI,TQ1(MAXP),TQ2(MAXP),TIME1(MAXP),TIME2(MAXP)

c Common block /geom/

      INTEGER ISHAPE,ISYM,M,MP1,ISTEP
      DOUBLE PRECISION H,L,DZ

c Common block /tim/

      DOUBLE PRECISION TTIME,DT,PDT

      common/bound/ibc1,ibc2,nbc1,nbc2,ti,TQ1,TQ2,time1,time2,
&/geom/ISHAPE,ISYM,M,MP1,ISTEP,H,L,DZ,
&/prop/dcp,tdc,aldc,kp,tk,alk,ntdc,naldc,ntk,nalk,
&/KIN/A1,A2,EA1,EA2,M0,M1,DENS,HT,VA1,VA2,VEA1,VEA2,A3,EA3,D0,D1,D2
&/MOD/MODEL,
&/TIM/TTIME,DT,PDT

      pi = dacos(-1.0d0)

c Weighting functions for Crank-Nicolson finite difference method:

c weighting coefficients for d2T/dz2:
c for time t:

```

```

        beta=0.50d0
c      for time t+1:
        nu=0.50d0

c      weighting coefficients for dT/dt:
c      for time t:
        omega=-1.0d0
c      for time t+1:
        gama=1.0d0

        dzz=1.0d0/dz
        if(Ishape.eq.2)then
            aar=2.0d0*pi*h
        else
            if(Ishape.eq.3)then
                aar=4.0d0*pi
            endif
        endif

c      Call Subroutine HEAT to determine heat of reaction

        IF (MODEL.NE.1)CALL HEAT(T,AL,DAL,DT,MP1,ALAVG,AL_5,DAL_5)

        do 10 i=1,mp1

c      slab

        if(Ishape.eq.1)then
            ar(i)=h
            arl(i)=h
        else

c      cylinder

        if(Ishape.eq.2)then
            ar(i)=aar*(i-1)*dz
            arl(i)=ar(i)+aar*dz/2.0d0
        else

c      sphere

        ar(i)=aar*((i-1)*dz)**2.0d0
        arl(i)=aar*((i-1)*dz+dz/2.0d0)**2.0d0
        endif
        endif

c      Find heat generation term from dalphi/dt:

        HDEN = HT*DENS*DZ
10      continue

        CALL PFIND(T,AL,M,CK,CSD,DT,DZ)

c      *****

c      1st boundary point

        AVG1 = (AR(1)+AR1(1))*0.50d0
        a(1)=0.0d0
        IF (IBC1.EQ.1) THEN

```

```

      B(1) = 1.0D0
      C(1) = 0.0D0
      D(1) = BCTQ(2,1)
ENDIF
IF (IBC1.EQ.2) THEN
  c(1)=nu*dzz*CK(1)*ar1(1)
  dc=-beta*dzz*CK(1)*ar1(1)

  b(1)=-gama*CSD(1,1)*avg1-c(1)
  db=omega*CSD(1,1)*avg1-dc
  DDD(1)=(-beta*BCTQ(1,1)-nu*BCTQ(2,1)-HDEN*DAL(1)*0.50d0)*ar(1)
  d(1)=db*t(1,1)+dc*t(2,1)+ddd(1)
ENDIF

c *****
c
c interior points

  do 20 i=2,m
    AVG1 = (AR(I)+AR1(I))*0.50d0
    AVG2 = (AR(I)+AR1(I-1))*0.50d0
    a(I) = nu*dzz*CK(I-1)*ar1(i-1)
    da = -beta*dzz*CK(I-1)*ar1(i-1)

    c(I) = nu*dzz*CK(I)*ar1(i)
    dc = -beta*dzz*CK(I)*ar1(i)

    b(I) = -gama*(CSD(I,1)*avg2+CSD(I,2)*avg1)-a(i)-c(i)
    db = omega*(CSD(I,1)*avg2+CSD(I,2)*avg1)-da-dc
    DDD(I) = -HDEN*DAL(I)*ar(I)
    d(I) = da*t(i-1,1)+db*t(i,1)+dc*t(i+1,1)+DDD(I)
20  continue

c *****
c 2nd boundary point

  AVG2 = (AR(mp1)+AR1(M))*0.50d0
  c(mp1)=0.0d0

  IF (IBC2.EQ.1) THEN
    A(MP1) = 0.0D0
    B(MP1) = 1.0D0
    D(MP1) = BCTQ(2,2)
  ENDIF
  IF (IBC2.EQ.2) THEN
    a(mp1)=nu*dzz*CK(M)*ar1(m)
    da=-beta*dzz*CK(M)*ar1(m)

    b(mp1)=-gama*CSD(mp1,2)*avg2-a(mp1)
    db=omega*CSD(mp1,2)*avg2-da
    ddd(MP1)=(-beta*BCTQ(1,2)-nu*BCTQ(2,2)-HDEN*DAL(MP1)*0.50D0)
    1      *ar(mp1)
    d(mp1)=da*t(m,1)+db*t(mp1,1)+ddd(MP1)
  ENDIF
  return
end

c *****

SUBROUTINE HEAT(T,AL,DAL,DT,MP1,ALAVG,AL_5,DAL_5)

PARAMETER (MAXM=101,MAXP=100,R=8.314D0)

```

IMPLICIT DOUBLE PRECISION (A-H,P-Z)

DOUBLE PRECISION AL (MAXM), AL_5 (MAXM), ALAVG, C1, C2, C3, D3, DAL (MAXM),
1 DAL_5 (MAXM), DEXP, DT, MEXP, NEXP, SUM, T (MAXM, 2), TT

C Declare variables in common block.

DOUBLE PRECISION A1, A2, EA1, EA2, M0, M1, DENS, HT, VA1, VA2, VEA1,
1 VEA2, A3, EA3, D0, D1, D2

COMMON /KIN/A1, A2, EA1, EA2, M0, M1, DENS, HT, VA1, VA2, VEA1, VEA2, A3, EA3,
1 D0, D1, D2

C Extent of cure is found assuming an autocatalyzed second order reaction

C

C Use Ryan and Dutta method for $a < 0.5$:

C $da/dt = (c1+c2*a**m) (1-a)**(2-m)$;

C where, $c1 = A1 \exp(-E1/T*R)$, $c2 = A2 \exp(-E2/T*R)$, $m = m0+m1*(T-273.15)$

C

C Use E. Scott's method for $a > 0.5$:

C $da/dt = (da/dt) (a=.5) + c3*(0.5-a) \exp(-D*(0.5-a))$

C where, $c3 = A3 \exp(-E3/T*R)$, $D = d0+d1*(T-273.15)$

C

SUM = 0.0D0

DO 100 J = 1, MP1

C

C For extent of cure < 0.5 :

C

IF (AL(J) .LE. 0.50D0) THEN

MEXP = M0+M1*(T(J,1)-273.15D0)

NEXP = 2.0D0-MEXP

C1 = A1*EXP(-EA1/(T(J,1)*R))

C2 = A2*EXP(-EA2/(T(J,1)*R))

DAL(J) = (C1+C2*(AL(J)**MEXP))*(1.0D0-AL(J))**NEXP

AL_5(J) = AL(J)

DAL_5(J) = DAL(J)

ELSE

C

C For extent of cure > 0.5 :

C

AL_5(J) = 0.50D0

MEXP = M0+M1*(T(J,1)-273.15D0)

NEXP = 2.0D0-MEXP

C1 = A1*EXP(-EA1/(T(J,1)*R))

C2 = A2*EXP(-EA2/(T(J,1)*R))

DAL_5(J) = (C1+C2*(AL_5(J)**MEXP))*(1.0D0-AL_5(J))**NEXP

TT = 150.0D0-(T(J,1)-273.15D0)

DEXP = D0+D1*TT+D2*TT*TT

IF (DEXP.LT.0.50D0) DEXP = 0.5D0

DIFAL = AL_5(J)-AL(J)

C3 = A3*EXP(-EA3/(T(J,1)*R))

DAL(J) = DAL_5(J)+DIFAL*C3*EXP(-DEXP*DIFAL)/(HT*1D-3)

IF (DAL(J) .LT. 0.0D0) DAL(J) = 0.0D0

ENDIF

AL(J) = AL(J)+DT*DAL(J)

IF (AL(J) .GT. 1.0D0) THEN

AL(J) = 1.0D0

DAL(J) = 0.0D0

ENDIF

SUM = SUM+AL(J)

100 continue

ALAVG = SUM/MP1

```

RETURN
END

```

```

C *****

```

```

SUBROUTINE BCFIND (TIME,BCTQ)

PARAMETER (MAXP=100)

IMPLICIT DOUBLE PRECISION (A-H,P-Z)

DOUBLE PRECISION TIME,BCTQ(2,2)

```

```

C Common block /bound/
  INTEGER IBC1,IBC2,NBC1,NBC2
  DOUBLE PRECISION TI,TQ1(MAXP),TQ2(MAXP),TIME1(MAXP),TIME2(MAXP)

  common/bound/ibc1,ibc2,nbc1,nbc2,ti,TQ1,TQ2,time1,time2

```

```

C First boundary condition

```

```

      DO J = 2,NBC1
        JM1 = J-1
        IF (TIME.LE.TIME1(J)) THEN
          BCTQ(2,1) = TQ1(JM1)+(TIME-TIME1(JM1))*(TQ1(J)-TQ1(JM1))/
& (TIME1(J)-TIME1(JM1))
          GOTO 10
        ENDIF
        BCTQ(2,1) = TQ1(NBC1-1)+(TIME-TIME1(NBC1-1))*(TQ1(NBC1)-
& TQ1(NBC1-1))/(TIME1(NBC1)-TIME1(NBC1-1))
        ENDDO
10    CONTINUE

```

```

C Second boundary condition

```

```

      DO J = 2,NBC2
        JM1 = J-1
        IF (TIME.LE.TIME2(J)) THEN
          BCTQ(2,2) = TQ2(JM1)+(TIME-TIME2(JM1))*(TQ2(J)-TQ2(JM1))/
& (TIME2(J)-TIME2(JM1))
          GOTO 20
        ENDIF
        BCTQ(2,2) = TQ2(NBC2-1)+(TIME-TIME2(NBC2-1))*(TQ2(NBC2)-
& TQ2(NBC2-1))/(TIME2(NBC2)-TIME2(NBC2-1))
        ENDDO
20    CONTINUE

      RETURN
      END

```

```

C *****

```

```

SUBROUTINE PFIND (T,AL,M,CK,CSPD,DT,DZ)

PARAMETER (MAXm=101)

IMPLICIT DOUBLE PRECISION (A-H,P-Z)

double precision TAVGK,TAVGDC(2),ALAVGK,ALAVGDC(2),CK(MAXM),
&CSPD(MAXM,2),t(maxm,2),AL(maxm),dt,dz

```

C Declare variables in common statements

C Common block /prop/

```

      INTEGER NTDC,NALDC,NTK,NALK
      DOUBLE PRECISION dcp(10,10),tdc(10),aldc(10),kp(10,10),tk(10),
&alk(10),cc

```

```

      COMMON /prop/dcp,tdc,aldc,kp,tk,alk,ntdc,naldc,ntk,nalk

```

C Common block /MOD/

```

      INTEGER MODEL

```

```

      COMMON /MOD/MODEL

```

```

      MP1 = M+1

```

```

      cc = 1.0d0*dz/2.0d0

```

C Look up table for thermal conductivity

```

      DO 100 I = 1,MP1
      IF (I.LE.M) THEN
      TAVGK = (T(I,1)+T(I+1,1))*0.50D0
      TAVGDC(1) = 0.75D0*T(I,1)+0.25D0*T(I+1,1)
      IF (MODEL.NE.1) THEN
      ALAVGK = (AL(I)+AL(I+1))*0.50D0
      ALAVGDC(1) = 0.75D0*AL(I)+0.25D0*AL(I+1)
      ENDIF
      ENDIF
      IF (I.GT.1) THEN
      TAVGDC(2) = 0.75D0*T(I,1)+0.25D0*T(I-1,1)
      IF (MODEL.NE.1) THEN
      ALAVGDC(2) = 0.75D0*AL(I)+0.25D0*AL(I-1)
      ENDIF
      ENDIF

```

C First find thermal conductivity

C For MODEL 1, thermal conductivity is a function of temperature only

```

      IF (MODEL.EQ.1) THEN
      IF (TAVGK.LE.TK(1)) THEN
      CK(I)=KP(1,1)+(TAVGK-TK(1))*(KP(2,1)-KP(1,1))/(TK(2)-TK(1))
      ENDIF

      IF (TAVGK.GT.TK(1).AND.TAVGK.LT.TK(NTK)) THEN
      DO J = 1,NTK
      IF (J.NE.NTK) THEN
      IF (TAVGK.LE.TK(J+1)) THEN
      CK(I)=KP(J,1)+(TAVGK-TK(J))*(KP(J+1,1)-KP(J,1))/
&      (TK(J+1)-TK(J))
      ENDIF
      ENDIF
      ENDDO
      ENDIF

      IF (TAVGK.GE.TK(NTK)) THEN
      CK(I)=KP(NTK,1)+(TAVGK-TK(NTK))*(KP(NTK,1)-KP(NTK-1,1))/
&      (TK(NTK)-TK(NTK-1))
      ENDIF

      ELSE

```

C For MODEL's 2 and 3, find thermal conductivity as a function of
C temperature and extent of cure

```

      IF (NTK.EQ.1.AND.NALK.EQ.1) THEN
        CK(I)=KP(1,1)
        GO TO 105
      ENDIF
      IF (TAVGK.LE.TK(1)) THEN
        IF (ALAVGK.LE.ALK(1)) THEN
          CK(I)=KP(1,1)+(TAVGK-TK(1))*(KP(2,1)-KP(1,1))/
&      (TK(2)-TK(1))+(ALAVGK-ALK(1))*(KP(1,2)-KP(1,1))/
&      (ALK(2)-ALK(1))
        ENDIF
        IF (ALAVGK.GT.ALK(1).AND.ALAVGK.LT.ALK(NALK)) THEN
          DO N = 1,NALK
            IF (N.NE.NALK) THEN
              IF (ALAVGK.LE.ALK(N+1)) THEN
                CK(I)=KP(1,N)+(TAVGK-TK(1))*(KP(2,N)-KP(1,N))/
&      (TK(2)-TK(1))+(ALAVGK-ALK(N))*(KP(1,N+1)-KP(1,N))/
&      (ALK(N+1)-ALK(N))
              ENDIF
            ENDIF
          ENDDO
        ENDIF
        IF (ALAVGK.GE.ALK(NALK)) THEN
          CK(I)=KP(1,NALK)+(TAVGK-TK(1))*(KP(2,NALK)-KP(1,NALK))/
&      (TK(2)-TK(1))+(ALAVGK-ALK(NALK))*(KP(1,NALK)-KP(1,NALK-1))/
&      (ALK(NALK)-ALK(NALK-1))
        ENDIF
      ENDIF

      IF (TAVGK.GT.TK(1).AND.TAVGK.LT.TK(NTK)) THEN
        DO J = 1,NTK
          IF (J.NE.NTK) THEN
            IF (TAVGK.LE.TK(J+1)) THEN
              IF (ALAVGK.LE.ALK(1)) THEN
                CK(I)=KP(J,1)+(TAVGK-TK(J))*(KP(J+1,1)-KP(J,1))/
&      (TK(J+1)-TK(J))+(ALAVGK-ALK(1))*(KP(J,2)-KP(J,1))/
&      (ALK(2)-ALK(1))
              ENDIF
              IF (ALAVGK.GT.ALK(1).AND.ALAVGK.LT.ALK(NALK)) THEN
                DO N = 1,NALK
                  IF (N.NE.NALK) THEN
                    IF (ALAVGK.LE.ALK(N+1)) THEN
                      CK(I)=KP(J,N)+(TAVGK-TK(J))*(KP(J+1,N)-KP(J,N))/
&      (TK(J+1)-TK(J))+(ALAVGK-ALK(N))*(KP(J,N+1)
&      -KP(J,N))/(ALK(N+1)-ALK(N))
                    ENDIF
                  ENDIF
                ENDDO
              ENDIF
              IF (ALAVGK.GE.ALK(NALK)) THEN
                CK(I)=KP(J,NALK)+(TAVGK-TK(J))*(KP(J+1,NALK)
&      -KP(J,NALK))/(TK(J+1)-TK(J))+(ALAVGK-ALK(NALK))
&      *(KP(J,NALK)-KP(J,NALK-1))/(ALK(NALK)-ALK(NALK-1))
              ENDIF
            ENDIF
          ENDIF
        ENDDO
      ENDIF

      IF (TAVGK.GE.TK(NTK)) THEN
        IF (ALAVGK.LE.ALK(1)) THEN

```

```

      CK(I) = KP(NTK, 1) + (TAVGK - TK(NTK)) * (KP(NTK, 1) - KP(NTK-1, 1)) /
&      (TK(NTK) - TK(NTK-1)) + (ALAVGK - ALK(1)) * (KP(NTK, 2) - KP(NTK, 1)) /
&      (ALK(2) - ALK(1))
    ENDIF
    IF (ALAVGK.GT.ALK(1).AND.ALAVGK.LT.ALK(NALK)) THEN
      DO N = 1, NALK
        IF (N.NE.NALK) THEN
          IF (ALAVGK.LE.ALK(N+1)) THEN
            CK(I) = KP(NTK, N) + (TAVGK - TK(NTK)) * (KP(NTK, N)
&            - KP(NTK-1, N)) / (TK(NTK) - TK(NTK-1)) + (ALAVGK - ALK(N))
&            * (KP(NTK, N+1) - KP(NTK, N)) / (ALK(N+1) - ALK(N))
          ENDIF
        ENDIF
      ENDDO
    ENDIF
    IF (ALAVGK.GE.ALK(NALK)) THEN
      CK(I) = KP(NTK, NALK) + (TAVGK - TK(NTK)) * (KP(NTK, NALK)
&      - KP(NTK-1, NALK)) / (TK(NTK) - TK(NTK-1)) + (ALAVGK - ALK(NALK))
&      * (KP(NTK, NALK) - KP(NTK, NALK-1)) / (ALK(NALK) - ALK(NALK-1))
    ENDIF
  ENDIF
ENDIF
ENDIF

```

C Next find density-specific heat, CSPD(1) and CSPD(2):

105 DO 50 NC = 1,2

C For MODEL 1, density-specific heat is a function of temperature only

```

    IF (MODEL.EQ.1) THEN
      IF (TAVGDC(NC).LE.TDC(1)) THEN
        CSPD(I, NC) = DCP(1, 1) + (TAVGDC(NC) - TDC(1)) * (DCP(2, 1) - DCP(1, 1)) /
&        (TDC(2) - TDC(1))
      ENDIF

      IF (TAVGDC(NC).GT.TDC(1).AND.TAVGDC(NC).LT.TDC(NTDC)) THEN
        DO J = 1, NTDC
          if(j.ne.ntdc) then
            IF (TAVGDC(NC).LE.TDC(J+1)) THEN
              CSPD(I, NC) = DCP(J, 1) + (TAVGDC(NC) - TDC(J)) * (DCP(J+1, 1)
&              - DCP(J, 1)) / (TDC(J+1) - TDC(J))
            ENDIF
          endif
        ENDDO
      ENDIF

      IF (TAVGDC(NC).GE.TDC(NTDC)) THEN
        CSPD(I, NC) = DCP(NTDC, 1) + (TAVGDC(NC) - TDC(NTDC)) * (DCP(NTDC, 1)
&        - DCP(NTDC-1, 1)) / (TDC(NTDC) - TDC(NTDC-1))
      ENDIF

    ELSE

```

C For MODEL's 2 and 3, find specific heat as a function of temperature
C and extent of cure

```

    IF (NTDC.EQ.1.AND.NALDC.EQ.1) THEN
      CSPD(I, NC) = DCP(1, 1)
      GO TO 50
    ENDIF
    IF (TAVGDC(NC).LE.TDC(1)) THEN

```

```

IF (ALAVGDC (NC) .LE. ALDC (1)) THEN
  CSPD (I, NC) = DCP (1, 1) + (TAVGDC (NC) - TDC (1)) * (DCP (2, 1) - DCP (1, 1)) /
  & (TDC (2) - TDC (1)) + (ALAVGDC (NC) - ALDC (1)) * (DCP (1, 2) - DCP (1, 1)) /
  & (ALDC (2) - ALDC (1))
ENDIF
IF (ALAVGDC (NC) .GT. ALDC (1) .AND. ALAVGDC (NC) .LT. ALDC (NALDC)) THEN
  DO N = 1, NALDC
    IF (N.NE.NALDC) THEN
      IF (ALAVGDC (NC) .LE. ALDC (N+1)) THEN
        CSPD (I, NC) = DCP (1, N) + (TAVGDC (NC) - TDC (1)) * (DCP (2, N) -
        & DCP (1, N)) / (TDC (2) - TDC (1)) + (ALAVGDC (NC) - ALDC (N)) *
        & (DCP (1, N+1) - DCP (1, N)) / (ALDC (N+1) - ALDC (N))
      ENDIF
    ENDIF
  ENDDO
ENDIF
IF (ALAVGDC (NC) .GE. ALDC (NALDC)) THEN
  CSPD (I, NC) = DCP (1, NALDC) + (TAVGDC (NC) - TDC (1)) * (DCP (2, NALDC) -
  & DCP (1, NALDC)) / (TDC (2) - TDC (1)) + (ALAVGDC (NC) - ALDC (NALDC)) *
  & (DCP (1, NALDC) - DCP (1, NALDC-1)) / (ALDC (NALDC) - ALDC (NALDC-1))
ENDIF
ENDIF

IF (TAVGDC (NC) .GT. TDC (1) .AND. TAVGDC (NC) .LT. TDC (NTDC)) THEN
  DO J = 1, NTDC
    IF (J.NE.NTDC) THEN
      IF (TAVGDC (NC) .LE. TDC (J+1)) THEN
        IF (ALAVGDC (NC) .LE. ALDC (1)) THEN
          CSPD (I, NC) = DCP (J, 1) + (TAVGDC (NC) - TDC (J)) * (DCP (J+1, 1) -
          & DCP (J, 1)) / (TDC (J+1) - TDC (J)) + (ALAVGDC (NC) - ALDC (1)) *
          & (DCP (J, 2) - DCP (J, 1)) / (ALDC (2) - ALDC (1))
        ENDIF
      IF (ALAVGDC (NC) .GT. ALDC (1) .AND. ALAVGDC (NC) .LT. ALDC (NALDC)) THEN
        DO N = 1, NALDC
          IF (N.NE.NALDC) THEN
            IF (ALAVGDC (NC) .LE. ALDC (N+1)) THEN
              CSPD (I, NC) = DCP (J, N) + (TAVGDC (NC) - TDC (J)) * (DCP (J+1, N) -
              & DCP (J, N)) / (TDC (J+1) - TDC (J)) + (ALAVGDC (NC) - ALDC (N)) *
              & (DCP (J, N+1) - DCP (J, N)) / (ALDC (N+1) - ALDC (N))
            ENDIF
          ENDIF
        ENDDO
      ENDIF
      IF (ALAVGDC (NC) .GE. ALDC (NALDC)) THEN
        CSPD (I, NC) = DCP (J, NALDC) + (TAVGDC (NC) - TDC (J)) * (DCP (J+1,
        & NALDC) - DCP (J, NALDC)) / (TDC (J+1) - TDC (J)) + (ALAVGDC (NC) -
        & ALDC (NALDC)) * (DCP (J, NALDC) - DCP (J, NALDC-1)) / (ALDC (NALDC) -
        & ALDC (NALDC-1))
      ENDIF
    ENDIF
  ENDDO
ENDIF

IF (TAVGDC (NC) .GE. TDC (NTDC)) THEN
  IF (ALAVGDC (NC) .LE. ALDC (1)) THEN
    CSPD (I, NC) = DCP (NTDC, 1) + (TAVGDC (NC) - TDC (NTDC)) * (DCP (NTDC, 1) -
    & DCP (NTDC-1, 1)) / (TDC (NTDC) - TDC (NTDC-1)) + (ALAVGDC (NC) - ALDC (1))
    & * (DCP (NTDC, 2) - DCP (NTDC, 1)) / (ALDC (2) - ALDC (1))
  ENDIF
  IF (ALAVGDC (NC) .GT. ALDC (1) .AND. ALAVGDC (NC) .LT. ALDC (NALDC)) THEN
    DO N = 1, NALDC
      IF (N.NE.NALDC) THEN

```

```

      IF (ALAVGDC (NC) .LE. ALDC (N+1) ) THEN
        CSPD (I, NC) = DCP (NTDC, N) + (TAVGDC (NC) - TDC (NTDC) ) *
&         (DCP (NTDC, N) - DCP (NTDC-1, N) ) / (TDC (NTDC) - TDC (NTDC-1) ) +
&         (ALAVGDC (NC) - ALDC (N) ) * (DCP (NTDC, N+1) - DCP (NTDC, N) ) /
&         (ALDC (N+1) - ALDC (N) )
      ENDIF
    ENDIF
  ENDDO
ENDIF
IF (ALAVGDC (NC) .GE. ALDC (NALDC) ) THEN
  CSPD (I, NC) = DCP (NTDC, NALDC) + (TAVGDC (NC) - TDC (NTDC) ) *
&   (DCP (NTDC, NALDC) - DCP (NTDC-1, NALDC) ) / (TDC (NTDC) - TDC (NTDC-1) ) +
&   (ALAVGDC (NC) - ALDC (NALDC) ) * (DCP (NTDC, NALDC) - DCP (NTDC, NALDC-1)
&   ) / (ALDC (NALDC) - ALDC (NALDC-1) )
ENDIF
ENDIF
ENDIF
50   CONTINUE
100  CONTINUE

do i = 1, mp1
  DO KK = 1, 2
    CSPD (I, KK) = CSPD (I, KK) * cc / dt
  ENDDO
enddo
RETURN
END

C *****

      subroutine output (nprint, headtq, t, tavg, time, al, alavg, al_5, dal_5,
1      val)

      parameter (maxp=100, maxm=101)

      integer model

      double precision al (maxM), abcd, alavg, val, tavg, tavg1, abc (5), time,
1      T (MAXM, 2), AL_5 (MAXM), DAL_5 (MAXM)

      character outfil*12, hh11*29, hh22*21, prunit*6

C Declare variables in common statements

C Common block /ttl/
      character title*20, ttlfil*4, ttlprp*4, ttlkin*4

C Common block /kin/

      DOUBLE PRECISION A1, A2, EA1, EA2, M0, M1, DENS, HT, VA1, VA2, VEA1,
1      VEA2, A3, EA3, D0, D1, D2

C Common block /prop/
      INTEGER NTDC, NALDC, NTK, NALK
      DOUBLE PRECISION dcp (10, 10), tdc (10), aldc (10), kp (10, 10), tk (10),
&alk (10)

C Common block /bound/
      INTEGER IBC1, IBC2, NBC1, NBC2
      DOUBLE PRECISION TI, TQ1 (MAXP), TQ2 (MAXP), TIME1 (MAXP), TIME2 (MAXP)

C Common block /geom/
      INTEGER ISHAPE, ISYM, M, MP1, ISTEP

```

DOUBLE PRECISION H,L,DZ

```

C   Common block /tim/
      DOUBLE PRECISION DT, TTIME, PDT

      common/ttl/title,ttlfil,ttlprp,ttlkin,
      &/mod/model,
      &/KIN/A1,A2,EA1,EA2,M0,M1,DENS,HT,VA1,VA2,VEA1,VEA2,A3,EA3,D0,D1,D2
      &/prop/dcp,tdc,aldc,kp,tk,alk,ntdc,naldc,ntk,nalk,
      &/bound/ibcl,ibc2,nbcl,nbc2,ti,TQ1,TQ2,time1,time2,
      &/geom/ISHAPE,ISYM,M,MP1,ISTEP,H,L,DZ,
      &/TIM/TTIME,DT,PDT

C   NPRINT = 0 if printing input parameters and headings
C   NPRINT = 1 if printing temperature and/or extent of cure
C   NPRINT = 2 if printing end line

      IF (NPRINT.EQ.0) THEN
        GO TO 1100
      ELSE
        if (nprint.eq.1) then
          go to 1200
        else
          go to 1300
        endif
      endif

1100 write(outfil,1000)ttlfil,'out.dat'
1000 format(' ',a,a)
      open(unit=12,name=outfil(1:12),type='new',carriagecontrol='list')
      write(12,1)title
1   format(' ',3x,'Title: ',a20,/3x,'-----',//,14x,'Input Para',
+ 'meters',/,14x,16('-'))
      if(model.ne.1) then
        write(12,3)'Kinetic Parameters; Extent of Cure < 0.5:'
3   format(' ',/, ' ',A,/)
        write(12,5)'Pre-exponential factor, Ln(A1), (Ln(1/sec)).',LOG(A1)
        write(12,5)'                               Ln(A2), (Ln(1/sec)).',LOG(A2)
        abcd=ea1/1000.0d0
        write(12,6)'Activation energy const., Ea1, (kJ/mole)...',abcd
6   format(3x,A,f8.2)
        abcd=ea2/1000.0d0
        write(12,6)'                               Ea2, (kJ/mole)...',abcd
        write(12,4)'Exponent, M0, (dimensionless).....',M0
        write(12,4)'                               M1, (dimensionless).....',M1
4   format(3x,A,e10.4)
        write(12,3)'Extent of Cure > 0.5:'
        write(12,5)'Pre-exponential factor, Ln(A3), (Ln(1/sec)).',LOG(A3)
        abcd=ea3/1000.0d0
        write(12,6)'Activation energy const., Ea3, (kJ/mole)...',abcd
        write(12,4)'Diffusion constant, D0, (dimensionless)....',D0
        write(12,4)'                               D1, (dimensionless)....',D1
        write(12,4)'                               D2, (dimensionless)....',D2
        WRITE(12,7)'Density (kg/m3).....',DENS
7   FORMAT(/,3X,A,F10.1)
        WRITE(12,7)'Total heat of reaction (J/kg).....',HT
        if(model.eq.3) then
          abcd=vA1**0.50d0
          write(12,5)'St. dev. of rate constant, A1, (1/sec).....',abcd
5   FORMAT(3X,A,F8.4)
          abcd=vA2**0.50d0
          write(12,5)'St. dev. of rate constant, A2, (1/sec).....',abcd
          abcd=vea1**0.50d0/1000.0d0
          write(12,5)'St. dev. of Ea1 (kJ/mole).....',abcd

```

10

11

12

13

14

15

16

17

18

19

20

22

23

```

abcd=veal**0.50d0/1000.0d0
write(12,5)'St. dev. of Ea2 (kJ/mole).....',abcd
endif
endif
write(12,10)'Thermal Properties'
10  format(' ',/, ' ',A,/)
write(12,11)'Thermal conductivity table:'
11  format(3x,A)
    if(model.eq.1)then
        do i = 1,ntk
            write(12,12)tk(i),'C',kp(i,1),'W/mC'
12      format(6x,f6.2,1x,a,2x,f6.2,1x,a)
        enddo
    else
        do i = 1,ntk
            write(12,13)tk(i),'C',(alk(n),kp(i,n),n = 1,nalk)
13      format(5x,f6.2,a,2(3x,f6.3,3X,f6.2,'W/mC'),4(/,12x,
& 2(3x,f6.3,3X,f6.2,'W/mC'))
        enddo
    endif
write(12,14)
14  format(' ',/)
write(12,11)'Density-Specific Heat table:'
    if(model.eq.1)then
        do i = 1,ntdc
            write(12,15)tdc(i),'C',dcp(i,1),'m/s2'
15      format(6x,f6.2,1x,a,2x,E10.4,1x,a)
        enddo
    else
        do i = 1,ntdc
            write(12,16)tdc(i),'C',(ALDC(n),DCP(I,n),n = 1,naldc)
16      format(5x,f6.2,a,2(3x,f6.3,3X,E10.4,'m/s2'),4(/,12x,
& 2(3x,f6.3,3X,E10.4,'m/s2'))
        enddo
    endif
write(12,14)
abcd=ti-273.150d0
write(12,17)abcd
17  format(' ',/, ' ', 'Initial Condition:',/, ' ',2x,'Product temp.'
+, ' (C) at time=0 .....',f6.2)

```

c product geometry

```

    if(Ishape.eq.1)then
        if(Isym.eq.1)l = 1*2.0d0
        write(12,18)l
18      format(' ',/, ' ', 'Slab Geometry:',/,3x,'thickness (m)',
+26(' '),f10.6)
    else
        if(Ishape.eq.2)then
            write(12,20)l
20      format(' ',/, ' ', 'Cylindrical Geometry:',/,3x,'radius (m)',
+29(' '),f10.6)
        else
            write(12,22)l
22      format(' ',/, ' ', 'Spherical Geometry:',/,3x,'radius (m)',
+29(' '),f10.6)
        endif
    endif
endif

```

c boundary conditions

```

if(Ibcl.eq.1)then
  write(12,23)'Temperature Boundary Condition (IBC1)'
23  format(' ',/,3x,a,/)
  else
    write(12,23)'Heat Flux Boundary Condition (IBC1)'
  endif
do i = 1,nbc1
  if(Ibcl.eq.1)then
    write(12,24)'Temperature (C) at ',time1(i),' sec.....',tQ1(i)
24  format(6x,a,f8.1,a,f9.2)
    else
      write(12,24)'Heat Flux (W/m2) at ',time1(i),' sec.....',TQ1(i)
    endif
  endif
enddo

if(Ibc2.eq.1)then
  write(12,23)'Temperature Boundary Condition (IBC2)'
  else
    write(12,23)'Heat Flux Boundary Condition (IBC2)'
  endif
do i = 1,nbc2
  if(Ibc2.eq.1)then
    write(12,24)'Temperature (C) at ',time2(i),' sec.....',
&TQ2(i)-273.15D0
    else
      write(12,24)'Heat Flux (W/m2) at ',time2(i),' sec.....',TQ2(i)
    endif
  endif
enddo

c Temperature history

  write(12,100)title
100 format(' ',/,' ',/,'Title= ',a20,/)
  if(Isym.eq.1)then
    write(12,110)
110 format(' ',/,'Note: Distribution is symmetrical;'/,6x,'results',
+' are shown for half-thickness only.'/)
  endif

  hh22='DISTRIBUTION HISTORY'
  if(headtq.eq.1)then
    hh11='          TEMPERATURE (C)          '
  else
    hh11='TEMPERATURE (C) & EXTENT OF CURE'
  endif
  write(12,120)hh11,hh22
120 format(' ',/,' ',/,' ',17x,a,/,23x,a,/,19x,27('-'),/)
  if(model.eq.1)then
    write(12,130)
130 format(' ',32x,'position (m)',/,' ',7x,'time',5x,':',40x,
&'|Avg Temp')
    else
      write(12,135)
135 format(' ',32x,'position (m)',/,' ',7x,'time',5x,':',40x,
&'|Avg Temp ')
    endif
  do i = 1,5
    abc(i)=(i-1)*ISTEP*dz
  enddo
  if(model.eq.1)then
    write(12,137)abc(1),abc(2),abc(3),abc(4),abc(5)
137 format(' ',16x,':',5(f8.4))
  else

```

```

        if(model.eq.2)then
            write(12,140)abc(1),abc(2),abc(3),abc(4),abc(5)
140    format(' ',16x,':',5(f8.4),'|Ext Cure')
            else
            write(12,145)abc(1),abc(2),abc(3),abc(4),abc(5)
145    format(' ',16x,':',5(f8.4),'|Ext Cure| StD(%)')
            endif
        endif
        if(model.ne.3)then
            write(12,150)
150    format(' ',67('='))
            else
            write(12,155)
155    format(' ',72('='))
            endif

c Printout time heading

1200    tavg1 = tavg-273.150d0
        do i = 1,5
            abc(i)=t((i-1)*ISTEP+1,2)-273.150d0
        enddo
        prunit = '   sec:'
        write(12,190)time,prunit,abc(1),abc(2),abc(3),abc(4),abc(5),
& tavg1
190    format(' ',f10.2,1x,a,5(f7.2,1x),'|',f7.2,'C')

        if(headtq.eq.2)then

C Printout extent of cure values

        do i = 1,5
            abc(i)=al((i-1)*ISTEP+1)
        enddo
        if(model.eq.2)then
            write(12,210)abc(1),abc(2),abc(3),abc(4),abc(5),alavg
210    format(17x,':',5(f7.3,1x),'|',1x,f7.3)
            else
            write(12,215)abc(1),abc(2),abc(3),abc(4),abc(5),alavg,
& (val)**0.50d0
215    format(17x,':',5(f7.3,1x),'|',f7.3,1x,'|',f6.3)
            endif
        endif
        return

c Printout end line

1300    if(model.ne.3)then
            write(12,300)
300    format(' ',67('-'))
            else
            write(12,305)
305    format(' ',72('-'))
            endif
        close(unit=12)
        return
    end

c
c
c    program RANDNU

```

[illegible]

APPENDIX B

APPENDIX B

DATA ACQUISITION PROGRAM, *DATA_DA_AD*

B.1 Summary of Program

The data acquisition program, *DATA_DA_AD*, discussed in Chapter 4, is presented in this appendix. An outline of the program is given in Table B.1, and a listing of the program, written in Fortran 77 for a VaxstationII/GPX microcomputer is given in Table B.1.

Table B.1 Description of the Data Acquisition Program, *DATA_DA_AD*.

<u>Subroutine Title</u>	<u>Description</u>
PROGRAM DATA	Main program; contains data acquisition control software.
SUBROUTINE AUTO_ZERO	Calculates zeros (0°C) of amplifiers.
SUBROUTINE PROCESS_DATA	Averages and converts A/D data to temperature and heat flux.
SUBROUTINE SETUP_AMP	Sets gains, weights, and zeros for amplifiers.
SUBROUTINE SETUP_DATA	Initial set-up routine for data acquisition.
SUBROUTINE SETUP_POWER	Data input for D/A power supply.
SUBROUTINE TRANS_ADC	Converts binary data into volts.
SUBROUTINE TRANS_DAC	Converts volts into binary format.

B.2 Program Listing for DATA_DA_AD.FOR

```

PROGRAM DATA
c
c-----
c
c This program was written by Elaine Scott, 7/15/89, with the invaluable
c help of Mike McPherson of the MSU Case Center. It is based
c partly on Example 4-16, pages 4-217-219, VAXlab/LabStar Program-
c mers Guide.
c
c The purpose of this program is to read data from the A/D converters
c on the AXV11-Ca and AXV11-Cb boards, while writing to the D/A on
c the AXV11-Cb board.
c
c The program is designed to read thermocouple measurements (mV) and
c write voltages to a power supply to activate a heater. The
c output voltages of the power supply are also read. The thermo-
c couple measurements are converted to degrees centigrade (Type E
c TC), and are written to a file along with the power supply out-
c put. The file is compatible to the format required by the
c parameter estimation program, PROP1D.
c
c Other features of this program include data averaging over sampling
c interval and automatic 'zeroing' of input temperature data.
c
c-----
c
c IMPLICIT NONE
c
c Six external functions are used. Page numbers in descriptions refer
c to the Vaxlab/LabStar Programmers guide.
c
c EXTERNAL LIO$ATTACH      !Returns the device ID for the specified
c                          device. See pages 4-48 to 4-51.
c EXTERNAL LIO$DETACH      !Detaches the specified device, returns
c                          any associated storage to the system,
c                          and closes and deallocates associated
c                          VMS devices. See page 4-54.
c EXTERNAL LIO$READ        !Fills a buffer with data from the spe-
c                          cified device. See pages 4-58 to 4-59.
c EXTERNAL LIO$SET_I       !Sets up a device according to a parame-
c                          ter code and any number of interger
c                          values. See pages 4-60 to 4-61.
c EXTERNAL LIO$SET_R       !Sets up a device according to a parame-
c                          ter code and any number of real values.
c                          See pages 4-62 to 4-63.
c EXTERNAL LIO$WRITE       !Empties a buffer through the specified
c                          device. See pages 4-68 to 4-69.
c
c Include library containing external functions
c
c INCLUDE 'SYS$LIBRARY:LIOSET.FOR'      !External function symbol
c                                      definitions
c
c Define external functions
c
c INTEGER*4 LIO$ATTACH, LIO$DETACH, LIO$READ, LIO$SET_I,
c 1      LIO$SET_R, LIO$WRITE
c

```

c Declare integer variables

c

```

      INTEGER      AXA_ID      !AXV11-Ca device ID variable
      INTEGER      AXB_ID      !AXV11-Cb device ID variable
      INTEGER      AD_LENGTH_AXA !no. of data pts read (AXA)
      INTEGER      AD_LENGTH_AXB !no. of data pts read (AXB)
      INTEGER*2     BUFF_AD_AXA(8) !8 word buffer for A/D
      INTEGER*2     BUFF_AD_AXB(8) !8 word buffer for A/D
      INTEGER*2     BUFF_DA_AXB(500) !500 word buffer for D/A
      INTEGER      CAL_ZERO     !=1 for calculating zeros
      INTEGER      CLK_ID      !KVV11-C clock ID variable
      INTEGER      I,J,K,DUMMY !Dummy variables
      INTEGER      NAVG        !Total no. of data averaged
      INTEGER      NCHAN,NCHANA,NCHANB !No. channels (total, board)
      INTEGER      NDATAP      !Total no. data points
      INTEGER      NSAMPL      !No. data avg./samp. interval
      INTEGER      NSTEPS      !No. time steps for zeroing
      INTEGER*4     NVOLT      !No. voltages to be converted
      INTEGER      POWER      !Indicates use of D/A
      INTEGER      STATUS      !Status returned by LIO$

```

c

c Declare real variables

c

```

      REAL*4        GAIN(16)      !Gains for amplifiers
      REAL          HEAT_AREA     !Area of heated surf. (m*m)
      REAL          RATE          !Clock rate (Hertz)
      REAL          RESIST        !Resistance of heater (ohms)
      REAL          SRATE         !Interval rate
      REAL          TIMES(100)    !Times(s) for power supply
      REAL          VOLTS(100)    !Volts(v) for power supply
      REAL*4        WEIGH(16)     !Weights for amplifiers
      REAL*4        ZERO(16)     !Zeros for amplifiers

```

c

c Declare character variables

c

```

      CHARACTER*15   AMP(16)      !Electron amplifier number
      CHARACTER      BINARYFIL*20 !Binary data file
      CHARACTER      TEMPFIL*20   !Temperature data file
      CHARACTER      YN*2         !Yes/No (Y/N)

```

c

c Common statements

c

```

      COMMON /AMPLIFIER/ GAIN,WEIGH,ZERO,NAVG,NSTEPS,AMP
      COMMON /FILES/BINARYFIL,TEMPFIL
      COMMON /POWER/ BUFF_DA_AXB,NVOLT,POWER,HEAT_AREA,TIMES,VOLTS,
1      RESIST
      COMMON /SETUP/NCHAN,NCHANA,NCHANB,NDATAP,NSAMPL,RATE,SRATE

```

c

c*****

c

c Call SETUP_DATA to begin set up for data

c

```

      CALL SETUP_DATA

```

c

c Call SETUP_POWER to begin set up for input to D/A for power supply

c

```

      WRITE(*,10)'Do you want to input voltage values for D/A?'
1      ,'(N = no; F = enter data file; K = use keyboard)'
10     FORMAT(' ',/, ' ',5X,A,/, ' ',5X,A)
      READ(*,1)YN
1      FORMAT(A)
      IF(YN.NE.'N'.AND.YN.NE.'n') THEN
          CALL SETUP_POWER(YN)

```

```

ELSE
    POWER = 0
ENDIF

c
c Call SETUP_AMP to change gains, weights and/or zeros of amplifiers
c
    CALL SETUP_AMP(NCHAN,CAL_ZERO)
c
c Name output file for binary and temperature measurements. Binary
c data is stored during the experiment in case of unintended
c program interruption.
c
    WRITE(*,30)'Two data files (binary and temp.) are created:'
30  FORMAT(' ',/, ' ',72('*'),/, ' ',5X,A)
    WRITE(*,20)'File name for binary data file:'
    READ(*,1)BINARYFIL
    WRITE(*,20)'File name for temperature data file:'
20  FORMAT(' ',/, ' ',5X,A)
    READ(*,1)TEMPFIL
c
c End subroutine set up calls
c
c*****
c
c Begin hardware set up for data aquisition:
c
    WRITE(*,20)'Begin hardware set up:'
c
c First, attach devices:
c
c Attach the KWV11-C clock
c Gets a device ID for the KWV and tells LIO to use QIO I/O
c
    STATUS = LIO$ATTACH(CLK_ID, 'KZAO', LIO$K_QIO) !Attach to KWV
    IF(.NOT.STATUS) CALL LIB$SIGNAL(%VAL(STATUS))
c
c-----
c
c Attach AXV11-Ca device for A/D
c Gets a device ID for the AXVa and tells LIO to use QIO I/O
c
    STATUS = LIO$ATTACH(AXA_ID, 'AXAO', LIO$K_QIO) !Attach to AXVa
    IF(.NOT.STATUS) CALL LIB$SIGNAL(%VAL(STATUS))
c
c-----
c
c Attach AXV11-Cb device for A/D and D/A
c Gets a device ID for the AXVb and tells LIO to use QIO I/O
c
    IF(NCHANB.GT.0.OR.POWER.EQ.1)THEN
        STATUS = LIO$ATTACH(AXB_ID, 'AXB0', LIO$K_QIO) !Attach to AXVb
        IF(.NOT.STATUS) CALL LIB$SIGNAL(%VAL(STATUS))
    ENDIF
c
c*****
c
c Set up the clock
c rate = Hertz rate (a real number)
c function = repeat count
c trigger = immediate (this only sets up the start condition, the
c clock will be started by the LIO$READ from the A/D)
c
    STATUS = LIO$SET_R(CLK_ID, LIO$K_CLK_RATE, 1, RATE)

```

```

        IF(.NOT.STATUS)          CALL LIB$SIGNAL(%VAL(STATUS))
STATUS = LIO$SET_I(CLK_ID, LIO$K_FUNCTION, 1, LIO$K_REP_COUNT)
        IF(.NOT.STATUS)          CALL LIB$SIGNAL(%VAL(STATUS))
STATUS = LIO$SET_I(CLK_ID, LIO$K_TRIG, 1, LIO$K_IMMEDIATE)
        IF(.NOT.STATUS)          CALL LIB$SIGNAL(%VAL(STATUS))
C
C*****
C
C Set up AXVa and AXVb:
C
C AXVa:
C Synchronous interface (LIO$READ):
C
        STATUS = LIO$SET_I(AXA_ID, LIO$K_SYNCH, 0)
        IF(.NOT.STATUS)          CALL LIB$SIGNAL(%VAL(STATUS))
C
C Set up A/D:
C use A/D channels 0-7, depending on value of NCHANA
C
        STATUS = LIO$SET_I(AXA_ID, LIO$K_AD_CHAN, NCHANA, 0, 1, 2, 3,
1          4, 5, 6, 7)
        IF(.NOT.STATUS)          CALL LIB$SIGNAL(%VAL(STATUS))
C
C use a gain of one
C
        STATUS = LIO$SET_I(AXA_ID, LIO$K_AD_GAIN, NCHANA, 1, 1, 1, 1,
1          1, 1, 1, 1)
        IF(.NOT.STATUS)          CALL LIB$SIGNAL(%VAL(STATUS))
C
C Sweep through all channels on each clock tic:
C
        STATUS = LIO$SET_I(AXA_ID, LIO$K_TRIG, 1, LIO$K_CLK_SWEEP)
        IF(.NOT.STATUS)          CALL LIB$SIGNAL(%VAL(STATUS))
C
C End AXVa set up
C
C-----
        IF(NCHANB.GT.0.OR.POWER.EQ.1) THEN
C AXVb:
C Synchronous interface (LIO$READ):
C
        STATUS = LIO$SET_I(AXB_ID, LIO$K_SYNCH, 0)
        IF(.NOT.STATUS)          CALL LIB$SIGNAL(%VAL(STATUS))
C
C Set up A/D:
C Note, channel 4 is reserved for reading output of power supply,
C and channels 0-3 are for thermocouple output. QIO I/O requires
C channels to be in consecutive, ascending order; therefore, the
C fifth channel is designated for the power supply, instead of
C the last, and all five channels must be read regardless whether
C or not they are all used.
C
C WARNING: If additional amplifiers are installed, the channel
C designation must be changed!!
C
        STATUS = LIO$SET_I(AXB_ID, LIO$K_AD_CHAN, 5, 0, 1, 2, 3, 4)
        IF(.NOT.STATUS)          CALL LIB$SIGNAL(%VAL(STATUS))
C
C use a gain of one
C
        STATUS = LIO$SET_I(AXB_ID, LIO$K_AD_GAIN, 5, 1, 1, 1, 1, 1)
        IF(.NOT.STATUS)          CALL LIB$SIGNAL(%VAL(STATUS))
C

```

```

c Set up D/A:
c use D/A channel X
c
      STATUS = LIO$SET_I(AXB_ID, LIO$K_DA_CHAN, 1, 1)
      IF(.NOT.STATUS) CALL LIB$SIGNAL(%VAL(STATUS))
c
c Use immediate start burst mode for AXV11-Cb. This starts immediately
c on the LIO$READ call for the AXV11-Ca board:
c
      STATUS = LIO$SET_I(AXB_ID, LIO$K_TRIG, 1, LIO$K_IMM_BURST)
      IF(.NOT.STATUS) CALL LIB$SIGNAL(%VAL(STATUS))
      ENDIF
c
c End AXVb set up
c
c*****
c
c Initialize the power supply and open output file before starting the
c clock:
c
      IF(POWER.EQ.1) THEN
        STATUS = LIO$WRITE(AXB_ID,BUFF_DA_AXB(1),2,LIO$K_OUTPUT)
        IF(.NOT.STATUS) CALL LIB$SIGNAL(%VAL(STATUS))
      ENDIF
c
      OPEN(UNIT=10,NAME=BINARYFIL,TYPE='NEW',ERR=99)
c
c Now, initialize the experiment:
c
      WRITE(*,40)'Type "1 <CR>" to start data collection'
40  FORMAT(' ',/, ' ',72('*'),/, ' ',15X,A,/, ' ',72('*'),/)
      READ *,DUMMY
c
c-----
c
c Start the clock:
c
      STATUS = LIO$SET_I(CLK_ID, LIO$K_START,0)
      IF(.NOT.STATUS) CALL LIB$SIGNAL(%VAL(STATUS))
c
c-----
c
c Start loop:
c
      K = 2
      DO I = 1,NDATAP
c
c Write D/A values to power supply using AXVb
c
        IF(POWER.EQ.1) THEN
          IF(K.LE.NVOLT-1) THEN
            IF(TIMES(K).GE.I/RATE.AND.TIMES(K).LT.(I+1)/RATE) THEN
              STATUS = LIO$WRITE(AXB_ID,BUFF_DA_AXB(K),2,LIO$K_OUTPUT)
              IF(.NOT.STATUS) CALL LIB$SIGNAL(%VAL(STATUS))
              K = K+1
            ENDIF
          ENDIF
        ENDIF
c
c Read A/D values from thermocouples (channels 0-7 on AXVa and 0-3 on
c AXVb) and power supply (channel 4 on AXVb)
c
      STATUS = LIO$READ(AXA_ID, BUFF_AD_AXA(1),

```

```

1      2*NCHANA, AD_LENGTH_AXA, LIOSK_INPUT)
      IF (.NOT.STATUS)          CALL LIB$SIGNAL(%VAL(STATUS))
c
c Read all data for channel B
c
c WARNING: If additional amplifiers are installed, the number of
c channels read must be changed!!
c
      IF(NCHANB.GT.0.OR.POWER.EQ.1) THEN
        STATUS = LIO$READ(AXB_ID, BUFF_AD_AXB(1),
1          2*5, AD_LENGTH_AXB, LIOSK_INPUT)
        IF (.NOT.STATUS)          CALL LIB$SIGNAL(%VAL(STATUS))
      ENDIF
c
c Write data to file: The data from the AXV11-Ca are written on
c the first line, and the data from the AXV11-Cb, including
c output from the D/A, are written on the next line.
c
      WRITE(*,50)I,(BUFF_AD_AXA(J), J = 1,NCHANA),
1      (BUFF_AD_AXB(J), J = 1,NCHANB),BUFF_AD_AXB(5)
      WRITE(10,60) (BUFF_AD_AXA(J), J = 1,NCHANA),
1      (BUFF_AD_AXB(J), J = 1,NCHANB),BUFF_AD_AXB(5)
50     FORMAT(' ',I6,2X,8(I5,3X),/,9X,8(I5,3X))
60     FORMAT(' ',8(I5,3X),/,' ',8(I5,3X))
      ENDDO
c
c End loop
c
c-----
c
c Begin shutdown procedure
c
c Close binary data file
c
      CLOSE(UNIT=10)
c
c Terminate input voltage to power supply at the end of the run:
c
      IF(POWER.EQ.1) THEN
        STATUS = LIO$WRITE(AXB_ID,BUFF_DA_AXB(NVOLT),2,LIOSK_OUTPUT)
        IF (.NOT.STATUS)          CALL LIB$SIGNAL(%VAL(STATUS))
      ENDIF
c
c Detach devices:
c
      STATUS = LIO$DETACH(AXA_ID, )
      IF (.NOT.STATUS)          CALL LIB$SIGNAL(%VAL(STATUS))
      IF(NCHANB.GT.0.OR.POWER.EQ.1) THEN
        STATUS = LIO$DETACH(AXB_ID, )
        IF (.NOT.STATUS)          CALL LIB$SIGNAL(%VAL(STATUS))
      ENDIF
c
c Stop and detach the clock:
c
      STATUS = LIO$SET_I(CLK_ID,LIOSK_STOP,0)
      IF (.NOT.STATUS)          CALL LIB$SIGNAL(%VAL(STATUS))
      STATUS = LIO$DETACH(CLK_ID, )
      IF (.NOT.STATUS)          CALL LIB$SIGNAL(%VAL(STATUS))
c
c Data collection is complete
c
      WRITE(*,30)'Data collection is completed, now process data:'
c

```

```

c*****
c
c Start data analysis:
c
c First calculate zeros for amplifiers if needed.
c
c IF(CAL_ZERO.EQ.1)THEN
c   CALL AUTO_ZERO(POWER)
c ENDIF
c
c Now, average binary data over sampling interval, and convert
c binary data into millivolts and then to degrees centigrade.
c
c CALL PROCESS_DATA(POWER,HEAT_AREA,RESIST)
c
c All done now.... stop and end
c
c WRITE(*,70)'Program is completed.'
70  FORMAT(//,' ',72('*'),//,' ',5X,A,/)
c   GO TO 300
99  STOP      'Error during opening master data file'
300 STOP
c   END
c
c Fini!!
c
c
c*****
c
c End main program.
c
c Begin subroutines:
c   There are six subroutines in this program; they are listed in
c   alphabetical order:
c   Title           Arguments           Brief Description
c
c-----
c
c AUTO_ZERO         POWER              Calculates zeros(OC) of amplifiers
c PROCESS_DATA      POWER,HEAT_AREA    Avgerages & converts A/D data
c SETUP_AMP         NCHAN,CAL_ZERO     Sets gain, weight, zero for ampl.
c SETUP_DATA        (none)             Initial set up for data aquisition
c SETUP_POWER       YN                 Data input for D/A
c TRANS_DAC         VOLTS,BUFF_DA_AXB  Converts volts to binary format
c
c*****
c*****
c
c SUBROUTINE AUTO_ZERO(POWER)
c
c This subroutine calculates the zeros (C) for the amplifiers, based
c on initial isothermal data.
c
c IMPLICIT NONE
c
c Declare integer values
c
c INTEGER I,J,K          !Dummy
c INTEGER NAVG           !Total no. of data averaged
c INTEGER NCHAN,NCHANA,NCHANB !Total number of channels
c INTEGER NDATAP         !Total no. data points
c INTEGER NSAMPL         !No. data avg./samp. interval
c INTEGER NSTEPS         !No. time steps for zeroing
c INTEGER NZERO          !No. of zeros changed

```

```

      INTEGER NWEIGH      !No. of weights changed
      INTEGER POWER      !Indicates use of D/A
c
c  Declare real values
c
      REAL*4      AVGZERO(100,16) !Binary data to be averaged
      REAL*4      CONV(16)        !Inter. value for zeros
      REAL*4      GAIN(16)        !Gains for amplifiers
      REAL        RATE            !Clock rate (Hertz)
      REAL        SRATE           !Interval rate
      REAL        SUMI(16)        !Sum of binary data
      REAL        SUMAVG          !Average binary data
      REAL        SUMWGH          !Average weights
      REAL*4      WEIGH(16)       !Weights for amplifiers
      REAL*4      ZERO(16)       !Zeros for amplifiers
c
c  Declare character values
c
      CHARACTER*15  AMP(16)       !Electron amplifier number
      CHARACTER     BINARYFIL*20  !Binary data file
      CHARACTER     TEMPFIL*20    !Temperature data file
      CHARACTER     YN*2         !Yes/No (Y/N)
c
c  Common statement
c
      COMMON /AMPLIFIER/ GAIN,WEIGH,ZERO,NAVG,NSTEPS,AMP
      COMMON /FILES/BINARYFIL,TEMPFIL
      COMMON /SETUP/NCHAN,NCHANA,NCHANB,NDATAP,NSAMPL,RATE,SRATE
c
c *****
c
c  The zero's are calculated internally by averaging the first NSTEPS
c  data points for each thermocouple prior to the onset of applied heat
c  flux, and determining the difference between the overall average and the
c  average value for each thermocouple.
c-----
c
c  Read in first NAVG values from binary data file (BINARYFIL)
c
      OPEN(UNIT=20,NAME=BINARYFIL,STATUS='OLD')
      DO J = 1,NSTEPS
        K = (J-1)*NCHAN
        READ(20,*)(AVGZERO(J,I), I = 1,NCHANA)
        IF(NCHANB.GT.0.OR.POWER.EQ.1) THEN
          READ(20,*)(AVGZERO(J,NCHANA+I), I = 1,NCHANB+POWER)
        ENDIF
      ENDDO
c
c  Close binary data file
c
      CLOSE (UNIT=20)
c-----
c
c
c  Check weights and recalculate zeros if you find bad thermocouples.
c
      WRITE(*,10)'Number','Amplifier','Weighting Factor'
      DO I = 1,NCHAN
        WRITE(*,20) I,AMP(I),WEIGH(I)
      ENDDO
      TYPE *
      WRITE(*,30)'Are corrected weighting factors OK? (Y/N)'

```

```

      READ(*,1)YN
c
c   Change weights if necessary
c
      IF(YN.EQ.'N'.OR.YN.EQ.'n')THEN
100    WRITE(*,30)'Enter number of weights you wish to change:'
      READ *,NWEIGH
      DO I = 1,NWEIGH
        WRITE(*,30)'Enter amplifier number and corrected weight:'
        READ *,J,WEIGH(J)
      ENDDO
      WRITE(*,10)'Number','Amplifier','Corrected Weights'
      DO J = 1,NCHAN
        WRITE(*,20)J,AMP(J),WEIGH(J)
      ENDDO
      WRITE(*,30)'Are corrected weights OK? (Y/N)'
      READ(*,1)YN
      IF(YN.EQ.'N'.OR.YN.EQ.'n')GO TO 100
      ENDIF
      SUMAVG = 0.0D0
      SUMWGH = 0.0D0
      DO I = 1,NCHAN
        SUMI(I) = 0.0D0
        SUMWGH = SUMWGH + WEIGH(I)
      ENDDO
c
c   Average data over all channels for NSTEPS time steps
c
      DO J = 1,NSTEPS
        DO I = 1,NCHAN
          SUMI(I) = SUMI(I) + AVGZERO(J,I)*WEIGH(I)
        ENDDO
      ENDDO
c
c   Adjust for gain
c
      DO I = 1,NCHAN
        SUMAVG = SUMAVG + SUMI(I)*GAIN(I)
      ENDDO
      SUMAVG = SUMAVG/SUMWGH
c
c   Calculate zeros
c
      DO I = 1,NCHAN
        CONV(I) = (SUMAVG-SUMI(I)*GAIN(I))/NSTEPS
      ENDDO
      CALL TRANS_ADC(0,NCHAN,CONV,ZERO)
1    FORMAT(A)
10   FORMAT(' ',/, ' ',3X,A,3X,A,7X,A)
20   FORMAT(' ',3X,I6,3X,A,3X,F6.3)
30   FORMAT(' ',/, ' ',A)
c
c   End AUTO_ZERO subroutine.
c
      RETURN
      END
c
c*****
c*****
c
      SUBROUTINE PROCESS_DATA(POWER,HEAT_AREA,RESIST)
c
c   This subroutine averages A/D data over each sampling interval, and

```

```

c      then converts the binary data to millivolts and then to degrees
c      centigrade.
c
c      IMPLICIT NONE
c
c      Declare integers variables
c
c      INTEGER I,J,K,L          !Dummy variables
c      INTEGER NAVG             !Total no. of data averaged
c      INTEGER NCHAN,NCHANA,NCHANB !No. channels (total, board)
c      INTEGER NCHANP1          !Includes voltage channel
c      INTEGER NDATAP,NDATA     !Total no. data points
c      INTEGER NSAMPL           !No. data avg./ (samp intrvl)
c      INTEGER NSTEPS           !No. time steps for zeroing
c      INTEGER POWER            ! =1 for output to D/A
c      INTEGER STATUS           !Status returned by LIO$
c
c      Declare real variables
c
c      REAL          AVG_DATA(1000) !Data to be avgeraged
c      REAL*4        GAIN(16)       !Gains for amplifiers
c      REAL          HEAT_AREA      !Area of heated surf. (m*m)
c      REAL          HEAT_FLUX      !Heat flux from heater
c      REAL          RATE,SRATE     !Clock rate (Hertz)
c      REAL          RESIST         !Resistance of heater (ohms)
c      REAL          SUM(16)        !Sums for averaging data
c      REAL          TEMP(16)       !Converted temps. from A/D
c      REAL          TIMSTP         !Time step for printout
c      REAL          VA(16)         !Millivolts from A/D
c      REAL*4        WEIGH(16)     !Weights for amplifiers
c      REAL*4        ZERO(16)      !Zeros for amplifiers
c
c      Declare character variable
c
c      CHARACTER*15    AMP(16)      !Electron amplifier number
c      CHARACTER       BINARYFIL*20 !Binary data file
c      CHARACTER       TEMPFIL*20   !Temperature data file
c
c      Common statement
c
c      COMMON /AMPLIFIER/ GAIN,WEIGH,ZERO,NAVG,NSTEPS,AMP
c      COMMON /FILES/BINARYFIL,TEMPFIL
c      COMMON /SETUP/NCHAN,NCHANA,NCHANB,NDATAP,NSAMPL,RATE,SRATE
c
c      *****
c
c      Open binary data file (BINARYFIL) and temperature data file (TEMPFIL)
c
c      OPEN (UNIT=20,NAME=BINARYFIL,STATUS='OLD')
c      OPEN (UNIT=30,NAME=TEMPFIL,TYPE='NEW')
c
c      Initialize arrays, etc.
c
c      NDATA = NDATAP/NSAMPL
c      NCHANP1 = NCHAN + POWER
c      DO J = 1,NCHANP1
c          SUM(J) = 0
c      ENDDO
c
c      -----
c
c      Read in data values from file
c

```

```

DO L = 1, NDATA
  DO J = 1, NSAMPL
    K = (J-1)*NCHANP1
    READ(20,*,ERR=99) (AVG_DATA(K+I), I = 1, NCHANA),
1      (AVG_DATA(K+NCHANA+I), I = 1, NCHANB+POWER)
c
c Average data over sampling interval
c
    DO I = 1, NCHANP1
      SUM(I) = SUM(I) + AVG_DATA(K+I)/NSAMPL
    ENDDO
  ENDDO
c
c -----
c
c Begin processing data
c
c Convert binary data into volts. Binary data is converted to
c voltages in subroutine TRANS_ADC assuming a linear relationship
c between the binary output and volts based on a calibrated curve.
c Voltage values are returned in VA.
c
    CALL TRANS_ADC(POWER, NCHANP1, SUM, VA)
c
    DO I = 1, NCHANP1
c
c Next, convert thermocouple values to degrees centigrade if channel is
c not reading from power supply.
c
      IF(POWER.EQ.1.AND.I.EQ.NCHANP1)GOTO 100
c
c First, adjust thermocouple data for gain and zeros (C), and then con-
c vert data to millivolts.
c
      VA(I) = (VA(I)*GAIN(I)+ZERO(I))/1000.0
c
c Voltages are then converted to temperatures using the thermocouple
c conversion routine in VAXlab/Lab-Star Programmers Guide. See
c Sec. 6.9, pages 6-17 to 6-19; pages 6-62 to 6-63; and Example 6-20
c on page 6-119 for details.
c
c Note, this subroutine is for Type E, Chromel-Constantan thermocouples.
c Input values are the voltages in microvolts, the number of data
c values to be converted, and output values are temperature in
c degrees centigrade and the operation status.
c
      CALL LSP$THERMOCOUPLE_E (VA(I), TEMP(I), 1, STATUS)
      IF(.NOT.(status)) CALL lib$signal(%val(status))
100    ENDDO
c
c Print out processed temperature data (C) to file (TEMPFIL)
c
    TIMSTP=SRATE*L
    IF(POWER.NE.1) THEN
      IF(NCHAN.LE.8) THEN
        WRITE(30,10) TIMSTP, (TEMP(I), I=1, NCHAN)
10      FORMAT(F10.3, 1X, 8(F6.2, 1X))
      ELSE
        WRITE(30,20) TIMSTP, (TEMP(I), I=1, NCHAN)
20      FORMAT(F10.3, 1X, 16(F6.2, 1X))
      ENDIF
    ELSE
c

```

```

c Calculate heat flux using measured voltage and resistance of heater
c   (power = (volts)*(volts)/resistance; heat flux = power/area)
c
c       HEAT_FLUX = VA(NCHANP1)*VA(NCHANP1)/(RESIST*HEAT_AREA)
c
c Write processed heat flux and temperature data to a file
c
c       IF(NCHAN.LE.8) THEN
c         WRITE(30,30) TIMSTP,HEAT_FLUX,(TEMP(I),I=1,NCHAN)
30      FORMAT(F10.3,1X,F8.1,1X,8(F6.2,1X))
c       ELSE
c         WRITE(30,40) TIMSTP,HEAT_FLUX,(TEMP(I),I=1,NCHAN)
40      FORMAT(F10.3,1X,F8.1,1X,13(F6.2,1X))
c       ENDIF
c     ENDIF
c
c End data processing
c
c -----
c
c Initialize summations
c
c       DO I = 1,NCHANP1
c         SUM(I) = 0.0
c         VA(I) = 0.0
c       ENDDO
c
c End loop
c
c     ENDDO
c
c *****
c
c Close binary data file and temperature file
c
c       CLOSE (UNIT=20)
c       CLOSE (UNIT=30)
c
c End data processing subroutine
c
c       RETURN
99  STOP      'Error while reading from data file'
c       END
c
c *****
c *****
c
c SUBROUTINE SETUP_AMP(NCHAN,CAL_ZERO)
c
c This subroutine sets up the Ectron amplifiers; user may change gains,
c weights and/or zeros if necessary.
c
c IMPLICIT NONE
c
c Define integer variables
c
c       INTEGER CAL_ZERO      !=1 for calculating zeros
c       INTEGER      I,J      !Dummy
c       INTEGER NAVG          !Total no. of data averaged
c       INTEGER NCHAN        !Total number of channels
c       INTEGER NGAIN        !No. of gains changed
c       INTEGER NSTEPS        !No. of time steps for zeroing

```

```

      INTEGER NWEIGH      !No. of weights changed
      INTEGER NZERO       !No. of zeros changed
c
c Define real variables
c
      REAL*4      GAIN(16)      !Gains for amplifiers
      REAL*4      WEIGH(16)     !Weights for amplifiers
      REAL*4      ZERO(16)     !Zeros for amplifiers
c
c Define character variables
c
      CHARACTER*15 AMP(16)      !Ectron amplifier number
      CHARACTER*1  YN           !Yes/no (Y/N)
c
c Common statement
c
      COMMON /AMPLIFIER/ GAIN,WEIGH,ZERO,NAVG,NSTEPS,AMP
c
c Data statements for amplifiers
c Ectron amplifier numbers:
c
      DATA AMP(1),AMP(2),AMP(3),AMP(4),AMP(5),AMP(6),AMP(7),AMP(8),
1      AMP(9),AMP(10),AMP(11),AMP(12) / 'ECTRON_53661',
1      'ECTRON_53662','ECTRON_53663','ECTRON_53664',
1      'ECTRON_53665','ECTRON_53674','ECTRON_53675',
1      'ECTRON_53676','ECTRON_53677','ECTRON_53678',
1      'ECTRON_53973','ECTRON_53974' /
c
c Gain of Ectron amplifiers last checked on 3/16/89
c
      DATA GAIN(1),GAIN(2),GAIN(3),GAIN(4),GAIN(5),GAIN(6),GAIN(7),
1      GAIN(8),GAIN(9),GAIN(10),GAIN(11),GAIN(12) / 1.003,1.003,
1      0.996,0.999,0.998,0.995,1.002,1.000,0.999,0.999,1.028,
1      1.008 /
c
c Weights of Ectron amplifiers
c
      DATA WEIGH(1),WEIGH(2),WEIGH(3),WEIGH(4),WEIGH(5),WEIGH(6),
1      WEIGH(7),WEIGH(8),WEIGH(9),WEIGH(10),WEIGH(11),WEIGH(12)
1      / 1.00,1.00,1.00,1.00,1.00,1.00,1.00,1.00,1.00,1.00,1.00,
1      1.00 /
c
c Zeros are millivolt readings at 0C; last checked on 3/30/89.
c
      DATA ZERO(1),ZERO(2),ZERO(3),ZERO(4),ZERO(5),ZERO(6),ZERO(7),
1      ZERO(8),ZERO(9),ZERO(10),ZERO(11),ZERO(12) / 0.002,0.000,
1      0.000,-0.003,0.0005,0.001,-0.0025,-0.0005,0.0005,0.005,
1      0.0055,-0.004 /
c
c*****
c
c Set up amplifiers: change gains, weights and/or zeros if necessary:
c
      WRITE(*,10) 'Begin set up for amplifiers:'
c
c-----
c
c Change gain of amplifiers if necessary. Gains represent fractional
c output at 10V input (amps should read 0-10V; for example, if the
c amplifier instead read 0-9.99V, the gain would be 0.999)
c
      WRITE(*,40) 'Check gain of Ectron amplifiers:'
      TYPE *
```

```

        WRITE(*,20)'Number','Amplifier','Gain'
        DO J = 1,NCHAN
        WRITE(*,30)J,AMP(J),GAIN(J)
        ENDDO
c
c   You may change any number of gains that you want
c
        WRITE(*,40)'Do you want to change any of the gains? (Y/N)'
        READ(*,1)YN
        IF(YN.EQ.'Y'.OR.YN.EQ.'y')THEN
300    WRITE(*,40)'Enter number of gains you wish to change:'
        READ *,NGAIN
c
c   Amplifier numbers start from 1 and go to 12 (Ectron Amplifiers)
c
        DO I = 1,NGAIN
        WRITE(*,40)'Enter amplifier number and corrected gain:'
        READ*,J,GAIN(J)
        ENDDO
        TYPE *
        WRITE(*,20)'Number','Amplifier','Corrected Gain'
        DO J = 1,NCHAN
        WRITE(*,30)J,AMP(J),GAIN(J)
        ENDDO
c
c   Re-correct values if necessary
c
        WRITE(*,40)'Are corrected gains OK? (Y/N)'
        READ(*,1)YN
        IF(YN.EQ.'N'.OR.YN.EQ.'n')GO TO 300
        ENDIF
c
c-----
c
c   Change weights for amplifiers if necessary. Use a weight of 1.0 for
c   good thermocouples, and a weight of 0.0 for bad thermocouples.
c
        WRITE(*,40)'Check weights for Ectron amplifiers:'
        TYPE *
        WRITE(*,50)'Number','Amplifier','Weight'
        DO J = 1,NCHAN
        WRITE(*,60)J,AMP(J),WEIGH(J)
        ENDDO
        WRITE(*,40)'Do you want to change any of the weights? (Y/N)'
        READ(*,1)YN
        IF(YN.EQ.'Y'.OR.YN.EQ.'y')THEN
c
c   Change as many of the weights as you want.
c
400    WRITE(*,40)'Enter number of weights you wish to change:'
        READ*,NWEIGH
c
c   Amplifier numbers range from 1 to 12 (Ectron Amplifiers)
c
        DO I = 1,NWEIGH
        WRITE(*,40)'Enter amplifier number and corrected weight:'
        READ*,J,WEIGH(J)
        ENDDO
        TYPE *
        WRITE(*,20)'Number','Amplifier','Corrected Weight'
        DO J = 1,NCHAN
        WRITE(*,30)J,AMP(J),WEIGH(J)
        ENDDO

```

```

c
c   Re-correct values if necessary
c
      WRITE(*,40)'Are corrected weights OK? (Y/N)'
      READ(*,1)YN
      IF (YN.EQ.'N'.OR.YN.EQ.'n')GO TO 400
    ENDIF
c
c-----
c
c   Change zeros of amplifiers if necessary.  Zeros represent the ampli-
c   fier readings at 0C.  There are three options for the user here:
c   1.  use the zeros given; 2. let the program calculate the zeros;
c   3.  enter in zeros.
c
      WRITE(*,40)'Check zeros (at 0C) of Ectron amplifiers:'
      TYPE *
      WRITE(*,20)'Number','Amplifier','mV at 0C'
      DO J = 1,NCHAN
        WRITE(*,70)J,AMP(J),ZERO(J)
      ENDDO
      TYPE *
      WRITE(*,80)'Do you want the zeros to be recalculated for you?',
1      ' (Y/N)'
      READ(*,1)YN
      CAL_ZERO = 0
      NSTEPS = 0
      NAVG = 0
c
c   If user wants program to calculate zeros, the voltage values are
c   averaged over a number of time steps specified by the user.
c   The time step means the actual time step in which data is col-
c   lected, not the averaged sampling interval.  The temperatures
c   should be isothermal over this interval, with no externally
c   applied heat flux.
c
      IF (YN.EQ.'Y'.OR.YN.EQ.'y')THEN
        WRITE(*,90)'Enter number of time steps to average zeros over:'
1      ' (No heat flux should be applied over this interval.)'
        READ *,NSTEPS
        CAL_ZERO = 1
        NAVG = NSTEPS*NCHAN
      ELSE
c
c   User may change zeros by himself or herself
c
      WRITE(*,40)'Do you want to change any of the zeros? (Y/N)'
      READ(*,1)YN
      IF (YN.EQ.'Y'.OR.YN.EQ.'y')THEN
500    WRITE(*,40)'Enter number of zeros you wish to change:'
        READ*,NZERO
        DO I = 1,NZERO
          WRITE(*,40)'Enter amplifier number and corrected zeros:'
          READ *,J,ZERO(J)
        ENDDO
        TYPE *
        WRITE(*,20)'Number','Amplifier','Corrected mV at 0C'
        DO J = 1,NCHAN
          WRITE(*,30)J,AMP(J),ZERO(J)
        ENDDO
c
c   Re-correct values if necessary

```

```

c      WRITE(*,40)'Are corrected zeros OK? (Y/N)'
c      READ(*,1)YN
c      IF(YN.EQ.'N'.OR.YN.EQ.'n')GO TO 500
c      ENDIF
c      ENDIF
1      FORMAT(A)
10     FORMAT(' ',//,' ',72('*'),//,10X,A,/)
20     FORMAT(' ',3X,A,3X,A,7X,A)
30     FORMAT(' ',3X,I6,3X,A,3X,F6.3)
40     FORMAT(' ',//,' ',5X,A)
50     FORMAT(' ',3X,A,3X,A,5X,A)
60     FORMAT(' ',3X,I6,3X,A,3X,F6.4)
70     FORMAT(' ',3X,I6,3X,A,5X,F7.4)
80     FORMAT(' ',//,' ',5X,A,A)
90     FORMAT(' ',//,' ',5X,A,/, ' ',5X,A)
c
c      End set up for amplifiers
c
c      RETURN
c      END
c
c*****
c*****
c
c      SUBROUTINE SETUP_DATA
c
c      This subroutine provides the initial set up for data aquisition:
c
c      IMPLICIT NONE
c
c      Define integer variables
c
c      INTEGER  NCHAN,NCHANA,NCHANB      !No. channels (total, board)
c      INTEGER  NDATA                    !No. of data pts per channel
c      INTEGER  NDATAP                   !Total no. data points
c      INTEGER  NSAMPL                   !No. data avg/(samp intrvl)
c
c      Define real variables
c
c      REAL      RATE                    !Clock rate (Hertz)
c      REAL      SRATE                   !Interval rate
c
c      Define character variable
c
c      CHARACTER  YN*2                  !Yes/no (Y/N)
c
c      Common statement
c
c      COMMON /SETUP/NCHAN,NCHANA,NCHANB,NDATAP,NSAMPL,RATE,SRATE
c
c*****
c
c      First set up sampling interval, and number of samples to be averaged
c      over each sampling interval.
c
c      WRITE(*,10)'Begin set up for data aquisition'
c      WRITE(*,20)'Data is collected over a sampling interval and',
1      ' averaged for that interval.'
5      WRITE(*,30)'Enter sampling interval in seconds: '
c      READ *,SRATE
c      WRITE(*,40)'Enter no. of samples to be averaged per sampling ',
1      'interval:'

```

```

      READ *,NSAMPL
      RATE = 1.0*NSAMPL/SRATE
      WRITE(*,50)'rate =',RATE,' Hertz'
c
c   Next enter total number of data points for each channel and
c   the total number of channels.
c
      WRITE(*,40)'Enter total number of sampling intervals',
      1      ' for each channel:'
      READ*,NDATA
      NDATA*NSAMPL
      WRITE(*,30)'Enter total number of channels (max=12):'
      READ*,NCHAN
      IF(NCHAN.LT.8) THEN
        NCHANA = NCHAN
        NCHANB = 0
      ELSE
        NCHANA = 8
        NCHANB = (NCHAN-8)
      ENDIF
c
c   Allow user to change input values.
c
      TYPE *
      WRITE(*,30)'Do you want to change the above input values? (Y/N)'
      READ(*,1)YN
      IF(YN.EQ.'Y'.OR.YN.EQ.'y')GOTO 5
c
c   Initial set up complete
c
      1      FORMAT(A)
      10     FORMAT(' ',///,' ',72('*'),///,' ',20X,A,///,' ',72('*'),///)
      20     FORMAT(' ',10X,A,///,' ',5X,A,/)
      30     FORMAT(' ',5X,A)
      40     FORMAT(' ',5X,A,A)
      50     FORMAT(' ',/, ' ',10X,A,F8.3,A,/)
      RETURN
      END
c
c*****
c*****
c
      SUBROUTINE SETUP_POWER(YN)
c
c   This subroutine provides the initial set up for input to D/A for
c   power supply.
c
      IMPLICIT NONE
c
c   Define integer variables
c
      INTEGER*2      BUFF_DA_AXB(500)      !500 word buffer for D/A
      INTEGER J              !Dummy variable
      INTEGER*4      NVOLT      !No. voltages converted
      INTEGER POWER      !Indicates use of D/A
c
c   Define real variables
c
      REAL          HEAT_AREA      !Area of heated surf. (m*m)
      REAL          RESIST      !Resistance of heater (ohms)
      REAL          TIMES(100)    !times(s) for power supply
      REAL          VOLTS(100)    !volts(v) for power supply
c

```

```

c Define character variables
c
      CHARACTER      POWERFIL*20      !Data file for D/A input
      CHARACTER      YN*2      !Yes/no (Y/N)
c
c Common statement
c
      COMMON /POWER/ BUFF_DA_AXB,NVOLT,POWER,HEAT_AREA,TIMES,VOLTS,
      1      RESIST
c
c*****
c
c Set up program for heat flux:
c
      WRITE(*,10)'Begin set up for D/A to power supply:'
      POWER = 1
c
c Description of input file.
c
      WRITE(*,20)'A data file is created which contains the ',
      1      'desired input ','voltages for the power supply. ',
      1      'Set up the file as follows:',
      1      'line 1: Surface area of the heating unit (m*m)',
      1      '      (Divided by two for symmetrical case.)',
      1      'line 2: Total number of voltage data values (NVOLT)',
      1      'line 3: Time (sec), volts','.',',',
      1      'line NVOLT+2: Time (sec), volts ',
      1      'For, example, if you want to read 10 volts to the power',
      1      'supply at 20 sec and then read 0 volts at 40 sec from',
      1      'the ','start of the experiment, enter in from line ',
      1      '2 to line NVOLT+2:',
      1      'line 2: 2',
      1      'line 3: 20.,10.',
      1      'line 4: 40.,0.'
c
c Enter file name for input voltage data for power supply
c
      IF (YN.EQ.'F'.OR.YN.EQ.'f') THEN
        WRITE(*,30)'Enter input file name for power supply input:'
        READ(*,1)POWERFIL
        OPEN(UNIT=10,NAME=POWERFIL,STATUS='OLD')
c
c The heat flux area is area of heated surface (divided by two for
c the symmetrical case) (m*m).
c
      READ(10,*)HEAT_AREA
c
c Read the resistance of the heater in ohms.
c
      READ(10,*)RESIST
c
c Read the total number of voltage D/A input values.
c
      READ(10,*)NVOLT
c
c Start DO loop for voltages. The times (sec) and voltages (volts)
c are read in for the total number of voltage values.
c
c The actual desired output voltages from the power supply are to
c be read in. These values are converted to the output range of
c the computer (0 to 10 volts), and then a 2:1 divider is used to
c scale the voltage to the input required voltage for the
c HP 6024A DC power supply (0 to 5 volts). The power supply then

```

```

c   scales this input to 0 to 60 volts output to the heater.
c
c   The voltage will commence at the designated time and the signal
c   will continue until changed. The dummy variable starts from '2'
c   because an initial zero voltage is added later. A final zero
c   voltage is also added to turn off the power supply at the end
c   of the run.
c
c       DO J = 2,NVOLT+1
c           READ(10,*)TIMES(J),VOLTS(J)
c       ENDDO
c       ELSE
c
c   Or, enter voltage data by keyboard.
c   The variables are entered in the same order as described above.
c
c   First, enter heat flux area (m*m).
c
c       WRITE(*,30)'Enter area of heated surface (divide by 2) (m*m):'
c       READ(*,*)HEAT_AREA
c
c   Next, enter the resistance of the heater (ohms).
c
c       WRITE(*,30)'Enter resistance of heater (ohms):'
c       READ(*,*)RESIST
c
c   Enter the total number of voltage D/A input values.
c
c       WRITE(*,30)'Enter total number of voltage data values:'
c       READ(*,*)NVOLT
c
c   Now start the DO loop for D/A voltage data. See notes above.
c
c       WRITE(*,30)'Enter time (sec) and voltage (volts):'
c       DO J = 2,NVOLT+1
c           WRITE(*,40)J-1
c           READ(*,*)TIMES(J),VOLTS(J)
c       ENDDO
c   ENDIF
c
c   Initialize and shutdown power supply by imposing 0.0 volts at
c   time equal to 0 sec and at end of run.
c
c       NVOLT = NVOLT+2
c       VOLTS(1) = 0.0
c       VOLTS(NVOLT) = 0.0
c
c   Convert voltage input to integer values for D/A;
c   CALL TRANS_DAC subroutine to convert volts in to binary form.
c
c       CALL TRANS_DAC(NVOLT,VOLTS,BUFF_DA_AXB)
c
c   End set up for power supply
c
1   FORMAT(A)
10  FORMAT(' ',/, ' ',72(' '),/,10X,A,/)
20  FORMAT(11X,A,A,/,6X,A,A,/,7(/,16X,A),/,11X,A,/,6X,A,A,
1    /6X,A,A,/,3(/,16X,A))
30  FORMAT(' ',/, ' ',5X,A)
40  FORMAT(' ',I3,':')
50  FORMAT(' ',F10.2,5X,F10.2,5X,I10)
c
c   RETURN

```

```

END
C
C*****
C*****
C
      SUBROUTINE  TRANS_DAC(NVOLT,VOLTS,BUFF_DA_AXB)
C
C  This subroutine first scales the input voltage to the output voltage
C  of the VaxII/GPX (0 to 10V), and then converts the voltage
C  values to the binary form required for the D/A converter, using
C  a calibration chart by M. Loh, 7/30/89. The chart may be
C  found in the data aquisition notebook in RM A-32, RCE, MSU.
C
      IMPLICIT NONE
C
C  Define integer variables
C
      INTEGER*2      BUFF_DA_AXB(500)      !buffer for D/A
      INTEGER J      !Dummy variable
      INTEGER NVOLT   !Number of D/A voltage data
C
C  Define real variables
C
      REAL           VOLTS(100)             !volts(v) for D/A
      REAL           A                       !Y-intercept for volt/bin conv
      REAL           B                       !Slope for volt/binary convr
C
C*****
C
C  Based on calibration by M. Loh, scaling factor between the
C  output voltage signal from the VaxII/GPX and the output signal
C  from the HP 6024A DC power supply was found to be 6.012559. The
C  voltage was found to vary linearly with binary output, over the
C  voltage range from 0 to 10 volts. The conversion equation is:
C  binary = A + B*volts, where A = 2048.2235, and B = -34.02974.
C
C  Note: 10V is the maximum output for the VaxII/GPX computer. If more
C  than 60 V are read in as output to the power supply, it will be
C  scaled to 10 V for the D/A, and a warning statement will be
C  shown on the screen.
C
      A = 2048.2235
      B = -34.02974
      DO J = 1,NVOLT
C
C  Check to see if input voltage is greater than 60.0V and set to 60.0V
C  if it is. (60V is maximum voltage for HP 6024A power supply.)
C
      IF (VOLTS(J).GT.60.0) THEN
        VOLTS(J)=60.0
        WRITE(*,*)'WARNING: INPUT VOLTAGE GREATER THAN 60V; SET TO',
1          ' 60V!'
      ENDIF
C
C  Convert to binary format
C
      BUFF_DA_AXB(J) = A + B*VOLTS(J)
      ENDDO
      RETURN
      END
C
C  End subroutine TRANS_DAC
C

```

```

C*****
C
C      SUBROUTINE TRANS_ADC(POWER,NCHANP1,SUM,VA)
C
C      This subroutine converts binary output data to volts using a cali-
C      bration chart by M. Loh, 7/30/89. The chart may be found in
C      the data acquisition notebook in RM A-32, RCE, MSU. If the HP
C      power supply is used, the voltage is scaled from approximately
C      10 to 60 volts for heat flux calculations. (0 to 10 volts is
C      the range for the VaxII/GPX, while the actual voltage output
C      from the power supply is 0 to 60 volts.)
C
C      IMPLICIT NONE
C
C      Define integer variables
C
C      INTEGER J                      !Dummy variable
C      INTEGER NCHANP1                !Total number of channels
C      INTEGER POWER                   !Indicates use of D/A
C
C      Define real variables
C
C      REAL          B                 !Slope for volt/binary convr
C      REAL          SCALE              !Scaling factor
C      REAL          SUM(16)           !Sums for averaging data
C      REAL          VA(16)            !Millivolts from A/D
C
C*****
C
C      Based on calibration by M. Loh, the voltage was found to vary linear-
C      ly with binary output from 0 to 4095. The conversion equation
C      is: volts = B*binary, where B = 0.00243503.
C
C      SCALE = 6.52543
C      B = 0.00243503
C      DO J = 1,NCHANP1
C         VA(J) = B*SUM(J)
C         IF(J.EQ.NCHANP1.AND.POWER.EQ.1)VA(J) = VA(J)*SCALE
C      ENDDO
C      RETURN
C      END
C
C      End subroutine TRANS_ADC
C
C*****
C
C
C      \ /_____ \
C CCCCCCCCCCCCCCCCCCCCCCCCCCCCCCCCCCCCCCCC \ /_____ \ CCCCCCCCCCCCCCCCCCCCCCCCCCCCCCCCCCCCCCCC
C..... /_____ \ \_____ / .....
C!!!!!!!!!!!!!!!!!!!!!! / / \ \!!!!!!!!!!!!!!!!!!!!!!
C////////// | | e -< | \\\\\\\\\\\\\\\\\\\\\\\\\\\\\\\
C\\\\\\\\\\\\\\\\\\\\\\\\\\\\\\\ | | \_/ | ///////////////
C!!!!!!!!!!!!!!!!!!!!!! \ \ / \!!!!!!!!!!!!!!!!!!!!!!
C..... \_____ \ / .....EPS
C CCCCCCCCCCCCCCCCCCCCCCCCCCCCCCCCCCCCCCCC CCCCCCCCCCCCCCCCCCCCCCCCCCCCCCCCCCCCCCCC
C
C
C*****

```

APPENDIX C

APPENDIX C

PARAMETER ESTIMATION RESULTS FROM EXPERIMENTAL REPETITIONS USING CURED COMPOSITE SAMPLES

This appendix contains the results from the estimation of the thermal properties, namely the estimated effective thermal conductivity perpendicular to the fiber axis and the estimated effective density-specific heat product, of the cured $[0^\circ]_{24}$ AS4/EPON 828 composite samples for each repetition with approximate initial temperatures of 25°C, 50°C, 75°C, 100°C, and 125°C in Tables C.1-C.5 respectively. The results for the estimated thermal properties for each repetition of the experiments using cured $[0^\circ, \pm 30^\circ, \pm 60^\circ, 90^\circ]_{2(\text{sym})}$ samples with initial temperatures of approximately 25°C, 50°C, and 75°C are given in Tables C.6-C.8, respectively.

Table C.1. Estimated Effective Thermal Conductivity, k , Perpendicular to the Fiber Axis and Density-Specific Heat, ρc , of Cured [0°] AS4/EPON 828-mPDA Composites from Experiments with an Initial Temperature of Approximately 25°C.

Exper. No. ^a	Repet. No. ^a	Temperature Range (°C)	k (W/m°C)	ρc (kJ/m ³ °C)	RMS ^b (°C)
1.1	1	26 - 58	0.803	1,590	0.440
	2	26 - 57	0.805	1,580	0.480
	3	26 - 57	0.803	1,570	0.480
	4	32 - 53	0.780	1,580	0.173
	5	35 - 54	0.776	1,590	0.210
	6	26 - 45	0.769	1,570	0.299
	7	30 - 49	0.817	1,590	0.259
	8	30 - 48	0.818	1,550	0.250
	9	30 - 49	0.805	1,600	0.232
1.6	1	27 - 45	0.794	1,590	0.249
	2	29 - 47	0.792	1,550	0.255
	3	29 - 48	0.808	1,540	0.240
	4	25 - 44	0.798	1,590	0.284
	5	25 - 45	0.799	1,590	0.234
	6	25 - 45	0.790	1,580	0.340
1.11	1	26 - 46	0.767	1,560	0.190
	2	26 - 46	0.748	1,560	0.146
	3	27 - 47	0.742	1,580	0.138
	4	26 - 46	0.730	1,560	0.127
	5	26 - 46	0.737	1,550	0.130
	6	26 - 46	0.744	1,540	0.147

a. Experiment and repetition numbers refer to those in Table 4.2.

b. Root mean squared error of calculated versus experimental temperatures.

Table C.2. Estimated Effective Thermal Conductivity, k , Perpendicular to the Fiber Axis and Density-Specific Heat, ρc_p , of Cured [0°] AS4/EPON 828-mPDA Composites from Experiments with an Initial Temperature of Approximately 50°C.

Exper. No. ^a	Repet. No. ^a	Temperature Range (°C)	k (W/m°C)	ρc_p (kJ/m ³ °C)	RMS ^b (°C)
1.2	1	52 - 76	0.797	1,650	0.334
	2	53 - 76	0.789	1,640	0.363
	3	52 - 75	0.783	1,670	0.431
	4	54 - 74	0.794	1,620	0.202
	5	54 - 74	0.795	1,650	0.240
	6	54 - 74	0.797	1,660	0.252
1.7	1	50 - 67	0.855	1,700	0.242
	2	50 - 67	0.868	1,660	0.223
	3	50 - 67	0.866	1,660	0.209
	4	50 - 67	0.877	1,740	0.575
	5	50 - 67	0.870	1,740	0.336
	6	50 - 67	0.868	1,680	0.222
	7	52 - 70	0.850	1,620	0.145
	8	52 - 69	0.897	1,670	0.198
	9	49 - 66	0.852	1,680	0.202
	10	50 - 68	0.875	1,640	0.203
	11	51 - 68	0.847	1,640	0.159
	12	51 - 68	0.895	1,710	0.229
1.12	1	52 - 71	0.775	1,620	0.117
	2	52 - 71	0.773	1,620	0.108
	3	53 - 73	0.797	1,610	0.168
	4	53 - 72	0.805	1,620	0.205
	5	52 - 71	0.818	1,550	0.208
	6	52 - 71	0.771	1,610	0.141

a. Experiment and repetition numbers refer to those in Table 4.2.

b. Root mean squared error of calculated versus experimental temperatures.

Table C.3. Estimated Effective Thermal Conductivity, k , Perpendicular to the Fiber Axis and Density-Specific Heat, ρc_p , of Cured [0°] AS4/EPON 828-mPDA Composites from Experiments with an Initial Temperature of Approximately 75°C.

Exper. No. ^a	Repet. No. ^a	Temperature Range (°C)	k (W/m°C)	ρc_p (kJ/m ³ °C)	RMS ^b (°C)
1.3	1	78 - 99	0.796	1,670	0.408
	2	78 - 99	0.801	1,680	0.420
	3	76 - 98	0.809	1,680	0.414
	4	78 - 98	0.815	1,720	0.323
	5	78 - 97	0.827	1,710	0.323
	6	78 - 97	0.811	1,700	0.356
1.8	1	75 - 92	0.924	1,830	0.220
	2	75 - 91	0.900	1,820	0.203
	3	75 - 91	0.926	1,760	0.209
	4	75 - 91	0.919	1,820	0.211
	5	75 - 91	0.915	1,830	0.208
	6	75 - 91	0.922	1,820	0.209
1.13	1	77 - 94	0.825	1,780	0.126
	2	75 - 93	0.811	1,740	0.146
	3	77 - 95	0.802	1,760	0.206
	4	77 - 95	0.782	1,770	0.190
	5	77 - 95	0.779	1,760	0.139
	6	77 - 95	0.783	1,760	0.129

a. Experiment and repetition numbers refer to those in Table 4.2.

b. Root mean squared error of calculated versus experimental temperatures.

Table C.4. Estimated Effective Thermal Conductivity, k , Perpendicular to the Fiber Axis and Density-Specific Heat, ρc_p , of Cured [0°] AS4/EPON 828-mPDA Composites from Experiments with an Initial Temperature of Approximately 100°C.

Exper. No. ^a	Repet. No. ^a	Temperature Range (°C)	k (W/m°C)	ρc_p (kJ/m ³ °C)	RMS ^b (°C)
1.4	1	102 - 119	0.812	1,780	0.289
	2	102 - 122	0.844	1,910	0.303
	3	102 - 123	0.844	1,900	0.312
	4	102 - 120	0.830	1,980	0.237
	5	102 - 120	0.829	2,020	0.274
	6	102 - 120	0.847	2,000	0.241
	7	101 - 119	0.784	1,850	0.330
	8	103 - 119	0.804	1,830	0.282
	9	103 - 120	0.822	1,840	0.258
	10	102 - 119	0.841	1,830	0.300
	11	102 - 118	0.876	1,910	0.249
	12	102 - 118	0.847	1,950	0.555
1.9	1	100 - 115	0.969	1,950	0.178
	2	100 - 115	0.959	2,000	0.178
	3	100 - 115	0.963	1,930	0.187
	4	100 - 115	0.979	1,960	0.195
	5	100 - 115	0.961	1,960	0.179
	6	100 - 115	0.996	1,970	0.183
1.14	1	100 - 115	0.806	1,850	0.112
	2	100 - 115	0.808	1,850	0.115
	3	100 - 115	0.815	1,850	0.116
	4	100 - 115	0.816	1,810	0.142
	5	100 - 115	0.825	1,850	0.146
	6	100 - 115	0.824	1,790	0.145

a. Experiment and repetition numbers refer to those in Table 4.2.

b. Root mean squared error of calculated versus experimental temperatures.

Table C.5. Estimated Effective Thermal Conductivity, k , Perpendicular to the Fiber Axis and Density-Specific Heat, ρc_p , of Cured [0°] AS4/EPON 828-mPDA Composites from Experiments with an Initial Temperature of Approximately 125°C.

Exper. No. ^a	Repet. No. ^a	Temperature Range (°C)	k (W/m°C)	ρc_p (kJ/m ³ °C)	RMS ^b (°C)
1.5	1	126 - 145	0.814	2,150	0.447
	2	126 - 145	0.820	2,220	0.481
	3	126 - 145	0.834	2,170	0.436
	4	127 - 144	0.870	1,980	0.465
	5	127 - 145	0.894	2,000	0.454
	6	127 - 145	0.874	1,940	0.398
	7	128 - 144	0.965	1,960	0.297
	8	128 - 144	0.911	2,000	0.288
	9	128 - 144	0.934	1,990	0.239
1.10	1	126 - 141	1.006	2,070	0.189
	2	126 - 141	0.998	2,130	0.156
	3	126 - 141	1.004	2,110	0.163
	4	126 - 141	1.013	2,110	0.157
	5	126 - 140	1.014	2,090	0.167
	6	126 - 140	1.028	2,050	0.206
1.15	1	126 - 140	0.862	1,990	0.093
	2	126 - 140	0.880	1,910	0.104
	3	126 - 140	0.870	1,930	0.121
	4	126 - 140	0.875	1,920	0.100
	5	126 - 140	0.874	1,940	0.099
	6	126 - 140	0.881	1,920	0.104

a. Experiment and repetition numbers refer to those in Table 4.2.

b. Root mean squared error of calculated versus experimental temperatures.

Table C.6. Estimated Effective Thermal Conductivity, k , Perpendicular to the Fiber Axis and Density-Specific Heat, ρc_p , of Cured $[0^\circ, \pm 30^\circ, \pm 60^\circ, 90^\circ]_2$ (s y n) AS4/EPON 828-mPDA Composites from Experiments with an Initial Temperature of Approximately 25°C.

Exper. No. ^a	Repet. No. ^a	Temperature Range (°C)	k (W/m°C)	ρc_p (kJ/m ³ °C)	RMS ^b (°C)
1.16	1	25 - 32	0.697	1,780	0.922
	2	25 - 32	0.690	1,800	0.991
	3	25 - 32	0.667	1,720	0.950
	4	25 - 37	0.660	1,680	0.767
	5	25 - 45	0.685	1,830	0.897
	6	25 - 42	0.648	1,670	0.637
	7	28 - 45	0.716	1,680	0.166
	8	28 - 45	0.727	1,680	0.168
	9	28 - 49	0.659	1,520	0.176
	10	29 - 49	0.696	1,560	0.183
	11	29 - 48	0.713	1,590	0.200
1.19	1	26 - 49	0.716	1,540	0.246
	2	29 - 53	0.754	1,610	0.194
	3	25 - 48	0.765	1,610	0.268
	4	25 - 49	0.750	1,610	0.250
	5	31 - 55	0.813	1,640	0.247
	6	30 - 53	0.800	1,630	0.206

a. Experiment and repetition numbers refer to those in Table 4.2.

b. Root mean squared error of calculated versus experimental temperatures.

Table C.7. Estimated Effective Thermal Conductivity, k , Perpendicular to the Fiber Axis and Density-Specific Heat, ρc_p , of Cured $[0^\circ, \pm 30^\circ, \pm 60^\circ, 90^\circ]_2$ (s y m) AS4/EPON 828-mPDA Composites from Experiments with an Initial Temperature of Approximately 50°C .

Exper. No. ^a	Repet. No. ^a	Temperature Range ($^\circ\text{C}$)	k ($\text{W/m}^\circ\text{C}$)	ρc_p ($\text{kJ/m}^3\ ^\circ\text{C}$)	RMS ^b ($^\circ\text{C}$)
1.17	1	52 - 76	0.723	1,660	0.134
	2	53 - 76	0.708	1,640	0.183
	3	52 - 75	0.709	1,620	0.176
	4	54 - 74	0.724	1,650	0.302
	5	54 - 74	0.726	1,630	0.165
	6	54 - 74	0.709	1,690	0.413
1.20	1	50 - 67	0.809	1,710	0.326
	2	50 - 67	0.802	1,700	0.383
	3	50 - 67	0.805	1,700	0.352
	4	50 - 67	0.767	1,680	0.403
	5	50 - 67	0.766	1,680	0.353
	6	50 - 67	0.766	1,640	0.222

a. Experiment and repetition numbers refer to those in Table 4.2.

b. Root mean squared error of calculated versus experimental temperatures.

Table C.8. Estimated Effective Thermal Conductivity, k , Perpendicular to the Fiber Axis and Density-Specific Heat, ρc_p , of Cured $[0^\circ, \pm 30^\circ, \pm 60^\circ, 90^\circ]_2$ (s y m) AS4/EPON 828-mPDA Composites from Experiments with an Initial Temperature of Approximately 75°C.

Exper. No. ^a	Repet. No.	Temperature Range (°C)	k (W/m°C)	ρc_p (kJ/m ³ °C)	RMS ^b (°C)
1.18	1	78 - 96	0.735	1,740	0.151
	2	78 - 96	0.743	1,730	0.153
	3	78 - 97	0.738	1,730	0.177
	4	78 - 96	0.747	1,700	0.155
	5	78 - 97	0.759	1,680	0.194
	6	78 - 97	0.745	1,720	0.151
1.21	1	76 - 98	0.721	1,750	0.415
	2	77 - 96	0.884	2,240	0.623
	3	76 - 97	0.757	1,720	0.490
	4	76 - 96	0.744	1,740	0.423
	5	76 - 97	0.748	1,740	0.432
	6	76 - 97	0.749	1,730	0.426

a. Experiment and repetition numbers refer to those in Table 4.2.

b. Root mean squared error of calculated versus experimental temperatures.

BIBLIOGRAPHY

BIBLIOGRAPHY

- Acitelli, M. A., R. B. Prime, and E. Sacher, 1971, "Kinetics of Epoxy Cure: (1) The System Bisphenol-A Diglycidyl Ether/m-phenylene Diamine," *Polymer*, 12:445-463.
- Alifanov, O. M. and N. V. Kernov, 1981, "Determination of External Thermal and Load Parameters by Solving the Two-Dimensional Inverse Heat-Conduction Problem," translated from *Inzhenerno-Fizicheskii Zhurnal*, 1981, 41(4):581-586, *Journal of Engineering Physics*, 41(4):1049-1053.
- Alifanov, O. M. and V. V. Mikhailov, 1979, "Solution of the Nonlinear Inverse Thermal Conductivity Problem by the Iteration Method," translated from *Inzhenerno-Fizicheskii Zhurnal*, 1978, 35(6):1123-1129, *Journal of Engineering Physics*, 35(6):1501-1506.
- Alifanov, O. M. and S. V. Rumyantsev, 1987, "Formulas for the Discrepancy Gradient in the Iterative Solution of Inverse Heat-Conduction Problems. II. Determining the Gradient in Terms of a Conjugate Variable," translated from *Inzhenerno-Fizicheskii Zhurnal*, 1987, 52(4):668-675, *Journal of Engineering Physics*, 52(4):489-495.
- Barton, J. M., 1985, "The Application of Differential Scanning Calorimetry (DSC) to the Study of Epoxy Resin Curing Reactions," *Advances in Polymer Science 72 Epoxy Resins and Composites I*, Springer-Verlag, New York, pp. 111-154.
- Beck, J. V., 1966, "Transient Determination of Thermal Properties," *Nuclear Engineering and Design*, 3:373-381.
- Beck, J. V., 1987, "PROP1D", Parameter Estimation Computer Program, Michigan State University, East Lansing, MI 48824
- Beck, J. V., 1989, "PROP1DMA", Parameter Estimation Computer Program (revised version), Michigan State University, East Lansing, MI 48824
- Beck, J. V. and S. Al-Araji, 1974, "Investigation of a New Simple Transient Method of Thermal Property Measurement," *Journal of Heat Transfer*, 96(1):59-64.
- Beck, J. V. and K. J. Arnold, 1977, *Parameter Estimation in Engineering and Science*, John Wiley & Sons, New York.
- Borchardt, J. and F. Daniels, 1957, "The Application of Differential Thermal Analysis to the Study of Reaction Kinetics," *Journal of American Chemical Society*, 79:41-46.
- Boyer, G. T. and W. C. Thomas, 1985, "An Analytical Investigation of Charring Composite Undergoing Thermochemical Expansion," *American Society of Engineers Paper No. 85-HT-54*.
- Brennan, J. J., L. D. Bentsen, D. P. H. Hasselman, 1982, "Determination of the Thermal Conductivity and Diffusivity of Thin Fibres by the Composite Method," *Journal of Materials Science*, 17:2337-2342.

- Chern, C.-S., and G. W. Poehlein, 1987, "A Kinetic Model for Curing Reactions of Epoxides with Amines," *Polymer Engineering and Science*, 27(11):788-795.
- Courville and J. V. Beck, 1988, "Measurement of Field Thermal Performance Parameters of Building Envelope Components," *ASHREA Transactions*, 94(Part 2):1595-1612.
- Digital Equipment Corporation, 1986, *VAXlab/LabStar Programmers Guide*, AA-HX04B-TE, Digital Equipment Corporation, MA.
- Dul'nev, G. N., M. A. Eremeev, Y. P. Zarichnyak, and E. N. Koltunova, 1977, "A Combined Numerical Method for Determining the Conductance of Composite Bodies," translated from *Inzhenerno-Fizicheskii Zhurnal*, 1977, 32(2):284-291, *Journal of Engineering Physics*, 32(2):174-180.
- DuPont Company Instrument Systems, 1985, *910 Differential Scanning Calorimeter Operator's Manual*, DuPont Company Instrument Systems, Wilmington, DE 19898.
- Ectron Corporation, 1982, *Instruction Manual 687 DC Amplifier and Options A/O*, Ectron Corporation, San Diego, CA.
- Farnia, K., 1976, *Computer-Assisted Experimental and Analytical Study of Time / Temperature-Dependent Thermal Properties of the Aluminum Alloy 2024-T351*, Ph.D. Dissertation, Department of Mechanical Engineering, Michigan State University, East Lansing, MI 48824.
- Fava, R. A., 1968, "Differential Scanning Calorimetry of Epoxy Resins," *Polymer*, 9:137-151.
- Golovchan, V. T., and A. G. Artemenko, 1987, "Heat Conduction of Orthogonally Reinforced Composite Materials," translated from *Inzhenerno-Fizicheskii Zhurnal*, 51(2):260-297, 1986, Plenum Publishing Corporation.
- Griffis, C. A., R. A. Masumura, and C. I. Chang, 1981, "Thermal Response of Graphite Epoxy Composite Subjected to Rapid Heating," *Journal of Composite Materials*, 15:427-442.
- Hagnauer, G. L., B. R. LaLiberte, and D. A. Dunn, 1983, "Isothermal Cure Kinetics of an Epoxy Resin Prepreg," *Epoxy Resin Chemistry II*, R. S. Bauer, ed., American Chemical Society Symposium Series 221, pp. 229-244.
- Han, L. S. and A. A. Cosner, 1981, "Effective Thermal Conductivities of Fibrous Composites," *Journal of Heat Transfer*, 103(5):387-392.
- Harris, J. P., B. Yates, J. Batchelor, and P. J. Garrington, 1982, "The Thermal Conductivity of Kevlar Fibre-Reinforced Composites," *Journal of Materials Science*, 17(9):2925-2931.
- Hasselman, D. P. H. and L. F. Johnson, 1987, "Effective Thermal Conductivity of Composites with Interfacial Thermal Barrier Resistance," *Journal of Composite Materials*, 21:508-515.
- Hawley, M. C., L. T. Drzal, A. Asmussen, Jr., and J. V. Beck, 1988, "Study of Interface/Interphase in Thick Section Composites Annual Technical Report 1986-1988," submitted to: University of Illinois / Office of Naval Research.
- Henderson, J. B. and J. A. Wiebelt, 1987, "A Mathematical Model to Predict the Thermal Response of Decomposing, Expanding Polymer Composites," *Journal of Composite Materials*, 21:373-393.

- Henderson, J. B., J. A. Wiebelt, and M. R. Tant, 1985, "A Model for the Thermal Response of Polymer Composite Materials with Experimental Verification," *Journal of Composite Materials*, 19:579-595.
- Huag, E. J. and Arora, J. S., 1979, *Applied Optimal Design*, John Wiley and Sons, NY.
- Ishikawa, T., 1980, "Analysis and Experiments on Thermal Conductivities of Unidirectional Fiber-Reinforced Composites," *Heat Transfer - Japanese Research*, 9(3):41-53.
- James, B. W., G. H. Wostenholm, G. S. Keen and S. D. McIvor, 1987, "Prediction and Measurement of the Thermal Conductivity of Composite Materials," *Journal of Physics; D: Applied Physics*, 20(3):261-268.
- Kamal, M. R., S. Sourour, and M. Ryan, 1973, "SPE 31st Annual Technical Conference Proceedings," pp. 187. In Barton, J. M., 1985, "The Application of Differential Scanning Calorimetry (DSC) to the Study of Epoxy Resin Curing Reactions," *Advances in Polymer Science 72 Epoxy Resins and Composites I*. Springer-Verlag, New York, pp. 111-154.
- Lamm, P., 1989, "Notes on the Adjoint Method for Estimating Functions," Personal communication.
- Lee, H. J. and R. E. Taylor, 1975, "Thermophysical Properties of Carbon/Graphite Fibers and mod-3 Fiber-Reinforced Graphite," *Carbon*, 13:521-527.
- Lee, W. I., A. C. Loos, and G. S. Springer, 1982, "Heat of Reaction, Degree of Cure, and Viscosity of Hercules 3501-6 Resin," *Journal of Composite Materials*, 16:510-520.
- Loh, M., 1989, "Two-Dimensional Heat Transfer Studies in Carbon Composite Materials," *Diplomarbeit*, Michigan State University, East Lansing, MI; Rheinisch-Westfaelisch Technische Hochschule Aachen, Aachen, FRG.
- Loos, A. C., and G. S. Springer, 1983, "Curing of Epoxy Matrix Composites," *Journal of Composite Materials*, 17(3):135-169.
- Mijović, J., 1986, "Cure Kinetics of Neat Versus Reinforced Epoxies," *Journal of Applied Polymer Science*, 31:1177-1187.
- Mijović, J., J. Kim, and J. Slaby, 1984, "Cure Kinetics of Epoxy Formulations of the Type used in Advanced Composites," *Journal of Applied Polymer Science*, 29:1449-1462.
- Mijović, J., and H. C. Mei, 1987, "An Apparatus for Measurement of Thermal Conductivity of Neat Epoxies and their Composites," *Polymer Composites*, 8(1):53-56.
- Mijović, J. and H. T. Wang, 1988, "Modeling of Processing of Composites Part II - Temperature Distribution during Cure," *SAMPLE Journal*, March/April, pp. 42-55, 191.
- Mijović, J. and H. T. Wang, 1989, "Cure Kinetics of Neat and Graphite-Fiber-Reinforced Epoxy Formulations," *Journal of Applied Polymer Science*, 37:2661-2673.
- Moroni, A., J. Mijović, E. M. Pearce, and C. C. Foun, 1986, "Cure Kinetics of Epoxy Resins and Aromatic Diamines," *Journal of Applied Polymer Science*, 32:3761-3773.

- Mottram, J. T. and R. Taylor, 1987a, "Thermal Conductivity of Fibre-Phenolic Resin Composites. Part I: Thermal Diffusivity Measurements," *Composites Science and Technology* 29:189-209.
- Mottram, J. T. and R. Taylor, 1987b, "Thermal Conductivity of Fibre-Phenolic Resin Composites. Part II: Numerical Evaluation," *Composites Science and Technology* 29:211-232.
- Osman, A. M., 1987, *Estimation of Transient Heat Transfer Coefficients in Multi-Dimensional Problems by Using Inverse Heat Transfer Methods*, Ph.D. Dissertation, Department of Mechanical Engineering, Michigan State University, East Lansing, MI 48824.
- Pappalardo, L. T., 1977, "DSC Evaluation of Epoxy and Polyimide-Impregnated Laminates (Prepregs)," *Journal of Applied Polymer Science*, 21:809-820.
- Parker, W. J., R. J. Jenkins, C. P. Butler, and G. L. Abbott, 1961, "Flash Method of Determining Thermal Diffusivity, Heat Capacity, and Thermal Conductivity," *Journal of Applied Physics*, 32(9):1679-1684.
- Prime, R. B., 1970, Analytical Calorimetry, 2:201, in Barton, J. M., 1985, "The Application of Differential Scanning Calorimetry (DSC) to the Study of Epoxy Resin Curing Reactions," *Advances in Polymer Science* 72 Epoxy Resins and Composites I, Springer-Verlag, New York, pp. 111-154.
- Prime, R. B., 1973, "Differential Scanning Calorimetry of the Epoxy Cure Reaction," *Polymer Engineering Science*, 13:365-371.
- PLOTIT^R, 1989, Scientific Programming Enterprises, Haslett, MI 48840.
- Rabek, J. F., 1980, *Experimental Methods in Polymer Chemistry; Physical Principles and Applications*, John Wiley and Sons, NY.
- Rich, M., 1987, Personal Communication.
- Ryan, M. E. and A. Dutta, 1979, "Kinetics of Epoxy Cure: a Rapid Technique for Kinetic Parameter Estimation, *Polymer*, 20(2):203-206.
- Scientific Programming Enterprises, 1987, "PlotIT^R Reference Manual", Scientific Programming Enterprises, Haslett, MI 48840.
- Schechter, L., J. Wynstra, and R. P. Kurkky, 1956, "Glycidyl Ether Reactions with Amines," *Industrial and Engineering Chemistry*, 48:94-97.
- Schimmel, Jr, W. P., J. V. Beck, and A. B. Donaldson, 1977, "Effective Thermal Diffusivity for a Multimaterial Composite Laminate," *Journal of Heat Transfer*, 99:466-470.
- Sichina, W. J., "Autocatalyzed Epoxy Cure Predictions using Isothermal DCS Kinetics," DuPont Application Brief No. TA-93.
- Sichina, W. J., 1989, "Effects of Annealing on the Observed Tg of a Glassy Polymer," The TA Hotline, DuPont Company Instrument Systems, Fall.
- Smith, I. T., 1961, "The Mechanism of the Crosslinking of Epoxide Resins by Amines," *Polymer*, 2:95-108.
- Sourour, S. and M. R. Kamal, 1976, "Differential Scanning Calorimetry of Epoxy cure: Isothermal Cure Kinetics," *Thermochemica Acta*, 14:41-59.

- Springer, G. S. and S. W. Tsal, 1967, "Thermal Conductivities of Unidirectional Materials," *Journal of Composite Materials*, 1:166-173.
- Tant, M. R., J. B. Henderson, and C. T. Boyer, 1985, "Measurement and Modelling of the Thermochemical Expansion of Polymer Composites," *Composites*, 16(2):121-126.
- Taylor, R. E. and B. H. Kelsic, 1986, "Parameters Governing Thermal Diffusivity Measurements of Unidirectional Fiber-Reinforced Composites," *Journal of Heat Transfer*, 108:161-165.
- Tortorelli, D. A., R. B. Haber, and S. C-Y. Lu, 1989, "Design Sensitivity Analysis for Nonlinear Thermal Systems," accepted for publication in *Computer Methods in Applied Mechanics and Engineering*.
- Tu, J. S., 1988, *Solution of General Two-Dimensional Inverse Heat Conduction Problems and One-Dimensional Inverse Melting Problems*, Ph.D. Dissertation, Department of Mechanical Engineering, Michigan State University, East Lansing, MI 48824.
- Vinson, J. R. and R. L. Sleskowsky, 1987, *The Behavior of Structures Composed of Composite Materials*, Martinus Nijhoff Publishers, Dordrecht, MA.
- Walpole, R. E. and R. H. Myers, 1978, *Probability and Statistics for Engineers and Scientists*, 2nd Edition, Macmillan Publishing Co. NY.
- Waterbury, M. 1988, "Optimal Numerical Volumetric Analysis", computer software, Michigan State University, East Lansing, MI 48824.
- Ziebland, H., 1977, "The Thermal and Electrical Transmission Properties of Polymer Composites," in Chapter 7, *Polymer Engineering Composites*, M. O. W. Richardson, ed., Applied Science Publishers, LTD., London.

MICHIGAN STATE UNIV. LIBRA



31293007884178